SYNTHESIS, CHARACTERIZATION AND CATALYTIC PROPERTIES OF METALLOSILICATES WITH MEL TOPOLOGY

A THESIS
SUBMITTED TO THE
UNIVERSITY OF POONA
FOR THE DEGREE OF
DOCTOR OF PHILOSOPHY
(IN CHEMISTRY)

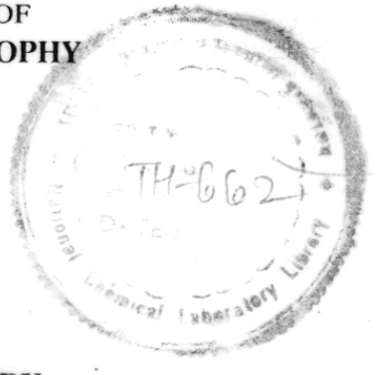

by

J. SUDHAKAR REDDY

CATALYSIS DIVISION
NATIONAL CHEMICAL LABORATORY
PUNE-411 008 (INDIA)

MAY 1992

– TO MY BELOVED PARENTS

CERTIFICATE

Certified that the work incorporated in the thesis "**Synthesis, Characterization and Catalytic Properties of Metallosilicate analogs with MEL Topology**" submitted by Mr. J. Sudhakar Reddy, for the degree of Doctor of Philosophy, was carried out by the candidate under my supervision in the National Chemical Laboratory, Pune. Such material as has been obtained from other sources has been duly acknowledged in the thesis.

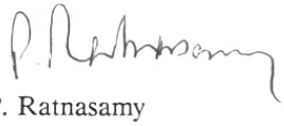

P. Ratnasamy
(Research Guide)

ACKNOWLEDGEMENTS

I wish to express my gratitude to Dr. P. Ratnasamy, Deputy Director, National Chemical Laboratory, Pune for his valuable guidance throughout the course of the investigation.

I am grateful to Dr. S. Sivasanker and Dr. Rajiv Kumar for their constant encouragement and many stimulating discussions.

I am thankful to Dr. A.V. Ramaswamy, Dr. S.G. Hegde and Dr. R. Vetrivel for their help during the present study.

I am also thankful to the scientific staff of the Catalysis Division and my numerous friends for their wholehearted co-operation in many ways.

Finally, my thanks are due to Council of Scientific and Industrial Research, New Delhi, for the award of a fellowship and the Director, National Chemical Laboratory, Pune for permitting me to submit this work in the form of thesis.

Reddy

J. Sudhakar Reddy

Contents...

CHAPTER - I

GENERAL INTRODUCTION

1.1. INTRODUCTION

Zeolites are microporous, crystalline aluminosilicates, having stable frameworks, constituted by cornersharing of all four oxygens of the $[SiO_4]^{4-}$ and $[AlO_4]^{5-}$ tetrahedral primary building units, in such a way that two Al-tetrahedra are not neighbors. The crystallographic unit cell of a zeolite may be represented as[1]:

$$M_{x/n}\,[(AlO_2)_x\,(SiO_2)_y\,Z\,H_2O$$

Where M is the cation of valence 'n' from group I or II or an organic cation. The ratio of y/x can be one to infinity. Z is the number of water molecules, which can be removed by heat and/or vacuum to get the porosity. In the as-synthesized form of the zeolite, the negative charge of the framework generated by aluminium is compensated by inorganic/organic cations. Al^{3+} ions in the zeolite lattice can be replaced by various trivalent and tetravalent metal ions like B^{3+}, Ga^{3+}, Fe^{3+}, Cr^{3+}, V^{4+}, Ti^{4+} and Zr^{4+}. The resultant materials are generally called metal-losilicates or molecular sieves.

Zeolites are classified according to their morphological characteristics[1,2,3,4], crystal structure[1,2,5], effective pore diameter[1,2,6], chemical composition[1,2,7] and natural occurrence[1,2].

There is no systematic nomenclature developed for molecular sieves. Milton and Breck used Arabic alphabets e.g., zeolites A, B, X, Y and L. Mobil and Union Carbide initiated the use of Greek alphabets, alpha, beta and omega. The zeolites having structures similar to mineral zeolites were assigned the name of the minerals eg., synthetic mordenite, chabazite, erionite, offretite etc.

International Zeolite Association (IZA) and International Union of Pure and Applied Chemistry (IUPAC) assigned[3,8] a three letter code to be used for a known framework topology, irrespective of its composition and distribution of various T-atoms (Si, Al, Ga, Ge, B, Be, Ti, V, etc.) eg., FAU (Faujasite, Y and X), MFI (Mobil five, ZSM-5), MEL (Mobil eleven, ZSM-11), MOR (Mordenite), TON (Theta-1, ZSM-22) etc.

1.2. ZEOLITE SYNTHESIS

Since 1950, approximately 150 synthetic zeolites have been made, while about 40 natural zeolites are known. Natural zeolites form by the reaction of mineralizing aqueous solution with solid aluminosilicates. The number of zeolites synthesized or found in nature are a few percent of the theoretically possible configurations. Zeolite synthesis has been studied

systematically[1,2,12,13]. Crystal growth occurs from the solution phase and the level of supersaturation is controlled by the dissolution of the amorphous gel solid. In contrast to the zeolite, the solid amorphous gel is structurally disordered and its T-atoms (T = Si or Al) have a lower connectivity, Q, than those of zeolite[9] (Q = 3.5 and 4, respectively). Hence the gel is more reactive and more soluble than the zeolite. The chief role of the solid gel is to supply silicate and aluminosilicate species to the solution and control its composition by solubility equilibria[10]. These depend on the structure and composition of the solid phase and are thus sensitive to the way in which the gel is prepared and to the ingredients used to prepare it. Gels of identical stoichiometry can have different solution phase compositions; this can have a marked effect on the crystallization reactions[11].

The zeolite crystallization is different from other crystallization processes in that the level of supersaturation is not readily controlled. The high supersaturations normally encountered give many nuclei and lead to rapid crystal growth; consequently the crystals are small and often faulted or intergrown. These effects are reduced if the solid phase of the reaction mixture is itself a zeolite. In such recrystallizations, the supersaturation is usually less than that sustained by amorphous gel solids and consequently the crystals are larger and more perfect[14].

Sand[15] has summarized the following important events occurring during the crystallization of zeolites:

- Precipitation of a gel phase
- Dissolution of the gel
- Nucleation of zeolite structure
- Continued crystallization and crystal growth
- Dissolution of the initial meta-stable phase
- Nucleation of a more stable metastable phase
- Continued crystallization and crystal growth of the new crystalline phase while the initial crystals are dissolving
- Dissolution of the metastable phase
- Nucleation of the equilibrium phase and
- Crystallization and crystal growth of the final crystalline phase.

The stabilization of the zeolite product is brought about by the guest species that fills the channels and cavities of the aluminosilicate framework. A simple thermodynamic treatment shows[14] that these guest species lower the chemical potential of the framework. The aluminous zeolites require inorganic cations and water molecules, whereas the hydrophobic clathrasils are filled with neutral organic species[16].

A guest species that is an especially good fit to the zeolite void phase is referred to as a template[12]. A template can be charged or neutral or an ionic pair. A test of a true template is that quite small changes in its structure should render it ineffective. Moretti *et al.*,[17] have reported a wide variety of neutral and ionic organic diamines and structures claimed to be produced as a result of these templates. The template sensitivity has been described by many authors[18-20]. The role of templates like tetraalkyl ammonium hydroxides may be to:

- act as donors of hydroxyl ions
- increase the solubility of aluminate and silicate ions
- organize the water molecules
- stabilize some structures
- balancing the framework charge
- effect the yield of the final product, and
- change the morphology

Although the organic cation has the primary structure directing role, secondary effects due to the presence of the inorganic cations cannot be completely excluded[21].

1.3. ISOMORPHOUS SUBSTITUTION

One of the greatest advantages of the zeolite molecular sieves is that the framework T-atom can be substituted by other bi, tri, tetra and pentavalent metal ions like Be, Ga, Fe, B, Cr, Ti, Zr, Sn, Ge, V and P. These materials are drawing increasing attention as catalysts with potentially unique properties.

Barrer[22] classified four types of isomorphous replacements in zeolites.

1. One guest molecule by another
2. One cation by another
3. One element by one of its isotopes
4. One element in tetrahedral position by another.

The first one is not important in catalytic applications. The second is useful in making bifunctional catalysts. The third one is useful in characterizing the zeolite materials. The last one is very important in substituting different elements into the zeolite framework. The first isomorphous substitution (in the lattice) was reported by Goldsmith, in which Si was replaced by Ge[23].

The modification of zeolites by isomorphous substitution may give new properties, which may lead to interesting catalytic applications. T-elements can occupy one or more of the following positions in the zeolites.

- Framework sites
- Inside the pores or on the external sites as a metal oxide
- Exchange positions
- Defect sites.

The possibility of metal substitution into the zeolite framework has been reviewed in many articles[2,24-29]. Pauling's theory[30] predicts the possibility of isomorphous substitution and the stability of that particular metal ion in the zeolite tetrahedral framework. According to the Pauling criterion, ρ ($\rho = r_c/r_o$, where r_o is the radius of oxygen and r_c is the cation radius), the metal ion is stable in the **tetrahedral** framework when it is in the range $0.414 > \rho > 0.225$. Values of Pauling criteria for some metal ions have been given in Table 1.1.

Table 1.1: Values of Pauling criterion for various elements[45].

Critical Values (ρ_{cr})	Coordination number at $\rho >$ ρ_{cr}	Corresponding cations
$\rho > 0.732$	8	Pb^{2+}, Sn^{2+}, Ti^{3+}, Eu^{3+}, Nd^{3+}
$0.732 > \rho > 0.414$	6	In^{3+}, Mn^{2+}, Zn^{2+}, Hf^{4+}, Cu^{2+}, Sn^{4+}, Fe^{3+}, Mo^{6+}, Ti^{4+}, Pt^{4+}, Cr^{3+}, Ga^{3+}, Sb^{5+}, V^{4+}
$0.414 > \rho > 0.225$	4	Al^{3+}, Mn^{4+}, Ge^{4+}, V^{5+}, Si^{4+}, Cr^{6+}, P^{5+}, Se^{6+}, Be^{2+}
$0.225 > \rho > 0.147$	3	B^{3+}

According to this, the cations for which ρ is out of this range, the substitution is either impossible or could take place only on a limited scale. Some metal ions like Fe^{3+}, Ti^{4+}, Ga^{3+}, and V^{4+}, which are out of this range have been successfully substituted into the zeolite tetrahedral framework due to their stability in tetrahedral environments. The techniques, which are normally used[31,32] to find out whether the substitution has really occurred or not are given below.

- X-ray diffraction (unit cell parameters)
- IR spectroscopy (shift in the position of hydroxyl bands)
- MAS-NMR spectroscopy
- ESR spectroscopy
- UV-VIS spectroscopy
- Mössbauer spectroscopy
- XPS
- EDX-STEM

- Photoacoustic spectroscopy
- Ion-exchange capacities
- Catalytic properties

Isomorphous substitution can be performed either by direct hydrothermal synthesis or by post-synthesis methods. With the use of organic templating agents, a large number of elements have been incorporated into zeolite framework by hydrothermal synthesis. They include B, Fe, Cr, Co, Ti, Zr, Zn, Be, Hf, Mn, Mg, V and Sn. But, only the metallosilicates containing B, Ga, Fe and Ti have been sufficiently characterized to confirm the incorporation of the metal ions in the framework. Secondary synthesis methods have also been used to incorporate various metal ions like Al, Si, Fe, B, Ga, Ti and Te into the zeolite framework[33-36]. Isomorphous substitution modifies the strength of the Brönsted acid sites. In the case of ZSM-5, the acid strength is found to increase in the order: H-B-ZSM-5 < H-Fe-ZSM-5 < H-Ga-ZSM-5 < H-Al-ZSM-5[37].

In 1982, a new class of molecular sieves, called aluminophosphates (**ALPO**) containing equal moles of Al^{3+} and P^{3+} ions in the lattice have been reported by Wilson *et al.,*[38]. Recently, Davis *et al.,*[39] have reported 18-membered ring large pore molecular sieve, ALPO, designated as VPI-5. Metalaluminophosphate (**MeALPO**) molecular sieves, where a metal ion (Co, Fe, Mg, Zn, Fe, Be, B, Ga, Cr, Ti, V and Mo) has been substituted into the framework of ALPO[24,40] have also been synthesized. The next family of molecular sieves are silicoaluminophosphates (**SAPO's**), where silicon is substituted for aluminium or phosphorous in ALPO framework[41]. SAPO molecular sieves exhibit cation exchange and weak-to-mild acidic catalytic properties. As in the case of ALPO's, SAPO's exhibit excellent thermal and hydrothermal stability.

1.4. THERMAL AND HYDROTHERMAL STABILITIES

The geometry of the crystalline network is a major factor in its thermal stability. In general, thermal stability of a zeolite increases with its silica to alumina ratio[42,43]. The degree of thermal stability can be measured as a function of crystallinity loss by x-ray powder diffraction analysis, changes in surface area, volume, electrical conductivity, infrared spectra and thermal behavior[44]. The most versatile method is x-ray diffraction. XRD patterns can be recorded even at high temperatures upto 1273 K.

When zeolites are exposed to water vapor at elevated temperatures and/or pressures they yield more stable and less porous materials[45]. Studies of hydrothermal stability are of great importance to the regeneration processes used in association with the use of synthetic zeolites as catalysts, molecular sieves and drying agents. Mc Daniel and Maher were the first to report the ultrastable Y zeolite that was more thermally and hydrothermally stable than the typical Y zeolite[46]. The type of conditions used for heat treatment were important[47]. Thermally treating ammonium Y in flowing dry air produced an unstable product, whereas treatment in steam produced a stable product[48]. It has also been reported that calcining ammonium Y in ammonia produced a structurally different and stable product[49].

1.5. ACIDITY AND BASICITY IN ZEOLITES

1.5.1. Acidity

The acidity in zeolites arises mainly from the Brönsted acid sites associated with the framework trivalent metal ion. The treatment of protonic zeolites at high temperature causes the transformation of Brönsted sites into Lewis acid sites. Theoretically, the number of protons are equal to the number of AlO_4^- tetrahedra. Acidity increases with the Al content. Several methods have been developed to determine the number and strength of both types of acid sites[50-52].

- Titration methods.
- Adsorption of bases: Calorimetric measurements.
- Desorption of bases: Temperature Programmed Desorption (TPD).
- IR spectroscopy of OH groups.
- IR spectroscopy of adsorbed bases.
- ^{1}H MAS-NMR of OH groups and ^{13}C, ^{15}N or ^{31}P NMR or respective probes.
- UV-VIS spectroscopy.
- ESR spectroscopy.
- Test Reactions.

1.5.2. Basicity

The application of basic properties of zeolites in catalysis and adsorption has recently been reported by some workers[53-57]. Like acid sites, basic sites may be of the Brönsted or Lewis type. The first one consists of basic OH groups and the second of the framework oxygen atoms. The extent of charge on the oxygen determines their basic strength.

Most of the zeolites contain mainly Lewis basicity. The number of potential basic sites are equal to the number of oxygen atoms in the framework. The framework oxygen atoms are less mobile than the protons. Barthomeuf *et al.*[57], have extensively studied the basicity of zeolites. They have shown that the actual basic strength of a zeolite depends not only on the chemical composition but also on the structural environment of the framework oxygen.

1.6. SHAPE SELECTIVITY IN ZEOLITES

The intracrystalline surface area of zeolites is an inherent part of the crystal structure and hence they are topologically well defined. As a consequence, zeolites are able to restrict or prevent the passage of organic molecules based on size or steric effects. This effect is commonly referred to as **shape selectivity**. Shape selectivity of zeolites is the basis of many important industrial processes. The basic concepts of shape selectivity have been discussed in detail[58-61]. Recently, Chen[62] summarized the impact of shape selective zeolite catalysis on the petroleum and petrochemical industry. Various types of shape selectivities observed in zeolites are:

- Reactant Shape Selectivity[63]
- Product Shape Selectivity[64]
- Restricted Transition State Shape Selectivity[65]
- Molecular Traffic Control[66].

The effective pore size of zeolites can be determined by the sorption of hydrocarbons with increasing kinetic diameter. However, the differences in the crystal size and shape and the presence of meso pores can cause distinct differences. So, the following methods based on model reactions have been applied to determine the extent of shape selectivity quantitatively.

- Constraint Index[67]
- Refined Constraint Index[68]
- Spacious Index[69]
- o-/p- Index in m-xylene Isomerization[70]
- DEB distribution in EB disproportionation[71].

1.7. CATALYTIC PROPERTIES

Zeolites have advantages over conventional heterogeneous catalysts in many applications, involving acid, acid-base, base, oxidation, reduction and polyfunctional catalysis. The main features of zeolites and molecular sieves, which make them very attractive as catalysts and adsorbents are:

- Higher stabilities (thermal, hydrothermal and chemical).
- Well defined micropore systems and shape-selectivities.
- Easy preparation of bi-functional catalysts.
- Isomorphous substitution of the framework ions.
- Ease of regeneration to the initial activity.
- Non-corrosive nature.
- Ion-exchange properties.

Though zeolites have definite advantages, they have some disadvantages too. This has recently been reviewed by Perot and Guisnet[72]. The major disadvantages are the deactivation by irreversible adsorption of secondary products and the restriction of pore size to the bulkier molecules.

1.7.1. ACTIVE SITES

The activity of zeolites in acid catalyzed reactions originates from the tetrahedral framework aluminium atoms. They possess both Brönsted and Lewis acid sites. Silicalites do not have acidity. When Al is substituted by some other trivalent metal ion like B, Ga or Fe, the number of acid sites remain the same, but there may be a difference in the strength. However, when Al is replaced by a tetravalent ion (like Ti), the resultant molecular sieves do not show strong acidity[73]. However the replacement of Al by V provides both an oxidation site and an acid site[74,75] (see Fig.1.1).

1.7.2. COMMERCIAL CATALYTIC APPLICATIONS OF ZEOLITES

Zeolites are mainly used as cation exchangers, selective adsorbents and as catalysts. The largest catalytic application is catalytic cracking. The combination of acidity and shape selectivity, the feasibility of tailoring the number and strength of acid centers, isomorphous substitution and doping with metals provide good opportunity to use these catalysts in many industrial processes[76-79]. Some major commercial processes utilizing zeolite catalysts are reported in Table 1.2.

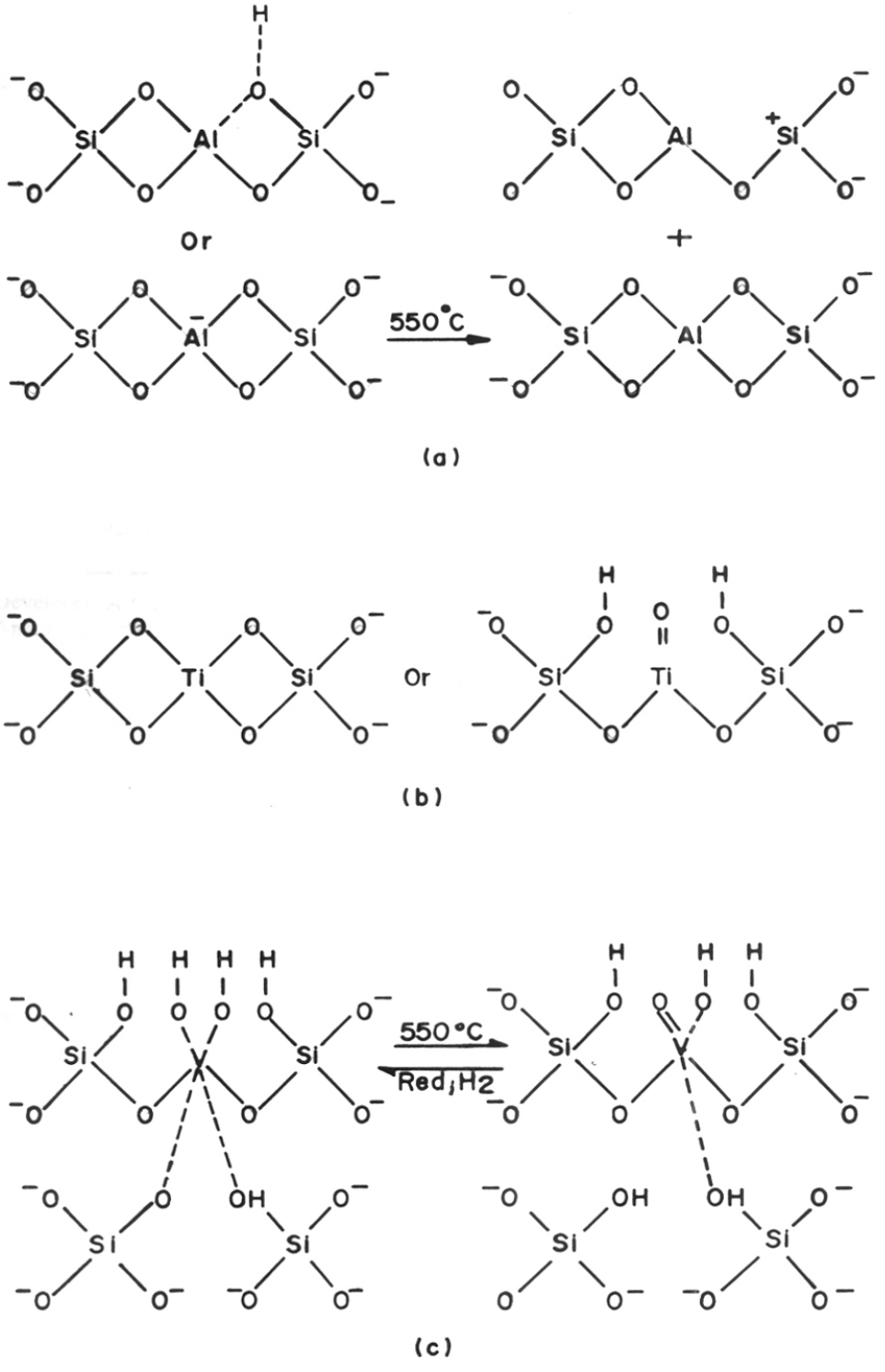

Fig.1.1. **Various types of active sites in zeolites.**
(a): aluminosilicates; (b): titaniumsilicates and (c): vanadiumsilicates.

Table 1.2. Commercial Processes Based on Zeolites[131].

Name of the Process	Purpose
Selecto forming	Octane Boosting
M-forming	-do-
Catalytic cracking	-do-
MDDW	Distillate Dewaxing
MLDW	Lube Dewaxing
M2-forming, Cyclar	Gas to Aromatics
MOGD	Light Olefins to Gasoline and Distillate
MTG	Methanol to Gasoline
MTO	Methanol to Light Olefins
MVPI, MLPI, MHTI	Xylene Isomerization
MTDP	Toluene Disproportionation
MEB, ALBENE*	Ethylbenzene Synthesis
Para-selective reactions	p-xylene Synthesis
	p-ethyltoluene Synthesis

*: Developed at National Chemical Laboratory, Pune and in commercial operation. (cf. NCL Annual Report 1989-90).

1.7.3. ORGANIC REACTIONS

Development of catalytic processes involving zeolites has focussed primarily on hydrocarbon transformations. Less priority has been given to catalytic transformations involving organic reactants that contain O, N and S, in which hetero atoms are retained in the products. The limited use of zeolites in the manufacture of organic fine chemicals is that many organic molecules are too bulky to enter into the zeolite channels. The application of zeolites in organic reactions has been comprehensively reviewed by many authors[80-86]. Some of the reactions are discussed in the following sections.

A. Condensation reactions

The condensation of aldehydes and ketones over zeolites has been studied extensively[87-93]. The base or acid catalyzed aldol condensation is a classical dehydration reaction of carbonyl compounds Condensation of acetone with H_2 at 353 K over Pd-ZSM-5 yields methyl isobutyl ketone[87]. Formaldehyde and isobutylene can be condensed to isoprene[88]. Subsequent condensations to a substituted dioxane have been reported with shape-selective zeolites like ZSM-5 and ZSM-11[89]. Iron containing ZSM-5 converts acetone selectively into 2,4-dimethyl phenol[90]. Isopulegol or citrenellol can be synthesized from citrenellal and isopropanol according to Meerwin-Pondorf-Verley reduction[91]. N-containing heterocycles can also be synthesized in the presence of NH_3[92,93].

Cyclic ethers and lactones react with ammonia and give cyclic imines or lactams[94]. Butyrolactone is converted to 2-pyrrolidine over Cu-Y zeolite[95].

B. Isomerizations and rearrangements

ZSM-5 has been reported to catalyze the isomerization of cresols, chloro toluenes, toluenitriles and toluidines[96]. The isomerization of aniline to 2-methylpyridine[97], 1,3-phenylenediamine to 4- and 6-amino-2-methylpyridine[98], olefins[85] and carbonyl compounds and derivatives[99] has been reported. Rearrangement of tetrahydrocyclopentadiene to adamantane[100], paraffins and olefins[85], 1,2-diols to carbonyl compounds (Pinacolone rearrangement), dihydro-5-(hydroxymethyl)-2-furanones to 3,4-dihydro-2-pyrones[85] (Wagner-Meerwin rearrangement) and epoxides to aldehydes[101,102] have also been reported over many zeolite catalysts. Isomerization of 1,3-dioxanes to 3-alkoxy propionaldehydes is also reported. The Beckmann rearrangement of cyclohexanone oxime to ε-caprolactam is catalyzed by X and Y zeolites[103]. The rearrangement of different aldoximes and ketoximes has also been reported[103,104].

C. Aromatic substitutions

Zeolite catalyzed alkylation of benzene, benzene derivatives and naphthalene have been studied extensively. The alkylating agent can be either alcohol or olefin. Alkylation reactions with longer chain alkenes or alcohols are carried out in the liquid phase to avoid the cracking of long chain alkenes and alcohols at high temperatures[105]. Para-alkylphenols can be prepared by alkylation of phenols with shape-selective zeolites[106]. Anilines also can be alkylated both in the liquid phase and in the gas phase[85]. The selectivity for toluidines is poor.

Zeolite-catalyzed Friedel-Craft's aromatic acylation reactions have also been reported[107]. Halogenation[108] and nitration[109] reactions have been studied in the gas and liquid phases over different zeolites in order to avoid corrosion and disposal problems. Hetero aromatic compounds also can be alkylated/acylated over zeolites[82]. Very high selectivities are obtained.

Aromatic hydroxylation of aromatic compounds has been reported to be catalyzed by ZSM-5[110], TS-1[73] and TS-2[111] using hydrogen peroxide as an oxidizing agent. TS-1, the Ti-analog of ZSM-5 catalyzes the direct hydroxylation of various aromatic compounds like benzene, toluene, ethylbenzene, phenol, cresol and anisole.

D. Aliphatic substitutions

Like the electrophillic substitutions in aromatic compounds, nucleophillic substitutions have also been studied in aliphatic compounds over many zeolite molecular sieves. Zeolites

containing alkali, alkaline earth or rare earth ions demonstrate very high selectivity for dimethyl amine from a mixture of methanol and ammonia[112,113]. Olefins also can be aminated to produce amines over zeolites[114]. Primary amines are relatively less active. Alcohols react with H_2S to give thiols[115]. The selectivities are better over zeolites compared to the conventional heterogeneous catalysts.

E. Oxidation reactions

The catalytic properties of zeolites in selective oxidation reactions have been reviewed by Tagiev[84]. Titaniumsilicate molecular sieves TS-1 and TS-2 have been reported to catalyze various oxidation reactions[73,116] like i) the hydroxylation of aromatic compounds, ii) epoxidation of olefins, iii) conversion of primary and secondary alcohols to aldehydes and ketones, iv) ammoximation of carbonyl compounds and v) sulfoxidation of thioethers. The advantage of titaniumsilicate molecular sieve catalysts compared to the conventional catalysts is that it is possible to use dilute aqueous hydrogen peroxide solution as the oxidant. The oxidation of various paraffins has also been reported[73,117]. A recent report[118] mentions that Pd and Fe containing zeolites catalyze the oxidation of paraffins with oxygen under mild conditions.

Lower olefins oxidize to carbonyl compounds in the gas phase over Pd/Cu-Y zeolites[119]. Zeolites doped with V, P or Zn catalyze the oxidation of C_4-C_{10} hydrocarbons to maleic anhydride[120].

F. Cyclizations

Diels-Alder cyclization reactions have been reported to be catalyzed by zeolites. The cyclodimerization of butadiene to vinyl cyclohexene has been carried out very selectively over Cu^IY[121]. Another example is the reaction of furan and methyl vinyl ketone over Cu^IY. Very low amounts of polymeric products are obtained over zeolites compared to the conventional catalysts.

1.8. MFI and MEL TYPE ZEOLITES

Mobil Research and Development Corporation has synthesized a variety of zeolites, denoted as ZSM, using organic cations. The members of this family are zeolites ZSM-4, -5, -8, -10, -11, -12, -18, -20, -21, -23, -34, -35, -38. This series may be divided into two impor-

tant families. The ZSM-5 family, which includes ZSM-11 and ZSM-8 and possessing unusual hydrophobic properties[122]. The second family includes ZSM-21, ZSM-35 and ZSM-38. These may be considered as synthetic ferrierite type zeolites.

ZSM-5 (MFI) and ZSM-11 (MEL) are remarkably stable as acidic catalysts. Unlike other zeolites, they have pores of uniform dimension and have no large supercages with smaller size windows. The absence of cavities, high silica-to-alumina ratios and the geometrical constraint imposed by the 10-membered ring pores are believed to contribute to their low coking tendencies[123-126]. This "non-aging" feature is one of the major reasons for the successful industrial application of these zeolites. ZSM-5 and ZSM-11 are commercially important shape-selective highly siliceous zeolite catalysts[59,127-130].

ZSM-5[131] and ZSM-11[132] are structurally extreme members of the pentasil family. The term pentasil was defined by Kokatailo and Meier[133] as a family of zeolites, whose frameworks are all formed by linking chains of 5-membered ring secondary building units. Pure siliceous analogs *viz.*, silicalite-1[134] and silicalite-2[135] have been reported for ZSM-5 and ZSM-11, respectively.

ZSM-5 has been synthesized with a variety of templates[16]. It has been synthesized even in the absence of a template[136]. However, compared to ZSM-5, a much smaller number of organics can be used as structure directing agents in the synthesis of ZSM-11[137,138]. The following templates have been used for the synthesis of ZSM-11.

- Benzyltriphenyl phosphonium (BTPhP) chloride
- Benzyltrimethyl ammonium (BTMA) hydroxide
- Tetrabutyl phosphonium (TBP) chloride
- Tetrabutyl ammonium (TBA) chloride
- Tetrabutyl ammonium (TBA) bromide
- **Tetrabutyl ammonium (TBA) hydroxide**
- 1,7-Diaminoheptane
- 1,8-Diaminooctane
- 1,9-Diaminononane
- 1,10-Diaminodecane
- Tripropyl amine.

Recently, Plank *et al.*[139] claimed the synthesis of ZSM-11 in the absence of a template. Chu[140] and Moretti *et al.*,[17] indicated that TBA and TBP ions are necessary as templates for the synthesis of ZSM-11. Tetraalkyl ammonium cations with alkyl groups bulkier than butyl such as pentyl, hexyl and heptyl groups yield exclusively ZSM-5[141]. The addition of TEA or TPA to TBA also yields ZSM-5[17]. ZSM-11 can be synthesized in the presence of NH_4^+-cation

without any alkali metal ion[135]. Valvocsik and Rollmann[18] have studied the effect of the chain length of the diamine used as template on the nature of the zeolite obtained. ZSM-11 was obtained only with 1,8-diaminooctane and 1,9-diaminononane. All other diamines gave ZSM-5 as a major product.

BTMA is an efficient template when the Al content in the gel is high[137]. TBA, TBP, BTPhP and 1,8-Diaminooctane are reported to be true templating agents, whereas BTMA is a pore filling template.

1.8.1. Crystallographic structure of ZSM-11 (MEL) and ZSM-5 (MFI)

Kokatailo *et al.*[132] have investigated the structure of ZSM-11 zeolite. The crystallographic data of ZSM-11 in comparison with ZSM-5 is summarized in Table 1.3.

Table 1.3: Comparison of Crystallographic Data of MFI and MEL Zeolites[3,131,132].

Crystallographic Parameters	MFI	MEL
Secondary Building units	Complex 5-1	Complex 5-1
Framework density (No. of T-atoms per 1000 (Å)^3	17.9 (Si + Al)	17.6 (Si + Al)
Channels	10-membered ring, intersecting	10-membered ring, intersecting
Fault planes	[100]	[100]
No. of T-atoms (Si+Al) per unit cell	96	96
No. of nonequivalent T-atoms	12	7
Unit cell composition	$Na_n Al_{nSi}96\text{-}nO_{192}\ 16H_2O$ (with n < 27 and typically about 3	$Na_n Al_{nSi}96\text{-}nO_{192}\ 16H_2O$ (with n < 16 and typically about 3)
Crystal symmetry/ Space group symmetry	Orthorhombic/P_{nma}	Tetragonal/$1\bar{4}m2$
Unit cell dimensions	a = 20.1 Å; b = 19.9 Å; c = 13.4 Å	a = b = 20.1 Å; c = 13.4 Å

The pure silica analog of MEL was also reported by Bibby *et al.*[135]. The framework topology of ZSM-11 was derived from modelling and distance least squares (DLS) refinement[142]. The simulated x-ray powder diffraction pattern was similar to that of the experimental pattern of H-ZSM-11. The powder diffraction patterns of ZSM-5 and ZSM-11 are given in Fig.1.2. The peaks at 9.06, 13.9, 15.5, 16.5, 20.8, 21.7, 24.4, 26.6 and 27.0 degrees 2θ are absent in the XRD pattern of ZSM-11. In addition peaks at 8.8, 14.8, 17.6, 23.1, 23.9 and 29.9 degrees 2θ are singlets in the ZSM-11 pattern, and not doublets as in the ZSM-5 pattern. These differences also occur in the XRD pattern of silicalite-1 and silicalite-2. Because of

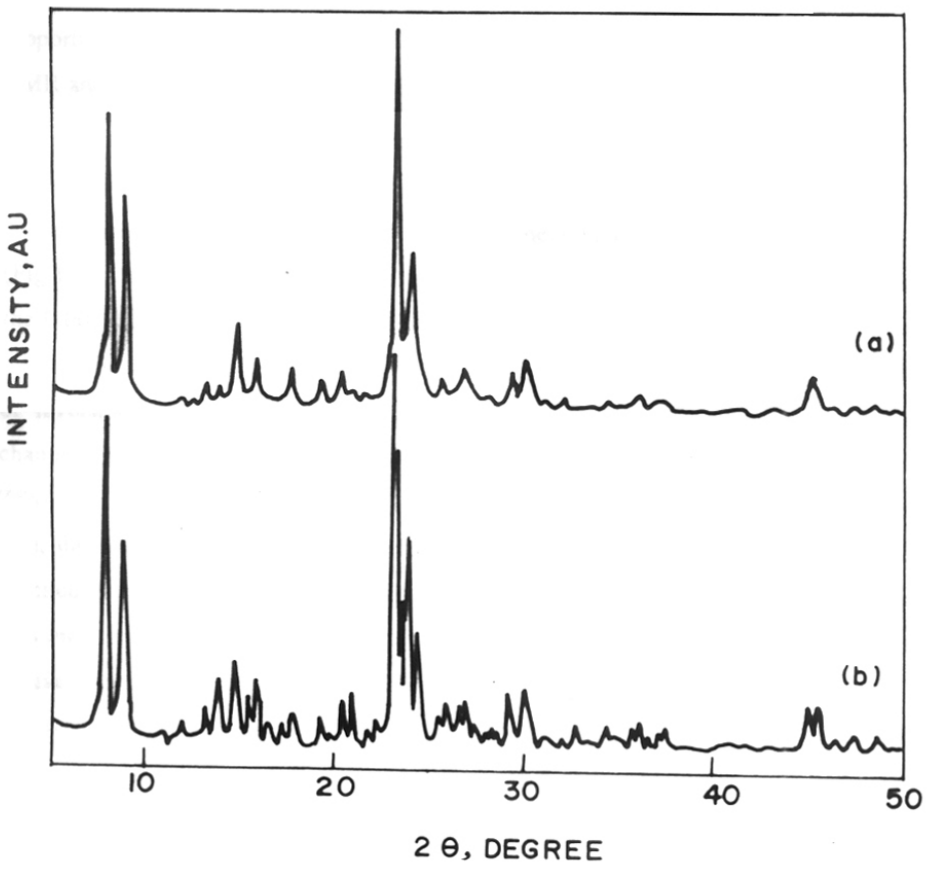

Fig.1.2. X-ray diffraction patterns of Al-MEL (a) and Al-MFI (b) calcined at 823 K.

peak superpositions in ZSM-5 and ZSM-11, it is very difficult to identify the intergrowths quantitatively[137]. The presence of intergrowths of ZSM-5 in ZSM-11 has been detected by various techniques like high resolution electron microscopy[143,144] and x-ray powder diffraction[132]. A good correlation between the x-ray and electron diffraction patterns for the relative amounts of ZSM-11 and ZSM-5 has been observed[145]. The presence of substantial amounts of diffuse scattering in certain regions of the observed pattern indicated the existence of a high proportion of stacking faults in ZSM-11[143,146,147]. Toby *et al.*[148] have used a high resolution NMR and synchrotron x-ray powder diffraction to study the structure of ZSM-11.

In the ZSM-11 and ZSM-5 structure groups, the secondary building units (Fig.1.3 a), made up of 5 membered rings, are joined along [001] to form chains (Fig.1.3 b), which pack laterally along [010]. The ZSM-5 structure is generated when adjacent [100] planes or sheets (Fig.1.3 c) are related to one another by inversion (*i*) and ZSM-11 structure is obtained when the [100] sheets are related to one another by mirror symmetry (σ) (Fig.1.4). Infinite series of intermediate structures may be obtained by applying reflection transformations (σ) to ZSM-5 or inversion transformation (i) to ZSM-11 (Fig.1.4 a). Such transformations lead to the channel systems shown in Fig.1.4 b. This results in two types of intersecting channels in ZSM-5, with 10-membered ring openings, one with an elliptical cross section (0.51 nm X 0.53 nm), the other one being circular (0.55 nm). In the case of ZSM-11, both the channels are identical (0.51 X 0.55 nm). The cavities formed in ZSM-5 by the intersection of these channels are equivalent, having a maximum diameter of 0.9 nm, whereas in ZSM-11 two types of intersections exist, one possessing the same volume as those present in ZSM-5 and the other one with a larger volume (30 % excess). With the crystallograpic data a theoretical channel length per unit cell[149] can be calculated. For ZSM-5 and ZSM-11, its value is 8.8 and 8.0 nm, respectively[149,150]. Another important structural difference between MFI and MEL is the presence of four 4-MR's per unit cell in the former structure and eight 4-MR's per unit cell in the latter.

1.8.2. Comparison of the Properties of MFI and MEL Zeolites

The acidity, sorption, catalytic and shape-selective properties of MEL zeolites have been compared with MFI in the literature[26,28,127-130]. The acidity of H-Y, H-ZSM-5 and H-ZSM-11 zeolites followed the decreasing order[143]. H-ZSM-5 > H-ZSM-11 > H-Y. It has been reported that ZSM-11 has a smaller number of stronger acid sites compared to ZSM-5[26,28,151]. From the IR spectroscopy of hydroxyl groups, it has been found that a large amount

Fig.1.3. Schematic diagram of the pentasil unit (a), SBU (b) and pentasil layer (c). (Ref. 133 b)

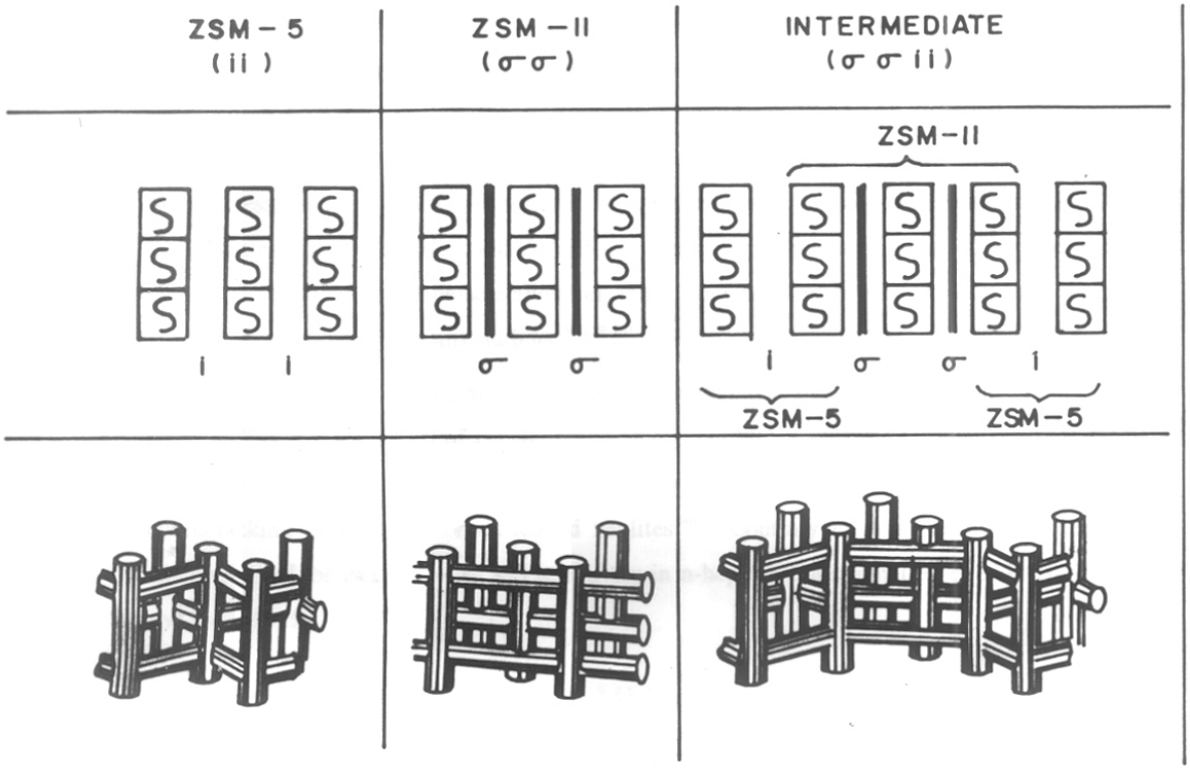

Fig.1.4. **Channel systems in pentasil structures with ii, σ σ and σ σ ii sequences of layers.** (Ref. 133 b)

of terminal silanol groups are present in ZSM-11 samples as compared to ZSM-5[151,152]. Jaifen and Yiwei[153] reported that with an increase in the Si/Al ratio of ZSM-11, its catalytic activity changed only to a small extent and the number of its strong acid sites did not change, though the number of weak acid sites decreased.

Sorption and diffusion properties of ZSM-11 and ZSM-5 have been studied by many investigators[78,150,154,155]. Some authors[78,150,155] reported that the sorption capacity of ZSM-5 is higher than that of ZSM-11. Contradictory results have been obtained by others[154].

ZSM-5 has been reported to exhibit unusual reaction selectivities and catalytic stabilities. ZSM-11 has been shown to exhibit similar catalytic properties like ZSM-5[156-158]. The Constraint Index, the ratio of the relative cracking rate constants of 3-methyl pentane and n-hexane, is found to be almost the same for ZSM-5 and ZSM-11[67] (8.3 and 8.7, respectively). Nevertheless, because of the difference in their channel structure and dimensions of the channel intersections, ZSM-11 and ZSM-5 are expected to show significant difference in their shape-selectivity. The shape-selectivity of these two zeolites in various reactions has been studied systematically by many authors[154,159-161].

The formation of C_9-aromatics is favoured more over ZSM-11 than over ZSM-5[28,152,153,160] in the alkylation of p-xylene with methanol and in methanol conversion. Both the zeolites exhibited significant difference in the product distribution in the isomerization and hydrocracking of n-decane on Pt-loaded zeolites[146]. Contrary to these results, Giannetto *et al.*[162] observed the same activity and selectivity in n-heptane transformation over Pt-H-ZSM-11 and Pt-H-ZSM-5.

1.8.3. Isomorphous substitution in MFI and MEL zeolites

The isomorphous substitution of various bi, tri and tetravalent elements has been successfully achieved in the MFI structure[24,163-167]. Be^{2+} is the only bivalent metal ion substituted into the zeolite framework. Not much work has been done in the case of MEL structure. Ione *et al.*[25,26,168] have done a systematic study of various metal ions in the MEL structure. They have claimed the incorporation of B, Ga and Fe. Ga-MEL has also been synthesized by refluxing silicalite with $Ga(NO_3)_3$ solution[169]. Recently we have also reported the isomorphous substitution of Ga[170], Fe[171] and Ti[111] into the MEL framework. In all these cases significant evidence has been obtained to show that these metal ions are present in the zeolite framework.

1.9. TITANIUMSILICATE MOLECULAR SIEVES

Young[172] claimed the synthesis of the titaniumsilicate molecular sieve, TS-1 (MFI structure) in 1967. But sufficient evidence was not available to show that the Ti was present in the lattice. After about 20 years, Taramasso *et al.*[167] claimed the synthesis of TS-1. In 1986, Perego *et al.*[73] published their results on the synthesis, characterization and catalytic properties of TS-1. In the following years several publications appeared on the possibility of synthesis of various titaniumsilicates using different procedures including secondary synthesis methods and in the fluoride media. Though work on titaniumsilicates started only 6 years back, the systematic characterization and the numerous studies of these materials when compared to other metallosilicates show the potential usefulness of these molecular sieves.

The Pauling criterion, ρ for Ti is equal to 0.515, which shows that the substitution of Ti into the tetrahedral framework positions is difficult. TS-1 has been characterized using various techniques like XRD, IR, Raman, ^{29}Si NMR, UV-VIS, ESR, XPS, EXAFS, SEM-EDXL, FABMS and catalytic measurements. All these techniques have demonstrated that Ti^{4+} is isomorphously substituted into the silicalite framework. The catalytic activity of titaniumsilicate molecular sieves in various oxidation reactions has opened up new and interesting prospects in industrial shape-selective catalysis.

It has been shown that Ti is uniformly distributed in the crystal; each Ti is tetrahedrally coordinated to four -O-Si units. This type of distribution has been reported to be responsible for their activity in various oxidation reactions. Notari[173] has suggested the existence of "Restricted Transition State Shape Selectivity" in TS-1 in the hydroxylation of aromatic compounds, as the amount of tar formed was less on TS-1 compared to amorphous SiO_2-TiO_2. A great advantage of using titaniumsilicates in these reactions is that dilute hydrogen peroxide solution can be used as an oxidant.

1.10. OBJECTIVE OF THE THESIS

The catalytic activity of TS-1 in i) the hydroxylation of aromatic compounds ii) the epoxidation of olefins, iii) the ammoximation of cyclohexanone iv) the oxyfunctionalization of alkanes and v) the conversion of primary and secondary alcohols to aldehydes and ketones, respectively, has opened a new era in the production of organic fine chemicals. The hydroxylation of phenol to catechol and hydroquinone has already been commercialized by ENICHEM,

Italy. Though the synthesis of other titaniumsilicate molecular sieves has also been reported using different procedures, experimental proof for the presence of Ti in the framework is not available.

The main objective of this thesis is to study the synthesis, characterization and catalytic activity of titaniumsilicate analogs with MEL structure in detail. The results obtained in the synthesis, characterization and catalytic properties of TS-2 are reported in Chapter III. To-date, TS-1 and TS-2 are the only titaniumsilicate molecular sieves, for which evidence for the presence of Ti in the framework has been reported.

Detailed studies on the isomorphous substitution of Fe and Ga into the MEL lattice are not available. These studies are also being reported. The synthesis of MEL structures without any impurity of MFI structure is usually difficult. Studies on the effect of various parameters on the phase purity of MEL during its synthesis have been carried out. The crystallization rates of Al-, Ga- and Fe-MEL have also been studied. The p-/o- ratio in xylenes has been reported to be dependent on the structure of zeolites. We have investigated the influence of isomorphous substitution on the p-/o- ratio in m-xylene isomerization and deactivation rates in ethylbenzene disproportionation reactions. These results are reported in Chapter IV.

Further, the simultaneous incorporation of Ti and Al or Ga or Fe into the MEL framework is expected to produce zeolites with interesting properties, as these metallo-titanium-silicates will have dual catalytic functions *viz.,* acid centers and redox sites. Chapter V reports the synthesis, characterization and the catalytic properties of metallo-titanium-silicates in both acid catalyzed and oxidation reactions.

1.11. REFFERENCES

1. Breck, D.W., in "Zeolite Molecular Sieves", Wiley Pub., New York, 1974.
2. Barrer, R.M., In "Hydrothermal Chemistry of Zeolites", Academic Press, New York, 1982.
3. Meier, W.M. and Olson, D.H., in "Atlas of Zeolite Structure Types" (2nd Ed. 1987), Butterworths, London.
4. Bragg, W.L., in "The Atomic Structure of Minerals", Cornell University Press, Ithaca, New York (1937).
5. Meier, W.M., in "Molecular Sieves", Soc. Chem. Ind., London, 1968, p.10.
6. Sand, L.B., *Ecom. Geol.*, (1967) 191.
7. Flanigen, E.M., in "Proc. Of the 5th Int. Zeolite Conf." Ed. L.V.C. Rees, Heydon, London, 1980, p.760.
8. Barrer, R.M., *Pure and Appl. Chem.*, **51** (1979) 1091.
9. Glasser, L.S.D. and Lachowski, E.E., *J. Chem. Soc., Dalton Trans.*, (1980) 399.
10. Lowe, B.M., *Stud. Surf. Sci. Catal.*, **37** (1988) 1.
11. Mostowicz, R. and Sand, L.B., *Zeolites*, **2** (1982) 143.
12. Flanigen, E.M., *ACS Symp. Ser.*, **121** (1973) 119.
13. Sand, L.B., in "Proc. 5th Int. Conf. Zeolites", Ed. L.V.C. Rees, Heyden, London, 1980, p.1.
14. Barrer, R.M., in "Zeolites", *Stud. Surf. Sci. Catal.*, **24** (1985) 1.
15. Sand, L.B., *Pure and Appl. Chem.* **52** (1980) 2105.
16. Lok, B.M., Cannan, T.R. and Messina, C.A., *Zeolites*, **3** (1983) 282.
17. Moretti, E., Contesa, S. and Padovan, M., *Chim. Ind.*, **67** (1985) 21.
18. Valyocsik, E.W. and Rollmann, L.D., *Zeolites*, **5** (1985) 123.
19. Nan der Gaag, F.J., Jansen, J.C. and van Bekkum, H., *Appl. Catal.*, **17** (1985) 261.
20. Casci, J.L., *Stud. Surf. Sci. Catal.*, **28** (1986) 215.
21. Barrer, R.M. and Sieber, W., *J. Chem. Soc., Dalton Trans.*, (1977) 1020.
22. Ref.2, Chap.6.
23. Goldsmith, J.R., *Min. Mag.*, **29** (1952) 952.
24. Ref.24, p.205.
25. Ione, K.G. and Vostrikova, L.A., *Russ. Chem. Rev.*, **56(3)** (1987) 231.
26. Ione, K.G., Vostrikova, L.A. and Mastikhin, V.M., *J. Mol. Catal.*, **31** (1985) 355.
27. Taramasso, G., Perego, G. and Notari, B., in "Proc. 5th Int. Zeolite Conf.", Napoli, Ed. L.V.C. Rees, Heydon, London, 1980, p.40.
28. Tielen, M., Geelen, M. and Jacobs, P.A., *Acta. Phys. Chem.*, **31** (1985) 1.
29. Xuren, X. and Wenqin, P., *Stud. Surf. Sci. Catal.*, **24** (1985) 27.
30. Pauling, L., in "The Nature of Chemical Bond", Goskhimizdat, Moscow, 1947.

31. Ben Taarit, Y., in "Zeeolite Microporous Solids: Synthesis, Structure, and Reactivity", Eds. E.G. Derouane *et al.*, NATO ASI Series, Kluwer Academic Publishers, 1991, p.291.

32. Vedrine, J.C., in "Guidlines for Mastering the Properties of Molecular Sieves", Eds. D. Barthomeuf *et al.*, NATO ASI Series, Series B: Physics Vol.221, Plenum, 1990, p.121.

33. Hamden, H. and Klinowski, J., *ACS Symp. Ser.*, **398** (1988) 329.

34. Yashima, J., Yamagishi, K., Namba, S. and Asaoka, S., *Stud. Surf. Sci. Catal.*, **37** (1988) 175.

35. Endoh, A., Nishimiya, K., Tsutsumi, K. and Takaishi, T., *Stud. Surf. Sci. Catal.*, **46** (1989) 779.

36. Kraushaar, B. and van Hoof, J.H.C., *Catal. Lett.*, **1** (1988) 81.

37. Ref. 24, p.240.

38. Wilson, S.T., Lok, B.M., Messina, C.A., Cannan, T.R. and Flanigen, E.M., *J. Am. Chem. Soc.*, **104** (1982) 1146.

39. Davis, M.E., Saldarriage, C., Montes, C., Graces, J. and Crowder, C., *Nature*, **331** (1988) 968.

40. Wilson, S.T. and Flanigen, E.M., *ACS Symp. Ser.*, **298** (1988) 329.

41. Lok, B.M., Messina, C.A., Patton, R.L., Gajek, R.L., Cannan, T.R. and Flanigen, E.M., U.S. Pat., 4, 440, 871 (1984).

42. Rabo, J.A., in "Zeolite Chemistry and Catalysis", Ed. F.M. Beringer, Am. Chem. Soc., Washington, D.C., 1976, p.285.

43. Bremer, H., Morke, W., Schodel, R. and Vogt, F., *Adv. Chem. Ser.*, **121** (1973) 249.

44. Barrer, R.M. and Langley, D.M., *J. Chem. Soc.*, (1958) 3804.

45. Dyer, A., in "An Introduction to Zeolite Molecular Sieves", John Wiley & Sons. Ltd., 1988, p.113.

46. Mc Daniel, C.V. and Maher, P.K., in "Molecular Sieves", Soc. Chem. Ind., London (1967) 186.

47. Kerr, G.T., *Adv. Chem. Ser.*, **121** (1973) 219.

48. Ward, J.W., *J. Catal.*, **27** (1972) 157.

49. Kerr, G.T. and Shipman, G.F., *J. Phys. Chem.*, **72** (1968) 3071.

50. van Hoof, J.H.C. and Roelofsen, J.W., *Stud. Surf. Sci. Catal.*, **58** (1991) 242.

51. Karge, H.G., *Stud. Surf. Sci. Catal.*, **65** (1991) 133.

52. Jacobs, P.A., in "Carboniogenic Activity of Zeolites", Elsevier, Amsterdam, 1977, p.33.

53. Sideronko, Y.N., Galich, P.N., Gutyrya, V.S., Il in, V.G. and Neimark, I.E., *Dokl. Akad. Nauk.*, SSSR, **173** (1967) 132.

54. Yashima, T., Sato, K., Hayasaka, T. and Hara, N., *J. Catal.*, **26** (1972) 303.

55. Ono, Y., *Stud. Surf. Sci. Catal.*, **5** (1980) 19.

56. Unland, M.L. and Barker, G.E., in "Catalysis of Organic Reactions", Ed. W.R. Moser, Chem. Ind. Ser. 5, Marcel Dekker Inc., New York, 1981, p.51.

57. Barthomeuf, D., *Stud. Surf. Sci. Catal.,* **65** (1991) 157 and references cited therein.

58. Chen, N.Y. and Weisz, P.B., *Chem. Eng. Progr.*, Symp. Ser., **63** (1967) 86.

59. Csicsery, S.M., *ACS Monogr.*, **171** (1976) 680.

60. Derouane, E.G., in "Interrelation Chemistry", Eds. M.S. Whittingham and A.J. Jacobson, Academic Press, New York, 1982, p.101.

61. Venuto, P.B., *Adv. Chem. Ser.* **102** (1971) 260.

62. Chen, N.Y in "Shape Selective Catalysts in Industrial Applications", Eds. W.E. Garwood and F.G. Dwyer, Marcel Dekker, Inc., New York, 1989.

63. Chen, N.Y. and Garwood, W.E., *Catal. Rev. Sci. Eng.,* **28** (1986) 1.

64. Weisz, P.B., *Stud. Surf. Sci. Catal.,* **7A** (1981) 3.

65. Csicsery, S.M., *J. Catal.,* **23** (1971) 124.

66. Derouane E.G. and Gabelica, Z., *J. Catal.,* **65** (1980) 486.

67. Frillette, V.J., Haag, W.O. and Lego, R.M., *J. Catal.,* **67** (1981) 218.

68. Martens, J.A., Tielon, M., Jacobs, P.A. and Weitkamp, J., *Zeolites,* **4** (1984) 98.

69. Wietkamp, J., Ernst, S. and Kartge, H.G., *Erdol Kohle-Erdgas-Petrochem.,* **37** (1984) 457.

70. Dewing, J.J., *J. Mol. Catal.,* **61** (1990) 173.

71. Weitkamp, J., Ernst, S., Jacobs, P.A. and Karge, H.G., *Erdoel Khole-Erdgas-Petrochem.,* **39** (1984) 13.

72. Perot, G. and Guisnet, M., *J. Mol. Catal.*, **61** (1990) 173.

73. Perego, G., Bellussi, G., Corno, C., Taramasso, M., Buonomo, F., and Esposito, A., Stud. Surf. Sci. Catal., **28** (1986) 129.

74. Riggutto, M.S. and van Bekkum, H., *Appl. Catal.,* **68** (1991) L1.

75. Rao, P.R.H.P. and Ramaswamy, A.V., *J. Catal.,* (Accepted)

76. Heinemam, H., *Catal. Rev. Sci. Eng.,* **23** (1981) 315.

77. Wiesz, P.B., Frilette, V.I. and Golden, R.L., *J. Catal.,* **1** (1962) 301.

78. Wu, E.L., Landolt, G.R. and Chester, A.W., *Stud. Surf. Sci. Catal.,* **28** (1986) 547.

79. Chen, N.Y., in "Industrial Applications of Shape Selective Catalysts", Ed. J.W. Ward, Elsevier, Amsterdam, 1987.

80. Van Bekkum, H. and Kouwenhoven, H.W., *Stud. Surf. Sci. Catal.,* **41** (1988) 45.

81. Isakov, Y.I. and Minachev, U.M., *Russ. Chem. Rev.,* **51** (1982) 1188.

82. Maxwell, I.E., *Adv. Catal.,* **31** (1982) 2.

83. Tobias, M.A., U.S. Pat., 3, 728, 408, (1973) assigned to Mobil Oil Corp.

84. Tagiev, D.B. and Minachev, Kh.M., *Russ. Chem. Rev.,* **50** (1981) 1009.

85. Hölderich, W.F., Hesse, M. and Näumann, F., *Angew. Chem. Int. Ed. (Engl.),* **27** (1988) 226.

86. Hölderich, W.F. and Van Bekkum, H., *Stud. Surf. Sci. Catal.,* **58** (1991) 631.

87. Huang, T.J. and Haag, W.O., U.S. Pat., 4,339,606 (1982); EP 112 821 (1986).

88. Weissermel, K. and Arpe, H.J., *Industrielle Organishe Chemie*, Verlag Chemie, Weinheim (1978) p.108.

89. Chang, C.D., Lang, W.H. and Morgan, N., EP 13 600 (1980).

90. Servotte, Y and Jacobs, J. and Jacobs, P.A., in "Proc. ZEOCAT Symp., Siofok (Hungary) 1985, *Acta Phys. Chem (Szeged)* 1985, p.1.

91. Shabtai, J., Lazar, R. and Biron, E., *J. Mol. Catal.*, **27** (1984) 35.

92. van Bekkum, H. and Kouwenhoven, H.W., *Recl. Trav. Chim. Phy. Bas.*, **108** (1989) 283.

93. Chang, C.D. and Lang, W.H., U.S. Pat., 4,220,783 (1979).

94. Venuto, P.B. and Landis, P.S., *Adv. Catal.*, **18** (1968) 259.

95. Hatada, K., Shimada, M., Ono, Y. and Keli, T., *J. Catal.*, **37** (1975) 166.

96. Weigert, F.J., *J. Org. Chem.*, **52** (1987) 3296.

97. Chang, C.D. and Perkins, P.D., *Zeolites*, **3** (1983) 298.

98. Le Blanc, H. and Puppe, L., Ger, Offen. D.E 3, 332,687 (1985).

99. Hölderich, W.F., *Pure & Appl. Chem.*, **58** (1986) 1838.

100. Honna, K., Sugimoto, M., Shimizu, N. and Kurisaki, K., *Chem. Lett.*, (1986) 315.

101. Neri, C. and Buonomo, F. EP. 100 117 (1983), Enichem Anic., S.p.A.

102. Aomura K., Nitta, M. and Matsumoto, S., *Kogakubu Kenkyu Hokoku (Hokaido Daigaku)* **67** (1973) 171.

103. Landis, P.S. and Venuto, P.B., *J. Catal.*, **6** (1966) 245.

104. Olson, K.D., EP. 251 168 (1988).

105. Burress, G.T., EP 12 514 (1980).

106. Wu, M.M., U.S. Pat., 4,391,998 (1983).

107. Gauthier, C., Chiche, B., Finiels, A. and Geneste, P., *J. Mol. Catal.*, **50** (1989) 219.

108. Mortel, T.M., Oudijn, D., Vleugel, C.J., Roelofsen, D.P. and Van Bekkum, H., *J. Catal.*, **60** (1979) 110.

109. Schumacher, J. and Wang, K., EP 53 031 (1982); EP 78 247 (1983); U.S. Pat., 4,107,220 (1978).

110. Chang, C.D. and Hellring, S.D., U.S. Pat., 4,578,521 (1986).

111. Reddy, J.S., Kumar, R. and Ratnasamy, P., *Appl. Catal.*, **58** (1990) L1.

112. Tompsett, A.J., EP 76 034 (1982).

113. Mochida, I., Yasutake, A., Fujitsu, H. and Takeshita K., *J. Catal.*, **82** (1983) 313.

114. Fales, H.S. and Peterson, J.O.H., EP 39 918 (198) assigned to Air Products.

115. Ziólek, M. and Bresinska, I., *Zeolites*, **5** (1985) 245.

116. Reddy, J.S. and Sivasanker, S., *Ind. J. Technol.*,

117. Parton, R.F., Jacobs, J.M., Huybrechts, R.R. and Jacobs, P.A., *Stud. Surf. Sci. Catal.*, **46** (1989) 163.

118. *Chem. Eng. News* 28.09.1987, p.27, Report on Work of C.A. Tolman.

119. Ball, W.J. and Stewart, D.G., U.S. Pat., 4,376,104 (1980).

120. Moorehead, E.L., U.S. Pat., 4,604,370 (1986).

121. Maxwell, I.E., Downing, R.S., de Boer, J.J. and van Langen, S.A., *J. Catal.,* **61** (1980) 485.

122. Argauer, R.J. and Landolt, G.R., U.S. Pat., 3,702,886, (1972).

123. Walsh, D.E. and Rollmann, L.D., *J. Catal.,* **56** (1979) 195.

124. Rollmann, L.D. and Walsh, D.E., *J. Catal.,* **56** (1979) 139.

125. Rollmann, L.D. and Walsh, D.E., in "Progress in Catalyst Deactivation", The Hague, 1982, p.81.

126. Derouane, E.G., *Stud. Surf. Sci. Catal.,* **20** (1985) 221.

127. Weisz, P.B., *Pure Appl. Chem.,* **73** (1980) 2091.

128. Olson, D.H., Haag, W.O. and Lago, R.M., *J. Catal.,* **61** (1980) 390.

129. Meisel, S.L., *Philos. Trans. R. Soc. London. Ser. A.*, **300** (1981) 157.

130. Dwyer, F.G., in "Catalysis of Organic Reactions", Ed. W.B. Moser, Marcel Dekker Inc., Ney York, 1981, p.39.

131. Kokatailo, G.T., Lawton, S.L., Olson, D.H. and Meier, W.M., *Nature*, **272** (1978) 437.

132. Kokatailo, G.T., Chu, P., Lawton, S.L. and Meier, W.M., *Nature*, **275** (1978) 119.

133. Kokatailo, G.T. and Meier, W.M., *Chem. Soc.,* Spec. Publ., **33** (1980) 133.

133b. Kokatailo, G.T. and Meier, W.M., "Pentasil Family of High Silica Crystalline Materials", paper presented at the conf. on zeolites, London, April 1979, Proc. of Chem. Soc., London.

134. Flanigen, E.M., Bennett, J.M., Grose, R.W., Cohen, J.P., Patton, R.L., Kirchner, R.M. and Smith, J.V., *Nature,* **271** (1978) 512.

135. Bibby, D.M., Milestone, N.B. and Aldridge, L.P., *Nature*, **280** (1979) 664.

136. Grose, R.W. and Flanigen, E.M., U.S. Pat., 4,257,885 (1981).

137. Jacobs, P.A. and Martens, J.A., *Stud. Surf. Sci. Catal.,* **33** (1987) 147.

138. Occelli, M.L., Ritz, G.P., Iyer, P.S. and Sanders, J.V., *ACS Symp. Ser.*, **368** (1988) 246.

139. Plank, C.J., Rosinski, E.J. and Rubin, M.K., U.S. Pat., 4,999,251 (1991).

140. Chu, P., U.S. Pat., 3,709,979 (1973).

141. Gabelica, Z., Cavez-Bierman, M., Bodart, P., Gourgue, A. and Nagy, J.B., *Stud. Surf. Sci. Catal.,* **24** (1985) 55.

142. Meier, W.M. and Villiger, H., *Z. Kristallogr.,* **129** (1969)) 411.

143. Millward, G.R., Ramdas, S., Thomas, J.M. and Barlow, M.T., *J. Chem. Soc., Faraday Trans.II,* **79** (1983) 1075.

144. Thomas, J.M. and Millward, G.R., *J. Chem. Soc., Chem. Commun.,* (1982) 1381.

145. Jablonski, G.A., Sand, L.B. and Gard, J.A., *Zeolites,* **6** (1986) 396.

146. Perego, G., Cesari, M. and Allegra, G., *J. Appl. Crystallogr.,* **17** (1984) 403.

147. Perego, G., Bellussi, G., Carati, A., Millini, R. and Fattore, V., *ACS Symp. Ser.*, **398** (1989) 360.

148. Toby, B.H., Eddy, M.M., Fyfe, C.A., Kokatailo, G.T., Strobl, H. and Cox, D.E., *J. Mater. Res.*, **3(3)** (1988) 563.

149. Gabelica, Z., Derouane, E.G. and Blom, N., *ACS Symp. Ser.*, **248** (1984) 219.

150. Jacobs, P.A., Beyer, H.K. and Valyon, J., *Zeolites,* **1** (1981) 161.

151. Auroux, A., Dexpert, H., Leclercq, C. and Vedrine, J.C., *Appl. Catal.,* **6** (1983) 95.

152. Datka, J. and Piwowarska, Z., *Zeolites* **8** (1986) 30.

153. Jiafen, H. and Yiwei, J., *Gaoden Xuexiao Huaxne Xuebao,* **7** (1986) 357.

154. Harrison, I.D., Leach, H.F. and Whan, D.A., *Zeolites*, **7** (1987) 21.

155. Ma, Y.H., Tang, T.D., Sand, L.B. and Hou, L.Y., *Stud. Surf. Sci. Catal.,* **28** (1986) 531.

156. Young, L.B., U.S. Pat., 4,082,805.

157. Kaeding, W.W., Wu, M.M., Young, L.B. and Burress, G.T., U.S. Pat., 4,197,413.

158. Kaeding, W.W., U.S. Pat., 4,082, 805.

159. Jacobs, P.A., Martens, J.A., Weitkamp, J. and Beyer, K., *Faraday Disc. Chem. Soc.,* **72** (1982) .

160. Derouane, E.G., Dejaifne, P., Gabelica, Z. and Vedrine, J.C., *Faraday Disc. Chem. Soc.,* **72** (1981) 331.

161. Sosa, R.C., Nitta, M., Deyer, H.K. and Jacobs, P.A., in "Proc. 6th Int. Zeolite Conf." Eds. D.H. Olson and A. Bisio, Reno, USA, 1983, p.508.

162. Giannetto, G., Perot, G. and Guisnet, M., *Stud. Surf. Sci. Catal.,* **24** (1986) 631.

163. Kaliaguine, S., Nagy, J.B. and Gabelica, Z., *Stud. Surf. Sci. Catal.,* **35** (1988) 381.

164. Iton, I.E., Beal, R.B. and Hodul, D.T., *J. Mol. Catal.,* **21** (1983) 151.

165. Hayashi, *Bull. Chem. Soc. Jpn.,* **59** (1982) 52.

166. Dongare, M.K., Singhj, P., Moghe, P.P. and Ratnasamy, P., *Zeolites, 11* (1991) 690.

167. Taramasso, M., Perego, G. and Notari, B., U.S. Pat., 4,410,501 (1983).

168. Ione, K.G., Vostrikova, L.A., Petvova, A.V. and Mastikhin, V.M., *Stud. Surf. Sci. Catal.*, **18** (1984) 151.

169. Xin-Sheng, L. and Thomas, J.M., *J. Chem. Soc., Chem. Commun.,* (1985) 1544.

170. Reddy, J.S., Reddy, K.R. and Kumar, R., in "Proc. 10th Natl. Symp. on Catal. And 4th INDO-USSR Symp. On Catal."Recent Developments in Catalysis, Theory and Practice, Eds. B. Viswanathan *et al.*, Narosa Pub., New Delhi, India, 1989, p.575.

171. Reddy, J.S., Reddy, K.R, Kumar, R. and Ratnasamy, P., *Zeolites*, **11** (1991) 553.

172. Young, D.A., U.S. Pat., 3,329,481 (1967).

173. Notari, B., *Stud. Surf. Sci. Catal.,* **37** (1987) 413.

CHAPTER - II

EXPERIMENTAL

2.1. SYNTHESIS

The reactants used in the synthesis of silicalite-2, TS-2, Al-MEL, Ga-MEL, Fe-MEL, Al-TS-2, Ga-TS-2 and Fe-TS-2 are listed in Table 2.1. The hydrothermal syntheses were carried out using 100 ml capacity stainless steel autoclaves (Fig.2.1) under static conditions. Before use, the reactors were thoroughly cleaned with 35% HF, and scraped and polished with a carbon brush to minimize the seeding effect of residual crystalline products.

Table 2.1. Specification of the reactants used in zeolite syntheses.

	Chemical Name	Chemical Formula	Purity, %
1.	Tetraethylorthosilicate, TEOS, (Fluka, AG)	$Si(OC_2H_5)_4$	98
2.	Tetrabutylorthotitanate, TBOT, (Fluka)	$Ti(OC_4H_9)_4$	98
3.	Aluminium isopropoxide, (Fluka)	$Al(OC_3H_4)_3$	100
4.	Aluminium nitrate	$Al(NO_3).9H_2O$	> 99
5.	Gallium nitrate, (Aldrich)	$Ga(NO_3)$	> 99
6.	Ferric nitrate	$Al(NO_3).9H_2O$	> 99
7.	Tetrabutyl ammonium hydroxide, TBA-OH, (Aldrich)	$(C_4H_9)_4NOH$	40 % aq. Solution (diluted to 20% before use)
8.	-do-	-do-	20 % methanolic solution
9.	1,8-Diamino octane, 1,8-DAO, (Aldrich)	$H_2N\text{-}(CH_2)_8\text{-}NH_2$	100

2.1.1. Titaniumsilicate, TS-2

Based upon some preliminary experiments, the following molar composition of the reaction mixture (gel/liquid) was chosen: $SiO_2/TiO_2 = 33$; TBA-OH/SiO_2 = 0.33 and H_2O/SiO_2 = 30. In a typical preparation (Fig 2.2), the following procedure was used: 61.0 g tetrabutyl ammonium hydroxide (TBA-OH) (20% solution, Aldrich) was added to 30 g tetraethylorthosilicate (TEOS). This mixture was stirred for about 30 minutes at 298 K. To the above mixture, a solution of 1.5 g tetrabutylorthotitanate (TBOT) in 5 g of dry isopropyl alcohol was added. The clear liquid, thus obtained was stirred for about 1 hour at 350 $\pm$ 2 K (to remove alcohol) before adding to it 76 g water. The resultant liquid was stirred for 30 minutes and autoclaved at 443 $\pm$ 2 K for 2 days. TS-2 with different Ti contents was synthesized by varying the amount of TBOT.

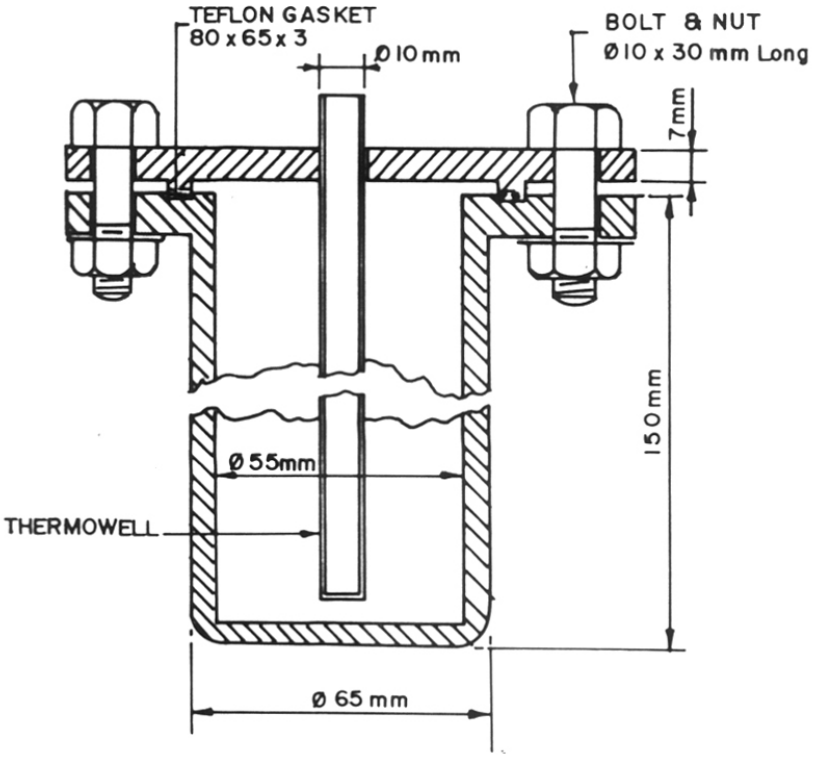

Fig.2.1. **Stainless steel (316) autoclave with teflon gasket for hydrothermal synthesis.**

2.1.2. Metallosilicates (M-MEL)

In the preparation of the ferrisilicates, to ensure that the species in the reactant mixture take up tetrahedral isomorphous positions, it is essential that the formation of the ferrisilicate gel occurs at a pH value between 3 and 4, thereby avoiding the precipitation of iron hydroxide. This was achieved by adding an acidic Fe(III) solution to TEOS. In the case of alumino- and gallosilicates, the formation of aluminium oxide and gallium oxide does not prohibit the incorporation of Al or Ga into the silicate framework.

The following molar gel compositions were used in the synthesis of M-MEL (where M = Al, Ga or Fe).

$SiO_2/M_2O_3 = 90$; $TBA/SiO_2 = 0.2$; $H_2O/SiO_2 = 30$

The synthesis procedures for M-MEL are shown in the form of a schematic diagram (Fig.2.2).

M-MEL (M = Al or Ga): In a typical procedure 36.6 g TBA-OH (20 % aq.) was added to 30 g TEOS under stirring. After about 20 min, the required amount of metal nitrate solution in 15 g water was added. Then 32 g water was added. The resultant mixture was stirred for 1 h before autoclaving. The crystallization was carried out at 443 ± 2 K for 1-2 days under static conditions.

Fe-MEL: 1.9 g of ferric nitrate in 15 g water was added to TEOS under stirring. This solution was stirred for about 30 min. Then 36.6 g TBA-OH (20 % aq.) was added followed by 32 g water. The final gel was stirred for about 1 h and autoclaved at 443 ± 2 K for 2-3 days.

2.1.3. Metallo-Titanium-Silicates

The following molar gel composition was used:

$SiO_2/M_2O_3 = 90$; $SiO_2/TiO_2 = 65$; $TBA/SiO_2 = 0.2$; $H_2O/SiO_2 = 30$

where M = Al, Ga or Fe.

The synthesis procedures for Al-TS-2, Ga-TS-2 and Fe-TS-2 (Fig.2.2) are given below:

Al-TS-2 and Ga-TS-2: 36.6 g TBA-OH (20 % aq. solution) was added to 30 g TEOS. The mixture was stirred for 20 min. A solution of 0.75 g TBOT (tetrabutylorthotitanate) in 5 g dry isopropyl alcohol was added to the above mixture slowly. To the above clear liquid, a solution

Fig.2.1. Schematic diagram for the synthesis of various MEL zeolites

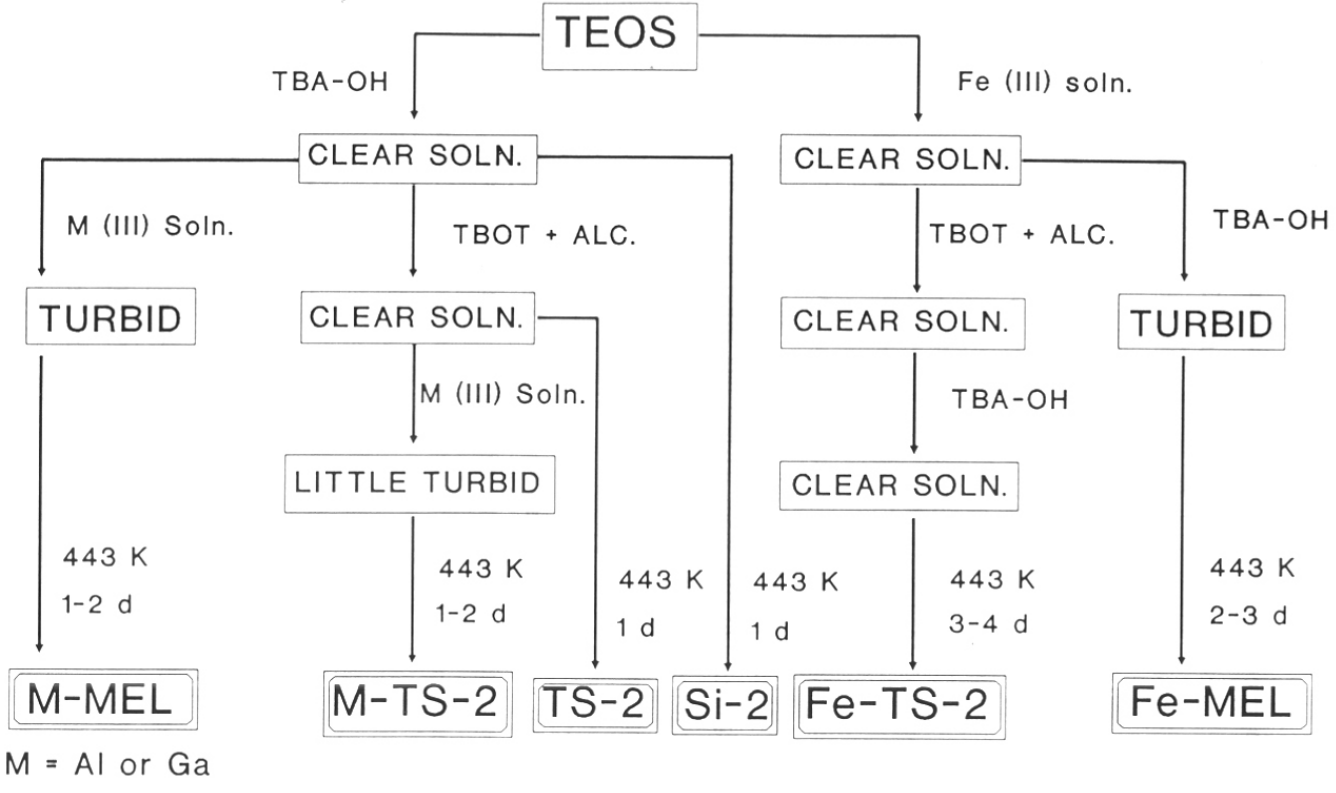

of 1.18 g aluminium nitrate or gallium nitrate in 15 g water was added before adding the remaining 32 g water. The resultant mixture was stirred for 1 h and autoclaved at 443 ± 2 K for 2 days under static conditions.

Fe-TS-2: 1.9 g ferric nitrate in 15 g water was added to 30 g TEOS under stirring. After about 30 min another solution of 0.75 g TBOT in 5 g isopropyl alcohol was added under vigorous stirring. Finally 36.6 g TBA-OH (20 % solution) and 32 g water was added. The resultant mixture was stirred for 1 h before autoclaving. The crystallization was carried out at 443 ± K for 3 days under static conditions.

After crystallization the solids were filtered, washed with water and dried at 398 K for 5 h.

2.1.4. Pretreatment procedure

All the zeolites synthesized above contain organic templates inside the channels. In order to characterize and use these zeolites in the catalytic reactions, it is necessary to remove the organic material from the zeolite pores and convert them into the hydrogen form. The as-synthesized material is placed in a petri-dish and calcined in a flow of nitrogen at 773 K for 4 h followed by passing dry air for 8 h. The temperature of the furnace was raised at a rate of 2.5 K/min.

The calcined material was refluxed twice in 1 M ammonium acetate solution (20 ml/g zeolite; 353 K for 6 h). After the exchange the material was filtered, washed thoroughly with deionized water and dried at 393 K for 10 h. The resultant NH_4^+-form was calcined at 723 K to get the catalytically active hydrogen form.

2.2. CHARACTERIZATION

2.2.1. Chemical analysis

An exact amount of sample was taken in a platinum crucible with lid and ignited to get the dry weight of the sample. The sample was then cooled in a dessicator and weighed. The difference in weights gave the loss on ignition. The anhydrous weight of the sample was noted. Anhydrous sample was treated with hydrofluoric acid (40 wt.%) and evaporated on a hot plate to remove silicon in the form of SiF_6. This treatment was repeated three times and the sample was again ignited, cooled in a dessicator and weighed. The loss in the weight of the sample was determined to get the content of silica. The residue was fused with potassium

pyrosulphate and dissolved in water. It was then analyzed by ICP (John Yvon JYU-38 VHR) and atomic absorption spectroscopy for estimating Na, K, Al, Ga, Fe and Ti. X-ray fluorescence spectrometer (Rigaku 3700) was also used to obtain the Si/Ti ratio.

2.2.2. X-ray diffraction

The samples synthesized during the course of the work under different conditions and different crystallization times were analyzed for qualitative and quantitative phase identification by x-ray powder diffraction (Rigaku (Model D/MAX III VC, Japan); Ni filtered Cu-Kα radiation; λ = 1.5404 Å). XRD was also used to identify the different phases. For calculating the x-ray crystallinity, XRD patterns were recorded between peaks 2 θ = 21.5-25.5, where the most intense peaks characteristic of the MEL zeolite structure occur.

The x-ray crystallinity was then calculated from the following equation:

$$\text{X-ray crystallinity} = \frac{\text{peak area between } 2\theta = 21.5\text{-}25.5^\circ \text{ of sample}}{\text{peak area between } 2\theta = 21.5\text{-}25.5^\circ \text{ of the standard sample}} \times 100$$

Silicon was used as an internal standard for calibrating the 2 θ values. The unit cell parameters were calculated for calcined samples from x-ray diffraction pattern scanned at a speed of 0.25 ° min^{-1}.

2.2.3. Infrared spectroscopy

The infrared spectra were recorded with a PYE UNICAM SP3 300 spectrometer in the frequency range 200-1300 cm^{-1} using the Nujol method. KCN was used as an internal standard. The IR crystallinity was determined using the formula:

$$\text{IR crystallinity} = \frac{\text{peak area of band at 550 } cm^{-1} \text{ of the product}}{\text{peak area of the band at 550 } cm^{-1} \text{ of the reference sample}} \times 100$$

In the range of 4000-1300 cm^{-1}, self supported wafers were used. For in-situ studies, a cell in which the temperature can be varied from liquid nitrogen temperature to 773 K was fabricated and used. This cell was connected to a volumetric adsorption apparatus (Micromeritics, USA, Model: accusorb-2000 E). The spectra were recorded with a Nicolet 60 SXB FTIR spectrometer.

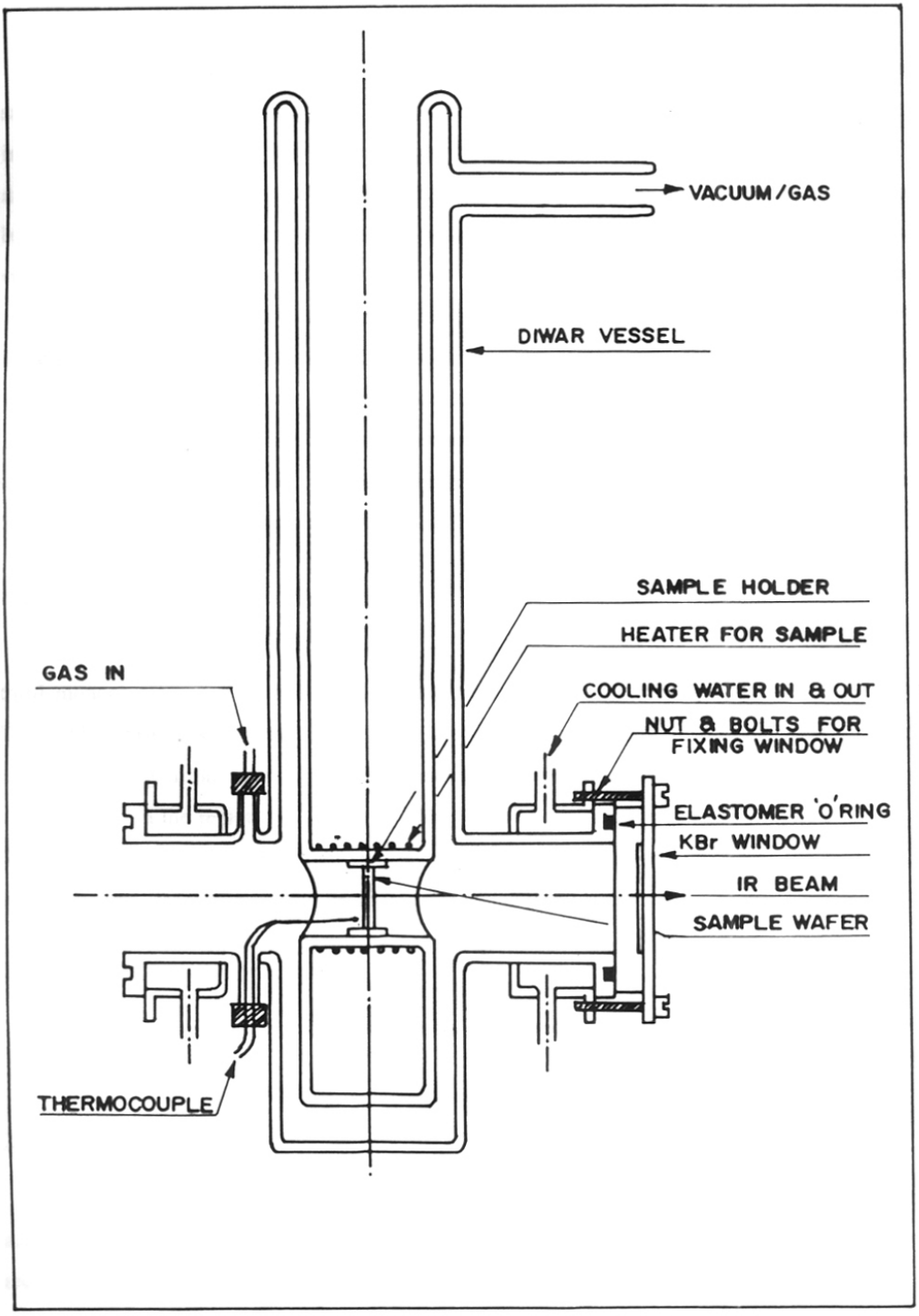

Fig.2.3. FT-IR transmittance cell.

The cell was basically a DEWAR flask with a modifications as shown in Fig. 2.3. The sample was pressed under pressure of 5 ton/inch^2 into a thin pellet (5-6 mgs/cm^2) and mounted in the sample holder (SH). It was then placed inside the heating compartment of the cell (HC) and aligned in line with the IR beam. The cell was sealed at both the ends by potassium bromide windows (KW) with the help of elastomer "O" rings. A thermocouple placed in close vicinity of the sample measured the temperature of the sample. The side tube at the top of the cell was connected to the high vacuum system. Cold water was constantly circulated through the cooling coil provided near the KBr windows. The sample was heated to 673 K with a heating rate of 5 K/min, under vacuum and maintained at this temperature for about 6 h and then cooled down to 323 K in vacuum. The spectra were recorded by averaging more than 100 scans with 2 cm^{-1} resolution. Vapors of pyridine were admitted to the sample though the adsorption manifold of the system.

2.2.4. Raman spectroscopy

Raman measurements in the photon-counting mode were performed using a SPEX 1442 third monochromator, a C31034 Ga-As-photomultiplier detector (PMT) system, and a SPEX DM1 DATAMATE spectrometer controller and data processor. The filtered radiation of 514.5 nm from an argon-ion laser formed the excitation source (for details see Ref.8). The spectra were scanned in the region 10-1210 cm^{-1} with steps of 2 cm^{-1} and an integration time of 20 sec. The data were plotted after a light smoothing by using the built-in software of the DM1 and subtracting the PMT dark counts [≈ 10 (photon counts)/sec].

2.2.5. UV-VIS spectroscopy

The UV-VIS diffuse reflectance spectra were recorded using Pye Unichem SP-8-100 UV-Visible spectrometer.

2.2.6. Thermal analysis

Simultaneous TG-DTA-DTG analyses of the crystalline phases were performed on an automatic derivatograph (Setaram TG-DTA92). The thermograms of the samples were recorded under the following conditions.

Weight of the sample	= 30 mg
Heating rate	= 10 K min^{-1}

Sensitivity

TG	= 25 mg
DTG	= 0.2 mv
DTA	= 0.1 mv
Atmosphere	= flowing air

Preheated and finely powdered α-alumina was used as reference material.

2.2.7. Scanning electron microscopy

The morphology of MEL samples was investigated using the scanning electron microscope (JEOL, JSM 5200). The sample was dusted on alumina and coated with a thin film of gold to prevent surface charging and to protect the zeolite material from thermal damage by the electron beam. In all the analyses a uniform film thickness of about 0.1 mm was maintained.

2.2.8. High resolution ^{71}Ga NMR studies

The high resolution MASNMR for ^{71}Ga were recorded at room temperature on a BRUCKER MSL-400 spectrometer at the Larmor frequency of 122.028 MHz in a 100 KHz spectral window. The free induction decays were collected under MASS and typically 2000 transients were accumulated to give an acceptable S/N. Before Fourier-transformation the FID was apodized with a 100 Hz exponential line broadening. ^{27}Al MASNMR spectra were recorded using Brucker MSL-300 NMR at the Larmor frequency of 78.0131 with a spinning speed of 4-5 MHz.

2.2.9. ESR and magnetic susceptibility

Magnetic susceptibilities and magnetic moments of the ferrisilicate and ferri-titanium-silicate molecular sieves were determined using a Faraday microbalance (Cahn Ventron, Cervitos, CA, USA). Brucker E-2000 spectrometer was used to record ESR spectrum of ferri- and ferri-titanium-silicates.

2.2.10. Mössbauer spectroscopy

The Mössbauer spectra were recorded with a conventional constant acceleration type Mössbauer spectrometer operating in multiscaler mode at room temperature in the presence of an externally applied magnetic field (4.13 T) perpendicular to the γ-beam.

2.2.11. Ion-exchange capacities

The calcined samples were treated with 1N NaCl for 2 h at 423 K to get Na-form of the zeolite. The Na-form was exchanged with 1N KCl solution for 2 h at 323 K. The solid was filtered, washed thoroughly with deionized water and dried at 373 K for 10 h. The resultant material (K-form) was analyzed for K and M (where M = Al, Ga or Fe).

2.2.12. Adsorption measurements

The sorption measurements for water, cyclohexane and n-hexane were carried out gravimetrically in a recording electromicrobalance (Model: Cahn-2000 G). The zeolite sample of about 60 mg was pressed into a pellet and weighed into an aluminium bucket which was attached to the balance. The system was evacuated down to a pressure of 10^{-6} torr at 673 K. After 2 hours, the temperature was lowered to the required value. The sorbate was admitted into the sample at a constant pressure and temperature and the weight gain was recorded as a function of time. After the experiment was over, the catalyst was evacuated and heated to 673 K at 10^{-6} torr and used for the next measurement.

2.2.13. Surface area measurements

Omnisorb 100 CX (supplied by COULTER Corporation, USA) unit was used for the measurement of nitrogen adsorption to determine surface areas. The samples were activated at 673 K for 2 hours in a high vacuum. After the treatment, the anhydrous weight of the sample was taken. The samples were then cooled to 94 K using liquid nitrogen. After this, the samples were allowed to adsorb nitrogen gas. Finally, the BET surface area was calculated.

2.2.14. Thermal and steaming treatments

The zeolite samples were heated in a muffle furnace to the desired temperature at a heating rate of 2.5 K/min. Then the samples were cooled to room temperature and kept in the desiccator over saturated ammonium chloride solution. The hydrothermal treatment was carried out in a tubular furnace with steam (100 %) at atmospheric pressure at the required temperature. These samples were subjected to XRD, IR, sorption and catalytic measurements.

2.3. CATALYTIC REACTIONS

The chemicals used in the various reactions are listed in Table 2.2

Table 2.2. Chemicals used in the catalytic reactions.

S.No.	Chemical Name	Source	Further purification
1.	Hydrogen peroxide, 30 % solution	S.d. Fine Chemicals, India.	Nil
2.	Phenol crystals, (AR grade)	-do-	Nil
3.	Benzene (AR)	-do-	Distilled
4.	n-hexane (AR)	-do-	-do-
5.	Cyclohexane	-do-	-do-
6.	Cyclohexanone	-do-	-do-
7.	Styrene/α-methyl styrene	-do-	Nil
8.	m-xylene	Aldrich, U.S.A.	Nil
9.	Ethylbenzene	-do-	Nil
10.	H_3C-$(CH_2)_n$-$CH=CH_2$ (n = 3, 4, 5, 9)	Aldrich	Nil

2.3.1. Liquid-phase reactions

A. Alkane oxidation

The catalytic reactions were carried out in stirred autoclaves (Parr Instrument Company, Illinois, USA) of 300 ml capacity at temperatures between 323 and 398 K under autogeneous pressure, using different mole ratios of hydrogen peroxide (26 wt.% aqueous solution) and alkane. In order to get a single liquid phase, acetone was used as a solvent. Typically 0.2 g of the catalyst was used in n-hexane oxidation and 1.0 g in the case of cyclohexane oxidation, as a fine powder (300-400 mesh). The duration of the runs was 5 h.

B. Hydroxylation and epoxidation

The catalytic runs were carried out in a four-necked glass flask (200 ml capacity) fitted with a mechanical stirrer, condenser, syringe feed pump (Sage Instruments, USA) and a septum. The temperature of the reaction vessel was maintained using an oil bath. The desired

temperature was obtained before adding H_2O_2 (26 wt.% aqueous solution) with stirring through a feed pump at the rate of 10 ml h^{-1} unless stated otherwise. The products (0.1 ml) were taken out periodically with a microlitre syringe and diluted with the solvent before analysis.

C. Ammoximation

The reactions were carried out in a three necked flask (250 ml); one neck was fitted with a mechanical stirrer, another with a condenser and the third one with a rubber septum. The temperature was maintained using an oil bath. The standard reaction conditions were: catalyst = 1g; temperature = 353 K and cyclohexanone : H_2O_2 : NH_3 molar ratio = 1 : 1 : 4. The reaction time was 5 hours. Hydrogen peroxide (26 wt.%) was injected through the septum using a feed pump (Sage Instruments, USA) over a period of 2 hours. After the addition of hydrogen peroxide, the reaction was continued for 3 more hours. After the completion of the reaction, the organic products were extracted with ether.

2.3.2. Fixed-bed atmospheric reactions

The powder form of zeolites was pressed into pellets in a hydraulic press with 1.5 cm die at pressures upto 10 ton/inch^2. These pellets were then gently crushed to 35-45 mesh size and then used in the catalytic reactions. The catalytic experiments were carried out in a fixed bed, down-flow, vertical silica reactor having diameter of 1.0 cm (Fig.2.4). 1.0 g (on anhydrous basis) of catalyst was loaded in the center of the reactor in such a way that the catalyst bed was sandwitched between inert porcelain beeds. The catalyst was activated at 723 K for 6 h in dry air before use. Then the temperature and gas flows were adjusted to the required value and the feed was injected using a syringe pump (Sage Instruments, Model 352, USA) at the required rate. The product samples were collected and periodically analyzed by GC.

After the completion of the reaction, the feed injection was stopped and the catalyst was flushed first with nitrogen and then a mixture of nitrogen and air (60 : 40 volume ratio approximately) was passed over the catalyst at 523 K. The temperature was slowly raised to 753 K. The regeneration was carried out at this temperature for 12 h. Then the catalyst was flushed again with dry nitrogen and cooled down to the reaction temperature for further use.

2.3.3. Product analysis

The products from hydroxylation, oxyfunctionalization, ammoximation, Beckmann rearrangement of cyclohexanone oxime and epoxidation reactions were analyzed in a gas chro-

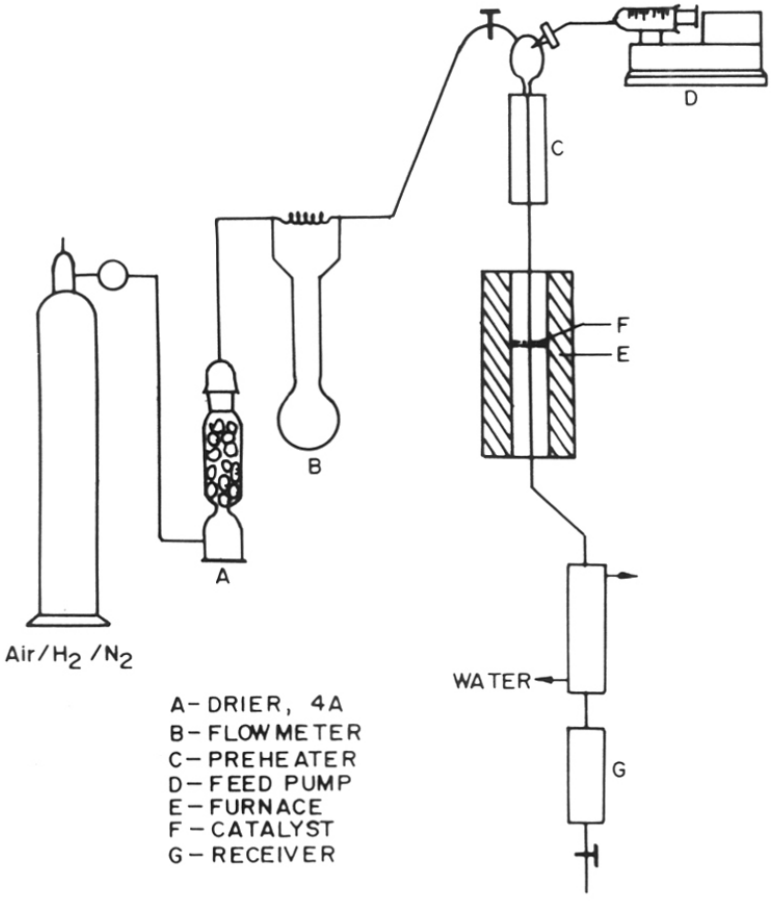

Fig.2.4. **Fixed bed, down-flow reactor used in this study.**

matograph (Hewlett Packard 5880 A) equipped with a capillary column (50 m X 0.25 mm cross linked methyl silicone gum). The products were identified by GC-MS (Shimadzu QCMS-QP2000A). Since the GC response of different compounds vary, standard samples were injected to determine the response factors. The product analyses were normalized using these GC response factors. The products of m-xylene isomerization and ethylbenzene disproportionation were analyzed in a Shimadzu 16A gas chromatograph using 2 meter long stainless steel column (3 mm i.d.) packed with 5 % Bentone-34 and 10 % diisodecylphthalate column.

CHAPTER - III

STUDIES ON THE TITANIUM SILICATE MOLECULAR SIEVE, TS-2 (MEL-ANALOG)

3.1. PART-I - SYNTHESIS AND CHARACTERIZATION OF TS-2

3.1.1. INTRODUCTION

Taramasso *et al.*[1] were the first to claim the direct synthesis of a crystalline, microporous titaniumsilicate (TS-1; MFI structure), confirming the predictions of Barrer[2] based on theoretical arguments that titaniumsilicates should be stable. Since then a number of reports on the synthesis[3-11], characterization[2-17] and catalytic properties[8-40] of TS-1 molecular sieves have appeared. Though the original investigators of TS-1 had reported[1] a minimum SiO_2/TiO_2 value of 39 for their samples, Thangaraj *et al.*[11] have been able to obtain TS-1 molecular sieves with SiO_2/TiO_2 ratios as low as 10 using an improved synthesis procedure.

Recently, we have reported a new titaniumsilicate molecular sieve, designated as TS-2 having MEL structure[41]. The synthesis[41-44], characterization[41-43] and catalytic properties[45-52] of this new titaniumsilicate have also been reported by us.

Titaniumsilicate molecular sieves are generally synthesized by hydrothermal procedures similar to those used in the synthesis of aluminosilicates. An alternate method for the synthesis of titaniumsilicates has been described by Kraushaar and van Hooff[7]. In this method, Al (III) is removed from the ZSM-5 framework with HCl treatment and the resultant material treated with $TiCl_4$ vapours in a stream of nitrogen at 673-773 K. The reaction can be described as follows:

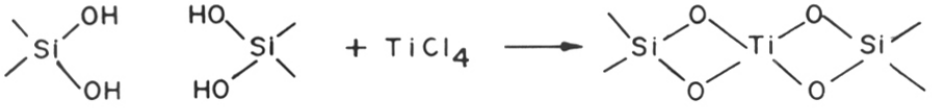

Evidence for the presence of Ti in the ZSM-5 framework has been obtained from i) the expansion in the unit cell parameters, ii) the appearence of the Si-O-Ti absorption band (IR) at 960 cm^{-1}, iii) the presence of a signal at -116 ppm in ^{29}Si NMR spectra and iv) the catalytic activity in the hydroxylation of phenol. Ferrini *et al.*[9] have also prepared TS-1 and titanium containing Y and mordenite by treating the corresponding zeolites with $TiCl_4$. All the samples exhibited an IR band at 960 cm^{-1}, characteristic of titaniumsilicates. But Y and mordenite samples were inactive in the hydroxylation of phenol indicating that most of the Ti in these samples was present as TiO_2. A similar secondary synthesis of TS-1 has also been tried by Carati *et al.*[16] using MFI-borosilicate instead of the aluminosilicate (ZSM-5). They found that

the deposition of extra framework TiO_2 occurs on the surface after some time. Notari[53] has pointed out that the formation of TiO_2 due to the hydrolysis of the $TiCl_4$ is not easy to prevent. Since even small amounts of TiO_2 deposited on titaniumsilicates can decompose H_2O_2 to H_2O and O_2 and reduce the activity dramatically, this method may not be of much use for preparing catalytically active titanaiumsilicates.

Skeels *et al.*[8] have synthesized titaniumsilicate molecular sieve analogs of ZSM-5, L, omega, phillipsite and faujasite by refluxing the corresponding dealuminated samples with diaminohexaflouro titanate ($(NH_4)_2TiF_6$) at 348-368 K for 2 h. The catalytic properties of these materials were not reported. The materials obtained by this method did not exhibit the 960 cm^{-1} band, characteristic of titaniumsilicates. The titaniumsilicate (TS-1) synthesized by us as per Skeels procedure was inactive in the hydroxylation of phenol, suggesting that Ti was not substituted into the framework of the zeolite matrix.

Synthesis of single crystals of titaniumsilicate in flouride media using $(NH_4)_3Ti(O_2)F_5$ has also been reported[54]. Evidence for the isomorphous substitution was obtained from the expansion in the unit cell parameters. Activity tests were, however, not carried out over these samples. Recently, the activity and selectivities of TS-1, synthesized by various methods, in selective oxidation reactions have been reported[29]. It was found that TS-1 synthesized following the procedures of Skeels[8] and Shilun[54] is inactive in the hydroxylation of phenol. TS-1 prepared in the presence of NaOH[55] was also found to be inactive.

A crystalline, three-dimensional, microporous titaniumsilicate composed of interconnected titanate octahedra and silicate tetrahedra with removable water and exchangeable cations has been reported[56]. The catalytic properties of this synthetic titaniumsilicate molecular sieve are not known. Since this material possesses six coordinated Ti atoms, the catalytic properties may be different from TS-1 and TS-2.

Very recently, titaniumsilicate molecular sieves, designated as ETS-4 and ETS-10 have been reported[57]. ETS-4 is a small-pore material having pore dimensions of approximately 4 A°, where as ETS-10 is a large-pore material with pore diameter of 8 A°. These materials also possess six coordinated Ti atoms.

Though many titaniumsilicate molecular sieves have been reported, clear evidence for the presence of Ti in the zeolite lattice has been obtained only for the MFI (TS-1) and the MEL (TS-2) structures.

The characteristic features of titaniumsilicate molecular sieves (TS-1 and TS-2) are:

- Ti atoms are located in vicariant positions in the place of Si atoms.
- Total absence of Al atoms and therefore strong acid sites.
- Uniform distribution of Ti atoms in the silicalite matrix; each Ti atom is surrounded by four -O-Si units.

3.1.2. RESULTS AND DISCUSSION

A. General synthesis procedure

The sequence and method of addition of reactants is very important[4,6,42] in the synthesis of titaniumsilicate molecular sieves. The formation of insoluble titanium oxide during the mixing of the reagents has to be avoided. Further, alkali metal hydroxides (such as NaOH, KOH etc.,) are detrimental to the incorporation of Ti in the lattice[44,53].

When tetraethylorthosiicate (TEOS), tetrabutylorthotitanate (TBOT) and a tetraalkylammonium hydroxide (TAA-OH) are mixed together, precipitation of TiO_2 or SiO_2 can occur under certain conditions. Kraushaar[4] has shown that the clear solution of the above mixture obtained using tetrapropyl ammonium hydroxide yields a titaniumsilicate, while a solution containing precipitated TiO_2 yields silicalite, without incorporation of Ti in the framework. The TiO_2 formed once does not dissolve back under the hydrothermal conditions used in the synthesis resulting in a material with poor incorporation of Ti. It is therefore important to prevent the formation of precipitates when TEOS, TBOT and tetrabutyl ammonium hydroxide (TBA-OH) are mixed.

The results of the effect of mode of addition of reactants on the hydrolysis behaviour of Ti and Si alkoxides are reported in Table 3.1.

The following procedure was adopted to avoid the precipitation of titanium oxide and to obtain a clear liquid reaction mixture :

1. TBOT was used as the source of Ti instead of the conventionally used tetraethylorthotitanate (TEOT), because the rate of hydrolysis of the former is slower[58,59]. Further the $Ti(OBu)_4$ was mixed with dry isopropyl alcohol to avoid its instantaneous hydrolysis to TiO_2.

2. Tetraethyl orthosilicate was used as a source of silica and was first hydrolyzed by adding tetrabutyl ammonium hydroxide solution before adding the Ti-butoxide solution because TBOT hydrolyzes faster than TEOS[59]. This method of addition provided a clear liquid by avoiding the formation of titanium oxide (Table 3.1) and facilitated the incorporation of titaniumsilicate.

Table 3.1. Effect of the mode of addition of template and Si and Ti alkoxides on the formation of titanium dioxide.

	Reactants	Observation
1	5 g $Si(OC_2H_5)_4$ + 5 g TBA-OH (aq.)	Clear solution
2	0.2 g $Ti(OC_4H_9)_4$ + 5 g TBA-OH (aq.)	TiO_2 formed
3	5 g $Si(OC_2H_5)_4$ + 0.2 g $Ti(OC_4H_9)_4$	Clear solution
4	5 g $Si(OC_2H_5)_4$ + 0.2 g $Ti(OC_4H_9)_4$ in 2 ml isopropyl alcohol	Clear solution
5	**5 g $Si(OC_2H_5)_4$ + 5 g TBA-OH (aq.) + 0.2 g $Ti(OC_4H_9)_4$ in 2 ml isopropyl alcohol**	**Clear solution**
6	5 g $Si(OC_2H_5)_4$ + 0.2 g $Ti(OC_4H_9)_4$ in isopropyl aocohol + 5 g TBA-OH	TiO_2 is formed
7	**5 g $Si(OC_2H_5)_4$ + TBA-OH (al.) + 0.2 g $Ti(OC_4H_9)_4$ in 2 ml isopropyl alcohol**	**Clear solution**
8	5 g $Si(OC_2H_5)_4$ + 0.2 g $Ti(OC_4H_9)_4$ in 2 ml isopropyl aocohol + 5 g TBA-OH (alc.)	Clear solution
9	5 g $Si(OC_2H_5)_4$ + 5 g TBA-OH (alc.)	Clear solution
10	0.2 g $Ti(OC_4H_9)_4$ + 5 g TBA-OH (al.)	TiO_2 formed

3. Finally the required quantity of water was added after removing the alcohol by heating at 332 K for 2 h.

The details of the synthesis procedure adopted in the preparation of TS-2 have already beed described in chapter II.

B. Kinetics of crystallization

The following gel composition was used to study the kinetics of crystallization

SiO_2/TiO_2 = 33; TBA-OH/SiO_2 = 0.2 and H_2O/SiO_2 = 20.

i. Effect of SiO_2/TiO_2 ratio

The effect of SiO_2/TiO_2 ratio on the crystallization of TS-2 is shown in Fig.3.1. curves 1-4 represent the crystallization rate from reaction mixtures with SiO_2/TiO_2 = 17, 33, 90 and 180, respectively. Fully crystalline material was obtained after 24 h. The development of crystallinity of the material with time was evident. Even after 25 days, no phase transformation was observed. The rate of crystallization increased with an increase in silica content in the reaction mixture. Similar observations have also been reported during the synthesis of high silica molecular sieves[60,61].

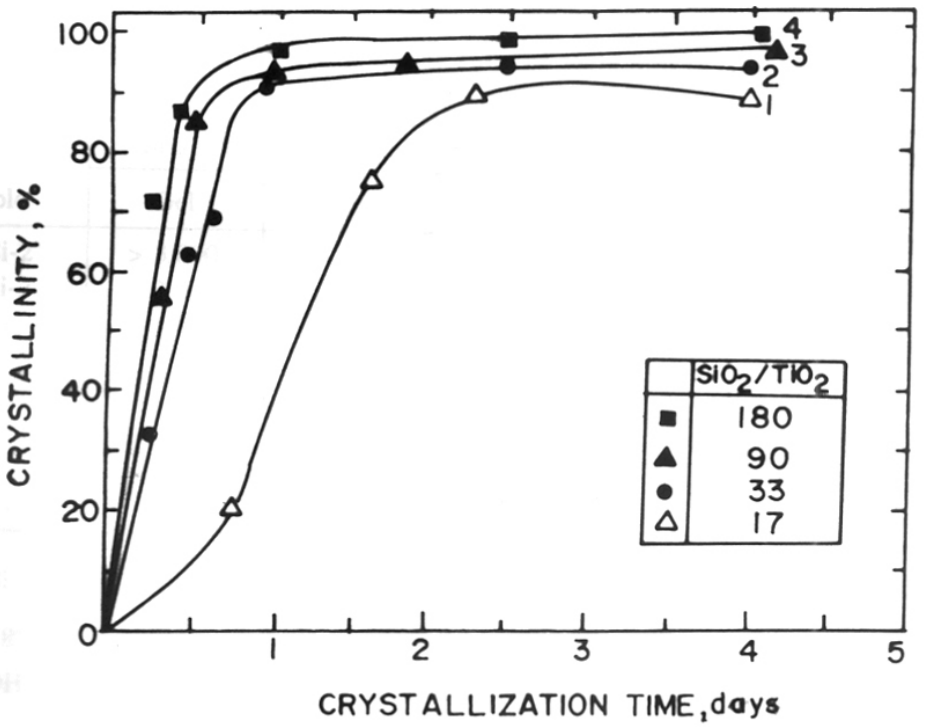

Fig.3.1. Effect of SiO_2/TiO_2 mole ratio on the crystallization of TS-2.
Molar gel composition: TBA-OH/SiO_2 = 0.2; H_2O/SiO_2 = 20. Crystallization temp.(K) = 443.

The interrelationship between the SiO_2/TiO_2 ratios of the reaction mixtures and the crystalline products and their corresponding yields are presented in Table 3.2. The pH of the mother liquor ranged between 12.5 and 12.7. No Ti was detected in the mother liquor after filtration of the crystallline products, indicating that Ti incorporation was generally efficient and complete (except in the case of samples 5 and 6, Table.3.2). With the increase in the SiO_2/TiO_2 ratio of the initial reaction mixture, Si^{4+} content of the mother liquor also increased leading to lower SiO_2/TiO_2 ratios in the solid products. As a result, the yield of the crystalline product decreased with increasing SiO_2/TiO_2 in the reaction mixture.

Table 3.2. Influence of SiO_2/TiO_2 molar ratio on yield and crystallization time.

Sample	SiO_2/TiO_2 molar ratio		Crystallization time, d	Yield (wt.%)	Particle size, μm
	Gel	Product			
Si-2[a]	> 3,000	> 3,000	1	70	6-8
Si-2	> 3,000	> 3,000	1	65	3-4
1	180	124	1	75	1.5-2
2	95	70	1	75	1-1.5
3	65	48	1	80	1-1.5
4	33	27	1.5	90	1-1.5
5	17	21	3	90	≈ 1
6	7	14	8	-	≈ 1

a: Si-2 = Silicalilte-2

Molar gel composition: TBA-OH/SiO_2 = 0.33; H_2O/SiO_2 = 30; SiO_2/TiO_2 varied except a: TBA-OH/SiO_2 = 0.2; H_2O/SiO_2 = 30. Crystallization Temp. (K) = 443.

ii. Influence of the organic base

Fig.3.2 depicts the effect of TBA-OH/SiO_2 molar ratio on the nucleation and crystallization of TS-2. The change in the pH of the mother liquor during the course of crystallization is also shown (curves A-D). At a very low concentration of TBA-OH (TBA-OH/SiO_2 = 0.1), both nucleation and subsequent crystallization were very slow (curve D). Further, fully crystalline material was not obtained even after 11 days. A slight increase in the TBA-OH/SiO_2 ratio from 0.1 to 0.13 significantly enhanced the rate of crystallization leading to a fully crystalline material after 3 days. However, the nucleation was found to be still slow (curve C). Further acceleration in nucleation and crystallization rates was observed (curve B) at TBA-OH/SiO_2 = 0.2; fully crystalline material could be obtained after 1 d at 443 K. TBA/SiO_2 ratio of 0.33 also produced fully crystalline material in 1 d. However, a further

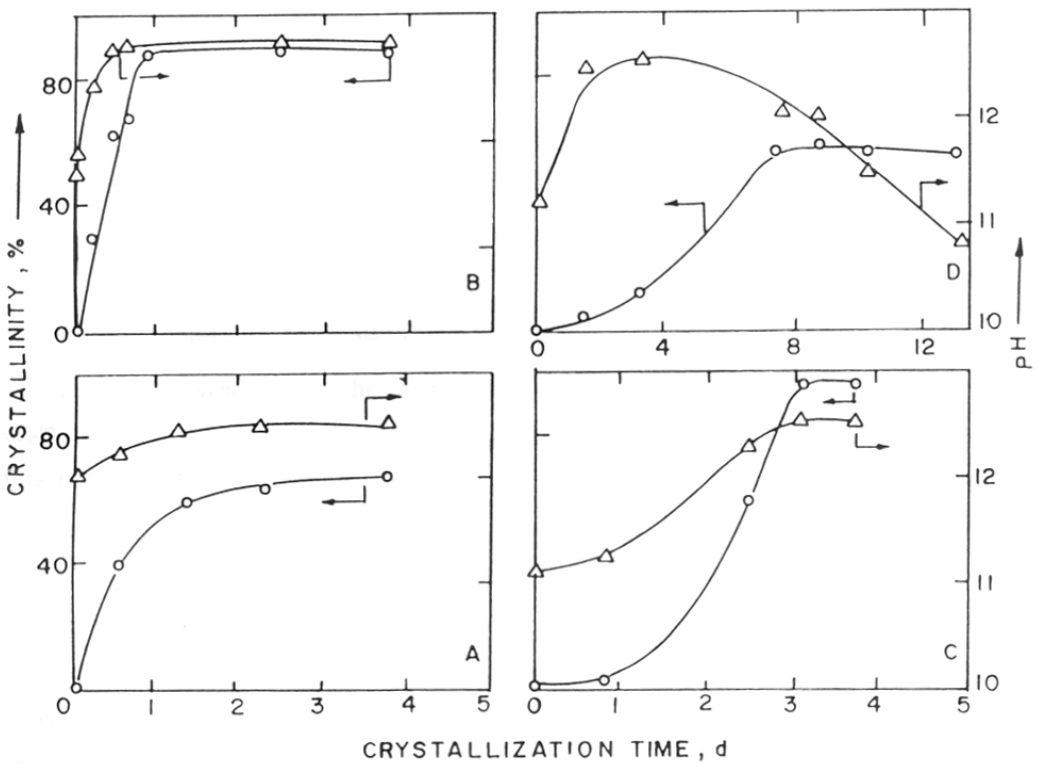

Fig.3.2. **Influence of the TBA-OH/SiO_2 molar ratio on the crystallization of TS-2.**

A-D correspond to values 0.67, 0.2, 0.13 and 0.1, respectively. The change in pH during crystallization is also plotted against crystallization time.

Molar gel composition: SiO_2/TiO_2 = 33; H_2O/SiO_2 = 20. Crystallization temp. (K) = 443).

increase in TBA-OH concentration (TBA-OH/SiO_2 = 0.67, curve D) decreased the yield of the crystalline (XRD) material to about 70 %. Perhaps, the very high alkalinity (high OH-concentration) of the TBA-OH caused the redissolution of the crystalline material. Similar results have been reported by Kraushaar in the case of TS-1[4].

The change in TBA-OH content also affects the alkalinity of the reaction mixture due to the highly basic nature of TBA-OH. The above observations may be a combined effect of templating as well as mineralizing/hydrolyzing action of TBA-OH in the synthesis of TS-2. However, it is clear from the curves A-D that there exists a definite range of TBA-OH/SiO_2 ratio for optimum crystallization of TS-2. A similar observation has also been made in the synthesis of aluminosilicate molecular sieves[60-64] indicating that this effect is, probably, a general phenomenon in the synthesis of high silica molecular sieves.

During the synthesis of the high silica aluminosilicate, EU-1 (ZSM-50), Casci and Lowe[64] found that a large increase in the pH of the mother liquor (i.e. Δ pH = pH_f-pH_i, where pH_f is the final pH of the mother liquor, and pH_i is the initial pH of the reaction mixture) during the crystallization indicated the formation of stable and highly crystalline material. Insignificant change or decrease in the value of Δ pH indicated either the redissolution of the less (meta) stable phase formed initially or the presence of amorphous material or both. Fig.3.3 (curves A-D) depict the pH changes with crystallization as a function of time. With the increase in TBA-OH/SiO_2 ratio, the initial pH of the reaction mixture (pH_i) also increases (curves A-D). A rise in pH accompanies the crystallization. The maximum Δ pH value (Ca. 1-1.2) is observed for compositions with TBA-OH/SiO_2 = 0.2 (curve B) and 0.13 (curve C). Both of these compositions produce fully crystalline material. When the TBA-OH/SiO_2 ratio of the reaction mixture is very high (0.67) or very low (0.1), the Δ pH is either very small (A) or even negative (D). Further these two extreme compositions yield only about 50-70% crystalline material.

In the case of aluminosilicates, the incorporation of SiO_2 into the framework leads to an increase in the pH[64], while the incorporation of AlO_2^- does not influence the pH significantly. This was explained to be due to an increase in the [free base] / [SiO_2] ratio (i.e. [M_2O-Al_2O_3] / SiO_2) in the remaining reaction mixture. However, in the case of Al and alkali free titanium-silicate systems, probably the incorporation of both Ti as well as Si increases the pH as the incorporation of Ti and/or Si units in the framework may result in an increase in the [free base] / [SiO_2+TiO_2] ratio in the remaining reaction mixture. Further, a sharp increase in both the Δ pH and crystallinity (Fig.3.2 curve B and C) indicates that titanium incorporation in the silica

network is quite fast and efficient under the optimum reaction conditions. The results (such as clear transparent liquid reaction mixture, and a quick rise in pH with crystallinity) indicate that the crystal growth occurs from reactive soluble species (≡Si-O-Ti≡) probably through a liquid phase transformation mechanism. Particle size decreased with increasing TBA-OH/SiO_2 ratio (Fig.3.3).

iii. Influence of water content

The influence of changing the H_2O/SiO_2 molar ratio in the initial reaction mixture on the crystallization of TS-2 is illustrated in Fig.3.4. The rate of crystallization increases slightly with a decrease in water content (H_2O/SiO_2). The average size of the crystals obtained from the mixtures having H_2O/SiO_2 = 10, 20 and 30 were 0.5, 1 and 1.5 μm, respectively. The faster rate of crystallization and smaller crystals obtained in the concentrated systems is attributed to the faster rate of nucleation in the concentrated systems.

iv. Influence of crystallization temperature

In all the above mentioned studies, the crystallization was done at 443 K. Fig.3.5 depicts the influence of temperature on nucleation and crystallization of TS-2. At 428 K (curve A) the crystallization rate was slower. At 458 K (curve C) the crystallization was slightly faster vis-a-vis that at 443 K (curve B). At all the temperatures (428-458 K), fully crystalline material was obtained.

v. Influence of Na+/SiO2 on the incorporation of Ti

It has been reported[3,44,53] that the presence of alkali metal in the reaction mixture may retard the incorporation of Ti. To study this effect systematically, varying amounts of sodium chloride were added to the reaction mixtures. The influence of Na on Ti incorporation was monitored by framework IR and catalytic activity in phenol hydroxylation. Table 3.3 compares the chemical composition and the ratio of the intensities of 960 cm^{-1}/550 cm^{-1} bands in the framework IR spectra of the crystalline material obtained from the reaction mixtures having Na^+/TiO_2 = 0, 1 and 2 (samples A, D and E, respectively). With an increase in Na^+/TiO_2 ratio from 0 to 2, the relative intensity of 960 cm^{-1} band, characteristic of titaniumsilicates decreases suggesting that the presence of alkali metal adversely affects Ti-incorporation. This is further confirmed by the very low catalytic activity of the crystalline material obtained from the Na containing systems compared to those obtained in the absence of Na (Table 3.3).

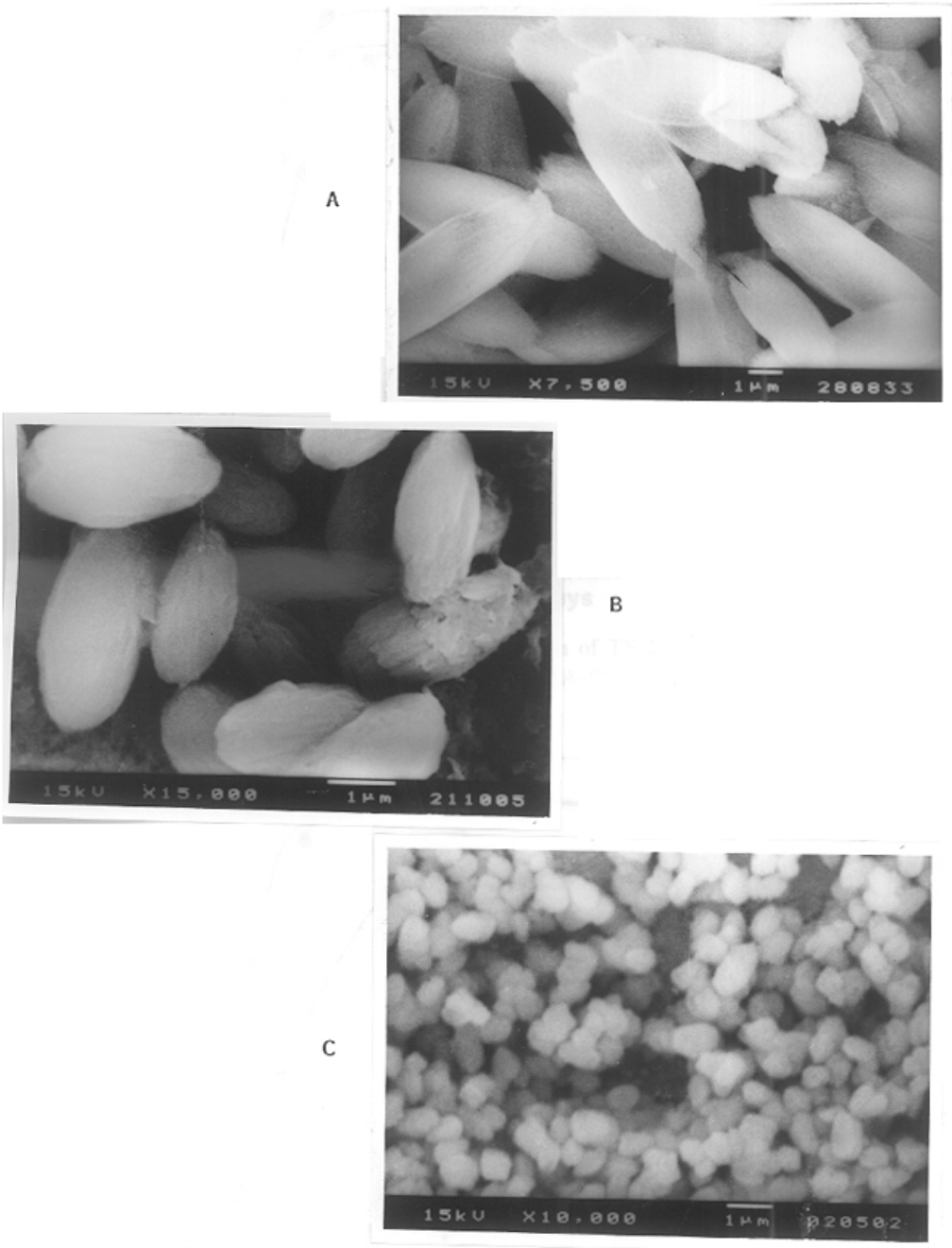

Fig.3.3. **SEM photographs of Silicalite-2 (A) and TS-2 (B,C).**
Molar gel composition: H_2O/SiO_2 = 30; SiO_2/TiO_2 = 30; TBA-OH/SiO_2 = 0.2, 0.13 and 0.33 for A, B and C, respectively. Crystallization temp. (K) = 443.

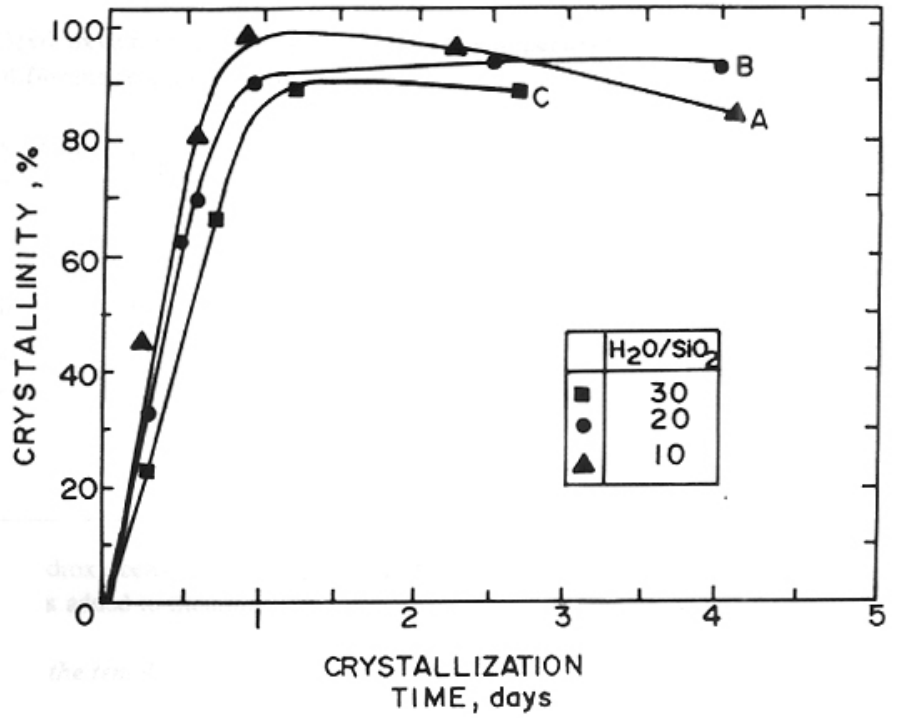

Fig.3.4. **Influence of dilution on the crystallization of TS-2.**
Molar gel composition: SiO_2/TiO_2 = 33; TBA-OH/SiO_2. Crystallization temp. (K) = 443.

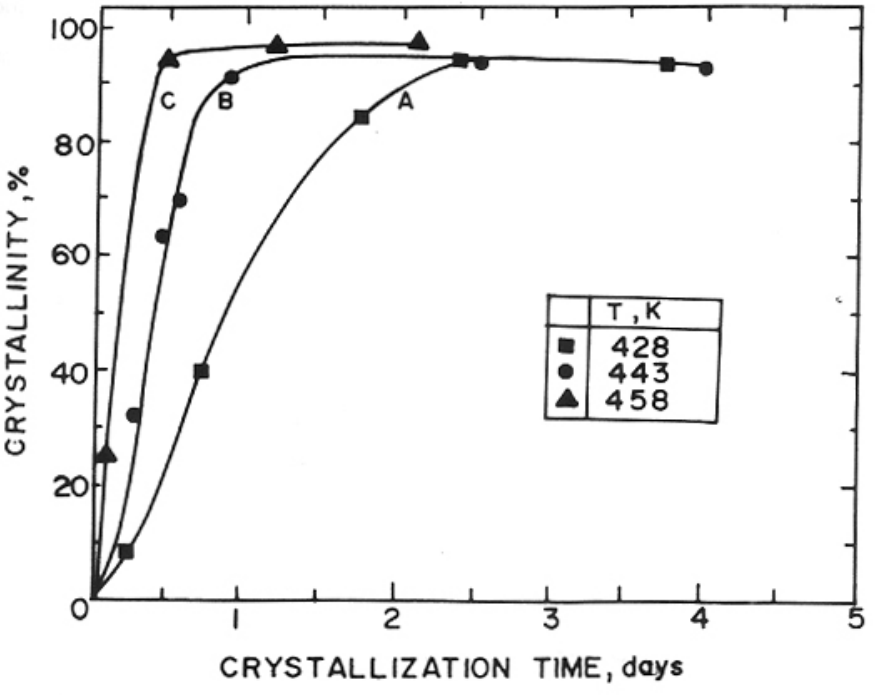

Fig.3.5. **Influence of crystallization temperature.**
Molar gel composition: SiO_2/TiO_2 = 33; TBA-OH/SiO_2 = 0.2; H_2O/SiO_2 = 20.

Table 3.3.Hydroxylation of phenol with hydrogen peroxide over TS-2 prepared from different reaction mixtures.

Reaction conditons: TS-2 = 1 g; Phenol = 10 g; Phenol/H_2O_2 (mole) = 3; Reaction time = 24h; Acetone = 20 ml; Temp. (K) = 338.

Sample No.	SiO_2/TiO_2		I_{970}/I_{550}	H_2O_2	Phenol convn.
	Initial	Product	cm^{-1}	Sel.[a]	(%,theoretical)
A (alcohol)	33	28	0.61	78.3	92.4
B (aq.clear)	33	27	0.59	75.8	87.1
C (aq.ppt)*	33	30	0.26	25.1	31.7
D (1:1 Na/Ti)	33	36	0.41	58.0	68.5
E (2:1 Na/Ti)	33	39	0.13	26.0	30.9

a: (mole dihydroxy benzenes formed / mole of H_2O_2 fed).
*: TBA-OH is added to titaniumsilicate mixture.

vi. Nature of the template

In one experiment, an aqueous solution of TBA-OH (40% Fluka) was used instead of 20% methanolic TBA-OH. There was not much change in the rate of crystallization and fully crystalline material was obtained when the precipitation of TiO_2 or gel formation was avoided. The incorporation of Ti in the crystalline material obtained from the titanosilicate gel was poor as suggested by framework IR, UV-VIS and catalytic data (Table 3.3, sample C).

Other organic bases such as 1,8 diamino octane and trimethyl benzyl ammonium hydroxide, which are known to produce ZSM-11[61], did not yield TS-2. Under identical synthesis conditions, no crystalline material was observed even after 20 days.

C. Characterization

i. X-ray diffraction

The XRD pattern of TS-2 (SiO_2/TiO_2 = 29) (Fig.3.6 A) matches well with that of silicalite-2 (Fig.3.6 B). The crystalline titaniumsilicate (TS-2) is free from any MFI (ZSM-5 or TS-1) type impurity, which is often present[65,66] in ZSM-11 (MEL) as an intergrowth. In the XRD pattern of TS-2, the lines at $2\theta \simeq 9.05°$ and 24.4° (characteristic of MFI structure) are completely absent[65,66]. Further a peak at $2\theta \simeq 45°$ is present as a singlet in MEL while in MFI it is observed as a clear doublet[66], suggesting that the TS-2 sample is a pure MEL-analog, without any MFI impurity.

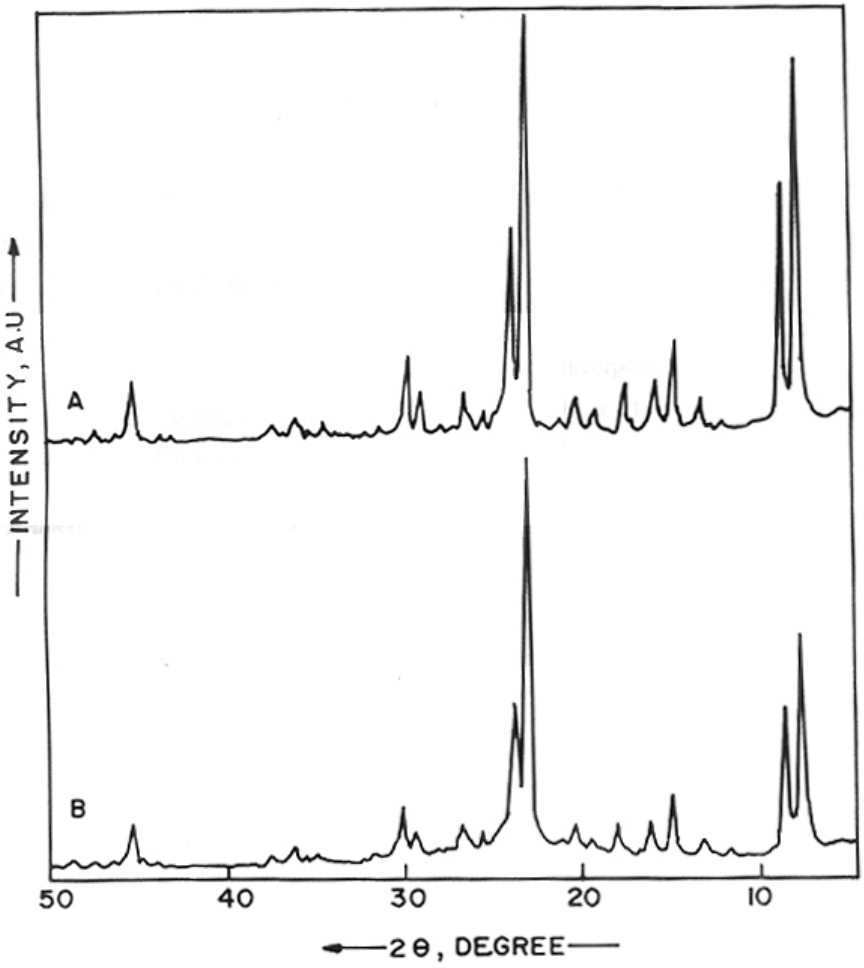

Fig.3.6. X-ray powder paterns of TS-2 (A) and Silicalilte-2 (B) calcined at 823 K.

The replacement of Si by the larger Ti^{4+} ions in the framework causes an increase in the lattice parameters and hence the unit cell volume. Fig.3.7 depicts the regular increase in the unit cell parameters a, c and volume, v with the increase in the Ti content of the TS-2. This is consistent with the incorporation of the larger Ti^{4+} ions in the silicalite-2 structure. The deviation in the case of sample 6 (SiO_2/TiO_2 = 14) (Table 3.2) is significant indicating that all the Ti in sample 6 is not incorporated into the framework. This fact is more clearly illustrated in Fig.3.8, where the XRD patterns of the samples 5 and 6, (calcined at 823) exhibit a peak at 2θ = 25.4° (Fig.3.8, curves A and B, see shaded area), characteristic of crystalline TiO_2 (anatase). After calcination at 1073 K, the intensity of the peak at 2θ = 25.4° increased further in the case of sample 6 (curve A) and not sample 5 (Fig.3.8, curves C and D). These results suggest the presence of exatra lattice Ti in sample 6. The maximum incorporation of Ti in TS-2, achieved during the present study, corresponds to a SiO_2/TiO_2 ratio = 21 (sample 5). A much larger incorporation of Ti has been claimed in the case of TS-1[67].

ii. Framework IR spectroscopy

The framework IR spectra of four TS-2 samples with different crystallinities and an amorphous titaniumsilicate gel calcined at 523 K are shown in Fig.3.9. As the crystallinity increases, the peaks characteristic of the MEL structure develop and become sharper. The peak at 575 cm^{-1} exhibits a direct correlation with XRD crystallinity. An additional IR peak around 970 cm^{-1}, characteristic of titaniumsilicate molecular sieves[3-6] and titaniumsilicate glasses[68] is also present in all the samples of TS-2. The absorption lines for the following groups: $(SiO)_3Si$-OH, (SiO_3)Si-O-Ti-, $(SiO)_2Ti{=}O$[16] are located in the same region. The 960 cm^{-1} band was originally attributed[3,18,22] to the >Ti=O group. However, Boccuti *et al.*[5] attributed this band to the Si-O stretching of the polarized $SiO-Si-O^{\delta-}-Ti^{\delta-}(IV)$ bond. The assignment of 960 cm^{-1} as a stretching mode of the titanyl group, >Ti=O was excluded[5,12] by them for the following reasons.

1) The electronic transitions of titanyl group are not present in the UV-VIS reflectance spectrum of TS-1,
2) The peak at 960 cm^{-1} does not show any tendency to exchange with $^{18}O_2$ even at 973 K temperature,
3) It is totally insensitive to reduction in molecular H_2 at 973 K, and
4) It is not perturbed by filling of the pores and channels with CO (which being a weak Lewis base, is expected to interact with the positive centers and to perturb them).

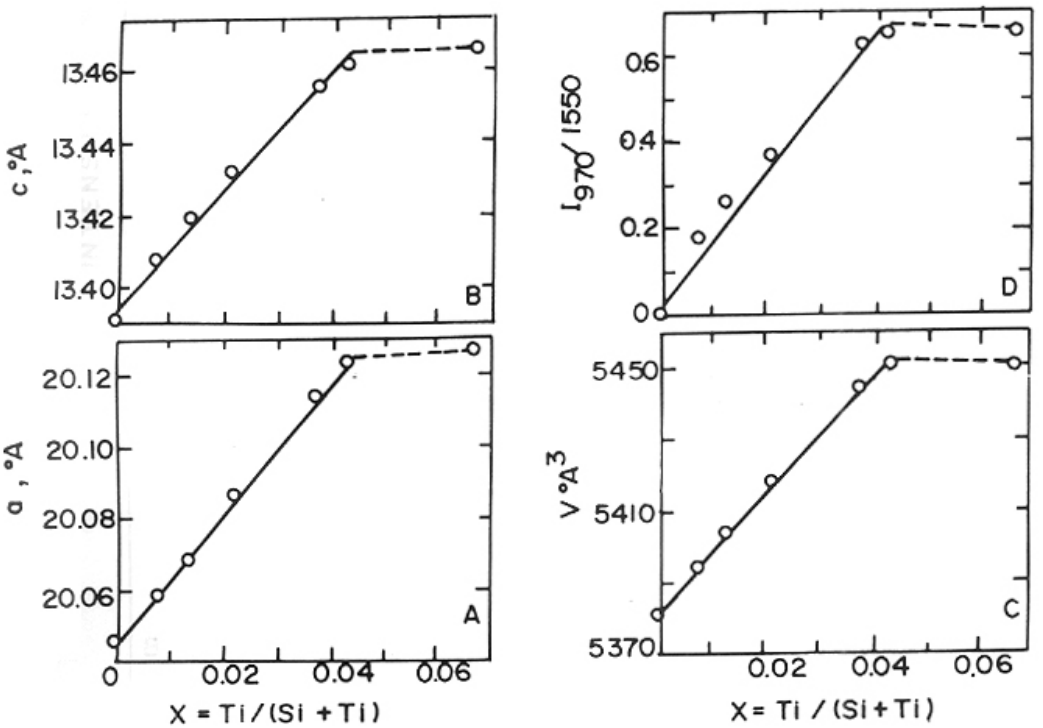

Fig.3.7. The unit cell parameters a = b (A), c (B) and volume, v (C) and ratio of intensities of 960/550 cm^{-1} IR bands vs mole fraction of titanium (x) (D) in various TS-2 samples.

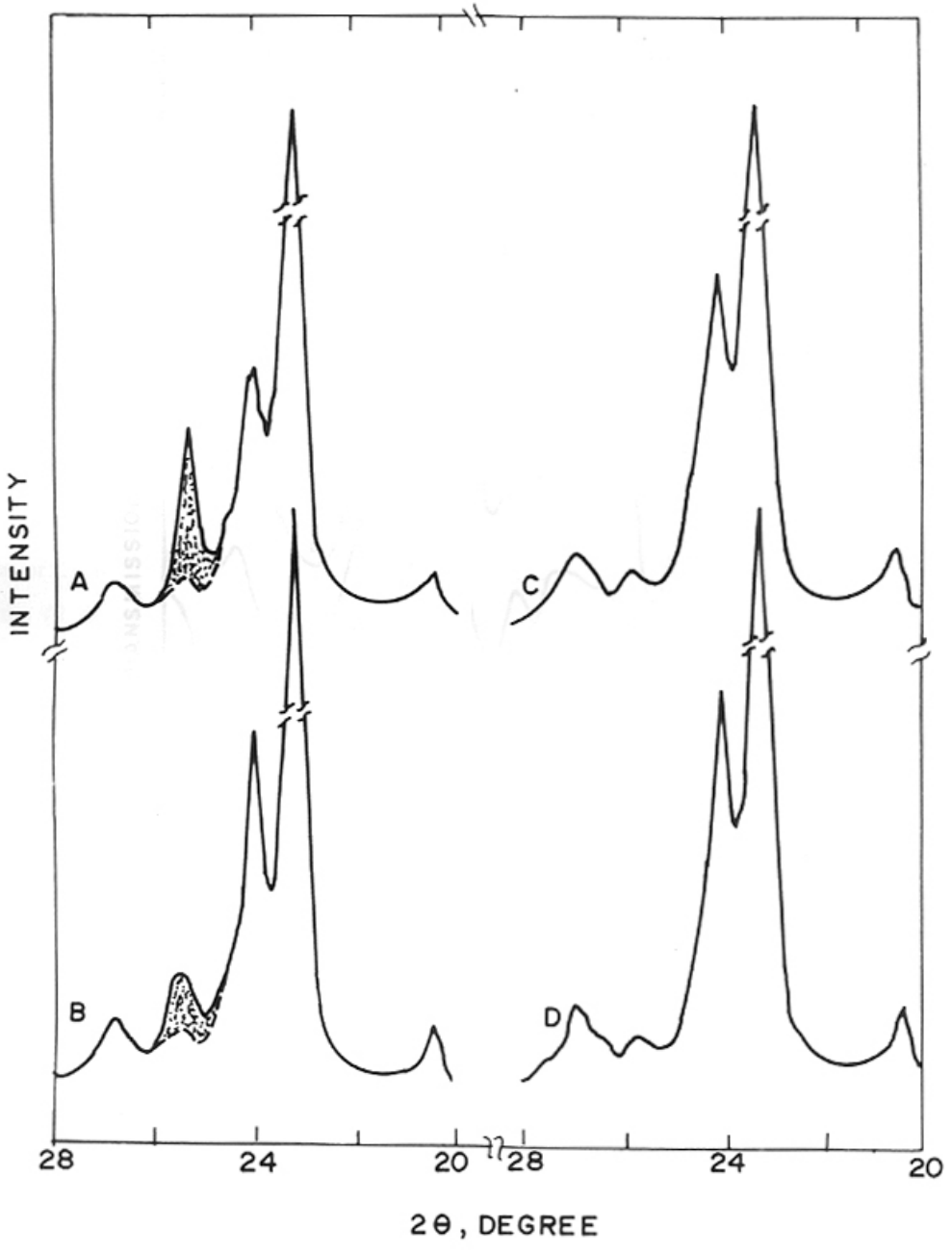

Fig.3.8. **X-ray powder patterns of samples 5 and 6, (Table 3.2) calcined at 1073 K (curves A and C) and at 823 K (curves B and D).**
The shaded area represents the enhancement of the intensity of XRD peak at 2 θ = 25.4° in sample 6 (curves A and B).

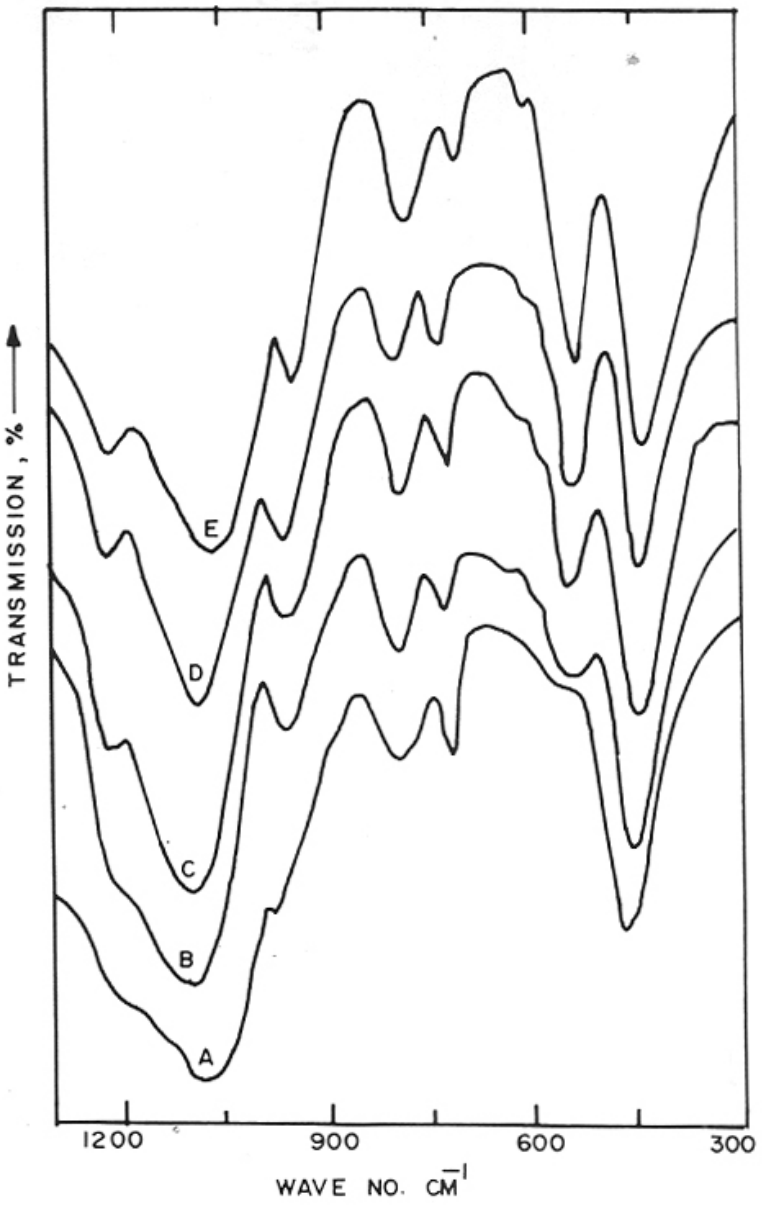

Fig.3.9. Framework IR spectra of calcined (823 K for 16 h) TS-2 samples.
Curves A-E represent samples with 0, 7, 32, 63 and 93 % crystallinity (XRD), respectively.
Molar gel composition: SiO_2/TiO_2 = 33; TBA-OH/SiO_2 = 0.2; H_2O/SiO_2 = 30. Crystallization Temp. (K) = 443.

Fig.3.10 depicts the IR crystallinity (calculated by comparing the ratio of the intensities of the IR bands at wavenumbers 550 and 400 cm^{-1}) vs XRD crystallinity of various samples. The IR crystallinity was always higher than the XRD crystallinity because the XRD technique requires a minimum long-range order of about 5 nm in the crystals. This observation indicates that smaller crystals (XRD amorphous) are formed in the beginning during crystallization.

The framework IR spectra of the TS-2 samples 1, 2, 4 and 5 (Table 3.2) are presented in Fig.3.11. An absorption band at 960 cm^{-1} is observed in all the samples. The intensity of this band increases with the Ti content of the TS-2. In Fig.3.7 D, the ratio of intensities of the IR bands at 960 cm^{-1} and 550 cm^{-1} band (the latter being characteristic of the MEL structure) is plotted against the Ti content of the calcined TS-2 samples. The observed increase in the value of this ratio with Ti content (except for sample 6) suggests a direct relation between the presence of Ti in the framework and the 960 cm^{-1} IR band. The 960 cm^{-1} band was not observed in the IR spectra of silicalite-2 which was synthesized under identical conditions. Again a deviation in the case of sample 6 (Fig.3.7 D), indicates the presence of extra lattice Ti (see unit cell data; Fig.3.7 A-C). Amorphous gels of both silicalite-2 and TS-2, exhibit a band at 960 cm^{-1}. This band disappears after calcination at 823 K in both cases. However, in the case of crystalline TS-2, the intensity of this band increases after calcination, while it decreases significantly in silicalite-2. These results indicate that the presence of the 950-970 cm^{-1} band in the IR spectrum of the as-synthesized Ti-containing molecular sieves may not be a conclusive evidence for the incorporation of Ti in the framework, though, it may also be due to such an incorporation. The presence of this band in the calcined titanium-silicate, however, confirms the incorporation of Ti in the framework.

iii. Raman spectroscopy

Raman spectra of TiO_2 (anatase), TS-2 and silicalite-2 are shown in Fig.3.12. TiO_2 exhibits a strong band at 140 cm^{-1}, in accordance with the reported data[92]. This band has been used to evaluate the amount of extra-framework Ti (up to 0.5 wt. % Ti) in titaniumsilicates[12]. Absence of this band in TS-2 indicates that most of the Ti is in the framework. A strong band at 970 cm^{-1} is observed only in the titniaumsilicate, TS-2. A similar band observed in the case of titaniumsilicate glasses, has been attributed to the vibrational mode of SiO_4 units bonded to Ti atoms in a polymeric structure[68,69]. These results show that Raman spectroscopy is a very good tool to determine the framework and non-framework Ti in titaniumsilicates.

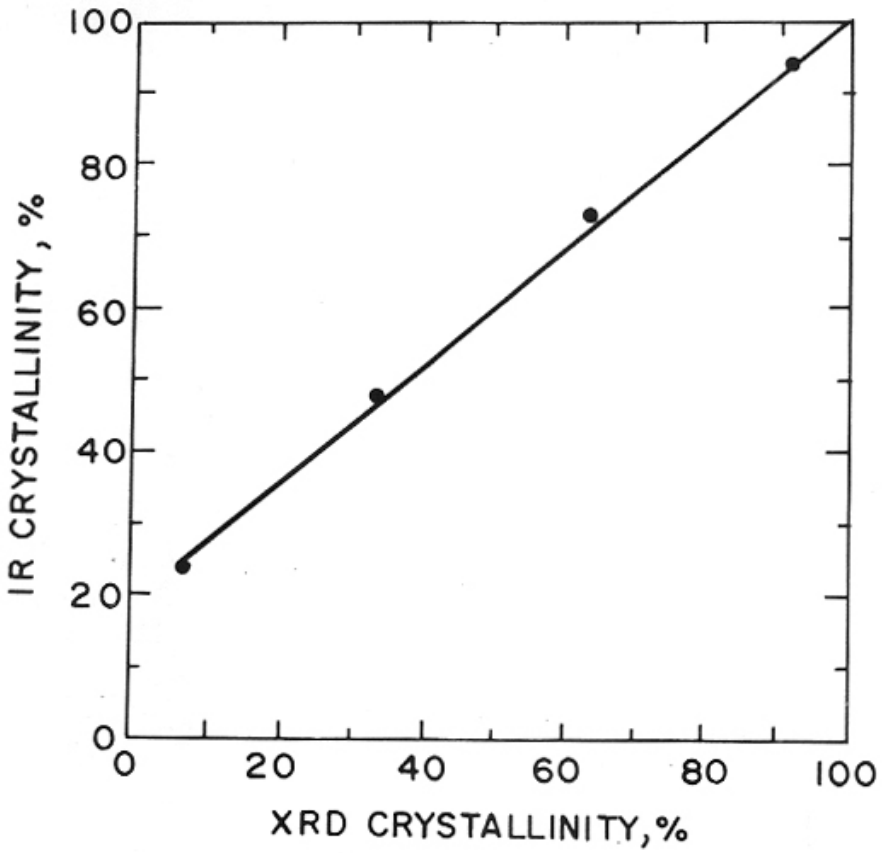

Fig.3.10. Relationship between x-ray crystallinity and IR crystallinity of TS-2 samples.

$$IR\ crystallinity = \frac{peak\ area\ of\ band\ at\ 550\ cm^{-1}\ of\ the\ sample}{peak\ area\ of\ the\ band\ at\ 550\ cm^{-1}\ of\ the\ reference\ sample} \times 100$$

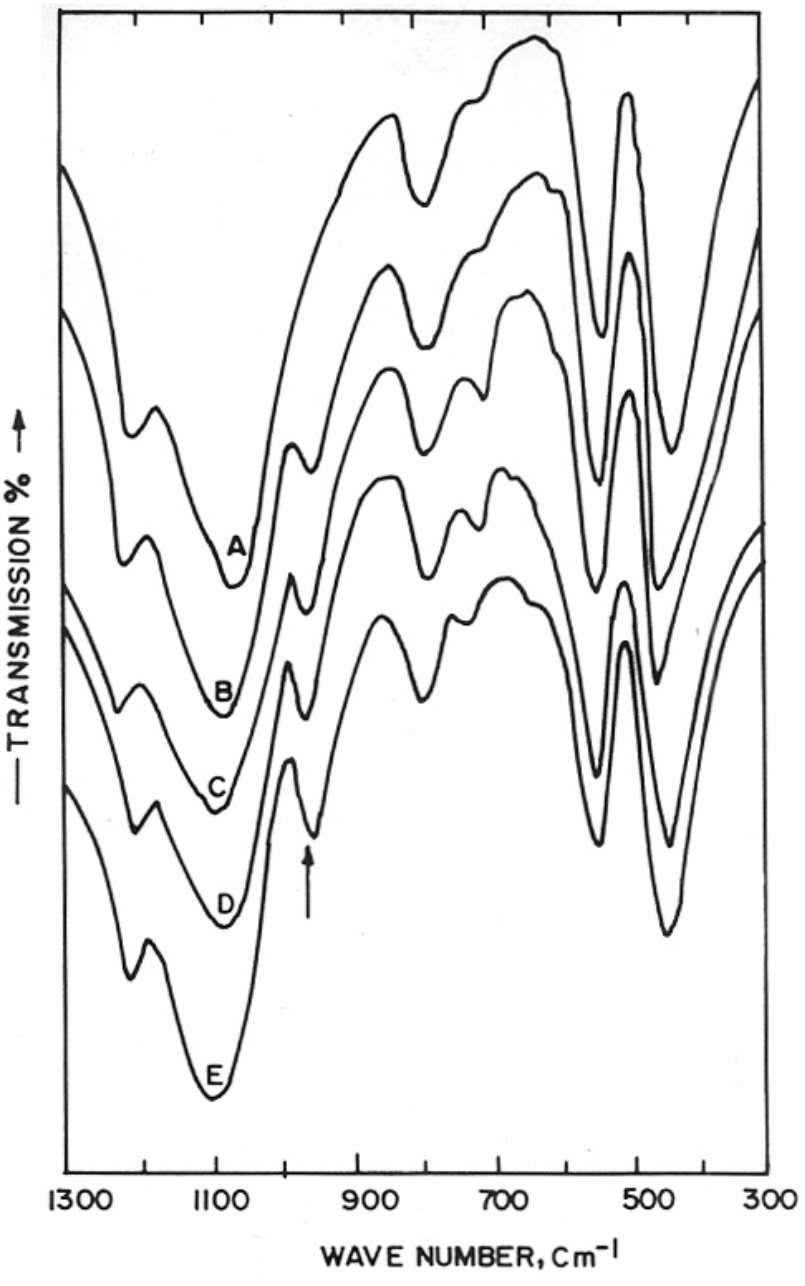

Fig.3.11. Framework IR spectra of silicalite-2 (curve A) and TS-2 samples 1, 2, 4 and 5 (curves B-E, respectively).

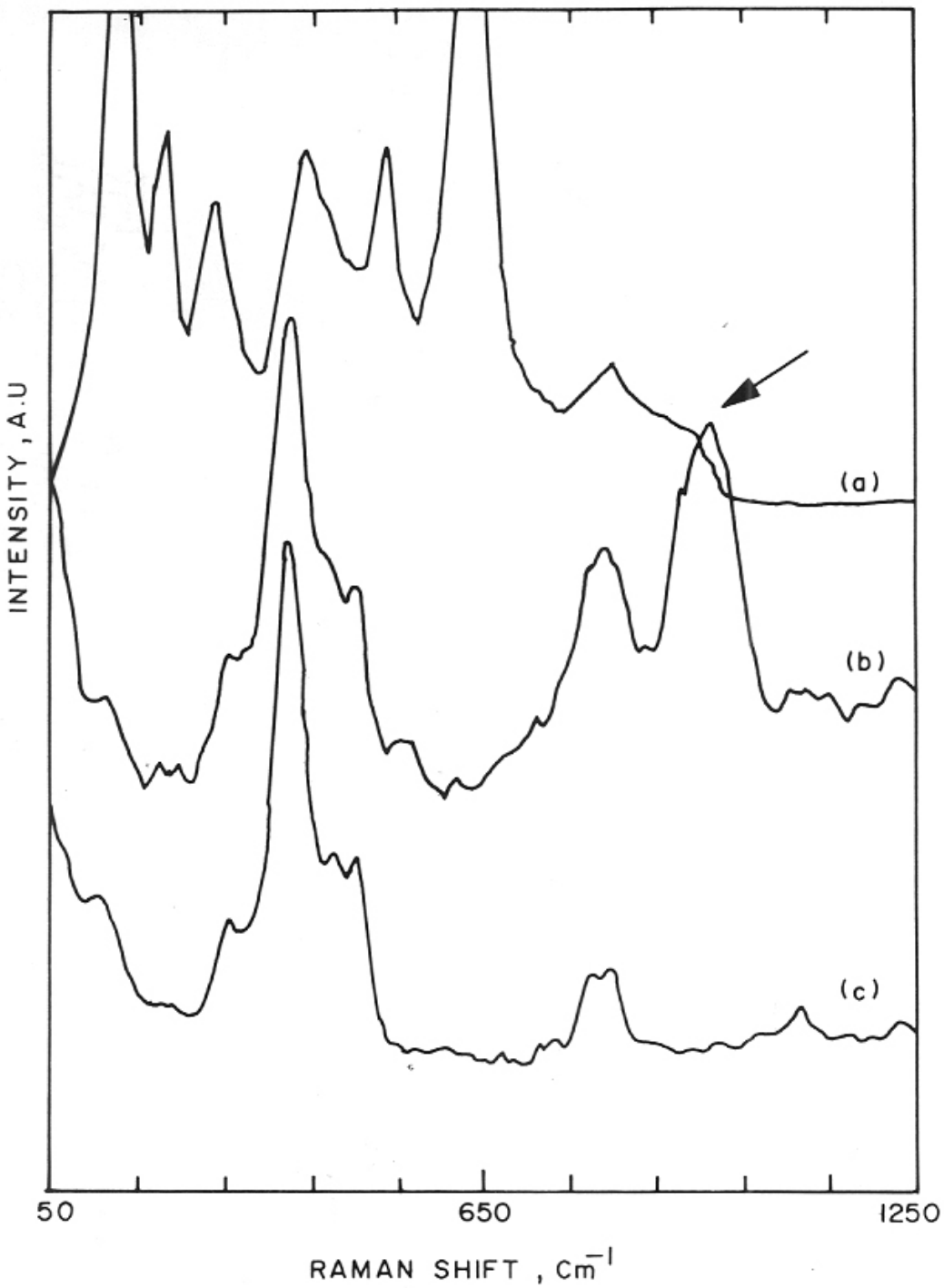

Fig.3.12. Raman spectra of TiO_2 (anatase) (a), TS-2 (b) and Silicalite-2 (c). Arrow indicates the band at 960 cm^{-1} in the case of TS-2.

iv. UV-VIS spectroscopy

The diffuse reflectance spectra of TS-2 (sample 4) and silicalite-2 are presented in Fig.3.13. TS-2 exhibits a strong band at around 212 nm (Fig.3.13, curve e); pure silicalite-2 does not show such a signal (curve f). A similar absorption around 212 nm has also been reported in the UV-VIS spectrum of TS-1[5,11,13]. The crystalline TiO_2 (anatase) has an absorption at around 330 nm (curve a) in agreement with reported values. This absorption around 212 nm is attributed to an electronic transition from ligand to metal involving isolated framework Ti(IV) in tetrahedral coordination[70]. The absorption due to isolated Ti(IV) in octahedral coordination is expected at about 240 nm. Fig.3.13 clearly indicates that the Ti is mainly present in the framework position in TS-2. Zecchina *el al.*[13] have used this technique for the quantitative determination of extraframework Ti in TS-1.

The UV-VIS spectra of the dried reaction mixtures used in the synthesis of samples B and C (Table 3.3) and the corresponding crystalline materials are also shown in Fig.3.13. The clear reaction mixture shows a band at 224 nm, where as the reaction mixture with TiO_2 precipitated in it exhibits a broad band at 256 nm. Since TiO_2 is present in the latter sample, the charge transfer band at 212 nm, characteristic of isolated tetrahedral Ti(IV), is shifted towards the value of anatase. The position of the bands in both samples is close to the values reported for isolated Ti(IV) in octahedral coordination. As the crystallization proceeds, the band at 224 nm of the clear solution shifts to 212 nm (tetrahedral Ti(IV)). But in the case of TiO_2 precipitated gel, three bands can be seen at 212, 262 and 380 nm (curve c). The bands at 262 and 380 nm may be due to an anatase like phase, where Ti-O-Ti linkages are present. These results demonstrate that the precursor titaniumsilicate mixture should be a clear solution to incorporate Ti efficiently into the zeolite framework. The results obtained in the hydroxylation of phenol over these samples are discussed in a later section.

The spectra recorded for M-MEL and M-TS-2 (where M = Al or Fe) are also shown in Fig.3.13. For comparison, a spectrum of TS-2 is also presented. Both Al-MEL and Al-TS-2 exhibit a band at about 214 nm, coinciding with that of TS-2. Fe-MEL has a band at 242 nm, characteristic of ferrisilicate molecular sieves[71]. As expected, Fe-TS-2 exhibits two bands at 212 and 242 nm, characteristic of isolated tetrahedral Ti(IV) and Fe(III), respectively, indicating that both Ti^{4+} and Fe^{3+} have been substituted into the MEL framework.

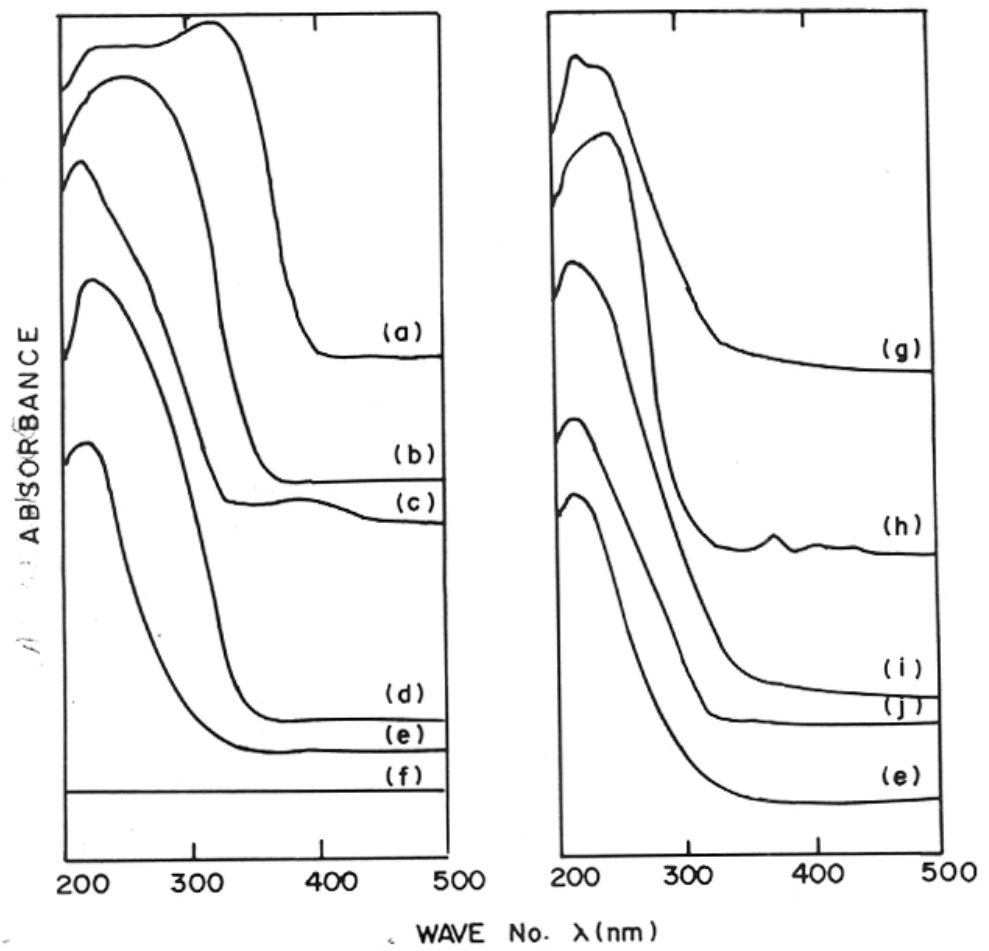

Fig.3.13. UV-VIS spectra of TiO_2, titaniumsilicates and MEL-analogs.
(a): anatase; (b): dried and calcined reaction mixture of TS-2, where TiO_2 is precipitated; (c): crystalline TS-2 (TiO_2 precipitated in the reaction mixture); (d): dried and calcined reaction mixture of TS-2; clear reaction mixture; (e): TS-2 obtained from clear solution; (f): Silicalite-2; (g): Fe-TS-2; (h): Fe-MEL; (i): Al-TS-2; (j): Al-MEL.

v. Adsorption

The adsorption capacities (at P/P_o = 0.5 and T = 298 K) of silicalite-2 and TS-2 (samples 4, 5 and 6 calcined at 823 and 1073 K) for n-hexane and cyclohexane are reported in Table 3.4. TS-2 has a sorption capacity comparable to that of silicalite-2. Sample 6 has a lower adsorption capacity probably due to the presence of occluded matter. After calcination at 1073 K, the adsorption capacity of sample 6 decreases further, due to partial blocking of the pores by occluded crystalline TiO_2 (anatase) (also see Fig.3.9). However, sample 4 and 5 do not show any change in sorption capacities after calcination at 1073 K.

Table 3.4. Adsorption properties of TS-2 samples[a].

	Si-2*	Sample 4		Sample 5		Sample 6	
Temp.(K)[b]	823	823	1073	823	1073	823	1073
n-Hexane	12.4	14.4	14.3	13.1	12.7	12.5	8.8
Cyclohexane	6.5	8.9	9.2	9.2	8.3	5.6	1.3

*: Si-2 = Silicalite-2
a: p/p_o = 0.5; Temp. (K) = 300 K; values reported are of absorbed per gram of sample
b: Calcination temperature.

vi. Scanning Electron Microscopy

The effect of SiO_2/TiO_2 ratio on the particle size of TS-2, determined using SEM are reported in Table 3.2. The substitution of Ti into the silicalite-2 framework decreases the particle size. SEM photographs of silicalite-2 and TS-2 synthesized with two different TBA-OH/SiO_2 ratios are presented in Fig.3.3. Particle size decreases with increase in the template concentration.

vii. Catalytic properties

It has been demonstrated[3,4,17,28,39] in the case of TS-1 that the catalytic activity in the hydroxylation of phenol with H_2O_2 originates from the framework titanium. We have also obtained similar results in the case of TS-2[40-42,45]. The activity of the titaniumsilicate, TS-2 in the hydroxylation of phenol indicates the presence of Ti species in the zeolite framework. The fact that the catalytic activity of titaniumsilicate molecular sieves in hydroxylation reactions originates from framework Ti is further confirmed by the complete inertness of silicalite-2

(Si-2), TiO_2 (both amorphous and crystalline), amorphous titaniumsilicate (obtained after drying, calcining and ion-exchanging the precursor amorphous gel used in the crystallization of TS-2) and physical mixtures of silicalite-2 and TiO_2 in this reaction.

In Table 3.3 the ratio of the intensities of IR peaks at 960 and 550 cm^{-1} is compared with catalytic activity (H_2O_2 selectivity and phenol conversion). The activity is found to be proportional to the intensity of the 960 cm^{-1} IR band. Aqueous TBA-OH also produces highly active TS-2 (sample B) provided care is taken to avoid the precipitation of TiO_2 during the mixing of the reactants, as otherwise TS-2 with low catalytic activity and low Ti incorporation is obtained (sample C).

D. Stabilities of MFI and MEL frameworks

i. Studies on hydrothermal/thermal stability

Thermal and hydrothermal stability of various elements like Al, Ga, Ge and B in the zeolite lattice positions has been studied extensively[72-74]. Severe thermal and hydrothermal treatments of zeolites result in the removal of these elements from the lattice positions, thereby lowering catalytic activities[75]. It is to be noted, that the presence of extraframework Al, Ga or Fe has also been found to enhance sometimes the catalytic activity of zeolites[74,76]. In the case of NU-1, Bellussi *et al.*[77] found that boron and ferrisilicate analogs are thermally less stable compared to alumino and gallosilicates. Thermal stability decreased in the following order: NU-1 > Ga-NU-1 > Fe-NU-1 > B-NU-1. The thermal stability of the Na-form of metallosilicates synthesized in the presence of tetrabutyl ammonium cation has been shown to decrease in the following order[78]: borosilicate < ferrisilicate ≈ TsVK < TsVM. Szostak *et al.*[79] have also reported that iron is thermally less stable in the zeolite framework than aluminium (at 823 K for 4 h; SiO_2/M_2O_3 = 55, where M = Al or Fe).

Though numerous studies have been carried out on the synthesis, characterization and catalytic properties of titaniumsilicate molecular sieves, the stability of Ti in the zeolite framework under thermal and hydrothermal conditions has not been examined in detail. The stability of Ti in a basic medium during the ammoximation of cyclohexanone has been examined by Petrini *et al*[80]. They found that Ti comes out of the framework and accumulates on the external surface of the solid. Reddy and Kumar[44] have shown that TS-2, thermally treated at 1073 K for 2 h possesses the same activity in the hydroxylation of phenol as the untreated one (calcined at 773 K). Recently, Genoni *et al.*[81] have reported that the framework

of TS-1 collapses at temperatures higher than 1100 K. Adsorption measurements using N_2 and p-xylene and TG and IR studies indicated the partial collapse of single crystallites and local collapse inside the channels.

In the case of metallosilicates, where a trivalent metal ion has been isomorphously substituted into the silicalite matrix, ion-exchange capacity can be used to determine the concentration of framework and non-framework metal ions quantitatively. Since titaniumsilicate molecular sieves do not exhibit any ion-exchange capacity, this method can not be used in their cases. Techniques are yet to be developed for the simultaneous quantitative estimation of the framework and extra-framework titanium in titaniumsilicate molecular sieves. However, the intensity of 960 cm^{-1} IR band and catalytic activity can be used to determine the extent of titanium present in the zeolite framework.

The results of our studies on the thermal and hydrothermal stabilities of TS-1 and TS-2 are described below.

XRD crystallinity and BET surface areas of silicalite-1, silicalite-2, TS-1 and TS-2 treated under thermal and hydrothermal (100 % steam) conditions are reported in Table 3.5. Crystallinity as well as surface area are found to decrease with increasing temperature of the treatment. In the case of titaniumsilicates, the structure remains intact even at 1173 K (Fig.3.14). However, under similar conditions, the structure of both the silicalites collapses; the silicalites transform into the stable crystabolite. The surface area of silicalites steamed at 1073 and 1173 K decreases to 2 m^2/g. Steaming at 973 K decreases the crystallinity of silicalite-2 to 53 %, while in the case of TS-2, crystallinity is still very high (96 %). Thermal stability of the silicalites is also less than that of titaniumsilicates. The surface area of TS-2 thermally treated at 1173 is more than that treated in the presence of steam, showing that stability in steam atmosphere is less.

In the case of titaniumsiloxanes, Andrianov and Zhdanov[82] have reported that Ti-O-Si linkages are more resistant towards hydrolysis than Si-O-Si linkages. The stability of M-O-Si linkage to hydrolysis decreases in the following order: Ti > Al > Sn. By analogy, Si-O-Ti linkages in zeolites may also be very stable.

The intensity of the band at 960 cm^{-1} in the IR spectra of titaniumsilicates TS-1 and TS-2 does not decrease even after steaming at 1273 K. This band has been attributed to the

Table 3.5. Effect of thermal and hydrothermal treatments on the surface area and crystallinity of titaniumsilicates and silicalites*

Catalyst	Steaming temp.(K)		Surface area		XRD crystallinity, %	Micro pore volume[a]
	Thermal	Hydrothermal	BET[+]	amorphous[++]		
TS-2	823	-	460	8	100	0.18
TS-2	-	973	389	47	96	0.18
TS-2	-	1073	359	25	92	0.14
TS-2	-	1173	291	13	83	0.11
TS-2	1173	-	394	43	87	0.14
TS-1	823	-	522	21	83	0.20
TS-1	-	1173	348	10	81	0.18
TS-1	1173	-	465	12	83	0.19
Silicalite-2	823	-	430	-	100	0.14
Silicalite-2	-	973	175	-	53	0.07
Silicalite-2	-	1073	-	2	0	-
Silicalite-2	1073	-	-	2	0	-
Silicalite-1	-	1073	-	2	0	-

*: All samples were calcined at 773 K prior to thermal/hydrothermal treatments.

+: S_{BET}, estimated from p/p_o = 0.006 to 0.05.

++: t-area, claculated from t-plots in the p/p_o range of 0.35 to 0.6.

a: Calculated from extrapolation of t-plots.

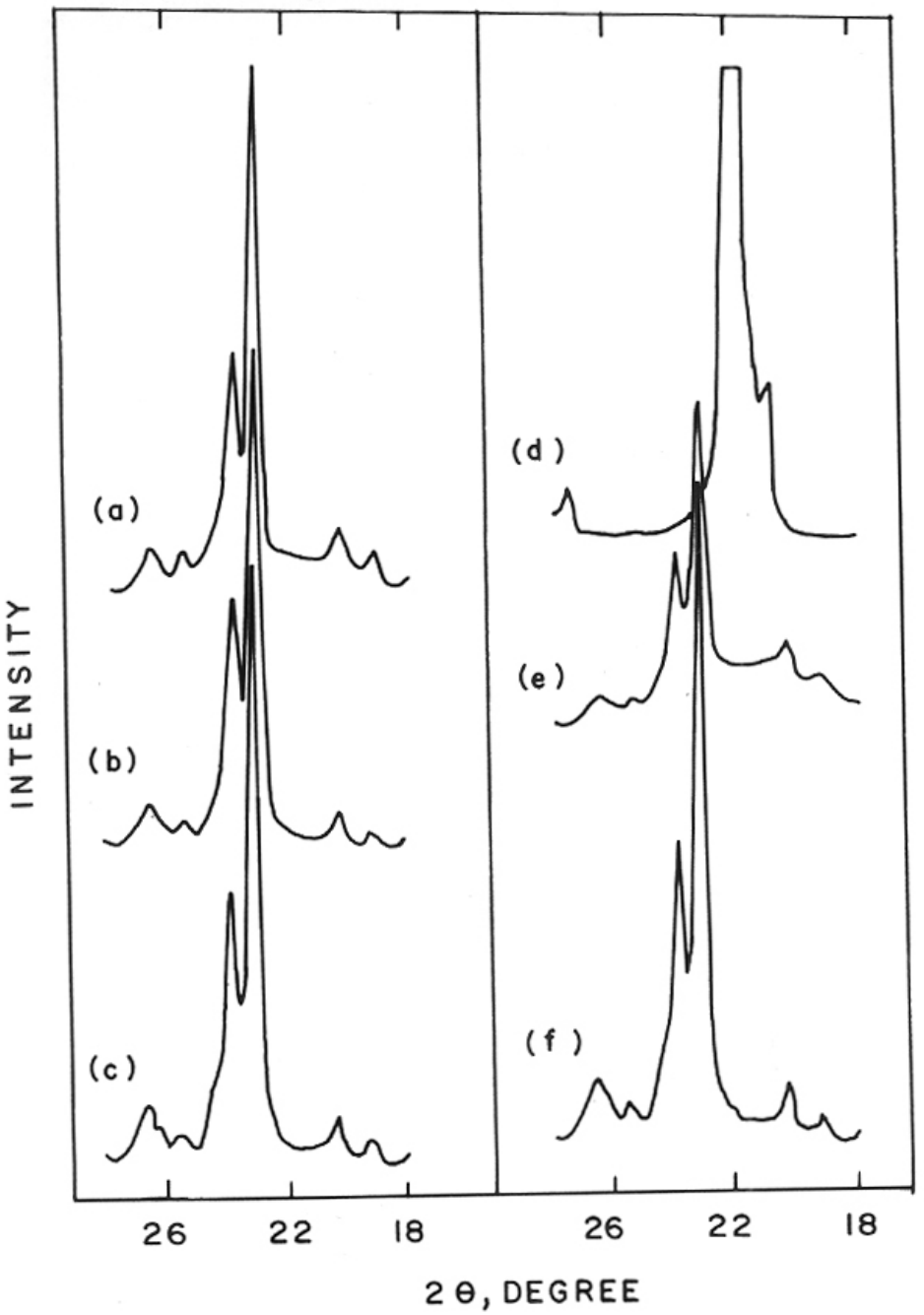

Fig.3.14: **X-ray diffraction patterns of TS-2 and silicalilte-2 pretreated at different conditions.**
(a): TS-2, steamed at 1173 K for 5 h; (b): TS-2, thermally treated at 1173 K for 5 h; (c): TS-2, calcined at 823 K for 16 h; (d): silicalite-2, thermally treated at 1173 K for 5 h; (e): silicalite-2, treated at 973 K for 5 h and (f): silicalite-2, calcined at 823 K for 16 h.

Table 3.6. Effect of thermal and hydrothermal treatments on TS-1 and TS-2 in the oxidation of n-hexane

Reaction conditions: Catalyst = 0.2 g; Temp. (K) = 373; Solvent = Acetone (20 ml); n-C_6 = 10 g; n-C_6 : H_2O_2 (moles) = 3; Reaction duration (h) = 5.

Catalyst[a]	Steamed at Temp. (K)	n-C_6 Conversion (wt. %)	H_2O_2 utilization[b] (mole %)	Break-up of products[c] 2-ol	2-one	3-ol	3-one	Others[d]	2-/3-ratio[e]	ol-/one ratio[f]
TS-2	823[g]	18.9	61.6	31.0	24.0	17.9	16.6	10.6	1.60	1.20
TS-2	973	14.5	44.9	30.8	22.0	19.0	15.7	12.2	1.51	1.31
TS-2	1073	5.9	12.3	26.2	14.8	16.9	15.0	27.1	1.29	1.45
TS-2	1173	4.8	6.8	22.3	11.2	15.8	11.0	39.7	1.25	1.72
TS-2	1173[g]	6.2	12.9	26.9	14.7	15.2	17.1	26.1	1.29	1.32
TS-1	823[g]	24.2	79.5	31.4	29.4	17.9	15.6	5.7	1.81	1.10
TS-1	1173	6.8	17.8	29.1	12.8	16.9	15.7	25.6	1.29	1.61
TS-1	1173[g]	8.8	27.0	18.6	21.2	10.6	23.9	25.7	1.15	0.65

a: TS-2: SiO_2/TiO_2 = 29; TS-1: SiO_2/TiO_2 = 22.

b: H_2O_2 utilized for mono functional product formation.

c: 2-ol = 2-hexanol; 2-one = 2-hexanone; 3-ol = 3-hexanol; 3-one = 3-hexanone.

d: Mostly oxygenates with more than one functional group.

e: 2-/3-ratio = (2-ol + 2-one/3-ol + 3-one).

f: -ol/-one = $\sum$ alcohols / $\sum$ ketones.

g: Thermal treatment in the absence of steam.

stretching mode of [SiO_2] bonded to titanium. The presence of this band at about the same intensity level in the steamed sample confirms that Si-O-Ti linkages are stable even under severe thermal and hydrothermal conditions.

The results of the studies on oxyfunctionalization of n-hexane are reported in Table 3.6. The activity decreases with increasing temperature of steaming in the case of both TS-1 and TS-2. However, thermally treated samples show slightly larger activity in this reaction compared to hydrothermally treated ones. Oxidation at 3-position and formation of the ketones increase with increasing steaming severity. The larger decrease in the XRD crystallinity and surface areas when compared to loss in intensity of the 960 cm^{-1} IR band of the thermally and hydrothermally treated samples indicates that cleavage of the Si-O-Si linkages is more. The larger decrease in the activity when compared to surface area and crystallinity loss is probably due to pore blockage by amorphous silica and not because the Ti has come out of the framework (IR data suggest the intactness of Si-O-Ti bonds). The relative crystallinities of TS-2 treated under thermal and hydrothermal conditions, calculated from different techniques have been reported in Table 3.7.

Table 3.7. Relationship between relative crystallinities calculated by different techniques and catalytic activity

Catalyst*	Relative crystallinity		Surface area	Catalytic
	XRD	IR	(Relative)	activity[a]
TS-2 (823/5)	100	100	100	100
TS-2 (973/5)	96	90	85	77
TS-2 (1073/5)	92	98	78	31
TS-2 (1173/5)	83	82	63	25
TS-2 (1173/5)[b]	87	-	76	33

*: Pretreatment condition: (Temp. K/h).
a: Oxyfunctionalization of n-C_6 (see Table 3.6 for details) (relative values).
b: Hydrothermal conditions.

ii. Theoretical studies on influence of isomorphous substitution in MFI

Recent studies based on lattice energy calculations[83] have revealed that TS-1 is more stable than silicalite-1 and ZSM-5. Extended Huckel Molecular Orbital calculations on suitable clusters have been used to study the stability changes in MFI lattice due to substitution of titanium, in the place of silicon.

Monomeric cluster models namely $T(OH)_4$, which represent the 12 crystallographically distinct sites of ZSM-5 lattice have been considered. The methodology of cluster generation was the same as the procedure reported by Fripiat *et al.*[84] and the geometry of the clusters were taken from a reported crystallographic study[85]. Further, to account for the effect of adjacent TO_4 group, a dimer cluster which is derived by replacing a OH group in the monomer by an $OSi(OH)_3$ group, namely $(OH)_3T\text{-}O\text{-}T(OH)_3$ was considered. For each site, four dimeric clusters were considered, wherein the adjacent tetrahedral group corresponded to the geometry of four neighbouring TO_4 groups. The calculations were carried out for the all-silica MFI framework corresponding to silicalite-1 as well as for Si-O-Ti clusters representing TS-1. The results of these calculations are given in Table 3.8.

Table 3.8. Energetics of isomorphous substitution in silicalite-1[83].

Crystallographic site in silicalite-1 in orthorhombic symmetry	Substitution energy of Al in silicalite-1	Substitution energy of Ti in silicalite-1
1	0.117	- 0.192
2	0.073	- 0.235
3	0.093	- 0.230
4	0.098	- 0.190
5	0.060	- 0.215
6	0.083	- 0.188
7	0.095	- 0.250
8	0.103	- 0.183
9	0.088	- 0.210
10	0.083	- 0.213
11	0.070	- 0.178
12	0.073	- 0.233

Lower stability of Al compared to Ti in pentasil zeolite framework is further evidenced by the results obtained from ^{27}Al NMR studies on an Al-TS-2 sample. When Al-TS-2 was steamed at 1073 K for 5 h, considerable amount of Al came out of the framework. Fig.3.15 clearly shows the presence of octahedral Al in the steamed sample (Fig.3.15 b), which is completely absent before steaming (Fig.3.18 a). The intensity of 960 cm^{-1} band in IR was retained even after steaming indicating the stability of Ti in the zeolite framework.

The results of the theoretical calculations could be summarized as:

1) The substitution of aluminium in silicalite-1 is an endothermic process; hence the lattice of Al-MFI will be less stable than silicalite-1.

2) The substitution of titanium in silicalite-1 is an exothermic process, hence the lattice of TS-1 will be more stable than silicalite-1.

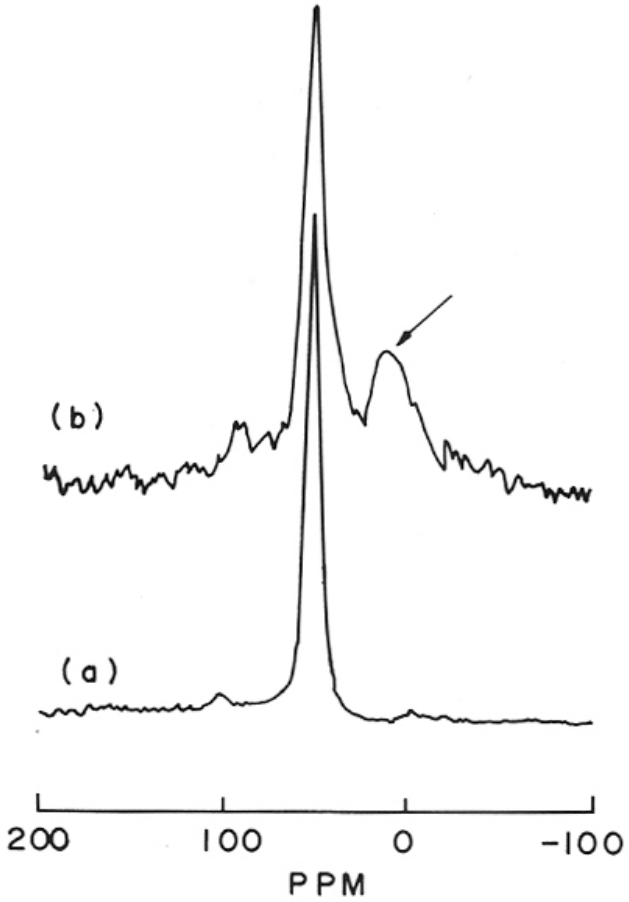

Fig.3.15. **^{27}Al MASNMR spectra of Al-TS-2 samples.**
a: calcined at 823 K for 16 h in dry air b: steamed at 1073 K for 5 h. Arrow indicates octahedral Al^{3+}.

3) The absolute values of energy can not be considered for quantitative prediction due to the small cluster model. However, the final lattice energy will be an additive property due to the large number of such substitutions. The preference energy of siting of titanium in the 12 sites lie within a small energy range. However, based on various sites, there could be a maximum of two titanium atoms in the repeating secondary building unit of MFI. This corresponds to a SiO_2/TiO_2 ratio of 6.

4) The sizes of the ions decide the substitution site in the lattice depending on the geometry of the site (T-O & T-O-T). The electron configuration and the electronegativity of the ions decide the stability of the lattice.

3.1.3. CONCLUSIONS

The following conclusions are drawn based on the detailed studies of the kinetics of crystallization and characterization of the new titaniumsilicate, TS-2 (MEL):

1) TS-2 can be readily synthesized using tetrabutyl ammonium hydroxide as the organic additive. Other organic bases (like 1,8 diamino octane or trimethylbenzyl ammonium hydroxide), which have been used in the preparation of the Al-analog, ZSM-11 do not produce TS-2. To efficiently synthesize a catalytically active titaniumsilicate (TS-2), the formation of TiO_2 and/or alkali metal titanates in the reaction mixture should be avoided, and the conditions which favour the formation of titaniumsilicate mixtures containing ≡Si-O-Ti≡ bonds should be adopted. Ti-tetrabutoxide is preferred over titanium tetraethoxide as a source of Ti, mainly because the hydrolysis of the former is slower.

2) Some analogies exist between the synthesis of titaniumsilicates (e.g. TS-2) and other high silica molecular sieves:
   i) an increase in the SiO_2/TiO_2 ratio in the reaction mixture and crystallization temperature enhances the rate of crystallization,
   ii) there exists an optimum range of [organic base]/[SiO_2] ratio and pH, below which the crystallization is extremely slow while high values retard the crystallization.

3) The incorporation of Ti in the tetrahedral silica framework is quite efficient under optimum reaction conditions. The increase in the pH of the mother liquor (Δ pH) with crystallization is caused by the incorporation of probably both Ti as well as Si in the framework.

4) With an increase in SiO_2/TiO_2 molar ratio, the yield of the crystalline material decreases. The maximum yield which could be obtained was 90 %.

5) Evidence for the presence of Ti in the MEL framework was obtained from XRD (a regular increase in the unit cell parameters with Ti content), framework IR spectroscopy (an

increase in the intensity of 970 cm^{-1} band with Ti content), Raman spectroscopy (presence of a band at 960 cm^{-1}), UV-VIS spectroscopic techniques and its catalytic activity in the hydroxylation of aromatics.

6) Experimental studies indicated higher stability for Ti in the zeolite framework when compared to Si and Al, confirming the results of recent theoretical studies.

3.2. PART-II - CATALYTIC PROPERTIES OF TS-2

The isomorphous substitution of Ti^{4+} in the ZSM-5 framework has led to interesting new routes for the production of organic fine chemicals. The titaniumsilicate analogs do not posses strong acidity, characteristic of the aluminosilicates. They however, catalyze interesting selective oxidation reactions in the presence of hydrogen peroxide. The most studied titaniumsilicate is TS-1, an ZSM-5 isomorph (MFI structure). This molecular sieve has been found to catalyze a number of organic reactions like the hydroxylation of aromatics[3,4,28,36], the selective oxidation of alkanes[21-23], the ammoximation of cyclohexanone[25,30] the selective oxidation of primary alcohols to aldehydes and secondary alcohols to ketones[3,25], the epoxidation of olefins[3,27,31,38], the oxidative dehydrogenation of ethanol to acetaldehyde in air[32] and the Beckmann rearrangement of cyclohexanone oxime[33,34]. TS-2 has also been reported to catalyze the ammoximation of carbonyl compounds[45,48], the selective oxidation of alkanes[46,48,50], the hydroxylation of aromatic compounds[42,47,48], the epoxidation of olefins[49], the Beckmann rearrangement of cyclohexanone oxime[86] and the sulfoxidation of thioethers[51]. Since both TS-1 and TS-2 do not possesses any acidity, they are catalytically inactive in Brönsted acid catalyzed reactions.

The aim of this section is to examine the catalytic properties of TS-2 in the following reactions:

1) Selective oxidation of alkanes
2) Ammoximation of carbonyl compounds
3) Hydroxylation of aromatic compounds
4) Epoxidation of olefins
5) Cleavage of C=C bond during epoxidation
6) Beckmann rearrangement of cyclohexanone oxime and
7) Oxidation of alcohols.

3.2.1. OXYFUNCTIONALIZATION OF ALKANES

The introduction of oxygen containing functional groups in alkanes has been reported over most homogeneous and heterogeneous catalysts[87-89] with monooxygen donor oxidants, like hydroperoxides, H_2O_2 and iodosobenzene. Molecular oxygen also has been used for the oxidation[87,90]. This reaction also has been reported to be catalyzed by a Pd-Fe zeolite[91] and metallo porphyrins[92]. Recently, the titaniumsilicate molecular sieve TS-1 was shown[21-23] to catalyze the oxyfunctionalization (selective oxidation) of alkanes by hydrogen peroxide with good selectivities.

We have found that the titaniumsilicate TS-2, also catalyzes the oxidation of alkanes with high selectivities[46,48,50].

A. Studies on n-hexane

The results of the studies using n-hexane as the substrate are presented below.

i. Activity of different catalysts

The oxidation of n-hexane was studied over a number of MEL isomorphs, *viz.*, silicalite-2, ZSM-11, Al-TS-2 and TS-2. For comparison, a blank experiment with a high surface area amorphous silica was also carried out. An experiment was also carried out with TS-1. The major products of the reaction are 2- and 3-hexanols and 2- and 3-hexanones. Small quantities of compounds with more than one functional group were also detected. However, these compounds have not been analyzed in detail. Also, 1-hexanol and hexanal were not detected.

The results are presented in Table 3.9. The most active catalysts are found to be TS-1 and TS-2. They are also the most selective for the formation of the mono-functional compounds. Al-TS-2, containing both Al and Ti is also catalytically active. On the other samples, the activities and selectivities are very low. The lower activity of Al-TS-2 when compared to TS-2 (both contain the same amount of Ti) is due to the rapid decomposition (and loss) of H_2O_2 by the acid (Al^{3+}) centers in the zeolite. It therefore appears that Ti^{4+} ions are responsible for the selective oxidation property of TS-2. If we examine the ratio of the 2-substituted to the 3-substituted compounds over the different catalysts (Table 3.9), we note that Ti activates the 2-position to a greater extent for insertion of the oxygen function. Similar results have also been reported by Huybrechts *et al.*[22] in their studies using TS-1. The larger conversion noted by us for TS-1 (compared to TS-2) could be due to differences in the structures, crystallite sizes and Ti-distribution in the two samples.

ii. Influence of Ti content of TS-2

Three TS-2 samples having different Ti contents (Ti/(Ti+Si) = 0.033, 0.014, 0.008) were examined for catalytic performance under identical conditions. The results are presented in Table 3.10. For comparison, the results obtained with silicalite-2 (Ti/(Ti+Si) ratio ≈ 0) are also included in the table. As expected, the activity and selectivity of the catalysts increased with increasing Ti content. However, the increase in activity is not in proportion to the increase in the Ti content of the samples if we examine the data obtained after 5 h (Table 3.10). The influence of duration of run on conversion in the case of two different TS-2

Table 3.9. Oxidation of n-hexane over different zeolites with MEL structure

Reaction conditions: Catalyst (g)/mole n-C_6 = 1.76; Temp.(K) = 373; n-C_6 : H_2O_2 (moles) = 0.116 : 0.039; Reaction duration (h) = 5; Solvent = Acetone (20 ml).

Catalyst	n-C_6 conversion (wt. %)	H_2O_2[+] utilization (mole %)	Break-up of products (wt. %)[*]					2-/3- ratio[++]	Product[+++] selectivity
			2-ol	2-one	3-ol	3-one	Others		
TS-2[**]	18.9	61.6	31.0	24.0	17.9	16.5	10.6[a]	1.6	89.4
Al-TS-2	9.8	13.7	20.1	14.7	18.3	8.0	38.9[b]	1.3	61.1
AL-MEL	5.3	4.9	4.3	17.4	4.2	10.6	63.5[b]	1.5	36.5
Silicalite-2	3.3	3.1	7.0	7.7	4.9	7.5	72.9[c]	1.2	27.1
SiO_2[***]	3.7	4.7	8.4	11.1	6.5	9.4	64.6[c]	1.2	33.4
TS-1[**]	24.2	79.5	31.4	29.4	17.9	15.6	5.7[a]	1.8	94.3

* : 2-ol = 2-hexanol; 3-ol = 3-hexanol; 2-one = 2-hexanone and 3-one = 3-hexanone.

** : TS-2: SiO_2/TiO_2 = 29; Al-TS-2: SiO_2/TiO_2 = 70, SiO_2/Al_2O_3 = 74; AL-MEL: SiO_2/Al_2O_3 = 69; SiO_2/TiO_2 = 31.

*** : Fumed silica, type S-5005, supplied by Sigma Chemical Co., Mo, U.S.A.

\+ : H_2O_2 utilized for mono functional product formation.

++ : 2-/3- ratio = (2-ol + 2-one/3-ol + 3-one).

+++ : Product selectivity = (Σ 2- and 3- compounds/n-hexane reacted) X 100.

a : Mostly oxygenates with more than one functional group.

b : Methyl cyclopentane, benzene, alkyl benzenes and oxygenates.

c : Similar to b, but with additional unidentified oligomeric material.

Table 3.10: Influence of Ti content and catalyst concentration on the oxidation of n-hexane

Reaction conditions: Temp.(K) = 373; n-C_6 : H_2O_2 (moles) = 0.116 : 0.039; Reaction duration (h) = 5; Solvent = Acetone.

Ti(Si+Ti)	Amount of catalyst (g/mole)	n-C_6 convn. (wt. %)	$H_2O_2^+$ sel. (mole %)	Break-up of products (wt. %)[a]					-ol/-one ratio[b]	2-/3-ratio[c]	Product sel.[d]
				2-ol	2-one	3-ol	3-one	Others[e]			
0.000	1.7	3.3	3.1	7.0	7.7	4.9	7.5	72.9[f]	0.8	1.2	27.1
0.008	1.7	11.3	33.0	26.1	20.3	23.1	16.0	14.5	1.4	1.2	85.5
0.014	1.7	15.4	47.2	30.3	21.2	19.2	16.1	13.2	1.3	1.5	86.8
0.033	1.7	18.9	61.6	31.0	24.0	17.9	16.5	10.6	1.2	1.6	89.4
0.033	0.9	14.4	43.8	34.6	19.3	18.8	15.3	12.0	1.5	1.6	88.0
0.033	4.3	19.8	68.1	33.2	26.6	18.6	15.4	6.2	1.2	1.8	93.8
0.033	8.6	20.8	73.8	32.1	29.0	18.3	15.7	4.9	1.1	1.8	95.1

+ : H_2O_2 utilized for mono functional product formation.

a : 2-ol = 2-hexanol; 3-ol = 3-hexanol; 2-one = 2-hexanone and 3-one = 3-hexanone.

b : -ol/-one ratio = Σ alcohols/Σ ketones.

c : 2-/3- ratio = (2-ol + 2-one/3-ol + 3-one).

d : Product selectivity = (Σ 2- and 3- compounds/n-hexane reacted) X 100.

e : Mostly oxygenates with more than one functional group.

f : Similar to a, but with additional unidentified oligomeric material.

samples (with SiO_2/TiO_2 = 29 and 124) is presented in Fig.3.16 (curves (a) and (c). It is observed that though conversion increase with time, beyond 3 h the increase is small. Examining Table 3.10, it is noticed that both the 2-/3- ratio and alcohol/ketone ratio are affected by a change in the Ti-content. The increase of -ol/-one ratio with decreasing Ti-content suggests that Ti-ions also catalyze the oxidation of alcohols to ketones.

iii. Influence of concentration of catalyst

Table 3.11 presents the results of the experiments carried out with different amounts of catalyst. A general trend of increasing conversion and selectivity for mono-functional products with increasing catalyst concentration is noticed, the increase being small beyond a catalyst concentration of 1.7 g/mole n-hexane. Compared to the 2-/3- ratio the alcohol/ketone ratio is more influenced by an increase in the catalyst amount (Table 3.11). Fig.3.16 also depicts the influence of duration of run on conversion at two catalyst concentrations (curves (a) and (b)).

The trends reported in Fig.3.16 for both the influence of catalyst concentration (curves (a) and (b)) and Ti content (curves (a) and (c)) are in the same expected direction; since only the Ti species are active centres for the reaction, an increase in Ti content leads to a more rapid conversion of n-hexane. However, beyond 3-4 h, H_2O_2 in the mixture is totally depleted and further n-hexane conversion does not take place. The deplation of H_2O_2 is due to both non-selective decomposition (and loss) and selective consumption in the reaction. Blank experiments carried out both in the presence and absence of the catalyst showed that all the H_2O_2 decomposed within a 5 h period. Hence, there is always a competition between reaction and decomposition during the run. When more Ti is present in the system, the reaction rate is enhanced compared to the decomposition rate.

iv. Influence of feed composition (n-C_6/H_2O_2 ratio)

Keeping the concentration of n-hexane constant (0.116 moles), experiments were carried out with three different n-C_6/H_2O_2 (mole) ratios. The results are reported in Table 3.11. Conversion increases with increasing H_2O_2 content, but the product (mono-functional) selectivity decreases slightly because of the greater formation of secondary products with more than one functional group. The H_2O_2 utilization is also lower due to greator loss of H_2O_2 by decomposition. As expected, the alcohol/ketone ratio increases with decreasing H_2O_2 content.

Table 3.11. Influence of concentration of reactants

Reaction conditions: Catalyst (g)/mole n-C_6 = 1.7; Temp.(K) = 373; n-C_6 : H_2O_2 (moles) = 0.116 : 0.039; Reaction duration (h) = 5; Solvent = Acetone (20 ml).

Concentration of reactants (moles)		n-C_6 conversion	H_2O_2 utilization+	Break-up of products (wt. %)a					-ol/-one ratio[b]	Product selectivity [c]
n-C_6	H_2O_2	(wt. %)	(mole %)	2-ol	2-one	3-ol	3-one	Others[d]		
0.116	0.116	44.5	52.7	22.1	31.5	9.4	25.6	11.4	0.6	88.6
0.116	0.039	18.9	61.6	31.0	24.0	17.9	16.5	10.6	1.2	89.4
0.116	0.023	13.3	68.7	37.8	18.9	21.9	14.3	7.1	1.8	92.9

+ : H_2O_2 utilized for mono functional product formation.

a : 2-ol = 2-hexanol; 3-ol = 3-hexanol; 2-one = 2-hexanone and 3-one = 3-hexanone.

b : -ol/-one ratio = Σ alcohols/Σ ketones.

c : Product selectivity = (Σ 2- and 3- compounds/n-hexane reacted) X 100.

d : Mostly oxygenates with more than one functional group.

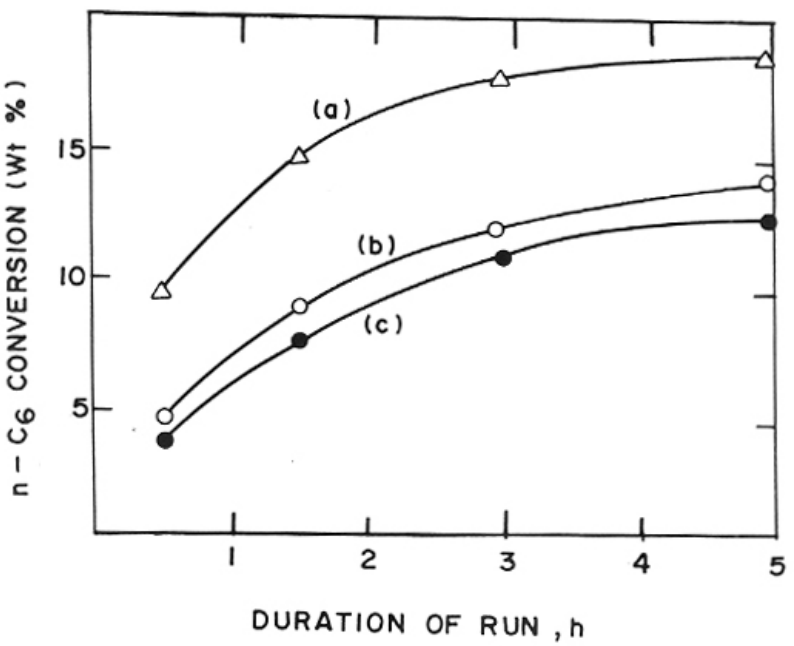

Fig.3.16. Influence of duration of run on n-hexane conversion.
Temp. (K) = 373; n-C_6 : H_2O_2 (mole) = 0.118 : 0.039; Solvent = Acetone.
(a): SiO_2/TiO_2 = 29, 1.7 g mol^{-1} n-C_6; (b): SiO_2/TiO_2 = 29, 0.9 g mol^{-1} n-C_6;
(c): SiO_2/TiO_2 = 124, 1.7 g mol^{-1} n-C_6.

v. Influence of temperature

Experiments carried out at different temperatures (Table 3.12) suggest the existence of an optimum temperature for maximum yields of the desired products (with single oxyfunctional group), H_2O_2 utilization and n-C_6 conversion. At high temperatures, n-C_6 conversion and H_2O_2 utilization are low because of greater H_2O_2 decomposition. At low temperatures, the formation of high boiling by-products (not identified in detail) decreases the product selectivity. The alcohol/ketone ratio decreases with temperature. The ratio of 2-/3- compounds also decreases with temperature suggesting activation of the 3- position with an increase of temperature.

vi. Influence of solvent

All the above studies were carried out with acetone as the solvent. The influence of other solvents on the conversion and product selectivities was next examined and the results are reported in Table 3.12. The reaction appears to be influenced by the solvent. n-C_6 conversion and selectivities (alcohol/ketone ratio and 2-/3- ratio) are influenced by the solvent. The influence of the solvent is probably very intricate, being a function of its polarity, molecular size, counter diffusion effects in the pores and interaction with the active centres.

B. Studies on cyclohexane

Among the alkane oxidation reactions, the conversion of cyclohexane to cyclohexanol and cyclohexanone is industrially very important. At present, the above reaction is carried out over transition metal catalysts with low conversions[93]. We have reported the oxyfunctionalization of cyclohexane with hydrogen peroxide in moderate yields using the TS-2[50]. These studies could lead to new commercial routes for the manufacture of cyclohexanol and cyclohexanone from cyclohexane.

The results of the reaction of cyclohexane with hydrogen peroxide in the presence of TS-2 are presented in Table 3.13. In all the experiments, the major products were cyclohexanol and cyclohexanone. Small amounts of compounds with more than one functional group were also detected. These compounds have not been estimated in detail. Increasing the temperature of the reaction increases cyclohexane conversion. Higher temperature also favours the formation of cyclohexanone. For example, the cyclohexanone to cyclohexanol (mole) ratio is 0.45 at 353 K, while it is 1.32 at 393 K (Table 3.13). Again, another factor that affects the relative yields of cyclohexanone and cyclohexanol is the amount of H_2O_2 used in the reaction. When the H_2O_2 : cyclohexanol mole ratios are 1.0 and 0.20, the cyclohexanone/cyclohexanol

Table 3.12. Influence of solvent and temperature on the oxidation of n-hexane

Reaction conditions: Catalyst (g)/mole n-C_6 = 1.7; n-C_6 : H_2O_2 (moles) = 0.116 : 0.039; Reaction duration (h) = 5.

Solvent	Temp. (K)	n-C_6 convn. (wt. %)	H_2O_2 sel.[+] (mole %)	Break-up of products (wt. %)[a]					-ol/-one ratio[b]	2-/3-ratio[c]	Product sel.[d]
				2-ol	2-one	3-ol	3-one	Others[e]			
Acetone	373	18.9	61.6	31.0	24.0	17.9	16.5	10.6	1.2	1.6	89.4
2-Butanone	373	6.0	14.4	12.1	17.1	21.0	18.2	31.6	0.9	0.7	68.2
Acetonitrile	373	12.3	37.8	20.1	9.7	45.9	12.6	11.7	3.0	0.5	88.3
NN DMF[f]	373	3.4	8.0	4.3	15.0	34.6	19.6	26.5	1.1	0.4	73.5
Acetone	323	5.9	13.1	48.4	7.3	20.7	4.2	19.4	6.0	2.2	80.6
Acetone	348	11.1	33.8	46.3	15.8	21.6	10.5	5.8	2.6	1.9	94.2
Acetone	398	17.1	56.9	22.1	24.6	15.6	23.3	14.4	0.8	1.2	85.6

+ : H_2O_2 utilized for mono functional product formation.

a : 2-ol = 2-hexanol; 3-ol = 3-hexanol; 2-one = 2-hexanone and 3-one = 3-hexanone.

b : -ol/-one ratio = Σ alcohols/Σ ketones.

c : 2-/3- ratio = (2-ol + 2-one/3-ol + 3-one).

d : Product selectivity = (Σ 2- and 3- compounds/n-hexane reacted) X 100.

e : Mostly oxygenates with more than one functional group.

f : N,N-dimethyl formamide.

Table 3.13. Oxidation of cyclohexane with H_2O_2[a]

SiO_2/TiO_2 ratio	Catalyst amount(g)	Temp. (K)	H_2O_2[b] (moles)	Cyclohexane conversion (mole %)	TON[c] (x 10^{-3})	H_2O_2 selectivity[d]	Product composition (mole %)		
							CH-OL[e]	CH-ONE[f]	Others[g]
29	1.0	373	0.038	13.0	1.57	42.2	60	34	6
48	1.0	373	0.038	9.8	1.92	30.4	62	31	7
124	1.0	373	0.038	7.0	3.66	20.0	65	25	10
29	1.0	353	0.038	5.8	0.67	23.1	64	29	7
29	1.0	393	0.038	15.8	1.82	59.3	41	54	5
29	1.0	373	0.102	27.8	3.21	31.4	44	45	11
29	1.0	373	0.024	7.3	0.84	70.0	64	31	5
29	0.2	373	0.038	7.5	4.51	20.3	40	29	31
29	0.5	373	0.038	11.7	2.82	36.3	52	35	13
22[h]	1.0	373	0.038	17.5	1.57	60.0	58	38	4

a: Duration of run = 5 h.

b: Cyclohexane 0.1190 moles; Solvent (Acetone) = 0.43 moles.

c: TON = turn over number, no. of mol. of cyclohexanone converted per Ti atom per sec.

d: H_2O_2 selectivity = (H_2O_2 consumed for cyclohexanol and cyclohexanone formation/Total H_2O_2 used) X 100.

e: CH-OL = cyclohexanol; f: CH-ONE = cyclohexanone.

g: Oxygenates like lactones and compounds with more than one functional group.

h: Catalyst = TS-1.

ratios are 1.02 and 0.48. It is found that the H_2O_2 selectivity (% of H_2O_2 usefully consumed) and product selectivity (selectivity for cyclohexanol and cyclohexanone) increases with temperature (studied upto 393 K). Similarly, they increase with a decrease in H_2O_2 concentration.

The activity and product selectivity increase with increasing Ti-content (decreasing SiO_2/TiO_2 ratios) suggesting that Ti ions are the active centres. The activities (at 373 K) of the three samples with SiO_2/Ti ratios of 29, 48 and 124, respectively, expressed as turn over numbers (TON = number of molecules of cyclohexane converted per Ti atom per second) are respectively 1.57 X 10^{-3}, 1.92 X 10^{-3} and 3.66 X 10^{-3}. Keeping the cyclohexane/H_2O_2 (mole) ratios constant at 3, the studies on the influence of catalyst amount were carried out at three different catalyst levels, *viz.*, 0.2, 0.5 and 1.0 g. The H_2O_2 content was kept low to achieve better H_2O_2 selectivities. Increasing the catalyst content increases the cyclohexane conversion as well as product selectivity. Further the TON decreases when the catalyst amount is increased: TON = 4.51 X 10^{-3}, 2.82 X 10^{-3} and 1.57 X 10^{-3} for 0.2, 0.5 and 1.0 g catalyst loadings, respectively.

C. Studies on other alkanes

Table 3.14 reports the results of the experiments carried out on different alkanes. The results reveal that conversion decreases with increasing carbon number in the case of the alkanes studied ($C_n > C_6$)[46]. The primary reason is the slower diffusion of the larger molecules into the zeolite channels. This is also apparent from the lower conversion of the bulkier branched hydrocarbon, 3-methyl pentane. When equimolar mixtures of n-hexane + 3-methyl pentane, n-hexane + 2,2-dimethyl butane and n-hexane + cyclohexane are simultaneously reacted, the faster diffusing n-hexane undergoes reaction preferentially (Table 3.14).

D. Conclusions

TS-2 is a good catalyst for the selective oxidation of alkanes by H_2O_2. The 2-position of the alkanes is the most favoured position for oxyfunctionalization, this preference increasing with carbon number of the alkane. An increase in the Ti content of TS-2 or its concentration in the reaction mixture increases the selective utilization of H_2O_2 and the rate of oxyfunctionalization. H_2O_2 concentration, temperature and nature of the solvent all have an influence on the alcohol/ketone ratio in the product.

Table 3.14. Reaction of other alkanes and alkane mixtures[a] over TS-2

Reaction conditions: Catalyst (g)/mole n-C_6 = 1.7; SiO_2/TiO_2 = 27; alkane : H_2O_2 (moles) = 0.116 : 0.039; Reaction duration (h) = 5; Solvent = Acetone (20 ml).

Alkane 1[b]	Alkane 2[c]	Conversion (wt.%)	
		Alkane 1	Alkane 2
n-C_6	--	18.9	--
n-C_7	--	18.2	--
n-C_8	--	16.5	--
n-C_{12}	--	13.5	--
n-C_6	3-M C_5	7.8	2.8
n-C_6	2,2-DM C_4	8.2	1.7
n-C_6	Cy C_6	12.3	1.8

a: Alkane mixtures = 50 mole % of each component.
b: n-C_6 = n-hexane; n-C_7 = n-heptane; n-C_8 = n-octane; n-C_{12} = n-dodecane.
c: 3-M C_5 = 3-methyl pentane; 2,2-DM C_4 = 2,2 dimethyl butane; Cy C_6 = cyclohexane.

3.2.2. AMMOXIMATION OF CARBONYL COMPOUNDS

A. Ammoximation of cyclohexanone

The production of cyclohexanone oxime is a major step in the manufacture of Nylon-6. The methods presently employed in the production of cyclohexanone oxime are associated with the coproduction of ammonium sulfate and the use of hazardous chemicals like oleum, halides and oxides of nitrogen[94]. There have been many attempts to modify the process to avoid the use of corrosive and environmentally undesirable reactants. Gas phase ammoximation using NH_3 and O_2 has been reported[95], but the yields have been low. Recently, the titaniumsilicate molecular sieve, TS-1 was found to catalyze the conversion of cyclohexanone into the oxime in the presence of NH_3 and H_2O_2 with high selectivities without the co-production of any ammonium sulfate[26]. Petrini *et al.*[96] have studied the stability and deactivation behaviour of TS-1 in this reaction. Three types of deactivation have been reported: i) slow dissolution of the framework ii) direct removal of framework Ti and iii) pore filling by by-products. We have reported our studies on the ammoximation of cyclohexanone and other carbonyl compounds using TS-2 as a catalyst in an attempt to identify the mechanism of the reaction[45].

i. Comparison of TS-2 with other catalysts

Silicalite-2, Al-MEL and TS-2 possess the same MEL framework structure. The difference between them lies in the composition of the framework. While silicalite-2 is a pure silica

molecular sieve, Al-MEL and TS-2 possess additionally Al^{3+} and Ti^{4+} ions, respectively in the lattice. While the presence of Al^{3+} lends acidity to the system, Ti^{4+} ions do not make the molecular sieve acidic. It is, therefore, interesting to compare the activities and selectivities of the MEL isomorphs, silicalite-2, Al-MEL, TS-2 and Al-TS-2, in the ammoximation of cyclohexanone. The results of the studies are presented in Table 3.15. The results obtained over TS-1[67] are also reported for comparison. Though the major product over most of the catalysts is the desired cyclohexanone oxime, by-products are also formed in considerable amounts over the non Ti-catalysts. The names and structures of the products formed in the reaction are given below.

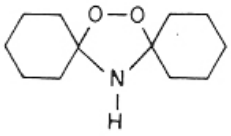

peroxydicyclohexyl amine

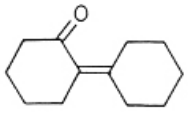

2-cyclohexylidene cyclohexanone

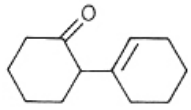

2-(1-cyclohex-1-en-1-yl)-cyclohexanone

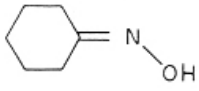

cyclohexanone oxime

An examination of the data (Table 3.15) reveals that the catalysts can be arranged in the following orders (increasing) for activity (conversion of cyclohexanone), selectivity for cyclohexanone oxime and its yield (conversion X selectivity).

Activity : TS-1 > TS-2 > SiO_2 > silicalite-2 > Al-TS-2 > Al-MEL

Selectivity : TS-1 > TS-2 > Al-TS-2 > silicalite-2 > Al-MEL > SiO_2

Yield : TS-1 > TS-2 > Al-TS-2 > silicalite-2 > SiO_2 > Al-MEL

The results show that while Ti increases the activity, Al-ions have just the opposite effect. This is clear from the lower activity of Al-TS-2 when compared to SiO_2 and silicalite-2. However, the selectivity for oxime is higher in the case of Al-TS-2 (which contains Ti-ions also) than silicalite-2 and SiO_2. The net yield of oxime is found to be dependent on the presence of Ti in the sample.

Table 3.15. Ammoximation of cyclohexanone over different catalysts

Reaction conditions: Temp. (K) = 353; Cyclohexanone : NH_3 : H_2O_2 (moles) = 0.102 : 0.40 : 0.102; Catalyst = 1 g; Reaction duration = 5 h.

Catalyst	AL-MEL	SiO_2[a]	Si-2[b]	TS-1[c]	SiO_2/TiO_2 molar ratio of TS-2			Al-T S-2[d]
					27	70	125	
Cyclohexanone Conversion (wt.%	17.7	55.3	44.9	90.1	84.5	53.5	35.1	19.1
Product distribution (wt.%)								
Cyclohexanone	82.3	44.7	55.1	9.9	15.5	46.5	64.9	80.9
Cyclohexanone Oxime	1.3	1.8	3.8	88.4	80.2	48.5	28.4	12.3
Peroxy-dicyclohexyl amine	12.0	47.1	34.4	0.2	3.2	4.2	4.4	2.2
Others[e]	4.4	6.4	6.7	0.1	1.1	0.8	2.3	4.5
Oxime selectivity (wt.%)	7.4	3.3	8.5	98.1	94.9	90.7	80.9	64.6

a: Fumed silica, Type S-5005, supplied by Sigma Chemical Co., Mo, U.S.A.

b: Si-2 = Silicalite-2; c: SiO_2/TiO_2 = 24; d: SiO_2/TiO_2 = 70; SiO_2/Al_2O_3 = 34

e: Others are 2-cyclohexylidene cyclohexanone and 2-(1-cyclohex-1-en-1-yl)-cyclohexanone.

The pure silica materials (SiO_2 and silicalite-2) favour the formation of peroxydicyclohexylamine, PDCA (a condensation product with NH_3 and H_2O_2), while the presence of Ti in the system favours the formation of the oxime suppressing the formation of PDCA. The reason for the low selectivity of the Al-containing samples (Al-TS-2 and Al-MEL) is the rapid decomposition of H_2O_2 over the Al^{3+} centers of the zeolite.

Blank experiments carried out in the absence of catalysts did not yield any oxime, though small amounts (<3 %) of PDCA were produced. Thus PDCA formation seems to be catalyzed by Si-OH groups on the surface of SiO_2 glass and the other catalysts.

The other by-products found in the experiments, *viz.*, 2-cyclohexylidene cyclohexanone and 2-(1-cyclohex-1-en-1-yl)-cyclohexanone are aldol condensation products and are obtained in much smaller quantities. The yields of these two compounds also are larger in the absence of Ti.

ii. Influence of temperature

The results of the experiments carried out at three different temperatures are presented in Table 3.16. It is noticed that increasing the temperature increases the conversion and at the same time decreases the formation of the by-products. Lower temperatures seem to favour the formation of the by-products. Similar results have also been reported by earlier workers[26] during their study of the reaction over TS-1. The slight decrease in conversion at 373 K, the highest temperature studied, is probably due to the rapid loss of the reactants, NH_3 and H_2O_2, at the higher temperature and their nonavailability for the reaction.

iii. Influence of catalyst amount

Increasing the catalyst concentration (Table 3.17) upto 10 g catalyst/mole of cyclohexanone increases the conversion and also decreases the formation of by-products, thereby increasing the selectivity for oxime formation. However, beyond the 10 g level, conversion does not increase, but selectivity improves further. In Table 3.15, the influence of increasing the Ti content of TS-2 on the reaction is reported. It is observed that increasing the Ti content increases both conversion and selectivity. The influence of increasing Ti content and catalyst amount are similar.

iv. Influence of solvents

The results reported in Tables 3.15-3.17 were carried out in the absence of a solvent in a 3 phase system, *viz.*, a solid catalyst phase and two liquid phases, an organic and an aqueous

Table 3.16. Influence of temperature of the oximation of cyclohexanone over TS-2

Reaction conditions: Catalyst = 1 g (SiO_2/TiO_2 = 27); Cyclohexanone : NH_3 : H_2O_2 (moles) = 0.102 : 0.40 : 0.102; Reaction duration = 5 h.

	Temperature, K		
	333	353	373
Cyclohexanone Conversion (wt.%)	77.6	84.5	82.0
Product distribution (wt.%)			
Cyclohexanone	22.4	15.5	18.0
Cyclohexanone Oxime	24.2	80.2	78.0
Peroxy dicyclohexyl amine	33.0	3.2	4.0
Others[a]	20.5	1.1	--
Oxime selectivity	31.2	94.9	95.1

a: Others are 2-cyclohexylidene cyclohexanone and 2-(1-cyclohex-1-en-1-yl)-cyclohexanone.

Table 3.17. Influence of catalyst concentration on the oximation of cyclohexanone over TS-2

Reaction conditions: SiO_2/TiO_2 = 27; Temp.(K) = 353; Cyclohexanone : NH_3 : H_2O_2 (moles) = 0.102 : 0.40 : 0.102; Reaction duration = 5 h.

	Catalyst concentration (g/mole of ketone)			
	0	5	10	15
Cyclohexanone Conversion (wt.%)	< 3.0	38.0	84.5	83.9
Product distribution (wt.%)				
Cyclohexanone	> 97	62.0	15.5	16.1
Cyclohexanone Oxime	0.0	29.7	80.2	80.7
Peroxy dicyclohexyl amine	< 3.0	5.8	3.2	2.8
Others[a]	0.0	2.5	1.1	0.4
Oxime selectivity	0.0	78.2	94.9	96.2

a: Others are 2-cyclohexylidene cyclohexanone and 2-(1-cyclohex-1-en-1-yl)-cyclohexanone.

phase. The addition of solvents like methanol and t-butanol converts the two liquid phases into a single one. The influence of adding solvents on the conversion and selectivity are presented in Table 3.18. Surprisingly, the addition of solvents decreased the conversion, but selectivity for the oxime was not affected significantly.

Table 3.18. Influence of solvents on the oximation of cyclohexanone over TS-2.

Reaction conditions: Catalyst = 1 g (SiO_2/TiO_2 = 27); Cyclohexanone : NH_3 : H_2O_2 (moles) = 0.102 : 0.40 : 0.102; Reaction duration (h) = 5; Solvent used 20 ml.

	Solvent		
	None	Methanol	t-butanol
Cyclohexanone Conversion (wt.%)	84.5	39.2	74.6
Product distribution (wt.%)			
Cyclohexanone	15.5	60.8	25.4
Cyclohexanone Oxime	80.2	37.2	69.1
Peroxy dicyclohexyl amine	3.2	1.4	5.3
Others[a]	1.1	0.6	0.2
Oxime selectivity	94.9	94.8	92.6

a: Others are 2-cyclohexylidene cyclohexanone and 2-(1-cyclohex-1-en-1-yl)-cyclohexanone.

v. Influence of duration of run

The influence of duration of the run on product formation was studied by analyzing samples of the reaction mixture at different intervals of time over a period of 5 h. The results are presented in Fig.3.17. The experiment was carried out in t-butanol with a small amount of catalyst (5 g per mole of cyclohexanone) to keep the conversion low. It is observed that conversion and selectivity for oxime increase steadily with time. The yield of by-products goes through a maximum. Initially when the concentration of the reactants, especially cyclohexanone and H_2O_2 are large, the condensation products are formed rapidly. After a certain time their formation decreases and at the same time they break down and transform into the desired cyclohexanone oxime.

vi. Influence of concentration of reactants

The results of the experiments carried out at different concentrations of the reactants are presented in Table 3.19. The results indicate that when cyclohexanone and hydrogen peroxide

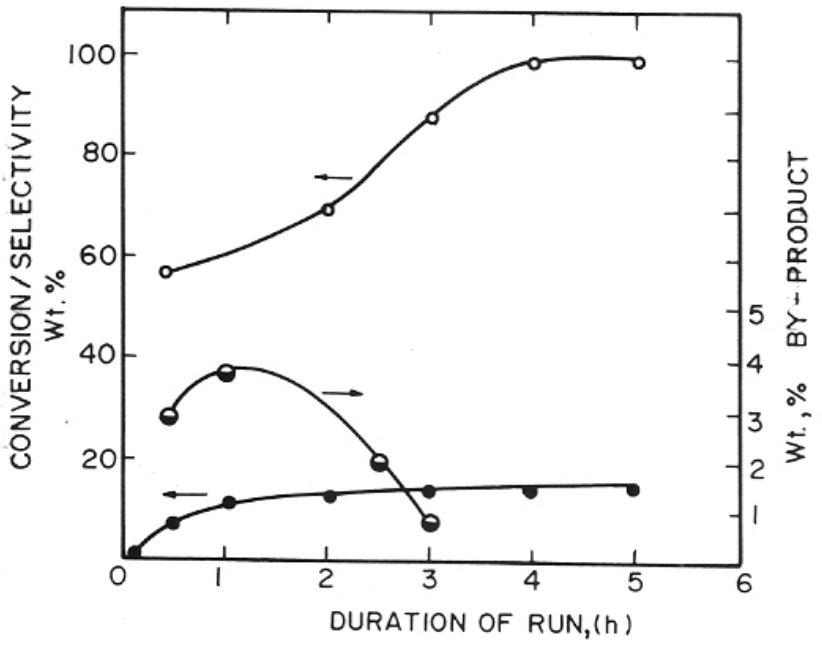

Fig.3.17. Influence of duration of run on product yield in the ammoximation of cyclohexanone.

(●): conversion of cyclohexanone; (O): selectivity for oxime; (◒): yield of by-products.

Table 3.19. Effect of concentration of reactants

Reaction conditions: Catalyst = 1 g (SiO_2/TiO_2 = 27); Temp.(K) = 353; Reaction duration = 2 h; Solvent = t-butanol; amount of solvent varied to keep total moles including solvent at 0.2.

Reactants (moles)			Cyclohexanone	Oxime	Product distribution, wt.%		
Cyclohexanone	H_2O_2	NH_3	conversion	selectivity	CH[a]	Oxime	Others[b]
0.01	0.02	0.02	38.2	100.0	61.8	38.2	0.0
0.02	0.02	0.02	25.4	100.0	74.6	25.4	0.0
0.04	0.02	0.02	22.1	63.7	77.9	14.1	8.0
0.02	0.01	0.02	22.0	100.0	88.0	12.0	0.0
0.02	0.04	0.02	27.4	89.4	72.6	24.5	2.9
0.02	0.02	0.01	37.8	94.0	62.0	35.5	2.5
0.02	0.02	0.04	26.8	100.0	73.2	26.8	0.0

a: CH : Cyclohexanone

b: Others are 2-cyclohexylidene cyclohexanone and 2-(1-cyclohex-1-en-1-yl)-cyclohexanone.

are in excess, the by-products are formed in significant quantities, and when ammonia is in excess when compared to either one of the other two reactants or when all the reactants are in equal quantities, the selectivity for the oxime is maximum.

vii. Mechanism of ammoximation over titaniumsilicate molecular sieves

Based on the results reported earlier, two possible mechanisms for the ammoximation of cyclohexanone can be written.

1) $\text{-Ti(=O)-} + H_2O_2 \longrightarrow \text{-Ti(-OH)-O-OH}$

$\text{-Ti-O-Si-} + H_2O_2 \longrightarrow \text{-Ti-O-OH} + \text{-Si-OH}$

$\text{-Ti-OOH} + NH_3 \longrightarrow NH_2OH + \text{-Ti-OH}$

$NH_2OH + \text{Cyclohexanone} \longrightarrow \text{Cyclohexanone oxime} + H_2O$

2)

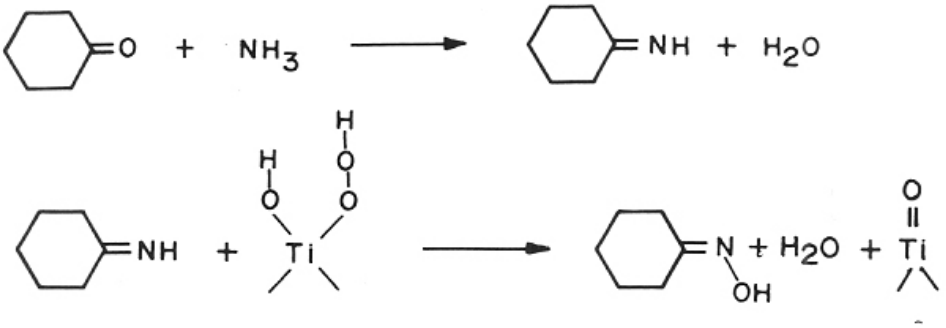

Evidence for the presence of -Ti=O, -Ti-OH and -Ti-O-Si groups in titaniumsilicates has already been reported by earlier workers[5,17,22]. Similarly, the transformation of -Ti=O or -Ti-O-Si- groups in the presence of H_2O_2 has also been reported[16,25]. -Ti-O-Si groups have been shown to possess an IR band at 960 cm^{-1}. On addition of H_2O_2, the 960 cm^{-1} band disappears and a new -Ti-OOH species with absorption in the visible region at 425 nm appears[21]. The 960 cm^{-1} band has, however, been attributed by some workers[3,17,22] to be due to -Ti=O species. In any case the formation of the peroxy titano complex -Ti-OOH is beyond doubt.

Recently, the formation of cyclohexanone imine over the titaniumsilicate, TS-1 has been confirmed[35]. This observation also supports the latter mechanism. The formation of imine over silica is also known[97]. The formation of the major by-product, peroxydicyclohexyl amine also occures via the imine. A possible mechanism for its formation could be:

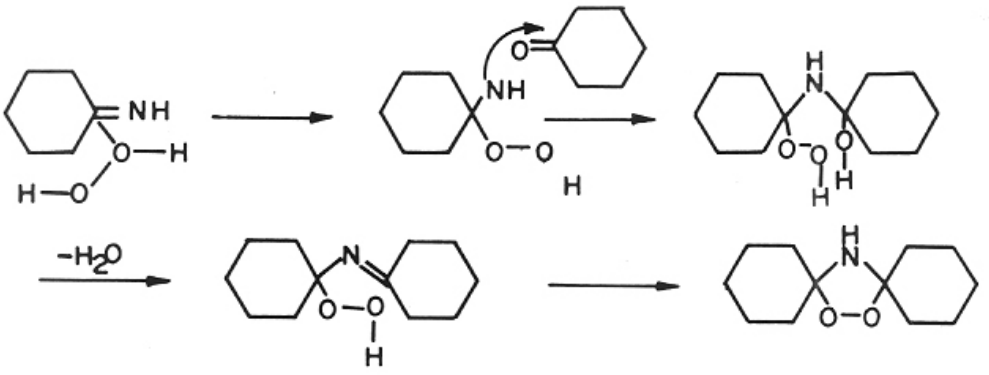

Evidence supporting the above mechanism are:

- Ti is not necessary to produce the by-product.
- PDCA yield is more when cyclohexanone and H_2O_2 concentrations are more.
- When Ti is present, the by-product (PDCA) formation is suppressed.

The suppression of the by-product arises from the rapid insertion of an 'O' from the peroxy titanium complex into the intermediate cyclohexylimine to produce the oxime.

B. Ammoximation of other carbonyl compounds

The ammoximation of a number of compounds with carbonyl groups was carried out under typical conditions. The results of the studies are presented in Table 3.20. The activity of the compounds followed the decreasing order: benzaldehyde > 2-butanone > cyclohexanone > acetophenone > benzophenone. The higher activity of benzaldehyde may be attributed to its more active carbonyl group; the activity of the carbonyl group increases with the positive charge of the carbonyl carbon. The low activity of benzophenone could be due to seric effects, and its difficulty in diffusing into the MEL pore system. The by-products obtained in the case of the different compounds were not condensation products in all the cases.

Table 3.20. Ammoximation of different carbonyl compounds over TS-2.

Reaction Conditons: Catalyst = 1 g (SiO_2/TiO_2 = 27); Temp.(K) = 353; Ketone : NH_3 : H_2O_2 (moles) = 0.102 : 0.40 : 0.102; Reaction duration (h) = 5.

Reactant	Conversion, wt.%	Selectivity to oxime, wt.%	Product distribution, wt.%	
			Oxime	By-products
Cyclohexanone	84.5	94.9	80.2	4.3
Benzaldehyde	100.0	96.0	96.0	4.0
Acetophenone	54.3	98.2	53.3	1.0
Benzophenone	0.4	50.0	0.2	0.2
2-butanone	85.0	98.2	83.5	1.5

C. Conclusions

TS-2 catalyzes the ammoximation of various carbonyl compounds. TS-2 produces cyclohexanone oxime with high selectivities, while silicalite-2 and SiO_2 produce large quantities of the condensation product, peroxydicyclohexylamine. Similarly, when the concentrations of cyclohexanone and H_2O_2 are larger than that of NH_3, the formation of the by-products is favoured.

3.2.3. HYDROXYLATION OF AROMATIC COMPOUNDS

A. Hydroxylation of phenol

The first commercial process utilizing titaniumsilicate (TS-1) as a catalyst is the hydroxylation of phenol to hydroquinone and catechol introduced by Enichem, Italy[18]. Some aspects of the **TS-1** catalyzed hydroxylation reaction have been revealed recently[25,53]. We have investigated the reaction using **TS-2** as the catalyst, and are presenting the results in this section.

Though the major reaction is the hydroxylation of phenol, other side reactions also take place. These are the oxidation of the dihydroxy benzenes to quinones, the further oxidation of the quinones into tar and the decomposition of H_2O_2. These reactions are shown below.

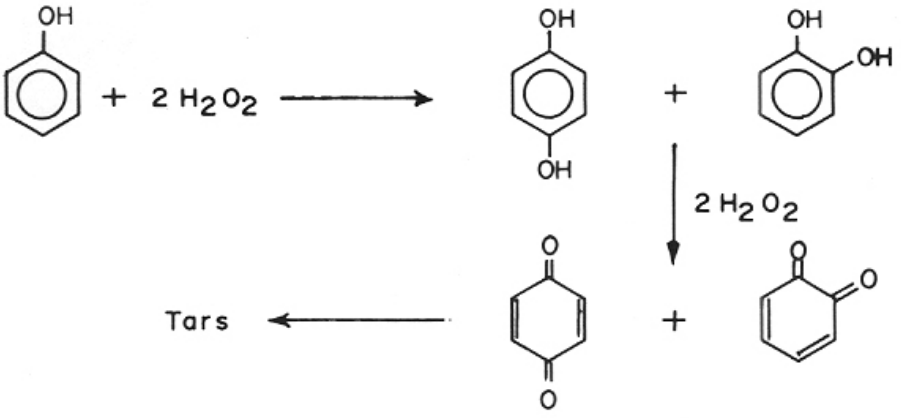

Like earlier reports[2,52], our studies also did not show the formation of meta-dihydroxy benzene (resorcinol). We will now discuss the influence of various parameters on the above reactions.

i. Mode of addition of H_2O_2

As the desired dihydroxy benzenes are intermediates in a sequence of reactions (shown above) and H_2O_2 takes part in both their formation and destruction, its (H_2O_2) concentration in the reaction medium is an important factor determining the yield of the hydroxy benzenes. In other words, the mode of H_2O_2 addition could be important.

Three different modes of H_2O_2 addition have been adopted: 1) add all the H_2O_2 in one lot in the beginning of the reaction (Fig.3.18 A), 2) add the H_2O_2 over a period of 1 h (Fig.3.18 B) and 3) add the H_2O_2 slowly over a period of 6 h (Fig.3.18 C).

The studies have been carried out at excess phenol conditions (phenol : H_2O_2 mole ratio = 3). In the early stages of the runs, the concentration of the secondary products (ortho benzoquinone, OBQ and para benzoquinone, PBQ) are considerably different in the three cases. However, after about 12 h, the product pattern, conversion levels and H_2O_2 selectivities are all only marginally different. The maximum H_2O_2 selectivity (defined as the mole % of H_2O_2 consumed in the formation of dihydroxy benzenes and quinones) is 70 % in the case of 1 h and 6 h additions, while it is slightly lower (66 %) when the H_2O_2 is added in one lot. In the earlier stages of the run, OBQ and PBQ are formed in considerable amounts, though these react further to become tarry products (not estimated). OBQ is more reactive and disppears faster than PBQ. It is also found that the sum of the o- products (catechol + OBQ) is more than the sum of the p- products (hydroquinone + PBQ) when H_2O_2 is in excess (added in one lot; see below).

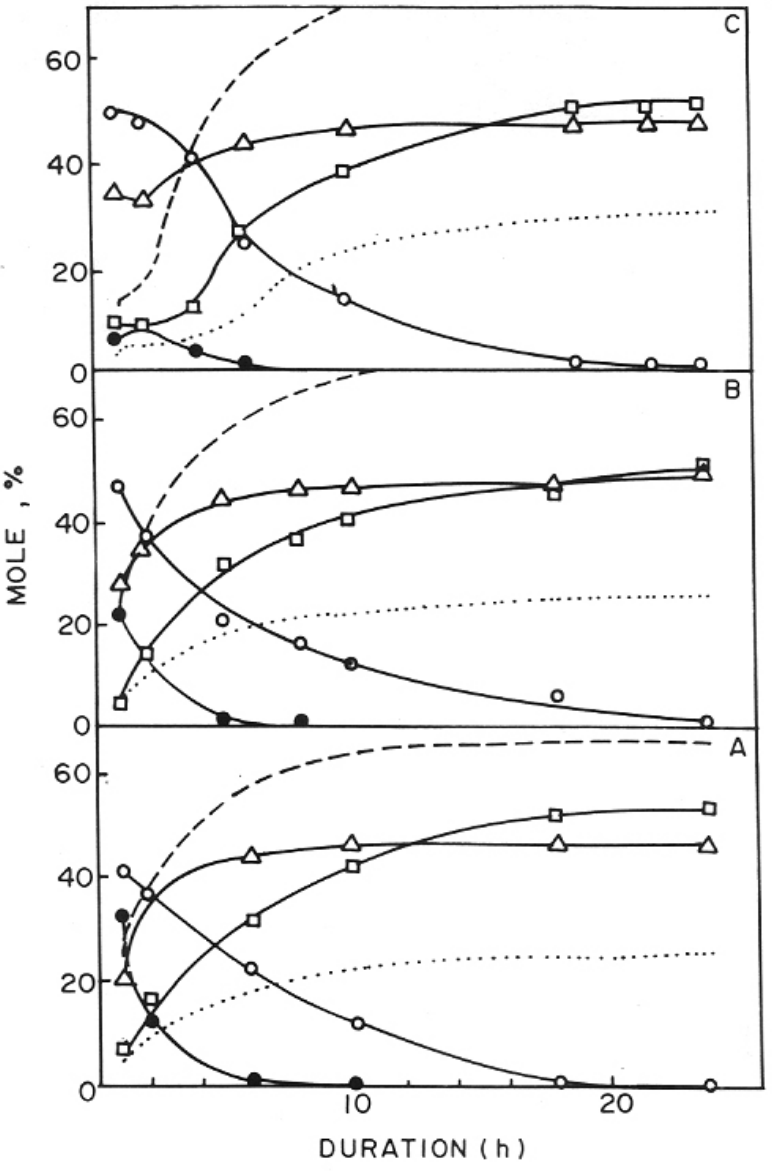

Fig.3.18. Influence of mode of addition of H_2O_2 on product distribution.
(A): addition in one lot; (B): addition over 1 h; (C): addition over 6 h.
(●): OBQ; (O): PBQ; (Δ): catechol; (□): hydroquinone; (---): H_2O_2 selectivity; (...): phenol conversion.
Reaction conditions: Temp.(K) = 342; Phenol/H_2O_2 (mole) = 3.0; Solvent = Acetone.

Mode of addition:	Rapid (one lot)	Slow	
		1h	6 h
o- : p- products ratio			
at 1 h	1.37	0.94	0.69
10 h	0.85	0.86	0.87

This suggests that hydroxylation at the o- position is more dependent on the concentration of H_2O_2 than hydroxylation at the p- position.

The yields (conversion x fraction in products) of OBQ and PBQ go through maxima with duration of run, the maximum being reached earlier by OBQ. The maximum amount of quinones in the product is also higher at higher H_2O_2 levels in the system (see also later section on influence of H_2O_2 concentration).

Separate experiments were carried out to study the reaction of pure hydroquinone and catechol with H_2O_2 in the presence and absence of TS-2. The studies have revealed the following results:

1) Both dihydroxy benzenes are oxidized by H_2O_2 in the absence of any catalyst, catechol oxidation being more rapid.
2) TS-2 increases the rate of oxidation of the dihydroxy benzenes by H_2O_2.
3) Tar formation takes place even in the absence of the catalyst and the influence of the catalyst on tar formation is not clear.

The above studies (Fig.3.18) have established that slow addition of H_2O_2 is preferable to addition in one lot. All further studies were therefore carried out with slow (1 h) addition of H_2O_2.

ii. Influence of Ti content of TS-2

The hydroxylation of phenol did not take place in the absence of any catalyst. Negligible conversion was recorded in the presence of silicalite-2, TiO_2 and an amorphous mixture of TiO_2 and SiO_2. The introduction of Ti into the silicalite lattice (TS-2), however, catalyzed the reaction, even at very low Ti contents. The influence of Ti content (of TS-2) on the reaction is presented in Table 3.21. The data were obtained after 24 h. Though the ratio of catechol to hydroquinone is not significantly affected by the Ti content, both conversion and selectivity increase with increase in Ti content.

Table 3.21. Effect of titanium content of TS-2 and catalyst amount.

Reaction conditions: Phenol/H_2O_2 (mole) = 3.0; H_2O_2 = 26 wt.% aq. solution; Temp.(K) = 342; Solvent = Acetone (20 ml); Reaction time (h) = 24.

Catalyst amount (g/mole of phenol)	SiO_2/TiO_2 ratio	H_2O_2 selectivity, %[a]	Phenol conversion[b]	Product distribution (mole %)[c]			
				OBQ	PBQ	CAT	HQ
10	29	70.0	26.8	0.0	0.9	49.3	49.9
10	48	64.0	24.3	0.0	1.1	49.7	49.2
10	70	51.1	19.6	0.0	1.0	49.5	49.5
10	124	39.2	15.0	0.0	0.5	50.3	49.2
20	29	72.3	27.2	0.0	0.0	48.4	51.6
5	29	47.8	14.8	6.5	22.1	41.4	30.0
2	29	23.0	4.6	25.5	42.4	22.8	9.3

a:

$$H_2O_2 \text{ selectivity} = \frac{H_2O_2 \text{ (mole) consumed in formation of dihydroxy benzenes (DHB) and quinones}}{\text{Total } H_2O_2 \text{ (mole) added}} \times 100$$

b: Phenol converted for the formation of the DHB and quinones (GC conversion).

a,b: Consumption for tar formation excluded.

c: Break up (in mole %) of products excluding tars.
OBQ = ortho benzoquinone; PBQ = para benzoquinone; CAT = Catechol; HQ = Hydroquinone.

iii. Effect of catalyst concentration

Use of larger amounts of TS-2 increases conversion and selectivity and also lowers the amount of quinones in the product (Table 3.21). In fact, at a catalyst concentration of 20 g/mole of phenol, neither OBQ nor PBQ is present in the product, while large amounts of OBQ and PBQ are present at and below a catalyst concentration of 5 g/mole of phenol. Fig.3.19 A presents the results (at different run durations) obtained at a catalyst loading of 20 g/mole phenol. Corresponding data for a catalyst loading of 10 g/mole phenol have been reported in Fig.3.18 B. Comparing the two figures, we note that the yield of quinones decreases more rapidly with time when more catalyst is present. This is due to the faster rate of conversion of phenol to dihydroxy benzenes at higher catalyst loadings, depleting the H_2O_2 available for further oxidation (quinones and tar). Consequently, the H_2O_2 selectivity is also higher (74 %) at 20 g than at 10 g catalyst loading (70 %).

iv. Influence of H_2O_2 concentration

The results show (Table 3.22) that for maximum useful utilization of H_2O_2 (H_2O_2 selectivity) and for minimum quinones formation, the phenol : H_2O_2 (mole) ratio must be kept as high as possible. However, lower H_2O_2 concentrations lead to lower phenol conversions. The influence of a higher H_2O_2 content (phenol : H_2O_2 mole ratio = 1) on the product composition at different run durations is presented in Fig.3.19 B. At the higher H_2O_2 concentration, not only more quinones are produced, they also persist in the product for a much larger duration (compare Fig.3.18 B and 3.19 B). These observations are similar to those made during the studies on mode of H_2O_2 addition (Fig.3.18). The o-/p- products ratio is also higher when H_2O_2 content is more (see below):

	Phenol : H_2O_2 (mole) ratio	
	1	3
o- : p- products ratio:		
at 1 h	1.56	0.94
6 h	1.14	0.86

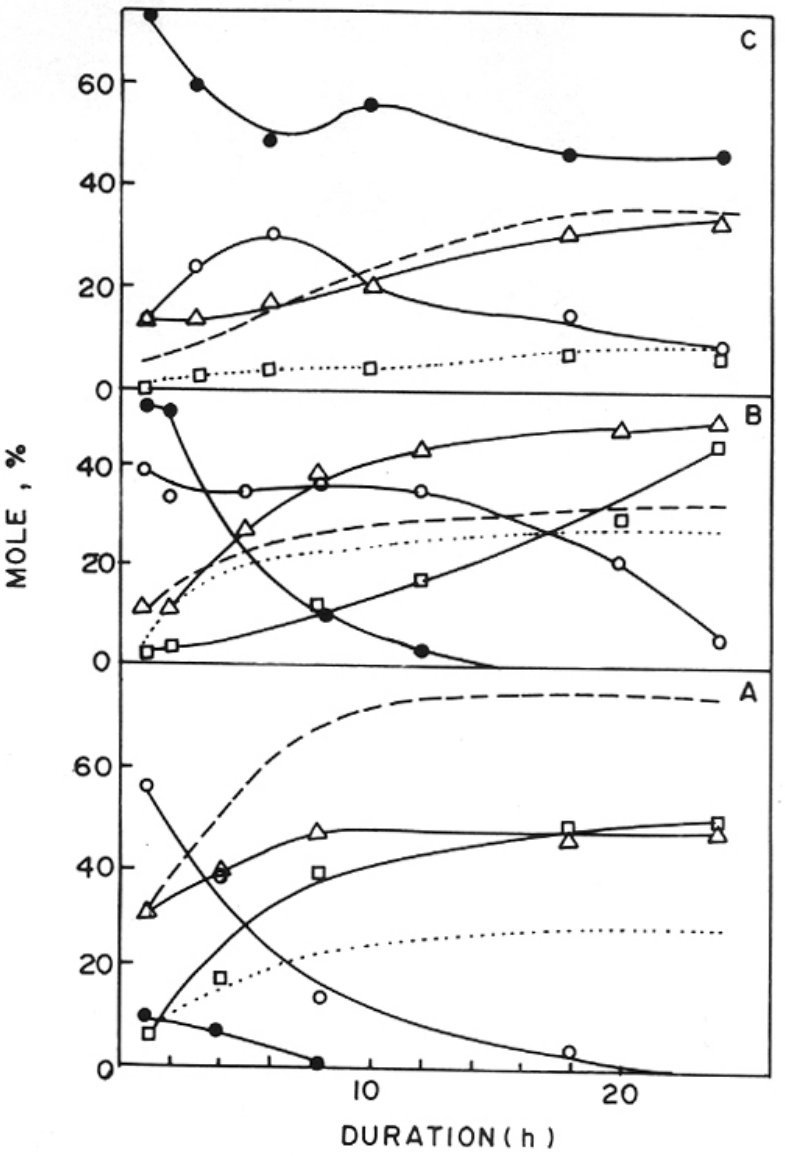

Fig.3.19. Influence of duration of run on product distribution.

(A): higher catalyst content (20 g mol^{-1} phenol); (B): longer duration of H_2O_2 addition (phenol : H_2O_2 mole ratio = 1); (C): lower reaction temperature (310 K).
(●): OBQ; (O): PBQ; (Δ): catechol; (□): hydroquinone; (---): H_2O_2 selectivity; (...): phenol conversion.

Reaction conditions: H_2O_2 is added in 1 h; solvent = acetone (20 ml); (A): Temp. (K) = 342; phenol : H_2O_2 mole ratio =3; (B): Temp. (K) = 342; phenol : H_2O_2 mole ratio = 1; (C): Temp. (K) = 310; phenol : H_2O_2 mole ratio = 3.

Table 3.22. Effect of temperature, solvent and H_2O_2 concentration

Reaction conditions: Catalyst = 10 g/mole of phenol (TS-2, SiO_2/TiO_2 = 29); H_2O_2 = 26 wt.% aq. solution; Reaction time (h) = 24.

Phenol:H_2O_2 (mole) ratio	Temp. (K)	Solvent	H_2O_2 selectivity, %[a]	Phenol conversion[b]	Product distribution (mole %)[c]			
					OBQ	PBQ	CAT	HQ
1	342	Acetone	27.5	26.1	0.0	5.4	49.4	45.0
3	342	Acetone	70.0	26.8	0.0	0.9	49.3	49.8
5	342	Acetone	75.9	17.4	0.0	0.0	51.7	48.3
3	310	Acetone	35.4	9.3	9.4	47.8	34.3	8.5
3	342	Acetone	70.0	26.8	0.0	0.9	49.3	49.8
3	342	Methanol	66.2	25.4	0.0	0.0	39.7	60.3
3	342	Acetonitrile	41.0	15.4	0.0	1.9	51.4	46.7
3	342	2-butanone	46.9	17.1	0.0	5.8	61.7	32.5

a:

$$H_2O_2 \text{ selectivity} = \frac{H_2O_2 \text{ (mole) consumed in formation of dihydroxy benzenes (DHB) and quinones}}{\text{Total } H_2O_2 \text{ (mole) added}} \times 100$$

b :Phenol converted for the formation of the DHB and quinones (GC values).

a,b: Consumption for tar formation excluded.

c: Break up (in mole %) of products excluding tars.
OBQ = ortho benzoquinone; PBQ = para benzoquinone; CAT = Catechol; HQ = Hydroquinone.

v. Influence of temperature

The results of the studies carried out in the temperature range 310 to 342 K are presented in Table 3.22. Both conversion and H_2O_2 utilization increase with temperature. The catechol/hydroquinone ratio (at the end of 24 h) is found to be dependent on temperature, the ratio being 4.08 at 313 K and 0.98 at 342 K.

At 310 K, significant quantities of OBQ and PBQ are present in the product even at the end of 24 h. Again the ratio of the o- / p- products is much higher at 310 K (7.49 after 1 h and 3.10 after 10 h) when compared to the values observed at 342 K (0.94 and 0.86) (Fig 3.22 C and 3.21 B).

vi. Influence of solvent

Acetone was used as the solvent in all the experiments reported earlier. Studies have also been carried out using other solvents (Table 3.22). The solvent affects both the conversion and H_2O_2 efficiency. Similarly the catechol/hydroquinone ratios are also influenced by the solvent, the ratios being 0.66 in methanol, 0.99 in acetone and 1.90 in 2-butanone. The amount of PBQ in the product is 5.8 % in the case of 2-butanone and nil in the case of methanol. Earlier workers[3,6,36] have also reported the influence of solvents (methanol and acetone) on the hydroxylation of phenol over TS-1. Tuel *et al.*[36] have recently suggested that catechol forms mainly on the outer surface. This was proved by using titaniumsilicate in the as-synthesized form, in which case catechol was the major product. The lower para-selectivity in the presence of acetone was explained on the basis that acetone is able to dissolve tars deposited on the surface of the zeolite crystal easily. The increase in para-selectivity with duration of run is due to the deactivation of external sites, which inhibits the formation of catechol.

vii. Mechanism of phenol hydroxylation

The hydroxylation of phenol exclusively at the o- and p- positions suggests the reaction to be a case of electrophilic substitution, involving probably $(OH)\delta^+$ species. We can now envisage the reaction to take place as follows:

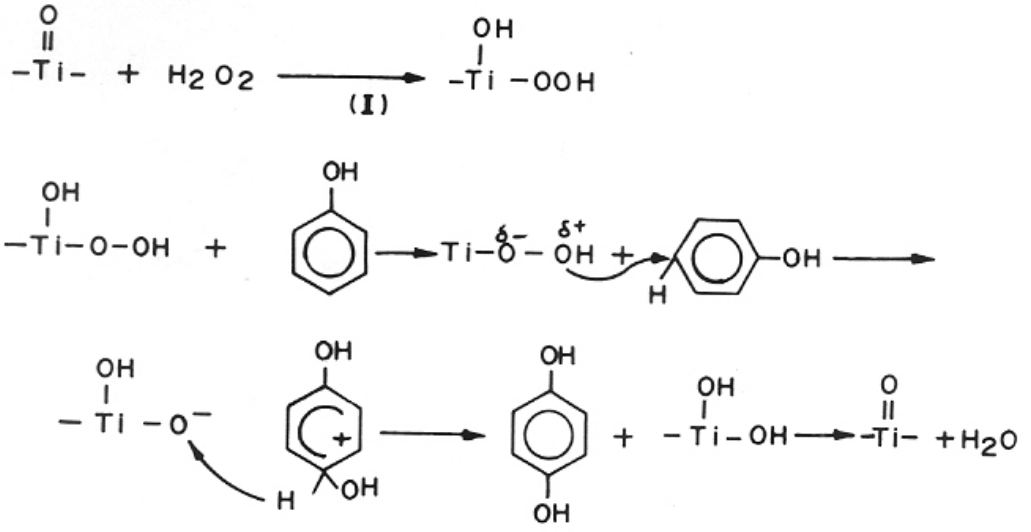

In the early stages of the reaction, especially in the presence of excess H_2O_2 or at lower temperatures, the amount of o- products formed is more than the amount of p- products. Tuel *et al.*[36] have suggested that the catechol formation is higher in the early stages of run when the major part of the reaction takes place on the external surface of the crystallites; the external surface gets deactivated faster with time. However, this does not explain the results of our studies on mode of H_2O_2 addition and inactiveness of bulky molecules like cumene, t-butylbenzene, naphthalene etc. We found that when the H_2O_2 concentration in the reaction mixture is low (see section on mode of addition) more HQ is produced even in the early stages of the run. In the hydroxylation of phenol with H_2O_2 in the presence of Fenton's reagent (Fe^{2+} ions) which is known to proceed by a free radical mechanism[98], the yield of o- products is generally more than 2 times the yield of the p- products. It is, therefore, likely that both ionic and radical type mechanism are operative during hydroxylation over TS-2, the importance of one mechanism over the other being dependent on the reaction conditions. Further, the external surface also, probably, influences the product pattern.

B. Hydroxylation of other aromatic compounds

TS-1 has been shown to catalyze the hydroxylation of various aromatic compounds[3]. TS-2 was also tried in the hydroxylation of other aromatic compounds and the results are reported in Table 3.23. The results indicate that the activities of the aromatic compounds depend on the electron density on the aromatic ring. This is further confirmed by the inactiveness of compounds containing electron withdrawing groups on the aromatic ring *viz.*, acetophenone, nitrobenzene, acetanilide, benzoic acid, benzaldehyde and phenyl acetate.

Similarly, as is expected in electrophilic substitution reactions, the o- and p- products predominate. In the case of benzene, the phenol formed in the reaction undergoes further hydroxylation to yield small amounts of dihydroxy benzenes and p-benzoquinone. The bulkier molecules like cumene, t-butylbenzene, napthalene and biphenyl are inactive, indicating that the active centres responsible for this reaction are mainly inside the zeolite channels.

Table 3.23. Hydroxylation of different aromatic compounds over TS-2.

Reaction conditions: Catalyst = TS-2 (SiO_2/TiO_2 = 29, 1g); Temp. (K) = 353; Solvent = Acetone (20 ml); Reaction time (h) = 24)

Reactant	Feed ratio[a]	H_2O_2 Sel.	Hydroxy products				
			ortho	meta	para	PBQ	Phenol
Benzene[b]	10	57	-	-	-	34	66
Toluene	10	54	38	1	60	-	-
Phenol	3	70	49	-	50	1	-
Phenol[c]	3	60	40	-	64	-	-
Anisol	3	60	36	-	64	-	-
Anisol[c]	3	51	31	-	69	-	-

a: Moles of aromatic compound/moles of H_2O_2 fed;
b: Temp. (K) = 300; No solvent is used.
c: Solvent = Methanol.

C. Conclusions

The titaniumsilicate molecular sieve, TS-2, catalyzes the hydroxylation of phenol to o- and p- dihydroxy benzenes with H_2O_2. The reaction is found to be catalyzed specifically by Ti ions in the molecular sieve. Higher phenol : H_2O_2 (mole) ratios, and higher catalyst loadings lead to better utilization of the H_2O_2 and higher conversion levels. The o- : p- dihydroxy benzene ratio in the product is influenced by the reaction temperature, the phenol : H_2O_2 (mole) ratio and the solvent.

3.2.4. STUDIES ON THE EPOXIDATION OF OLEFINS

Metal complexes containing Ti, V, Mo or W are known to catalyze the epoxidation of alkenes[99]. Heterogeneous catalysts like Ti/SiO_2 have also been reported to catalyze the epoxidation of alkenes with alkyl hydroperoxides[100]. TS-1 has been reported to catalyze the epoxidation reaction stereoselectively[101]. Selective monoepoxidation of compounds containing two double bonds (regioselectivity) has also been claimed[102]. When vinylbenzenes were used as reactants about 80 % selectivity for beta-phenylaldehydes was reported[103].

During a detailed study of the epoxidation of α-methylstyrene over TS-2, we noticed that, contrary to the earlier reports[103] significant amounts of carbonyl compounds arising from the cleavage of the olefinic bond were formed. The results are discussed in the following sections.

A. Epoxidation of α-methylstyrene

i. Activity of different catalysts

The results obtained in the conversion of α-methyl styrene to acetophenone over different zeolite catalysts are reported in Table 3.24. Acetophenone, α-methyl styrene epoxide and α-methyl styrene diol were the major products. Some unidentified products and 2-phenyl propionaldehyde were also present. Formaldehyde, the second product of the C-C bond cleavage was also identified, but the exact quantity was not determined. Similar products have been reported by Bõunnemann *et al.*[104] in the oxidation of 2,3-dimethyl-2-butene using acetylacetonatorhodium as the catalyst. In the epoxidation of styrene over TS-1, Neri *et al.*[103] have reported about 85 % selectivity for phenyl acetaldehyde. Though, we found that TS-1 exhibited a slightly better selectivity for the epoxide than TS-2, the overall selectivity was more for C=C bond cleavage over both TS-1 and TS-2. When Ti was incorporated into the zeolite framework the activity increased very sharply. TS-2 exhibited better selectivity for epoxide compared to Ga-MEL and Ga-TS-2 (gallo-titanium-silicate analogs of MEL). The presence of acid sites in Ga-MEL and Ga-TS-2 may cause the ring cleavage of the epoxide resulting in lower selectivities. Though both aluminosilicates and titaniumsilicates can catalyze the formation of an epoxide and cleave it to carbonyl compounds, cleavage may be most favoured over acid catalysts. Higher activity of TS-2 (SiO_2/TiO_2 = 75) and Ga-TS-2 (SiO_2/TiO_2 = 85; SiO_2/Ga_2O_3 = 70) compared to Ga-MEL (SiO_2/Ga_2O_3 = 78) indicates that the Ti^{4+} ions, substituted into the zeolitic framework play an important role in this reaction.

Table 3.24. Effect of various zeolite catalysts on reaction of α-methyl styrene with H_2O_2.

Reaction conditions: Catalyst wt. = 0.2 g; Temp. (K) = 353; α-methyl styrene : H_2O_2 (moles) = 2; Reaction time (h) = 20.

Catalyst	Olefin Convn. (% Theor.)	Product distribution, wt.%			
		Epoxide	>C=O	Diol	Others[a]
Y	43.6	16.0	51.6	20.2	12.2
Mordenite	40.6	5.6	54.5	35.6	4.3
Al-MFI	35.0	1.7	80.0	11.4	6.9
Alumina	38.6	7.8	53.4	24.4	14.5
Fumed silica	37.0	6.5	62.7	21.6	9.2
Silicalite-2	60.0	6.3	59.0	19.7	15.0
Al-MEL	52.8	7.6	52.3	27.7	12.0
Ga-MEL	68.4	5.1	54.1	26.4	14.4
Ga-TS-2	95.8	4.0	54.9	30.9	10.2
TS-2	100.0	9.1	42.9	37.9	10.1
TS-1	97.0	15.2	48.0	24.6	12.2

a: β-phenylpropionaldehyde, β-phenylpropionic acid and some unidentified compounds.

ii. Influence of solvent

Conversion of α-methylstyrene and the selectivity for epoxide decreases in the following order for various solvents (Table 3.25):

Olefin conversion : Acetonitrile ≈ Water > t-butanol > Methanol > Acetone
Epoxide selectivity: Acetone > Water > Acetonitrile > Methanol ≈ t-butanol

The major products are the diol and acetophenone. Water, t-butanol and acetonitrile exhibit a high selectivity (≈ 50 %) for the formation of acetophenone and methanol enhances the selectivity for the formation of the monomethyl ether (Table 3.25). Romano *et al.*[25] have shown that methanol is a good solvent for the epoxidation over TS-1. Nori *et al.*[103] have claimed about 95 % selectivity for the glycol monomethyl ether for various olefins using TS-1 as a catalyst. In the epoxidation of propylene, Clerici *et al.*[38] have claimed 87 % selectivity for the propylene oxide. The selectivity for the epoxide was improved further when 10 % SiO_2 was incorporated as a binder and the resultant TS-1/SiO_2 treated with sodium acetate.

The results obtained by the earlier workers suggest that the reaction conditions are very crucial. Small changes in the reaction conditions may affect dramatically the activity and

Table 3.25. Effect of nature of the solvent.

Reaction conditions: Catalyst = TS-2 (SiO_2/TiO_2 = 29; 0.2 g); Temp. (K) = 353; α-methylstyrene : H_2O_2 (mole) = 2.0; Reaction duration (h) = 20.

Solvent	Olefin conversion, (%, theoretical)	Product distribution, wt. %				
		Epoxide	>C=O[a]	Diol	Ketal/ ether[b]	Others[c]
Acetone	42	25.6	26.3	1.0	21.0	26.1
Acetone[d]	61	41.5	14.1	5.2	22.0	17.2
t-butanol	68	7.2	55.2	23.2	-	14.4
Acetonitrile	100	9.1	42.9	37.9	-	10.1
Acetonitrile[d]	100	19.2	48.0	20.6	-	12.2
Acetonitrile[e]	83	13.3	66.3	10.2	-	10.2
Water	100	12.2	52.4	15.0	-	20.4
Methanol	67	7.6	29.6	5.5	49.4	7.9

a: Product of carbon-carbon double bond cleavage.

b: Glycol ketal and glycol monomethyl ether of α-methylstyrene.

c: β-phenylpropionaldehyde, β-phenylpropionic acid and some unidentified compounds.

d: Catalyst = TS-1 (SiO_2/TiO_2 = 24; 0.2 g).

e: Temp. (K) = 298.

selectivities. When acetone is used as a solvent the diol is almost converted into the corresponding ketal. The formation of ketal from alcohol and acetone is an acid catalyzed reaction. When the diol and acetone were stirred at 353 K temperature without any catalyst, the reaction did not proceed.

iii. Influence of temperature

The selectivity for C = C bond cleavage in α-methylstyrene on reaction with H_2O_2 in acetonitrile solvent increased from 43 to 66 % on decreasing the temperature from 353 K to 298 K (Table 3.25), while the selectivity for the epoxide increased from 9 to 13 % and that of the diol decreased from 40 to 10 %.

iv. Influence of feed ratio and catalyst concentration

The influence of α-methylstyrene/H_2O_2 molar ratio in the feed on the epoxidation of α-methylstyrene is reported in Table 3.26. Acetone was used as a solvent in all the runs. At

higher molar ratios (lower H_2O_2 concentration) the selectivity for the epoxide increases and that for the cleavage of the C=C bond decreases. Excess H_2O_2 converts α-methylstyrene epoxide to acetophenone and formaldehyde.

The selectivity for the epoxide increases with increasing catalyst amount (Table 3.26). The selectivity for C=C bond cleavage, however, is not significantly affected.

B. Epoxidation of other olefins

Results obtained in the epoxidation of different olefins over TS-2 are reported in Table 3.27. For comparison, the results obtained over TS-1 are also reported. TS-1 shows better selectivity for the epoxide compared to TS-2. In both cases, greater than 50 % selectivity for the epoxide is obtained. The major products are the epoxide, the corresponding diols and carbonyl compounds (obtained from the cleavage of the carbon-carbon double bond). Products like β-phenylaldehyde, the corresponding carboxylic acids and some unidentified compounds are also obtained. When acetone is used as a solvent, ketals are obtained from the reaction of the diol and acetone.

In the present study, the selectivities for the epoxides of different olefins are in the range of 50-70 %. The cleavage of the carbon-carbon double band is unexpected and has not been reported over zeolites so far. This reaction is known to be catalyzed by potassium permanganate[105] in aqueous solutions. To investigate the phenomenon further, styrene epoxide and styrene diol were reacted separately under similar conditions. Major products obtained in the reaction of the epoxide are styrene diol and benzaldehyde. However, styrene diol in a separate reaction under similar conditions did not produce any benzaldehyde indicating that benzaldehyde is not formed via the diol. These experimental results show that the epoxide is cleaved, probably directly, to produce the carbonyl compound.

The reaction rate was found to decrease with increasing carbon number of the olefin (C_6 > C_8 > C_{12}) (Table 3.27), probably due to the decrease in diffusivity with increasing chain length. Such shape-selectivity effects are also probably responsible for the lower reactivity of cyclohexene compared to 1-hexene (Table 3.27). However, the higher activity of styrene and α-methylstyrene compared to cyclohexene indicates that not only the bulkiness of the molecule but also electron density at the double bond affects the activity.

Table 3.26. Effect of feed ratio and catalyst concentration

Reaction conditions: Catalyst = TS-2 (SiO_2/TiO_2 = 29); Temp. (K) = 353; Solvent = Acetone; Reaction duration (h) = 20.

Feed ratio	Catalyst amount, g	Olefin Conversion (%, theoretical)	Product distribution, wt. %				
			Epoxide	>C=O[a]	Diol	Ketol[b]	Others[c]
0.5	0.2	31.5	11.1	42.9	15.3	9.4	21.3
2.0	0.2	57.4	25.6	26.3	1.4	21.0	25.7
5.0	0.2	75.0	27.2	15.9	6.0	35.1	15.8
2.0	0.1	49.7	21.8	21.1	2.2	21.6	33.3
2.0	0.4	60.0	31.6	24.1	1.3	16.5	26.5

a: Acetophenone.

b: Ketal formed from the acetone and diol of corresponding olefin.

c: β-phenylpropionaldehyde, β-phenylpropionic acid and some unidentified compounds.

Table 3.27. Epoxidation of various olefins over TS-2

Reaction conditions: Catalyst = TS-2 (SiO_2/TiO_2 = 29; 0.2 g); Olefin/H_2O_2 (mole) = 2.0; Temp. (K) = 353; Reaction duration (h) = 5.

Reactant	Olefin Conversion (% theoretical)	Product distribution, wt. %				
		Epoxide	>C=O[a]	Diol	Ketal[b]	Others[c]
Styrene	70.0	54.3	19.7	8.0	7.1	10.9
Styrene[d]	67.6	76.0	2.9	1.9	2.5	2.4
α-methylstyrene	31.4	24.5	23.7	4.4	23.7	23.7
α-methylstyrene[d]	26.6	46.4	20.0	7.2	13.6	12.8
Cyclohexene	40.2	42.6	e	21.1	23.9	12.4
1-hexene	92.0	63.5	5.9	2.8	16.5	11.3
1-octene	56.4	66.3	5.3	e	12.4	16.0
1-dodecene	28.8	50.0	e	e	13.9	36.1

a: Product of carbon-carbon double bond cleavage.

b: Ketal formed from the acetone and diol of corresponding olefin.

c: β-phenylpropionaldehyde, β-phenylpropionic acid and some unidentified compounds

d: Catalyst = TS-1 (SiO_2/TiO_2 = 24; 0.2 g).

e: Not identified.

C. Mechanism of the formation and cleavage of epoxide

The formation of titanium-peroxo complexes upon addition of H_2O_2 to titaniumsilicate molecular sieves has already been discussed in earlier sections. From the above experimental results it is clearly seen that both alumino- and titaniumsilicates can catalyze the epoxidation of the olefin and the cleavage of the epoxide to carbonyl compounds. Since aluminosilicates and titaniumsilicate molecular sieves possess different types of active sites, one can envisage two different type of mechanisms taking place.

In the epoxidation of olefins over TS-1, Hubrechts *et al.*[106] have reported the following mechanism.

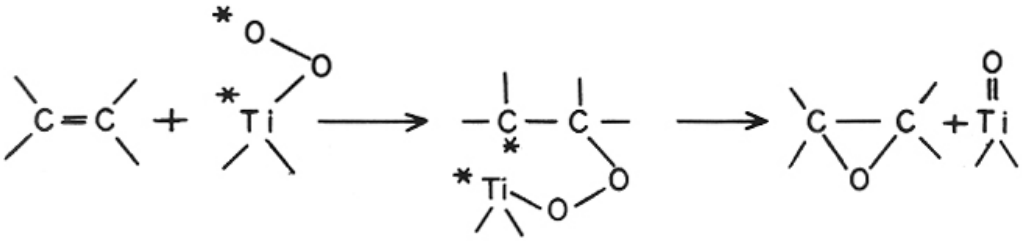

This mechanism can be extended to the cleavage of an epoxide to two carbonyl compounds. This mechanism may proceed through the formation of a stable 6 membered transition state, which later on dissociates into two carbonyl compounds. As Hubrechts *et al.*[106] have discussed in the case of epoxidation, this mechanism can also take place either by a radical or a non-radical mechanism. The possible radical mechanism is shown below:

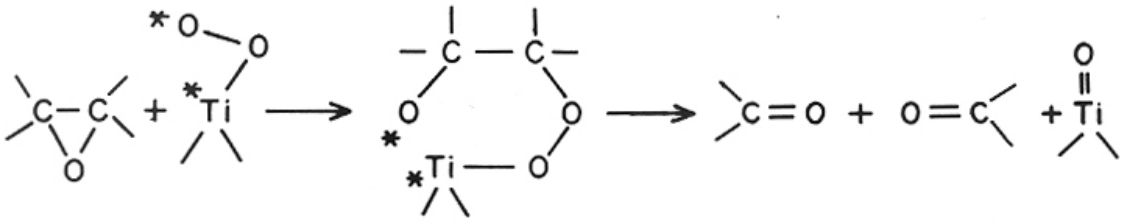

In the presence of aluminosilicates the following mechanism may take place for the formation of epoxide in the presence of hydrogen peroxide.

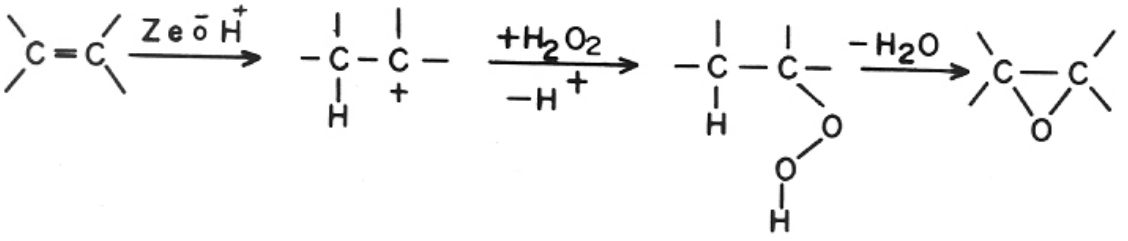

A possible mechanism for the cleavage of the epoxide over aluminosilicates to give two carbonyl compounds is:

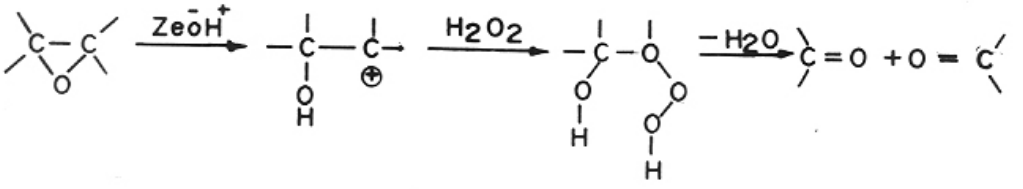

D. Conclusions

TS-2 catalyzes the epoxidation of olefins. Epoxide selectivity depends on various reaction parameters like feed ratio, temperature, catalyst concentration and nature of the solvent. Cleavage of the epoxide (to a carbonyl compound) is favoured when water, acetonitrile or t-butanol is used as a solvent and at lower temperatures. Glycol monomethyl ether and glycol ketal are formed as by-products, when methanol and acetone are used as solvents, respectively. The bulkiness of the olefin and electron density at its double bond are additional parameters that affect both the reaction rate and product selectivity.

3.2.5. BECKMANN REARRANGEMENT OF CYCLOHEXANONE OXIME

The Beckmann rearrangement of cyclohexanone oxime to ε-caprolactam (precursor to Nylon-6) is an important industrial process. This reaction is now being carried out using concentrated sulfuric acid[107] and is associated with disadvantages like the formation of 2-3 tons of the low-value by-product, ammonium sulfate, per ton of ε-caprolactam, and safety hazards, corrosion and environmental problems arising from the use of sulfuric acid.

Solid acid catalysts like alumina[108], heteropoly acids[109], silica-alumina[110] and zeolites like HY[112,113], ZSM-5[112] and mordenite[113] have been tried for this reaction. Sato *et al.*,[114,115] have reported that the Beckmann rearrangement takes place on the external surface of MFI (ZSM-5) zeolites. They found that the active sites for this reaction are the weaker or neutral centers present on the external surface of the crystallites.

The results obtained over different catalysts *viz.*, silicalite-2, TS-2, AL-MEL, Al-TS-2 and fumed silica are reported in Fig.3.20. The major product is ε-caprolactam. The by-products are cyclohexanone, cyclohexenone, cyanopentane and cyanopentene. The catalysts can be arranged in the following decreasing orders for the conversion of cyclohexanone oxime, selectivity for ε-caprolactam and deactivation rate.

Activity : TS-2 > silicalite-2 > SiO_2 > Al-TS-2 > AL-MEL.
Selectivity: TS-2 ≈ silicalite-2 > Al-TS-2 > AL-MEL > SiO_2.
Deactivation rate : TS-2 < silicalite-2 < SiO_2 < Al-TS-2 < AL-MEL.

In accordance with the earlier reports[116] over MFI zeolites, the presence of Al^{3+} in the MEL framework decreases the activity as well as the selectivity. Moreover, the incorporation of Ti into the framework improves the life of the catalyst (Silicalite-2) without significantly affecting the selectivity of the catalyst. Al-TS-2, where Al^{3+} and Ti^{4+} are substituted into the MEL framework has conversion and selectivity inbetween those of silicalite-2 and Al-MEL. The inset in Fig.3.20 presents the yield (conversion x selectivity / 100) of the lactam obtained over the different catalysts at different times on stream. Though similar yields of lactam are obtained over TS-2 and silicalite-2 upto about 20 h, there is a significant yield loss in the case of silicalite-2 beyond this time. The loss in yield is a result of a decrease in conversion and not selectivity. Apparently, the incorporation of Ti decreases catalyst deactivation. As expected, the incorporation of Al^{3+} in both silicalite-2 and TS-2 decreases both conversion and selectivity of both catalysts. Even amorphous SiO_2 yields more lactam than Al-MEL.

The influence of temperature on the conversion of cyclohexanone oxime and selectivity for ε-caprolactam over TS-2 and silicalite-2 is presented in Fig.3.21. The studies were carried out in the temperature range 543-613 K. Higher conversions and selectivities are obtained at higher temperatures over both the catalysts. The selectivity for lactam increases with time on stream at all the temperatures in the range studied (543-613 K). The increase in selectivity with time may be due to the deactivation of the strong acid sites by coke deposition, which

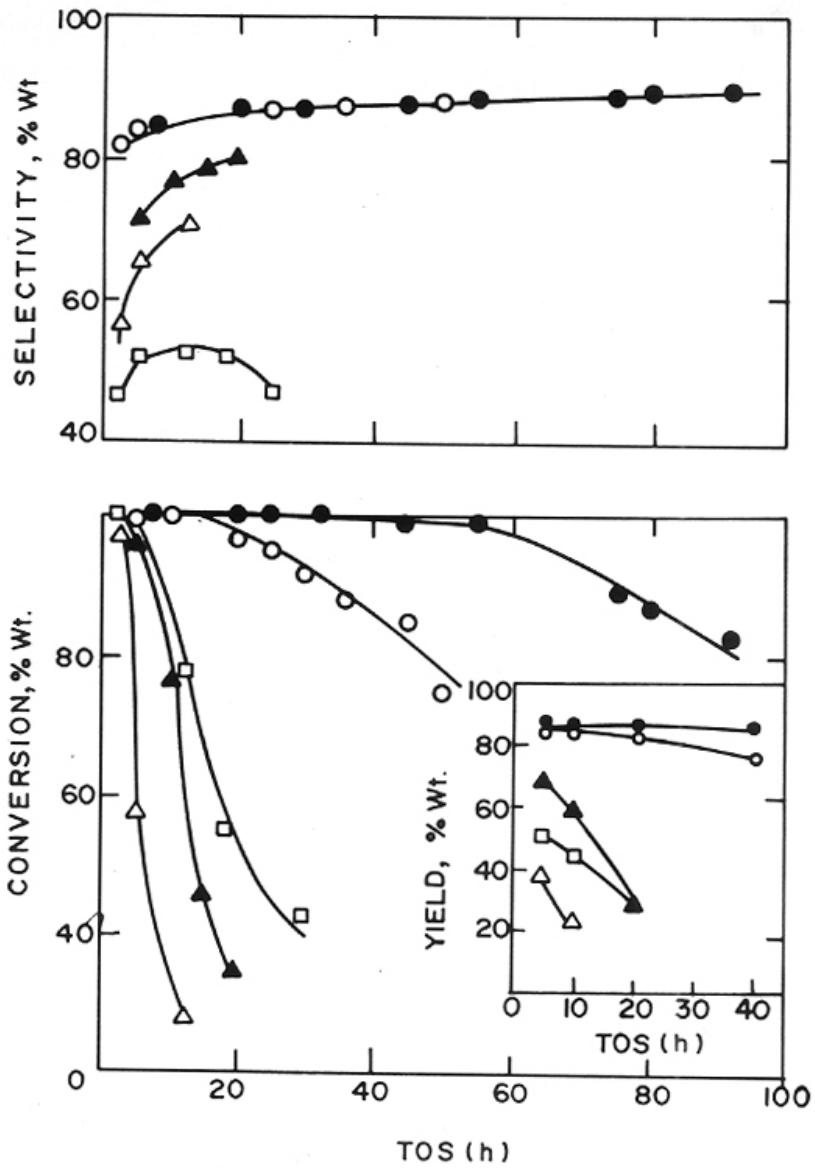

Fig.3.20. Influence of time on stream on conversion and selectivity over various MEL-analogs and fumed silica. **(Beckmann rearrangement)**
(Δ): Al-MEL; (▲): Al-TS-2; (□): Fumed silica; (Θ): silicalite-2; (●): TS-2.
Reaction conditions: Temp. (K) = 613; Press. = atm.; WHSV (h^{-1}) = 7.0; Feed = 6 wt.% oxime in benzene; Carrier gas = N_2 (5 ml/min.).

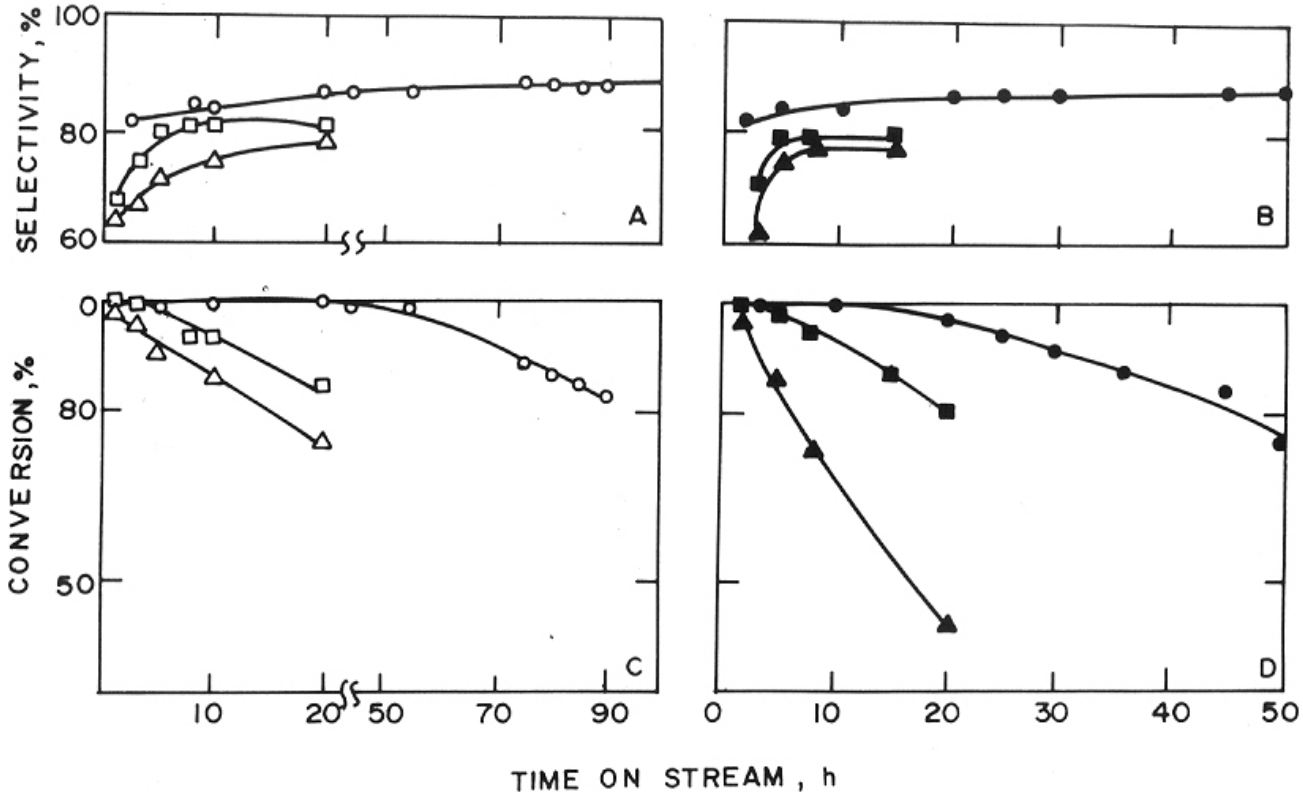

Fig.3.21. Influence of temperature on conversion and selectivity over silicalite-2 and TS-2. (Beckmann rearrangement)
(A) and (C): TS-2; (B) and (D): silicalite-2.
(Δ, ▲): 543 K; (□,■): 573 K; (O,●): 613 K.
Reaction conditions: Prss. = atm.; WHSV (h^{-1}) = 7.0; Feed = 6 wt.% oxime in benzene; Carrier gas = N_2 (5 ml/min.).

cause the formation of the by-products. Further, the deactivation rate decreases with increasing temperature. TS-2 is more resistant towards deactivation at all the temperatures vis-á-vis silicalite-2, though both exhibit similar selectivities for lactam formation.

The effect of space velocity and concentration of cyclohexanone oxime on the activity and selectivity of TS-2 and silicalite-2 are reported in Table 3.28. Higher space velocities lead to a higher concentration of the lactam in the product on both silicalite-2 and TS-2 probably due to a lower decomposition of the lactam, though a slight decrease in the conversion of cyclohexanone oxime is noticed. However, an increase in the concentration of the oxime decreases marginally both the selectivity and conversion.

A. Conclusions

MEL molecular sieves catalyze the Beckmann rearrangement of cyclohexanone oxime to ε-caprolactam. The incorporation of Ti into silicalite-2 framework increases the catalyst life and the selectivity for ε-caprolactam.

3.2.6. OXIDATION OF ALCOHOLS

Esposito *et al.*[37] have reported the oxidation of primary and secondary alcohols to aldehydes and ketones, respectively over TS-1. Very high selectivity for aldehydes (> 90%) has been reported without the subsequent oxidation to carboxylic acids. Recently, Romano *et al.*[25] have also reported the oxidation of various alcohols. Methanol was found to be less active compared to other alcohols, the activity for others decreasing with increasing carbon number.

The oxidation of some primary and secondary alcohols has also been carried out over TS-2. The results are reported in Table 3.29. Secondary alcohols are more selectively oxidized to ketones (≈ 100 %), where as in the case of primary alcohols, by-products like acetals, carboxylic acids and esters are obtained in minor quantities. Cyclohexanol is found to be less active compared to other alcohols.

Table 3.28. Effect of space velocity and oxime concentration

Reaction conditions: Temp. (K) = 613; Solvent = benzene; Carrier gas = N_2 (5 ml/min.); Press. = atm.; Time-on-stream (h) = 5.

Catalyst	WHSV, h^{-1}			Oxime, wt. %		
	3.5	7.0	15.0	6	10	15
TS-2						
Convn. %	100	99	97	100	100	95
Sel. %	83	86	94	84	84	82
Silicalite-2						
Convn. %	100	98	95	100	100	94
Sel. %	84	86	90	83	81	79

Table 3.29. Oxidation of various alcohols over TS-2

Reaction conditions: Catalyst = TS-2 (SiO_2/TiO_2 = 29, 1 g); Alcohol/H_2O_2 = 5.0; Temp. (K) = 338; Duration of run (h) = 5.

Reactant	H_2O_2 selectivity	Product selectivity[a]
Ethanol	78	85
Benzyl alcohol	72	92
Propyl alcohol	75	90
Isopropyl alcohol	75	100
Cyclohexanol	51	100

a: (aldehyde or ketone/alcohol conversion) x 100.

3.3. REFERENCES

1. Taramasso, M., Perego, G. and Notari, B., US Pat., 4,578,521 (1983).
2. Barrer, R.M., in Proceedings, 6th Intern. Zeolite Conf., Reno (USA), Eds. A. Bisio and D. Olson, Butterworths, Guildford, 1984, p.870.
3. Perego, G., Bellussi, G., Corno, C., Taramasso, M., Buonomo, F. and Esposito, A., *Stud. Surf. Sci. Catal.*, **28** (1986) 129.
4. Kraushaar, B., Ph.D Thesis., "Characterization and Modification of Zeolites and Related Materials", The Technical University of Endhoven, Eindhoven, The Netherlands, (1989).
5. Boccuti, M.R., Rao, K.M., Zecchina, A., Leofanti, G. and Petrini, G., *Stud. Surf. Sci. Catal.*, **48** (1989) 133.
6. Thangaraj, A., Ph.D Thesis, "Synthesis, Characterization and Catalytic Properties of Titaniumsilicate Molecular Sieves", University of Poona, Pune, India, (1991).
7. Kraushaar, B. and Van Hooff, J.H.C., *Catal. Lett.*, **1** (1988) 81.
8. Skeels, G.W. and Flanigen, E.M., *ACS Monograph*, **398** (1989) 421.
9. Ferrini, C. and Houvenhoven, H.W., *Stud. Surf. Sci. Catal.*, **55** (1990) 53.
10. Chen, M.C., Chu, S.J., Chang, N.S., Chen, T.K., Chuang. and Chen, L.Y., *Stud. Surf. Sci. Catal.*, **38** (1988) 253.
11. Thangaraj, A., Kumar, R, Mirajkar, S.P. and Ratnasamy, P., *J. Catal.*, **130** (1991) 1.
12. Zecchina, A., Spoto, G., Bordiga, S., Padovan, M., Leofanti, G. and Petrini, G., *Stud. Surf. Sci. Catal.*, **65** (1991) 671.
13. Zecchina, A., Spoto, G., Bordiga, S., Ferrero, A., Petrini, G., Leofanti, G. and Padovan, M., *Stud. Surf. Sci. Catal.*, **69** (1991) 251.
14. Tuel, A., Diab, J., Gelin, P., Dufaux, M., Dutel, J. and Taarit, B.Y., *J. Mol. Catal.*, **63** (1990) 95.
15. Behrens, P., Felsche, J., Vettr, S., Schulz-Ekloff, G., Jaeger, N.I. and Niemann, W., *J. Chem. Soc., Chem. Commun.*, (1991) 678.
16. Carati, A., Contarini, S., Millini, R. and Bellussi, G., ACS Symp. on Synthesis and Properties of New Catalysts, Boston 26th Nov-1 Dec., 1990., *Mat. Res. Soc.*, Ext Abstract (EA-24), (1990) 47.
17. Bellussi, G. and Fattore, V., *Stud. Surf. Sci. Catal.*, **69** (1991) 79.
18. Notari, B., *Stud. Surf. Sci. Catal.*, **37** (1987) 413.
19. Thangaraj, A., Kumar, R. and Ratnasamy, P., *Appl. Catal.*, **57** (1990) L1.
20. Hölderich, W., Hesse, M. and Näumann, F., *Angew. Chemie. Int. Ed. (Eng.)*, **27** (1988) 226.
21. Tatsumi, T., Nakamura, M., Negishi, S. and Tominaga, H., *J. Chem. Soc., Chem. Commun.*, (1990) 476; Nakumura, M., Nagishi, S., Yuasa, K., Tatsumi, T. and Tominaga, H., *Shokubai*, **32** (1990) 99.
22. Huybrechts, D.C., Bruyeker, L.D. and Jacobs, P.A., *Nature*, **345** (1990) 240.
23. Clerici, M.G., *Appl. Catal.*, **68** (1991) 249.

24. Clerici, M.G., Bellussi, G. and Romano, U., *J. Catal.,* **129** (1991) 159.

25. Romano, U., Esposito, A., Maspero, F., Neri, C. and Clerici, M.G., *Stud. Surf. Sci. Catal., 55* (1990) 33; Romano, U., Esposito, A., Maspero, F., Neri, C. and Clerici, M.G., *La Chimica & L'Industria,* **72** (1990) 610.

26. Roffia, P., Leofanti, G., Cesana, A., Mantegazza, M., Padovan, M., Petrini, G., Tonti, S. and Gervasutti, P., *Stud. Surf. Sci. Catal.,* **55** (1990) 43; Roffia, P., Leofanti, G., Cesana, A., Mantegazza, M., Padovan, M., Petrini, G., Tonti, S. and Gervasutti, P., *La Chimica & L'Industria,* **72** (1990) 598.

27. Tatsumi, T., Nakumara, M., Yuasa, K. and Tominaga, H., *Chem. Lett.,* (1990) 297.

28. Thangaraj, A., Kumar, R. and Ratnasamy, P., *J. Catal.,* **131** (1991) 294.

29. Huybrechts, D.R.C., Vaesen, I., Li, H.X. and Jacobs, P.A., *Catal. Lett.,*, **8** (1991) 237.

30. Thangaraj, A., Sivasanker, S. and Ratnasamy, P., *J. Catal.,* **131** (1991).

31. Nakamura, M., Negishi, S., Yuasa, K., Tatsumi, T. and Tominaga, H., 65th CATSJ Meeting Abstracts. No. B3, **32** (**2**) (1990) 101.

32. Rao, P.R.H.P., Thangaraj, A. and Ramaswamy, A.V., *J. Chem. Soc., Chem. Commun.,* (1991) 1139.

33. Thangaraj, A. and Sivasanker, S., in "Recent Developments in Catalysis: Theory and Practice" Eds. B. Viswanathan *et al.*, Norosa Publishing House, New Delhi, 1990, p.535.

34. Thangaraj, A., Sivasanker, S. and Ratnasamy, P., *J. Catal.,* (submitted).

35. Tvarci Zkova, Z., Habersberger, K., Zilkova, N. and Jíru., *Appl. Catal.,* **79** (1991) 105.

36. Tuel, A, Moussa-Khouzami, S. Taarit, Y.B. and Naccache, C., *J. Mol. Catal.,* **68** (1991) 45.

37. Esposito, A., Neri, C. and Buonuomo, F., U.S. Pat., 4,480,135 (1984).

38. Clerici, M.G., Bellussi, G. and Romano, U., *J. Catal.,* **129** (1991) 159.

39. Hage-Al Asswad, J., Nagy, J.B., Gabelica, Z. and Derouane, E.G., in "Proc. 8th Int. Zeolite Conf.", Amsterdam, July 10-14, RRR, 1989, p.475.

40. Kraushaar, B. and van Hooff, J.H.C., *Catal. Lett.*, **2** (1989) 43.

41. Reddy, J.S., Kumar, R. and Ratnasamy, P., *Appl. Catal.,* **58** (1990) L1.

42. Reddy, J.S. and Kumar, R., *J. Catal.,* **130** (1990)) 440.

43. Reddy, J.S., Hegde, S.G. and Ratnasamy, P., (unpublished results)

44. Reddy, J.S. and Kumar, R., *Zeolites*, **12** (1990) 95.

45. Reddy, J.S., Sivasanker, S. and Ratnasamy, P., *J. Mol. Catal.,* **69** (**3**) (1991) 383.

46. Reddy, J.S., Sivasanker, S. and Ratnasamy, P., *J. Mol. Catal.,* **70** (**3**) (1991) 335.

47. Reddy, J.S., Sivasanker, S. and Ratnasamy, P., *J. Mol. Catal.,* **71** (**3**) (1991) 373.

48. Reddy, J.S. and Sivasanker, S., *Ind. J. Technol.,* **30** (1992) 64.

49. Reddy, J.S., Kire, U.R., Mitra, R.B. and Ratnasamy, P., (communicated to J. Chem. Soc., Chem. Commun.).

50. Reddy, J.S, Sivasanker, S. and Ratnasamy, P., *Catal. Lett.*, **11** (1991) 241.

51. Reddy, R.S., Reddy, J.S., Kumar, R. and Kumar, P., *J. Chem. Soc., Chem. Commun.*, (1991) 84.

52. Reddy, J.S., Ratnasamy, P. and Mitra, R.B., (unpublished results).

53. Notari, B., *Stud. Surf. Sci. Catal.*, **60** (1990) 343.

54. Shilun, Q., Wenqin, P. and Shangqing, Y., *Stud. Surf. Sci. Catal.*, **49A** (1989) 133.

55. Lok, B.M.T., Marcus, B.K. and Flanigen, E., PCT WO 85/04853 (1985).

56. Chappman, D.M. and Roc, A.L., *Zeolites*, **10** (1990) 730.

57. *Chem. & Eng. News* **30** (1991) 31.

58. Bradley, D.C., in "Progress in Inorganic Chemistry" Ed. F.A. Cotton, Inter Science Publishers, Inc., New York, Vol.II, (1990) 316.

59. Schmidt, H, Scholze, H. and Kaiser, A., *J. Non-Cryst. Solids*, **63** (1984) 1.

60. Ernst, S., Jacobs, P.A., Martens, J.A. and Weitkamp, J., *Zeolites*, **7** (1987) 458.

61. Jacobs, P.A. and Martens, J.A., *Stud. Surf. Sci. Catal.*, **33** (1987) 58.

62. Bhat, R.N. and Kumar R., *J. Chem. Tech. Biotech.*, **48** (1990) 453.

63. Ernst, S., Kumar, R. and Weitkamp, J., in "Zeolite Synthesis", "Zeolite Synthesis" Eds. M.L. Occelli and H.E. Eobson ACS Monograph 398, Washington, DC, 1989, p.560.

64. Casci, J.L. and Lowe, B.M., *Zeolites*, **3** (1983) 186.

65. Kokatailo, G.T., Chu, P., Lawton, S.L. and Meier, W.M., *Nature*, **275** (1978) 119.

66. Jablonski, J.M., Sand, L.B. and Gard, J.S., *Zeolites*, **6** (1986) 396.

67. Thangaraj, A. and Sivasanker, S., *J. Chem. Soc., Chem. Commun.*, (1992) 123.

68. Best, M.F. and Condrate, R.A., *J. Mat. Sci. Lett.*, **4** (1985) 994.

69. Varshal, B.G., Denisol, V.N., Mavrin, B.N., Pavlova, G.A., Podonbedov, V.B. and Sterin, K.H.E., *Opt. Spectrosc.*, (USSR), **47** (1979) 344.

70. Jorgenson, C.K., in "Prog. Inorg. Chem." Ed. J. Lippard, Pub. John Wiley, New York, Vol. 12, 1970, p.101.

71. Lin, D., Ph.D Thesis No. 126-89 (1989), University of Clande Bernard, Lyon, France, 1986.

72. Bremer, H., Mörke, W., Schödel, R. and Vogt, E., *Adv. Chem. Ser.*, **121** (1973) 249.

73. Breck, D.W., in "Zeolite Molecular Sieves", Wiley Pub., New York, 1974.

74. Szostak, R in "Molecular Sieves, Principles of Synthesis and Identification", Van Nostrand, Reinhold, New York, 1989, p.221.

75. Wang, I., Chen, T., Chao, K. and Sai, T., *J. Catal.*, **60** (1979) 140; Nayak, V.S and Choudhary, V.R., *Appl. Catal.*, **10** (1984) 137.

76. Ball, W.J., Dwyer, J., Garforth, A.A. and Smith, W.J., *Stud. Surf. Sci. Catal.*, **28** (1986) 137.

77. Bellussi, G., Millini, R., Carati, A., Meddinelli, G. and Gervasini, A., *Zeolites*, **10** (1990) 642.

78. Vysotskii, A.V., Psarko, B.P., Simikova, A.A., Yaskina, V.A. and Krasnyatov, N.P., *Zh. Fiz. Khim.,* **62(5)** (1988) 1380.

79. Szostak, R., Nair, V. and Thomas, T.L., *J. Chem. Soc., Faraday Trans. I,* **83** (1987) 487.

80. Petrini, G., Cesana, A., De Alberti, G.,Genoni, A.F., Leofanti, G., Padovan, M., Paparatto, G. and Roffia, P., *Stud. Surf. Sci. Catal.,* **68** (1991) 761.

81. Genoni, F., Leofanti, G., Padovan, M., Petrini, N., Trezza, G. and Zecchina, A., Int. Symp., "Zeolite Chemistry and Catalysis", Prague, Sept 8-13, 1991, RRR, p.25.

82. Andrianov, K.A. and Zhdanov, A.A., *Vysokomolekul. Soedineniya,* **1** (1959) 894; Chem. Abstr. **54** (1960) 9348.

83. Vetrivel *et al.*, (unpublished results).

84. Fripiat, J.G., Andre, F.B., Andre, J.M. and Derouane, E.G., *Zeolites,* **5** (1985) 306.

85. Olson, D.H., Kokatailo, G.T., Lawton, S.L. and Meier, W.M., *J. Phy. Chem.,* **85** (1981) 2238.

86. Reddy, J.S., Sivasanker. and Ratnasamy, P., *Catal. Lett.,* (communicated).

87. Sheldon, A.A. and Kochi, J.K., in "Metal Catalyzed Oxidations of Organic Compounds", Academic Press, New York, 1981.

88. Lyons, J.E., *Appl. Catal.,* **3** (1981) 131.

89. Faraj, M. and Hill, C,C., *J. Chem. Soc., Chem. Commun.,* (1987) 1487.

90. Shilov, A.E., in "Activation of Saturated Hydrocarbons by Transition Metal Complexes", Reidel, Pordrecht, 1984, p.88.

91. Meunier, B., *Bull. Soc. Chim. Fr.,* (1986) 578.

92. Hubrechts, D.R.C., Parton, R.F. and Jacobs, P.A., *Stud. Surf. Sci. Catal.,* (1991) .

93. Kirk-othmer, in "Encyclopaedia of Chemical Technology" 3rd Ed. Vol.18., John Wiley and Sons, (1990) 476.

94. Ref.87, p.432.

95. Armor, J.N., *J. Catal.,* **70** (1981) 72.

96. Petrini, G., Cesano, A., De Alberti, G., Genoni, F., Leofanti, G., Padovan, M., Paparatto, G. and Roffia, P., *Stud. Surf. Sci. Catal.,* **68** (1991) 761.

97. Dreoni, D.P., Pinelli, D. and Trifiró, F., in "Preprints of 3rd European Workshop Meeting, New Developments in Selective Oxidation", Eds. B. Delmon and P.Ruiz, Vol.1, Université Catholique de Louvain, Louvain-la-Necule, 1991, 1991; Dreoni, D.P., Pinelli, D., Trifiró, F., Busca, G and Lorenzelli, G., Private communication.

98. Varagnat, J., *Ind. Eng. Chem. Prod. Res. Dev.,* **15** (1976) 212.

99. Weisz, P.B., *Stud. Surf. Sci. Catal.,* **28** (1981) 3.

100. Sheldon, *J. Mol. Catal.,* **7**, 107 (1980).

101. Eur. Pat. Appl. 315 248 (1988); Eur. Pat. 315 247 (1988).

102. Eur. Pat. 190 609 (1986).

103. Eur. Pat. 102 097 (1983).

104. Bönnemann, G., Brijoux, W., Pingel, N. and D.M.M. Rohe, in "Catalysis of Organic Reactions", Cheimcal Industries/22, Ed. R.L. Augustine, Marcel Dekker, Inc., New York, 1985, p.309.

105. House, H.O., in "Modern Synthetic Reactions" 2nd Ed., Ed. Benjamin, W.A., Menlo Park, CA, 1972, p.257.

106. Hubrechts, D.R.C., Buskens, P.L. and Jacobns, P.A., *J. Mol. Catal.,* **71** (1992) 129.

107. Kent, J.E. and Riegel, S., in "Handbook of Industrial Chemistry", 8th Ed., Van Nostrand, New York, 1983, p.402.

108. Immel, O., Schwarz, H.H., Starke, H. and Swodenk, W., *Chem. Eng. Techn.,* **56** (1984) 612.

109. Landis, P.S. and Venuto, P.B.,*J. Catal.,* **6** (1966) 245.

110. Venuto, P.B. and Landis, P.S., *Adv. Catal.,* **18** (1968) 259.

111. Hölderich, W., Messe, M. and Näumann, F., *Angew. Chem. Int. Ed. (Eng.),* **27** (1986) 187.

112. Corma, A., Garcio, H. and Primo, J., *Zeolites,* **11** (1991) 593.

113. Bell, W.K. and Chang, C.D, EP 056,698, 1988.

114. Sato, H., Ishii, N., Hirose, K. and Nakamura, S., *Stud. Surf. Sci. Catal.,* **28** (1986) 755.

115. Sato, H., Hitrose, K., Ishii, N. and Yamada, Y., EP 234,088, 1987.

116. Anajo, A., Burguet, M., Corma, A. and Fornes, V., *Appl. Catal.,* **22** (1986) 187.

CHAPTER - IV

STUDIES ON METALLOSILICATES WITH *MEL* TOPOLOGY

4.1. INTRODUCTION

The isomorphous substitution of Si or Al by other trivalent elements in zeolite frameworks has been reviewed by Barrer[1]. The replacement of Al by Fe in the framework of ZSM-5 has been reported by various workers[2-6]. Szostak and Thomas[7] have synthesized sodalite with significant quantities of iron in the framework (SiO_2/Fe_2O_3 = 6-30). Al free ferrisilicate analogs of zeolite Beta[8], ZSM-23[9], EU-11[10], mordenite[11], ZSM-20[12], ZSM-12[13] and Y[12] have been synthesized. Recently, Ratnasamy and Kumar[14] have reviewed the synthesis, characterization and catalytic properties of various ferrisilicates. The synthesis of the crystalline gallosilicate analogs of various zeolite structures have also been reported[15,16]. Ione *et al.*[17] have studied the possibility of isomorphous substitution of Si^{4+} by Me^{n+} cations of elements of group I-VIII (where n = 4) in the ZSM-11 structure using tetrabutyl ammonium cation as a template. Based on ESR measurements alone, it was concluded that only a small part of the total Fe^{3+} ions used could be incorporated in the tetrahedral framework of ZSM-11. The isomorphous substitution of various elements like B[18], Ga[17,19], Fe[17,20], Ti[21] and V[22] into the MEL framework has been achieved.

The extent of incorporation of metal ions in a zeolite framework depends on many factors like i) the nature of an element ii) the zeolite structure iii) the composition of the gel and iv) preparation methods. The nature of the metal oxides and the rates of hydrolysis of reactants also govern the extent of incorporation.

The availability of isostructural metallosilicate molecular sieves with different isomorphous substituents provides an opportunity to study the shape-selective properties and deactivation behavior of these materials as a function of their chemical nature. This may help in finding out whether the geometric features (pore structure, crystal morphology etc.) of a particular zeolite are the sole controlling factors in shape-selectivity or the chemical nature (substitutent) also influences the shape-selective properties.

This chapter describes the studies carried out on the

- incorporation of Ga and Fe in the MEL framework
- synthesis of pure MEL-analogs.
- investigation on the influence of isomorphous substitution on the p-/o-xylene ratio in the isomerization of m-xylene and catalyst life in the disproportionation of ethylbenzene.

4.2. RESULTS AND DISCUSSION

4.2.1. SYNTHESIS

The synthesis of Al-MEL (ZSM-11), Fe-MEL and Ga-MEL was carried out using TBA-OH as the template. Al-nitrate, Fe-nitrate and Ga-nitrates were used as the source of the metal ions. The general procedure for the synthesis was the formation of a metallosilicate gel with TEOS, TBA-OH and the metal source, and autoclaving it at the required temperature. The details of the synthesis procedure have been described in chapter II.

It is known that for the efficient synthesis of ferrisilicate molecular sieves the formation of insoluble, brown colored ferric hydroxides should be avoided by slowly adding the acidic ferric nitrate solution to the silicate solution. This way of addition facilitates the initial formation of a white or pale yellow ferrisilicate gel. After the formation of the ferrisilicate gel, the desired template is added. A similar procedure was adopted in the present case also, where a pure white gel resulted in highly crystalline and white Fe-MEL samples, free from MFI impurities (Fig.2.2). Since gallate ions are more stable at higher pH, the addition sequence does not influence much the incorporation of Ga into the MEL framework. When 1,8-diaminooctane (1,8-DAO) was used as a template, longer crystallization times were observed when compared to TBA. Crystal size was also larger in the 1,8-DAO system. However, both the templates produced pure MEL analogs. The rates of crystallization of Al-, Ga- and Fe-MEL are compared in Fig.4.1. The rate decreases in the following order: Al-MEL > Ga-MEL > Fe-MEL. Ball *et al.*[23] also have shown that aluminosilicates crystallize more rapidly compared to ferrisilicates. Different crystallization rates for different metallosilicates may be due to the different concentrations of the corresponding metal hydroxide species in the reaction mixture.

4.2.2. STUDIES ON THE PHASE-PURITY OF MEL

The intergrowth of ZSM-5 has frequently been observed during the hydrothermal synthesis of ZSM-11[24-30]. These intergrowths/impurities are believed to affect catalytic activity/selectivity. Hence, a study of the factors responsible for the occurrence of ZSM-5 phase/intergrowth along with ZSM-11 has been carried out.

Hou and Sand[24], in an almost Al-free system, observed that the formation of ZSM-11 and ZSM-5 strongly depends on crystallization temperature. ZSM-11 was formed at the lower temperatures (373-408 K) and ZSM-5 at higher temperatures (413-493 K). Jablonski *et al.*[25] found that an optimum amount of K^+ at 403 K favoured the formation of ZSM-11. Recently,

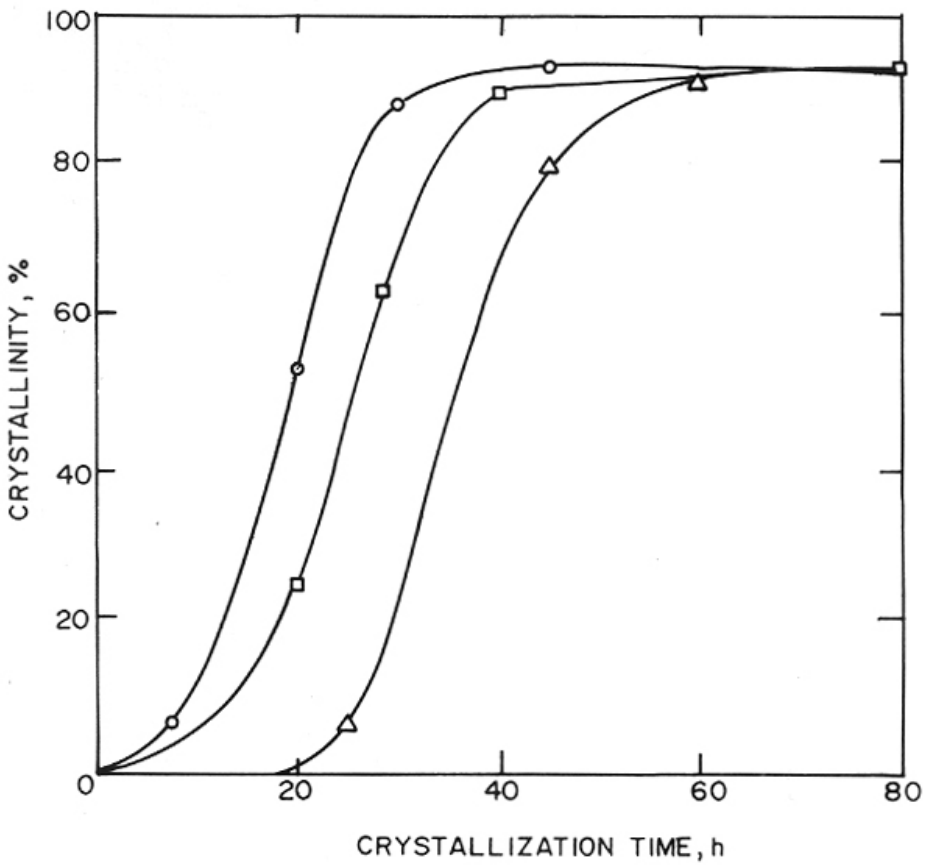

Fig.4.1. Influence of nature of the metal ion on the rate of crystallization of MEL analogs.
(○): Al-MEL; (□): Ga-MEL and (△): Fe-MEL.
Molar gel composition: SiO_2/M_2O_3 = 90; TBA-OH/SiO_2 = 0.2; H_2O/SiO_2 = 30).
Crystallization temp. (K) = 443.

Kaucic *et al.*[26] have observed that higher OH^-/SiO_2, SiO_2/Al_2O_3 ratios and temperature favour the formation of ZSM-5 impurity in ZSM-11 system. Further, tetrabutylphosphonium (TBP^+) ion was found to be more effective, compared to TBA^+, as a structure (MEL) directing agent. The use of trialkyl amines (such as tripropylamine or tributylamine) as structure directing agents resulted in ZSM-5/ZSM-11 mixtures[27].

In Al-free systems using TBA^+ as template, Bibby *et al.*[28] observed that the presence of alkali metal cations in the starting gel is detrimental to the phase purity of ZSM-11 (Silicalite-2); ZSM-5 (Silicalite-1) being the major phase. However, Kungang *et al.*[29] could synthesize Al-free ZSM-11 (Silicalite-2) in the presence of alkali metal chlorides from the molar composition: 3 NH_4OH : 0.3 ± 0.15 MCl : 8.5 SiO_2 : 100 H_2O (M = Li, Na, K, Rb or Cs). The formation of silicalite-2 in the presence of alkali metal ions has been explained on the basis of greater mutual repulsion of the hydrated alkali metal cations in the straight channels of ZSM-11 structure compared to that in the longer (and additionally) zigzag channels in ZSM-5 structure. Jacobs and Martens[30] have reported the synthesis of pure ZSM-11 in the presence of Na, using 1,8-diaminooctane as a template.

During our[31] studies on the crystallization of TS-2, no TS-1 impurity was observed under a broad range of SiO_2/TiO_2 and OH^-/SiO_2 ratios and at quite high crystallization temperatures (up to 458 K). No alkali metal or NH_4^+ salt/hydroxide was added and TBA-OH (20 wt.% methanolic or 40 wt.% aq. soln) was used as a template. This suggested that the presence of alkali metal cations, and not the crystallization temperature, may be the crucial factor favouring the occurrence of ZSM-5 type impurity during the synthesis of ZSM-11. In the present study, the effect of Na^+/SiO_2, OH^-/SiO_2, TBA-OH/SiO_2, temperature and the source and type of M^{3+} cations (M = Al, Fe or Ga) on the phase purity of ZSM-11 have been systematically examined. Relatively pure sources of SiO_2 (tetraethylorthosilicate), Al_2O_3 (aluminium isopropoxide) and TBA-OH were used to minimize the Na^+ or K^+ impurity originating from reactants, in the gel.

The following molar gel composition was used:

$$x\ Na^+ : y\ TBA : Al_2O_3 : 90\ SiO_2 : 2700\ H_2O$$

where x = 0, 4.5, 9, 18 or 36; y = 9, 18 or 36.

The influence of variables x or y on the nature of the product formed was monitored by x-ray diffraction (Rigaku, Model D/MAX III VC, Japan). The XRD pattern of MFI in the 2 θ range of 20° and 25° has four reflections at 23.1, 23.2, 23.9 and 24.4 degrees (Fig.1.2). In the

case of MEL, only two peaks at 2 θ = 23.1° and 23.9° are present. The ratio of the intensity of the peak at 24.4 to that at 23.1 in the XRD pattern of physical mixtures of ZSM-5 and ZSM-11 was found to correlate well with the actual amounts present upto 75 % MFI content (Fig.4.2). The percentage of MFI impurity in the synthesis products were determined from this graph (Fig.4.2).

The effect of the various synthesis parameters such as TBA^+/SiO_2, Na^+/SiO_2, OH^-/SiO_2 (i.e. (TBA-OH + NaOH)/SiO_2) molar ratios and temperature on the phase purity of MEL is reported in Table 4.1. Under the conditions of the study, temperature does not seem to affect the purity of the MEL samples (sample no. 1 and 2, Table 4.1). When NaOH was used, an equivalent amount (mole) of TBA-Br was added in the place of TBA-OH to maintain the TBA^+/SiO_2 and OH^-/SiO_2 mole ratios constant. Increasing the Na-content in the reaction mixture increased the MFI impurity to a larger extent (sample no. 3,4 and 5, Table 4.1). Even a small amount of Na (Si/Na = 20) gives about 25 % MFI impurity. When NaCl was used in the place of NaOH, MFI impurity decreased (sample no. 6 and 7, Table 4.1). At SiO_2/Na = 10, NaCl produced 15 % MFI, while NaOH produced about 55 % MFI impurity. These differences may be due to the differences in the nett OH^- ions available in the system. TBA-OH may not dissociate completely to give equivalent moles of OH^-, unlike NaOH. So, when NaOH (+ TBA-Br) is added to the reaction mixture, the OH^- ion concentration is more when compared to the NaCl + TBA-OH system.

When OH^- ion concentration was varied by adding different amounts of TBA-OH to the reaction mixture keeping all other parameters constant (sample no. 2,8, and 9), no adverse effect on the phase purity of MEL was observed. In all the three conditions (TBA-OH/SiO_2 = 0.1, 2 and 4), pure MEL was obtained. This indicates that a combination of both OH^- ion concentration and the presence of Na ions are responsible for the formation of MFI in MEL zeolites.

Scanning electron photographs of various metallosilicate MEL samples synthesized in the absence of Na (100 % MEL) are shown in Fig.4.3. All the three metallosilicate molecular sieves have nearly similar particle sizes in the range of 0.5-1.5 μm. SEM photographs of Al-MEL samples obtained in the presence of NaOH (sample no. 7) and NaCl (sample no. 4) are shown in Fig.4.4. When NaCl was added, the crystal size increased significantly, the crystal shape being cubic. In the presence of NaOH, smaller particles were obtained.

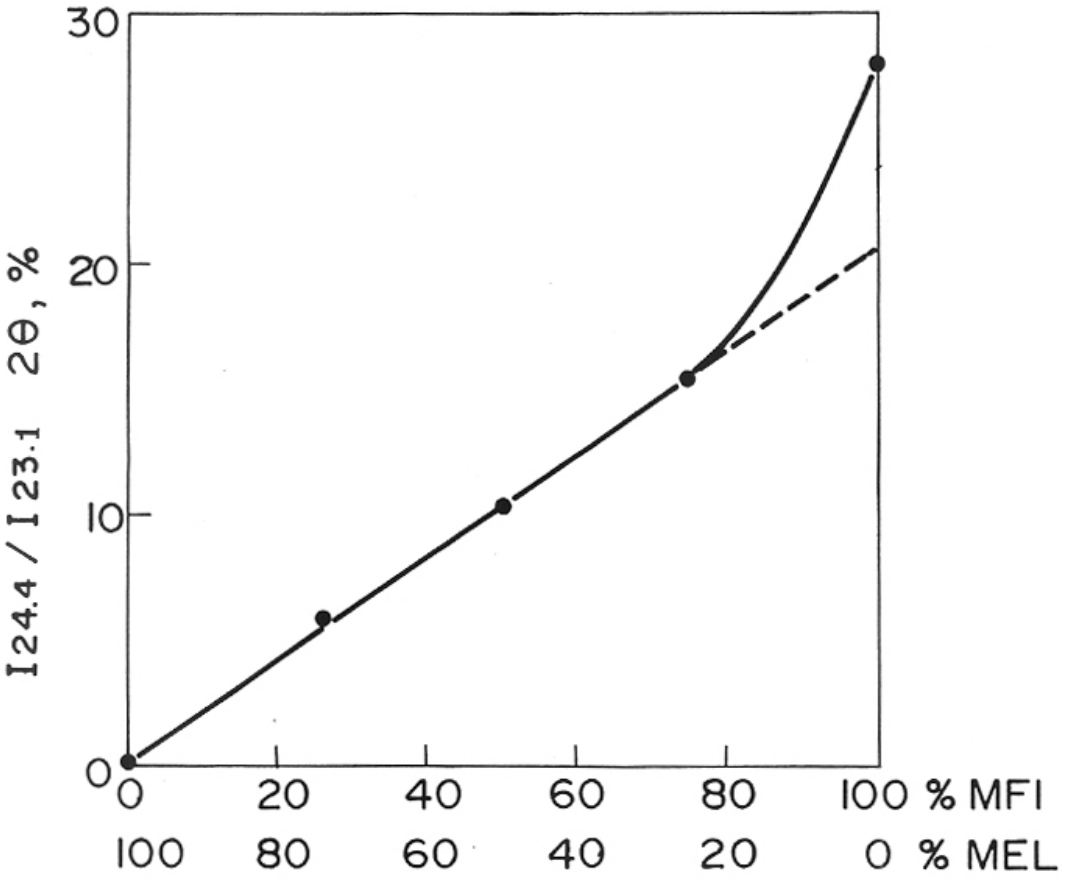

Fig.4.2. Relationship between the ratio of intensity of peaks at 2 θ = 24.4° to 23.1° ($I_{24.4}/I_{23.1}$) and composition of physical mixtures of ZSM-11 and ZSM-5.

Table 4.1. Effect of various synthesis conditions on the purity of MEL.

S.No.	$\frac{TBA-OH}{SiO_2}$	$\frac{TBA-Br}{SiO_2}$	$\frac{NaOH}{SiO_2}$	$\frac{NaCl}{SiO_2}$	$\frac{OH^{-b}}{SiO_2}$	Crystallization		Distribution, %	
						Temp.(K)	Time, d[c]	ZSM-11	ZSM-5
1.	0.2	-	-	-	0.2	413	3	100	0
2.	0.2	-	-	-	0.2	443	2	100	0
3.	0.15	0.05	0.05	-	0.2	443	2	75	25
4.	0.1	0.1	0.1	-	0.2	443	1	45	55
5.	0.0	0.2	0.2	-	0.2	443	2	40	60
6.	0.2	-	-	0.1	0.2	443	5	85	15
7.	0.2	-	-	0.4	0.2	443	4	45	55
8.	0.1	-	-	-	0.1	443	6	100	0
9.	0.4	-	-	-	0.4	443	1	100	0

a: SiO_2/M_2O_3 = 90; H_2O/SiO_2 = 30 (M = Al (Sample 1-10); Fe (Sample 11) or Ga (Sample 12) for samples 10-12, respective metal nitrate was used as metal source.

b: OH^-/SiO_2 = (TBA-OH + NaOH)/SiO_2.

c: time required to get fully crystalline material.

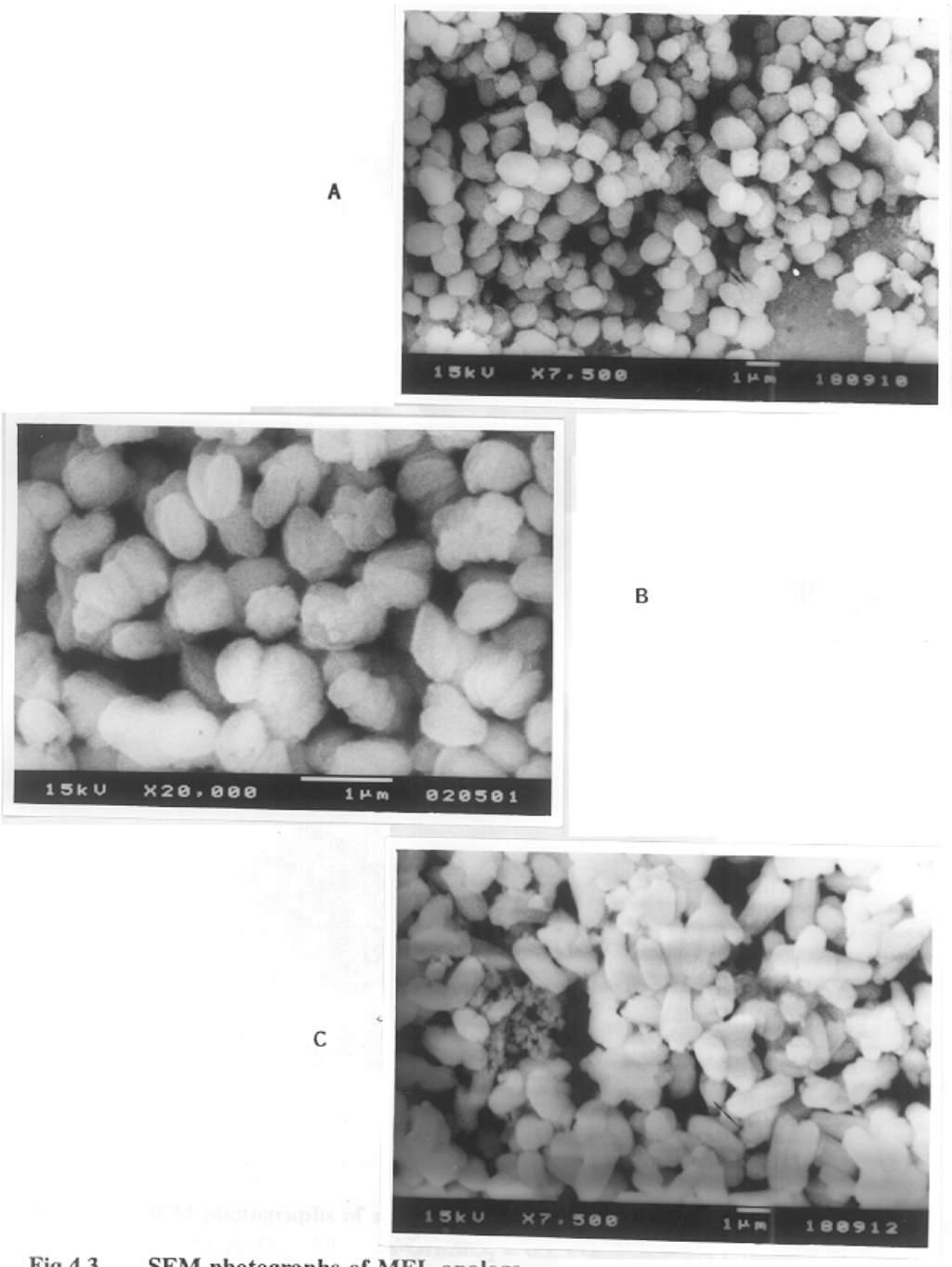

Fig.4.3. **SEM photographs of MEL-analogs.**
A: Al-MEL; B: Ga-MEL; C: Fe-MEL.

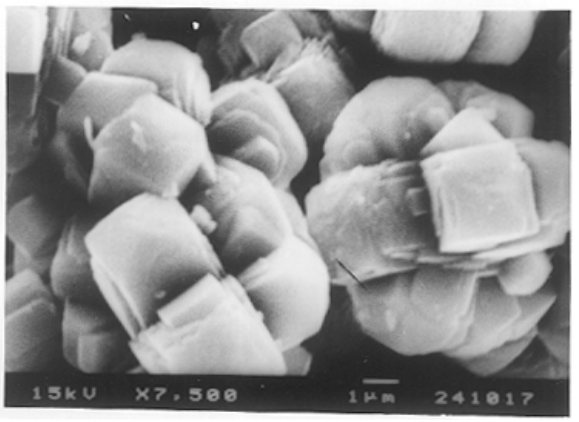

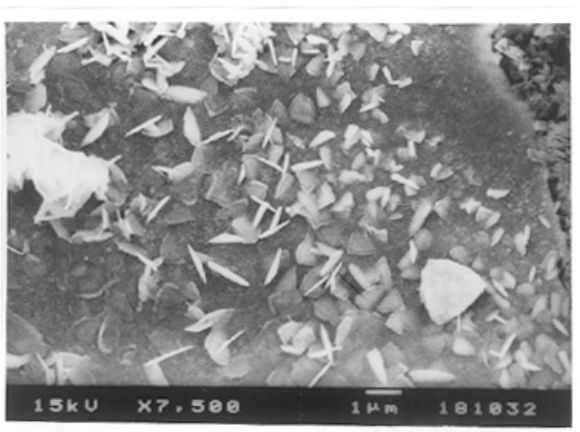

Fig.4.4. **SEM photographs of sample no.s 7 (A) and 4 (B).**
A: SiO_2/Al_2O_3 = 90; TBA-OH/SiO_2 = 0.2; Na/SiO_2 = 0.4 (NaCl).
B: SiO_2/Al_2O_3 = 90; TBA-OH/SiO_2 = 0.2; Na/SiO_2 = 0.1 (NaOH).

4.2.3. CHARACTERIZATION

A. Chemical analysis

The chemical composition of reactant gels as well as the final crystalline solids are given in Table 4.2. Because of the highly pure source of silica used (TEOS), the Al concentration in Fe-MEL and Ga-MEL was found to be negligible (SiO_2/M_2O_3 > 4000). Al could not be detected by NMR.

Table 4.2. Synthesis conditions and crystal size of various MEL-analogs.

	Zeolite	SiO_2/M_2O_3 (gel)[a]	SiO_2/M_2O_3 (product)[a]	Crystn. time, d	Crystal size, (μm)
1.	Al-MEL	45	37	1	≈ 1
2.	Ga-MEL	22	26	2	-
3.	Ga-MEL	45	35	1-2	≈ 1
4.	Ga-MEL	90	72	1	≈ 1
5.	Fe-MEL	22	20	5	1-2
6.	Fe-MEL	45	40	2-3	≈ 1
7.	Fe-MEL	90	78	2	≈ 1
8.	Fe-MEL[b]	45	35	9	< 1
9.	Fe-MEL[b]	68	57	8	1-2
10.	Fe-MEL[b]	90	81	8	2-3
11.	Ga-MEL[b]	45	39	8	2-3
12.	Al-MEL[b]	45	39	6	2-3

a: M = Al, Ga or Fe for Al-, Ga- and Fe-MEL, respectively.

b: 1,8-diamino octane was used as a template; gel composition: 30 1,8-DAO : 30 Na_2O : x M_2O_3 : 100 SiO_2; 2800 H_2O (where M = Al, Ga or Fe and x = 1.11, 0.74, 0.55, 1.11 and 0.11 for samples 8-12, respectively).

B. X-ray diffraction

The XRD patterns of the samples match well with that reported for MEL zeolites. Fig.4.5 depicts the influence of concentration of iron (Fe/(Fe+Si)) on the tetragonal unit cell parameters a, c and unit cell volume, v. The unit cell parameters of Ga-MEL having different Ga contents are reported in Table 4.3. A linear increase in the unit cell parameters and volume with the increase in iron or gallium contents in Fe-MEL and Ga-MEL, respectively, strongly suggest that the larger Fe and Ga atoms are present in the tetrahedral framework.

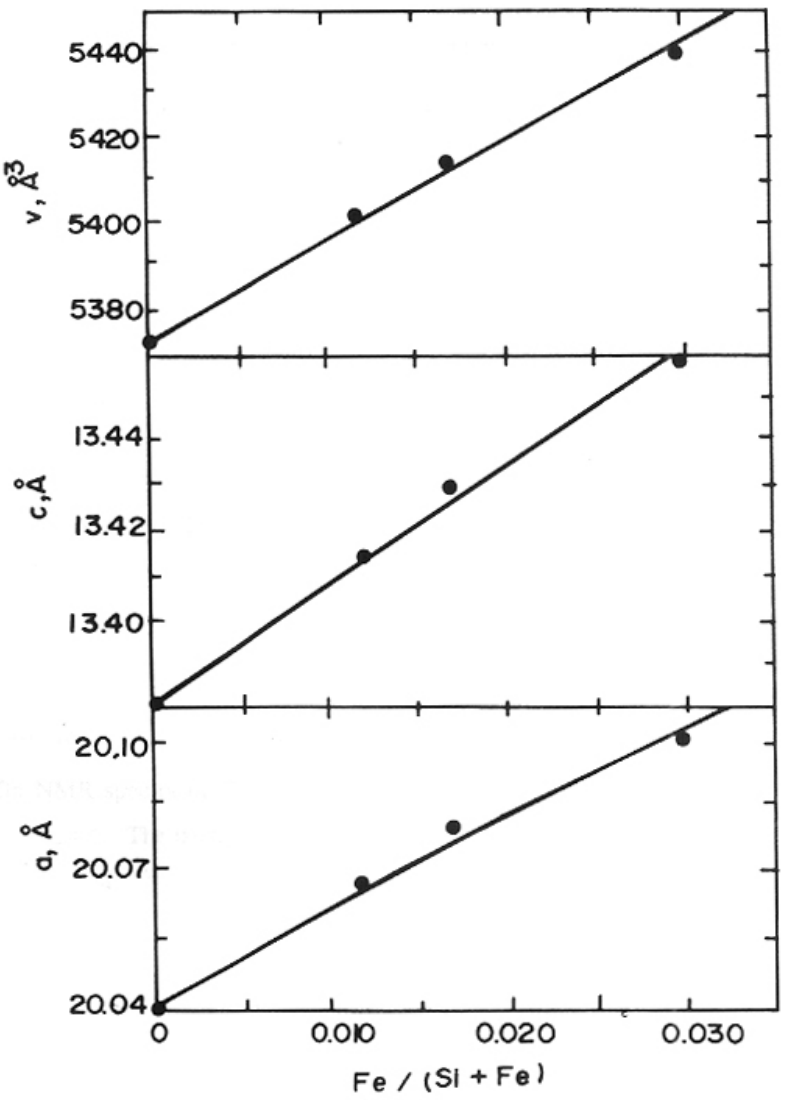

Fig.4.5. Lattice parameters a, c and volume, v as a function of mole fraction of iron in Fe-MEL.

Table 4.3. Unit cell parameters of Ga-MEL with different Ga contents and other MEL analogs.

Sample	Si/M[a]	Unit cell parameters		
		a=b, (Å)	c, (Å)	v, (Å)^3
Silicalite-2	> 4,000	20.046	13.391	5381.1
Al-MEL	37	20.052	13.432	5400.8
Ga-MEL	72	20.056	13.446	5408.6
Ga-MEL	35	20.060	13.457	5415.2
Ga-MEL	26	20.072	13.462	5423.6
Fe-MEL	40	20.102	13.460	5439.1

a: M = Al, Ga or Fe.

C. Framework IR spectroscopy

The framework IR bands (in the region of 200-1300 cm^{-1}) of calcined samples of Al-MEL, Ga-MEL and Fe-MEL were characteristic of MEL structure. A slight shift of the bands to lower wavenumbers arising from the replacement of Al by heavier Ga and Fe ions in lattice positions occurred in the case of the gallo- and ferrisilicates.

D. ^{71}Ga NMR studies

The ^{71}Ga NMR spectra of Ga-MEL with two different gallium contents and Ga-TS-2 are presented in Fig.4.6. The peak at about δ = 150 ppm is attributed to gallium in a tetrahedral oxygen environment[17,32,33].

E. Mössbauer spectroscopy

^{57}Fe Mössbauer measurement on Fe-MEL (sample 5, Table 4.2) at 297 K exhibited the values of isomer shift, δ = 0.23 mm/s, and line width, = 0.61 mm/s, suggesting the presence of tetrahedrally coordinated paramagnetic Fe^{3+} ions.

F. ESR & magnetic susceptibility measurements

The ESR spectrum of Fe-MEL (Fig.4.7) exhibited two signals at g = 4.3 and 2.0. Though an ESR signal at g = 4.3 can not be taken as a proof for the incorporation of Fe in the tetrahedral framework, its presence may be a necessary consequence of such an incorporation[34]. The ESR signals at g = 4.3 and g = 2.0 have been attributed to the presence of Fe^{3+} ions in distorted and undistorted symmetry, respectively. The values of magnetic moments measured at 94 and 297 K were 5.9 and 5.6 BM, respectively. The values for the corresponding calcined

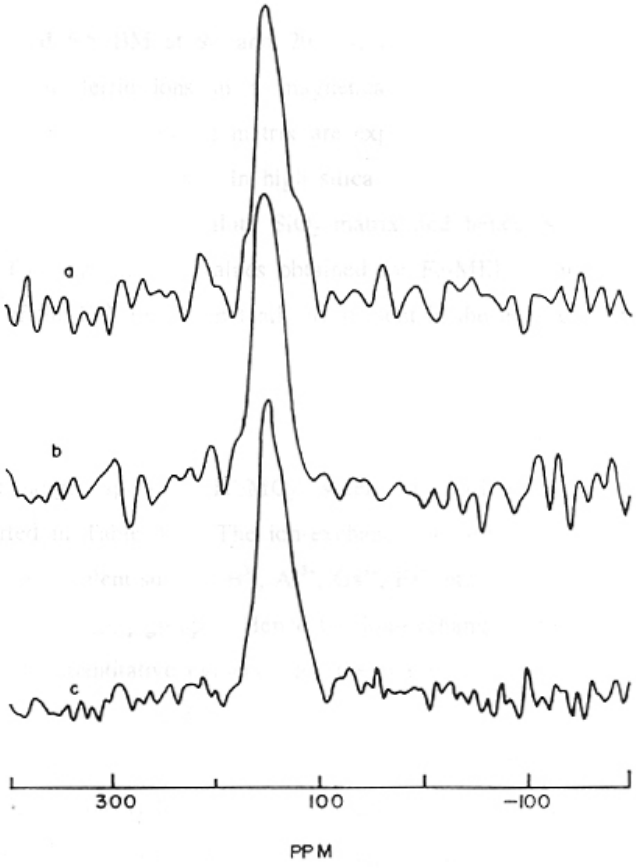

Fig.4.6. ^{71}Ga MASNMR spectra of Ga-TS-2 (SiO_2/Ga_2O_3 = 70; SiO_2/TiO_2 = 85) (a); Ga-MEL (SiO_2/Ga_2O_3 = 72 (b) and Ga-MEL (SiO_2/Ga_2O_3 = 26) (c).

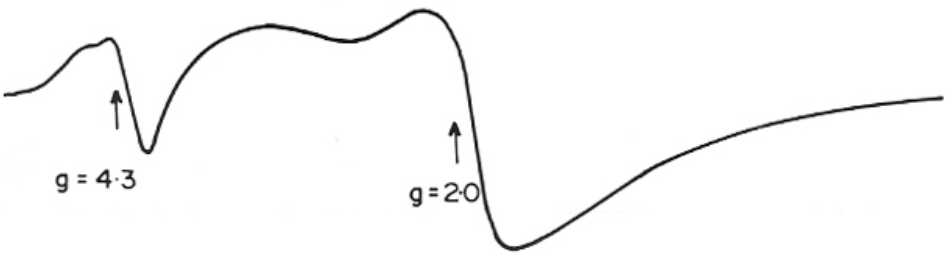

Fig.4.7. ESR spectra of calcined Fe-MEL recorded at 298 K.

samples were 5.8 and 5.5 BM at 94 and 297 K, respectively, indicating the presence of dispersed paramagnetic ferric ions in a magnetically dilute diamagnetic matrix. Non-interacting Fe^{3+} ions in a diamagnetic matrix are expected to possess an effective magnetic moment (μ_{eff}) below around 5.9 BM. In high silica ferrisilicate zeolites the framework Fe^{3+} ions are present in a magnetically dilute SiO_2 matrix and hence, should exhibit μ_{eff} value around 5.9 BM. The experimental values obtained for Fe-MEL, mentioned above, strongly suggest that most of the Fe^{3+} ions, if not all, are present in the tetrahedral zeolite framework positions.

G. Ion-exchange studies

The ion-exchange capacities (K^+/MO_2^-, where M = Al, Ga or Fe) of Al-, Ga- and Fe-MEL are reported in Table 4.4. The ion-exchange properties of metallosilicate zeolites (where metal ions are trivalent such as B^{3+}, Al^{3+}, Ga^{3+}, Fe^{3+} etc.) originate from the framework MO_2^- group bonded with SiO_2 groups. Hence the ion-exchange capacity of a zeolite can be taken as a direct and quantitative evidence for the presence of M^{3+} ions in the tetrahedral zeolite lattice. The large ion-exchange capacities exhibited by these zeolites provide strong evidence for the presence of most of the trivalent metals in the MEL framework. After steaming the Fe-MEL at 948 K for 1 h in 100 % steam, the K^+/FeO_2^- value was found to be 0.25. This considerable decrease in the ion-exchange capacity of steamed Fe-MEL and its brown color clearly indicated that most of the iron, which was originally present in the zeolite framework had come out from the lattice under the above hydrothermal treatment.

Table 4.4. Ion-exchange and adsorption capacities of metallosilicates.

Sample	Ion-exchange capacity, (K^+/MO_2^-)	Adsorption wt.%[a]	
		n-hexane	Cyclohexane
Silicalite-2	-	12.4	6.5
Al-MEL	0.90	12.4	6.9
Ga-MEL	0.90	12.5	6.6
Fe-MEL	0.84	12.3	6.2
Fe-MEL[b]	0.25	8.1	1.2

a: Temp. (K) = 298; p/p_o = 0.5.
b: Steamed at 948 K for 1 h in steam.

H. Adsorption studies

The adsorption capacities (at p/p_o = 0.5 and T = 298 K) of calcined, organic free samples of Ga-MEL and Fe-MEL for n-hexane and cyclohexane are compared with those of

Al-MEL and silicalite-2 in Table 4.4. High adsorption capacities (comparable with the values reported for ZSM-11) of these zeolites for n-hexane and cyclohexane indicate the absence of occluded material within the zeolite pores. When Fe-MEL was steamed, the sorption capacities, particularly for cyclohexane decreased sharply (Table 4.4), indicating that most of the iron had come out of the zeolite framework blocking the channels.

4.2.4. CATALYTIC PROPERTIES

A. Meta-xylene isomerization

The p-/o-xylene ratio (an indicator of para-selectivity) as well as selectivity for isomerization (Sel. Isom. = (o-xylene + p-xylene)/m-xylene converted) during the isomerization of m-xylene over these catalysts, are plotted against m-xylene conversion in Fig.4.8. The para-selectivity (p-/o-xylene ratio), particularly in the conversion range 5-20 %, followed the order: Al- > Ga- > Fe-MEL. However, the isomerization selectivity (Sel. Isom.) followed the reverse order (Fig.4.8), indicating that the disproportionation/transalkylation of m-xylene is suppressed considerably in the weakly acidic Fe-MEL and to a lesser extent in Ga-MEL analog.

Recently, Vorbeck *et al.*[35] have reported that H-Fe-MFI exhibited lower para-selectivity compared to H-Al-MFI. The samples containing both Al and Fe, H-Al,Fe-MFI, had intermediate para-selectivities. They attributed it to the slightly larger size of Al-MFI crystals (vis-á-vis Fe-MFI). They argue that larger crystals not only prolong the diffusion pathways but also exhibit a lower percentage of outer (non shape-selective) surface area. Both the factors should enhance the shape-selectivity. Although, longer pathways may not necessarily enhance shape-selectivity, as has been argued by Dewing and Dwyer[36], the enhanced non-selective contribution of acid sites located on the external surface to the overall p-xylene selectivity can not be ignored, as demonstrated by Hashmoto *et al*[37]. Further, Vorbeck *et al.*[35] have also speculated that the iron in Fe-MFI may overwhelmingly be located on the outer surface, thus significantly contributing to the non-shapeselective conversion of m-xylene.

Corma[38] on the other hand, has proposed that "**orbital control**" effects, *viz.,* the overall electronegativity of the zeolite, must also be taken into account when explaining p-xylene selectivity in C_7 and C_8 aromatic hydrocarbon reactions. Similarly, Pellet *et al.*[39], during the formation and isomerization of xylenes over CoAPSO-31 and MnAPSO-31, observed that shape-selective properties of these materials can not be explained on the basis of spatial effects (diffusion control) alone. The transition metal ions, as framework constituents appeared to

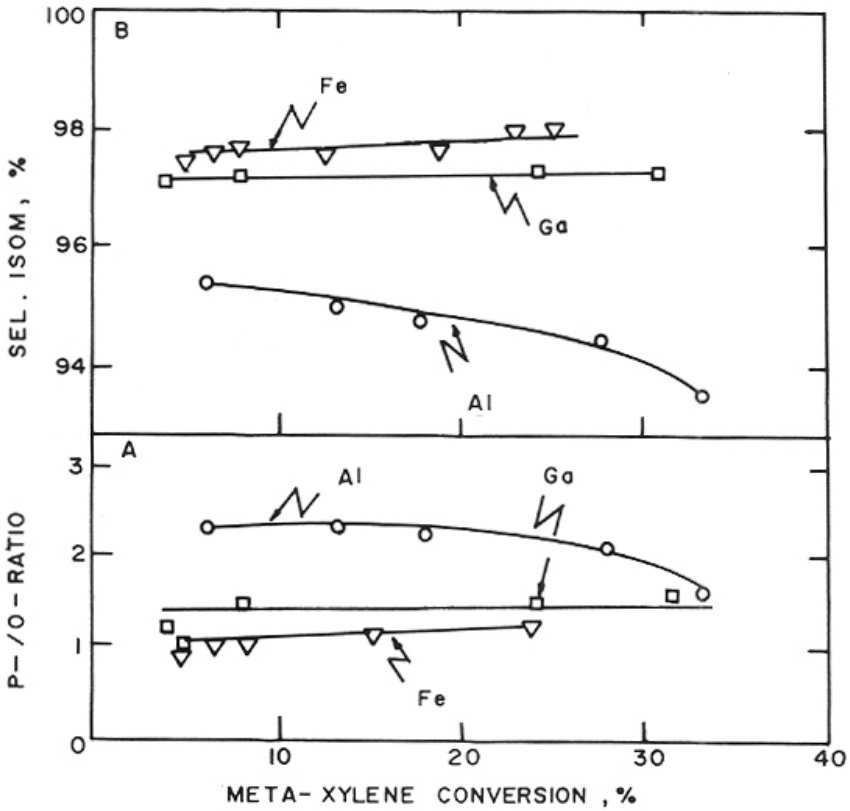

Fig.4.8. **Effect of m-xylene conversion on p-/o-xylene ratio and selectivity for isomerization.**
Press. = atm.; LHSV = 12, 8 and 4 for Al-, Ga- and Fe-MEL, respectively.

exert some special effect (d-character) on the catalytic performance independent of the acid strength and spatial constraints of the molecular sieve. A similar effect of Fe^{3+} ions (with almost no gap between LUMO and HOMO) may also be present in the case of ferrisilicate zeolites.

However, in the present work, all the samples studied had similar crystal size and shape, surface area, adsorption properties and SiO_2/M_2O_3 molar ratios (M = Al, Ga or Fe) (Tables 4.2 and 4.4). Hence the absence or low para-selectivity exhibited by H-Fe-MEL (vis-á-vis Ga-MEL and Al-MEL) can not be correlated with the morphological features of the catalyst.

Probably the chemical nature of the isomorphously substituted metal ions (such as their acid strength or hardness/softness of acid sites as well as the hardness/softness of the basicity of the reactants) play a significant role in controlling the apparent para-selective properties. This view is further supported by the results obtained in the isomerization of m-xylene over Al-TS-2, Ga-TS-2 and Fe-TS-2 (reported in the next Chapter).

B. Ethyl benzene disproportionation

In Fig.4.9 the conversion of ethylbenzene (EB) over H-Al-MEL, H-Ga-MEL and H-Fe-MEL is plotted against time on stream (TOS). The higher catalytic activity of H-Al-MEL compared to that of H-Fe-MEL in EB disproportionation, a typical Brönsted acid catalyzed reaction, can be attributed to the higher strength of the acid sites in Al-analogs compared to the ferrisilicate molecular sieves. The values of the molar ratio of diethyl benzene/benzene were between 0.7-0.8. H-Al-MEL deactivates very fast whereas H-Ga-MEL and H-Fe-MEL exhibit resistance to deactivation. This is a distinct advantage of H-Ga-MEL and H-Fe-MEL over the Al-analog. Weitkamp *et al.*[40] have suggested three criteria, to characterize medium pore zeolites using ethyl benzene as a test reaction: i) absence of induction period, ii) fast deactivation and iii) diethyl benzene/benzene (DEB/B) mole ratio of around 0.7-0.8. While the criteria (i) and (iii) are followed by the Al-, Ga- and Fe-analogs, criterion (ii) (i.e. fast deactivation) is obeyed by H-Al-MEL only. The lower acid strength of H-Fe-MEL and H-Ga-MEL compared to H-Al-MEL may be responsible for the slower rate of deactivation. The weaker acid sites probably suppress secondary reactions (like further disproportionation/dealkylation of products) which cause coke formation and/or blocking of the zeolite pores/pore openings. Since the active, acid sites could have been generated only by the protons associated with the framework Fe^{3+} or Ga^{3+} ions in Al-free ferri- and gallosilicates, the

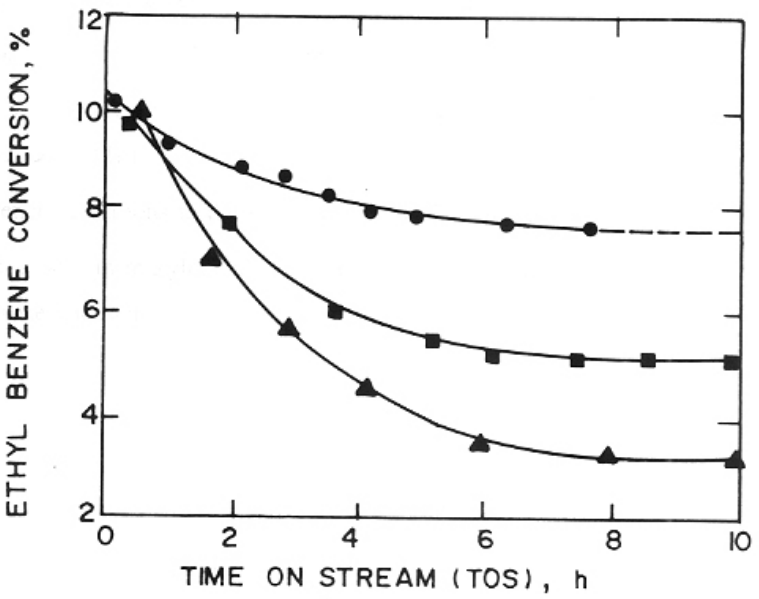

Fig.4.9. **Effect of time on stream on ethylbenzene conversion over Al- (▲), Ga- (■) and Fe-MEL (●).**
Temp. (K) = 553; LHSV = 12, 8 and 4 for Al-, Ga- and Fe-MEL, respectively.

significant activity and shape selectivity exhibited by Al-free H-Ga-MEL and H-Fe-MEL in acid catalyzed reactions (such as m-xylene isomerization and ethylbenzene disproportionation) provide additional strong evidence for the presence of most of the iron or gallium in the MEL framework.

4.3. CONCLUSIONS

Based on the above studies the following conclusions can be drawn:

1) Fe and Ga metal ions can be isomorphously substituted into MEL framework.

2) The rate of crystallization of metallosilicates decreases in the following order: Al-MEL > Ga-MEL > Fe-MEL.

3) The presence of Na ions in the reaction mixture favours the formation of MFI impurity.

4) p-/o-xylene ratio in m-xylene isomerization and deactivation rate in EB disproportionation decrease with acid strength.

4.4. REFERENCES

1. Barrer, R.M. "Hydrothermal chemistry of zeolites", Academic press, London, 1982, p.251
2. Ratnasamy, P., Borade, R.B., Sivasankar, S., Shiralkar, V.P. and Hegde, S.G. *Acta phys. Chem.*, **31** (1985) 137.
3. Ball, W.J., Dwyer, J., Garforth, A.A. and Smith, W.J. *Stud. Surf. Sci. Catal.*, **28** (1985) 137.
4. Szostak, R. and Thomas, T.L. *J. Catal.*, **100** (1986) 555
5. Meagher, A., Nair, V. and Szostak, R., *Zeolites* **8** (1988) 3.
6. Borade, R.B., *Zeolites*, **7** (1987) 398.
7. Szostak, R. and Thomas, T.L., *J. Chem. Soc., Chem. Commun.*, (1986) 155.
8. Kumar, R., Thangaraj, A., Bhat, R.N. and Ratnasamy, P., *Zeolites* **10** (1990) 85.
9. Kumar, R. and Ratnasamy, P., *J. Catal.*, **121** (1990) 89
10. Kumar, R., Thangaraj, A. in "Zeolites for Nineties", Recent Research Report, 8th IZC, Amstredam, Eds. J.C.Jansen *et al.*, Amsterdam, 1989, p.53.
11. Chandwadkar, A.J., Bhat, R.N. and Ratnasamy, P., *Zeolites* **11** (1991) 42.
12. Ratnasamy, P., Kotasthane, A.N., Shiralkar, V.P., Thangaraj, A. and Ganapathy, S., *ACS Symp. Ser.*, **398** (1989) 405.
13. Shizherg, L., Wenyang, X., Tao, D and Yizhao, Y., *Taiyuan Gogye Daxue Xuebao*, **20** (1989) 17.
14. Ratnasamy, P. and Kumar, R., *Catal. Today*, **9** (**4**) (1991) 329.
15. Szostak, R., in "Molecular Sieves: Principles of Synthesis and Identification", Van Nostrand, Reinhold, New York, 1989, p.212.
16. Barrer, R.M., Baynahm, J.W., Bultitude, F.W. and Meier, W.M., *J. Chem. Soc.*, (1959) 195.
17. Ione, K.G., Vostrikova, L.A. and Mastikhin, V.M., *J. Mol. Catal.*, **31** (1985) 355.
18. UK Pat., 2,023,562.
19. Reddy, J.S., Reddy, K.R. and Kumar, R., in "Proc. 10th Natl. Symp. on Catal. and 4th INDO-USSR Symp. on Catal."Recent Developments in Catalysis, Theory and Practice, Eds. B. Viswanathan *et al.*, Narosa Pub., New Delhi, India, 1989, p.575.
20. Reddy, J.S., Reddy, K.R., Kumar, R. and Ratnasamy, P., *Zeolites*, **11** (1991) 553.
21. Reddy, J.S., Kumar, R. and Ratnasamy, P., *Appl. Catal.*, **58** (1990) L1.
22. Rao, P.R.H.P. and Ramaswamy, A.V., *J. Catal.*, (in press).
23. Ball, W.J., Dwyer, J., Garforth, A.A. and Smith, W.J., *Stud. Surf. Sci. Catal.*, **28** (1986) 137.
24. Hou, L.Y. and Sand, L.B., in "Proc. 6th Int. Zeolite Conf.", Eds. D.H. Olson and A. Bisio, Reno, USA, 1983, p.887.
25. Jablonski,J.M., Sand,L.B. and GardJ.A., *Zeolites*, **6** (1986) 396.
26. Kaúcic, C., Gaspersic, S. and Hocevar, S., *Stud. Surf. Sci. Catal.*, **49A** (1989) 311.

27. Gabelica, Z., Derouane, E.G. and Blom, Nn, *Appl. Catal.*, **5** (1983) 109.

28. Bibby, D.M., Milestone, N.B. and Aldridge, L.P., *Naturen*, **280** (1979) 664.

29. Kungang, T. and Ruren, X., *Stud. Surf. Sci. Catal.*, **24** (1985) 73.

30. Jacobs, P.A. and Martens, J.A., *Stud. Surf. Sci. Catal.*, **33** (1987) 177.

31. Reddy, J.S. and Kumar, R., *Zeolites*, **12** (1992) 95.

32. Kentgens, A.P.M., Bayense, C.R., van Hoof, J.H.C., de Haan, J.W. and van de Ven, L.J.M., *Chem. Phys. Lett.*, **176(3,4)** (1991) 399.

33. Bayense, C.R., Kentgens, P.M., de Haan, J.W., van de Ven, L.J.M. and van Hooff, J.H.C., *J. Phy. Chem.*, **96** (1992) 775.

34. Kucherov, A.V. and Slinkin, A.A., *Zeolites*, **8** (1988) 10.

35. Vorbeck, G., Richter, M., Frincke, R., Parlitz, B., Schreier, E., Szulzewsky, K. and Zibrowius, B., *Stud. Surf. Sci. Catal.*, **65** (1991) 631.

36. Dewing, J. and Dwyer, J., *Zeolites*, (accepted)

37. Hashimoto, K., Masuda, T. and Kawase, M., *Stud. Surf. Sci. Catal.*, **46** (1989) 485.

38. Corma, A., in "Guidlines for Mastering the properties of Molecular Sieves", Eds. D. Barthomeuf *et al.*, NATO ASI Series B, Physics, Vol.221, Plenum Press, New York, 1990, p.299.

39. Pellet, G., Conghlin, P.K., Sharnshoum, E.S. and Rabo, J.A., *ACS Symp. Ser.*, **368** (1988) 512.

40. Weitkamp, J., Ernst, S., Jacobs, P.A. and Karge, H.G., Erdoel, Kohle-Erdgas-Petrochem., **39** (1986) 13.

CHAPTER - V

STUDIES ON METALLO-TITANIUM-SILICATES WITH *MEL* TOPOLOGY

5.1. INTRODUCTION

The simultaneous incorporation of a trivalent metal ion (eg., B^{3+}, Al^{3+}, Ga^{3+} or Fe^{3+}) alongwith Ti^{4+} in MFI and MEL structures has been reported recently[1-7]. These metallo-titanium-silicate molecular sieves have been found to be active in both oxidation reactions like titaniumsilicates[3], and in acid-catalyzed reactions like aluminosilicates. The activity of alumino-titanium-silicate (Al-TS-2) molecular sieves in oxidation reactions has been reported to be influenced by the trivalent metal ions[3]. Similarly, their activity in acid catalyzed reactions has been found to be affected by the presence of Ti in the framework[6].

This chapter describes the studies carried out on the synthesis, characterization and catalytic properties of alumino-titanium-silicate (Al-TS-2), gallo-titanium-silicate (Ga-TS-2) and ferri-titanium-silicate (Fe-TS-2) molecular sieves. A series of Al-TS-2 catalysts were prepared keeping the Al content constant and replacing Si by different amounts of Ti cations. The materials were characterized using XRD, framework IR, UV-VIS, adsorption, SEM, NMR and ion-exchange properties. The influence of the nature of the hetero metal ion and SiO_2/TiO_2 molar ratio on the rate of crystallization is described. Their catalytic properties in both oxidation (oxyfunctionalization of n-hexane and hydroxylation of benzene and phenol) and acid catalyzed reactions (m-xylene isomerization and ethylbenzene disproportionation) are reported. The acid strength of these metallo-titanium-silicates and the corresponding metallosilicates were examined by FTIR spectroscopy of adsorbed pyridine. The results are correlated with catalytic properties in m-xylene isomerization.

5.2. RESULTS AND DISCUSSION

5.2.1. SYNTHESIS

For better incorporation of Ti and Fe in framework positions, the formation of TiO_2 and Fe_2O_3 should be avoided during the synthesis. The addition of ferric nitrate solution to the titaniumsilicate mixture, as in the case of Al-TS-2 or Ga-TS-2, results in the formation of $Fe(OH)_3$ and eventually Fe_2O_3. To avoid the formation of $Fe(OH)_3$, a different procedure (described in detail in Chapter II) was adopted for Fe-TS-2; the ferric nitrate solution was added to TEOS followed by TBOT and the template. The addition sequence of reactants for the synthesis of Al, Ga and Fe-TS-2 has been shown in Fig.2.2 (Chapter II). The influence of the nature of the heterometal ion on the rate of crystallization of metallo- and metallo-titanium-silicates is shown in Fig.5.1. The metallosilicates crystallized faster compared to the

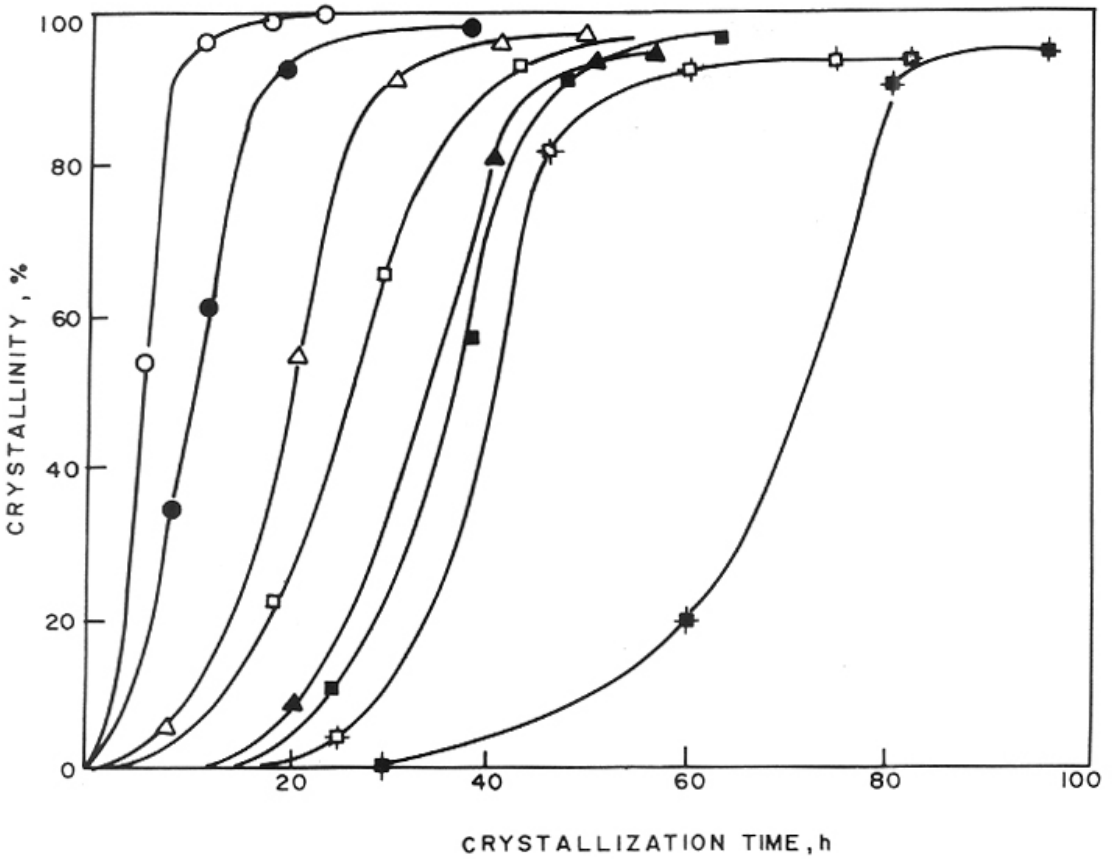

Fig.5.1. **Influence of the heterometal ion on the crystallization of metallo- and metallo-titanium-silicates.**
(○): **Silicalite-2;** (●): **TS-2;** (△): **Al-MEL;** (▲): **Al-TS-2;** (□): **Ga-MEL;** (■): **Ga-TS-2;** (☼): **Fe-MEL and** (✹): **Fe-TS-2.**
Molar gel composition: SiO_2/M_2O_3 = 90; TBA-OH/SiO_2; H_2O/SiO_2 = 30. Crystallization temp. (K) = 443.

corresponding metallo-titanium-silicate analogs. It is known that the incorporation of Al in high silica zeolites (such as MFI, MEL, MTT, MTW etc.,) is a slow process[7-9]. This phenomenon seems to be valid for Ga^{3+}, Fe^{3+} and Ti^{4+} also. The rate of crystallization of various metallo- and metallo-titanium-silicates (Fig.5.1) follows the decreasing order: Silicalite-2 > TS-2 > Al-MEL > Ga-MEL > Al-TS-2 > Ga-TS-2 > Fe-MEL > Fe-TS-2.

The influence of SiO_2/TiO_2 ratio in Al-TS-2 (at constant Al content) on the rate of crystallization is reported in Fig.5.2. With increase in Ti content, the rate of crystallization decreased. In the case of TS-2 also the rate of crystallization was found to decrease with increasing Ti content[10]. The rate of crystallization of Al-TS-2 samples with different Ti contents decreases in the following order: Al-MEL > Al-TS-2 (90,180) > Al-TS-2 (90,65) > Al-TS-2 (90,20), where the first value in parentheses is the SiO_2/Al_2O_3 ratio and the second one corresponds to the SiO_2/TiO_2 ratio of the reaction mixture.

5.2.2. CHARACTERIZATION

A. X-ray diffraction

The absence of reflections at 2θ = 9.05° and 24.4° and a doublet at 44-45°, (characteristic for MFI structure) in the XRD pattern of M-MEL and M-TS-2 samples confirms the absence of the corresponding MFI analogs. The molar composition and unit cell parameters of M-MEL, M-TS-2 (M= Al, Ga or Fe), TS-2 and silicalite-2 are reported in Table 5.1. The expansion in the unit cell increases in the following order: Silicalite-2 < Al-MEL < Ga-MEL < TS-2 < Al-TS-2 < Ga-TS-2 < Fe-MEL < Fe-TS-2.

B. Infrared spectroscopy

i. Framework IR

All titanium containing samples exhibited the characteristic IR band at 960 cm^{-1} (Fig.5.3), strongly suggesting the presence of Ti^{4+} ions in the tetrahedral zeolite framework in our samples. This band was not observed either in the IR spectra of silicalite or in metallosilicates (Fig.5.3). Forni *et al.*[2] have also observed this band in Al-TS-1. A small shift of the band at 1100 cm^{-1} towards lower wave numbers indicated the incorporation of the larger heteroatoms (Ti, Al, Ga or Fe) in the MEL framework. The intensity of the 960 cm^{-1} band increased with increasing Ti content in Al-TS-2.

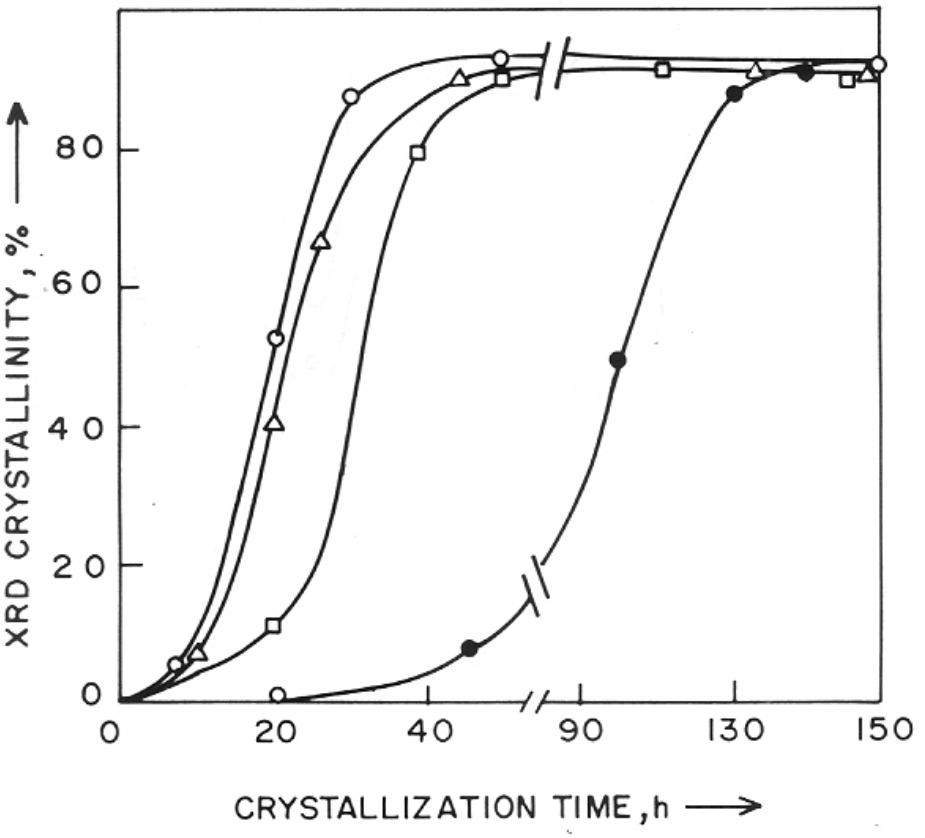

Fig.5.2. **Influence of SiO_2/TiO_2 molar ratio on the crystallization of Al-TS-2.**
(○): Al-MEL; (△), (□) and (●): Al-TS-2.
$TBA.OH/SiO_2$ = 0.2; SiO_2/Al_2O_3 = 90; SiO_2/TiO_2 = 0, 180, 65 and 20 for (○), (△), (□) and (●), respectively.

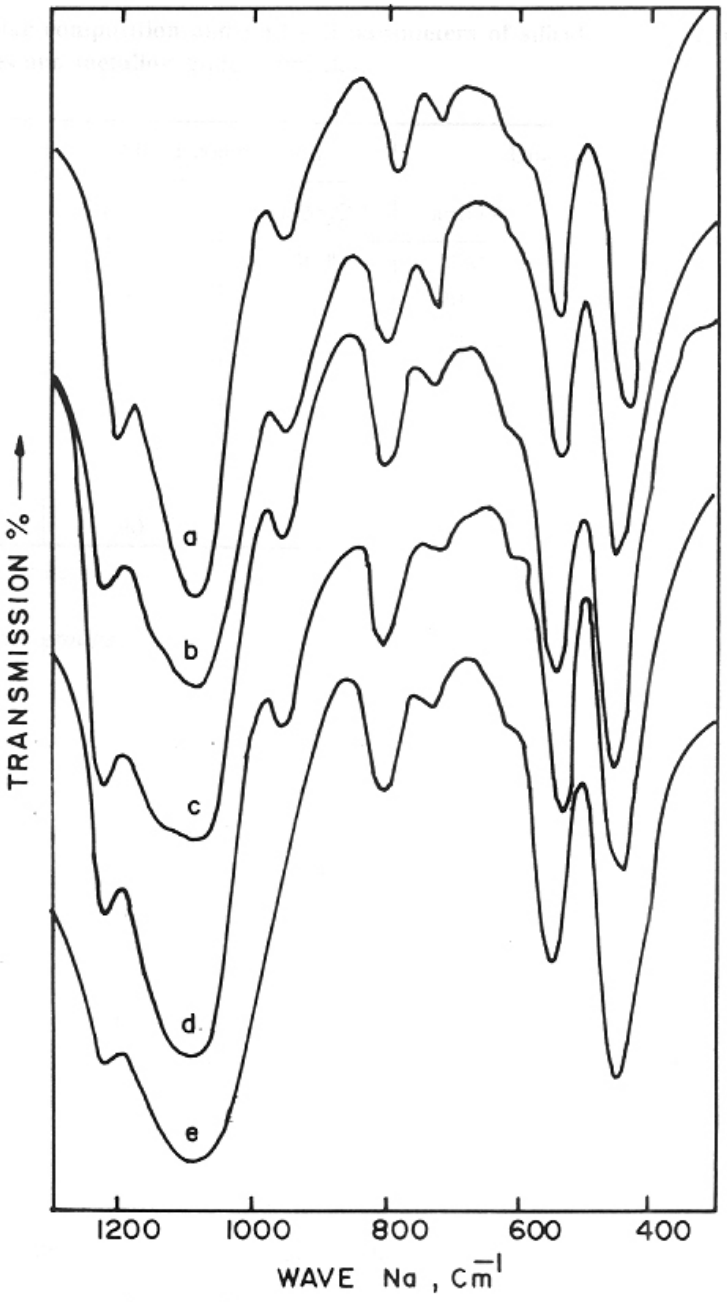

Fig.5.3. **Framework IR spectra of TS-2 (a), Fe-TS-2 (b), Ga-TS-2 (c), Al-TS-2 (d) and Al-MEL (e).**

Table 5.1. Molar composition and unit cell parameters of silicalite-2, TS-2, metallosilicates and metallo-titanium-silicates.

Catalyst	Molar composition		Unit cell parameters		
	SiO_2/TiO_2	SiO_2/M_2O_3[a]	a=b (Å)	c, (Å)	v,(Å)^3
Silicalite-2	--	> 4000	20.046	13.391	5381.1
TS-2	70	--	20.069	13.420	5405.1
Al-MEL	--	74	20.052	13.432	5400.9
Ga-MEL	--	78	20.060	13.457	5415.2
Fe-MEL	--	80	20.102	13.460	5439.1
Al-TS-2	92	60	20.094	13.427	5421.4
Ga-TS-2	85	70	20.108	13.460	5442.3
Fe-TS-2	90	66	20.137	13.459	5457.6

a: M = Al, Ga or Fe.

ii. Surface hydroxyl groups

FTIR spectra in the 4000-3100 cm^{-1} region for Al-MEL, Al-TS-2, TS-2 and silicalite-2 are presented in Fig.5.4 (Curves a-d, respectively). Absorption bands are observed at 3737 and 3608 cm^{-1} for Al-MEL, 3737, 3708 (Sh), 3608 and 3532 cm^{-1} (Sh) for Al-TS-2, 3732, 3708 and 3532 cm^{-1} for TS-2 and 3737 and 3532 cm^{-1} for silicalite-2. The band at 3737 cm^{-1} is assigned to the stretching vibrations of Si-OH groups (terminal and internal), the 3608 cm^{-1} band is assigned to Brönsted acid sites due to OH groups bridging Si and Al cations in the framework, the 3707 cm^{-1} band is assigned to hydrogen bonded Si-OH groups (terminal or internal) vicinal to Ti cations and the one at 3532 cm^{-1} being assigned to hydrogen bonded titanol (Ti-OH) groups vicinal to Si-OH groups. Similar assignments have been made for silicalite-1 and TS-1 by Boccuti *et al.*[11]. It should be noted that for Al-TS-2 samples, bands due to both Al and Ti cations in the framework (bridging hydroxyl groups and titanols) are present. It has earlier been reported[12] that in the synthesis medium of Al-TS-1 containing SiO_4, AlO_4^{-1} and TiO_4 tetrahedral units, corner sharing of AlO_4^{-1} and TiO_4 tetrahedra are least probable during the formation of secondary and tertiary building units. In view of the above observations, the surface species on TS-2 and Al-TS-2 can be represented as shown below (Scheme 1):

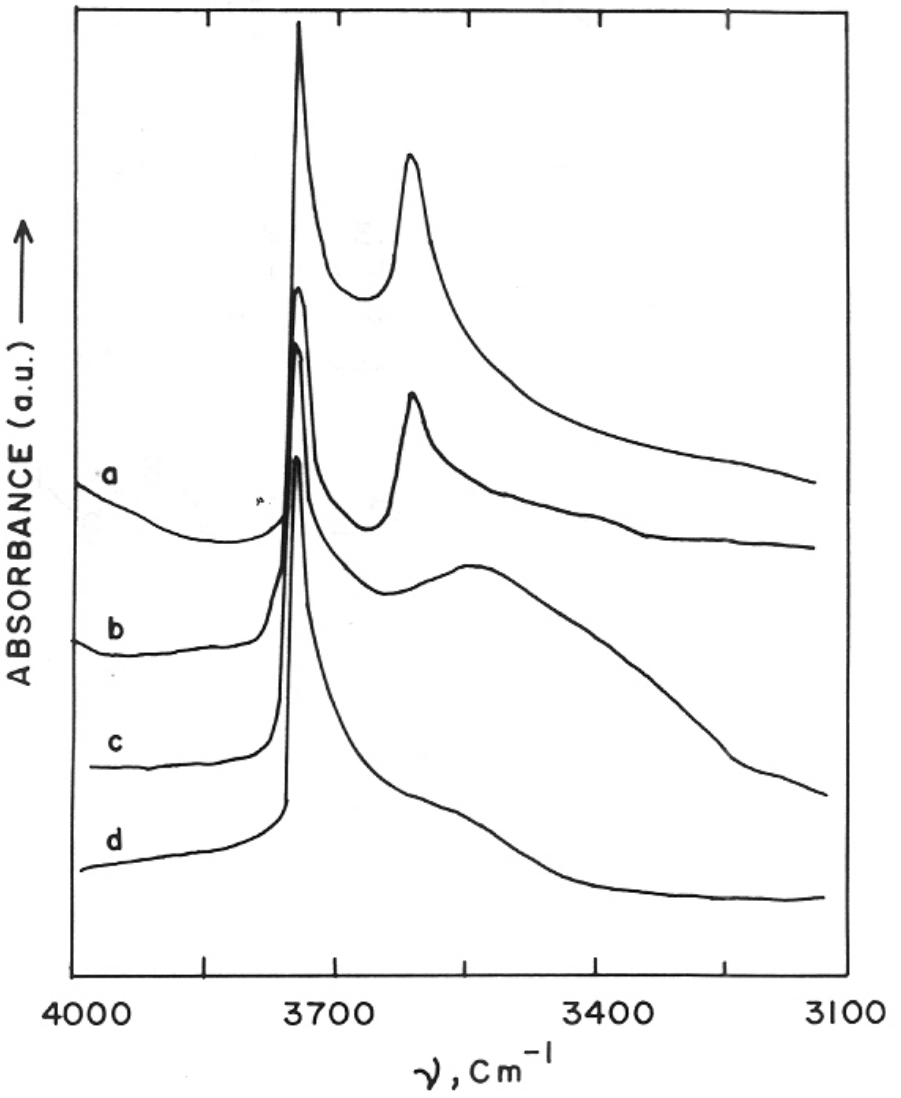

Fig.5.4. **FTIR spectra of Al-MEL (a), Al-TS-2 (b), TS-2 (c) and Silicalite-2 (d).** All samples were activated at 673 K in vacuum and cooled to 323 K.

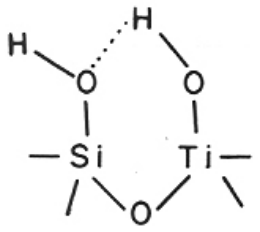

TS – 2

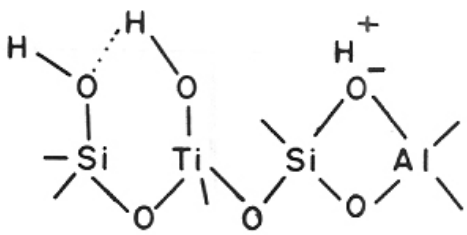

Al – TS – 2

SCHEME–I

It is observed that the intensity of the titanol groups (3530 cm^{-1}) depends on the temperature and time of evacuation, decreasing at temperatures higher than 673 K. On introducing H_2O on such a dehydroxylated sample, the intensity of the peak is restored (see below).

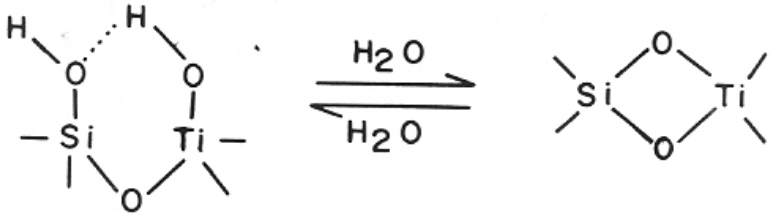

Because of the difference in electronegativity between Ti (1.4) and Si (1.8), the Si-O-Ti bridges formed on dehydroxylation are easily polarized and can, therefore, be easily rehydrated restoring the respective OH groups. In this respect, TS-2 is more hydrophilic than silicalite-2.

iii. Pyridine adsorption

FTIR spectroscopic study of pyridine adsorption has been widely used[13] in the determination of acid strength distribution of catalysts. The typical FTIR spectra of irreversibly adsorbed pyridine at 373 K on different samples (a-f in Table 5.2) are presented in Fig.5.5 (curves a-f). Vedrine *et al.*[14,15] have reported the IR spectra of pyridine adsorbed on Al-MEL. Absorption bands due to adsorbed pyridine were observed at 1640, 1628, 1550, 1495 and 1450 cm^{-1}. The bands at 1640 and 1550 cm^{-1} were ascribed to pyridinium ions. The bands at 1628, 1495 and 1450 cm^{-1} were assigned to pyridine molecules coordinated to Lewis acid sites. Similar assignments can be made for the spectra in Fig.5.5. The bands at 1633 and 1543 cm^{-1} are assigned to pyridinium ions, where as the bands at 1618, 1500 and 1452 cm^{-1} are assigned to pyridine bound to a Lewis acid site. The bands at 1447 and 1600 cm^{-1} are attributable to hydrogen bonding of the adsorbed pyridine molecules.

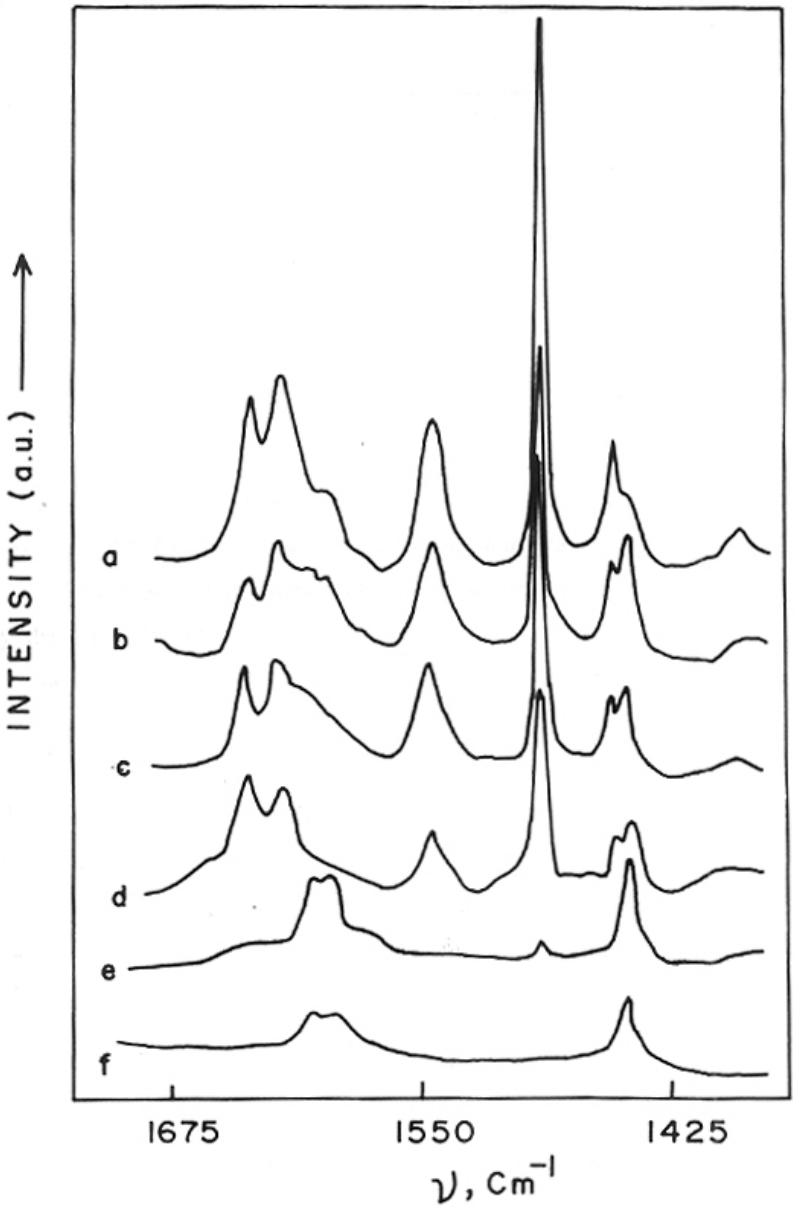

Fig.5.5. **FTIR spectra of chemisorbed pyridine.**
Curves a-f correspond to samples a-f (Table 5.2), respectively.

Table 5.2. Effect of Ti concentrationon the activity and selectivity in m-xylene isomerization

Sample No.	Unit cell composition	m-xylene conversion[a]	p-/o-xylene ratio
1.	$Si_{93.3}\ Al_{2.7}\ Ti_{0.0}$	22	2.4
2.	$Si_{92.9}\ Al_{2.5}\ Ti_{0.6}$	22	1.8
3.	$Si_{92.2}\ Al_{2.7}\ Ti_{1.1}$	19	1.6
4.	$Si_{91.3}\ Al_{2.4}\ Ti_{2.3}$	17	1.5
5.	$Si_{94.0}\ Al_{0.0}\ Ti_{2.0}$	4	-
6.	$Si_{96.0}\ Al_{0.0}\ Ti_{0.0}$	3	0.9

a: Reaction conditions: Temp. (K) = 573; LHSV (h^{-1}) = 4; H_2/m-xylene (mole) = 4.0.

In Fig.5.6, the normalized intensities of pyridinium ions (1543 cm^{-1}) and coordinatively adsorbed pyridine (1447 cm^{-1}) are plotted against the temperature of desorption. It is found that at 323 K, the intensity of Brönsted acid sites (1543 cm^{-1}) and Lewis acid sites (1447 cm^{-1}) are nearly the same for all samples. Brönsted acid sites are totally absent on TS-2 and silicalite-2 where as those on Al-MEL and Al-TS-2 decrease considerably on increasing the temperature of evacuation. It should be noted that on increasing the Ti mole fraction in Al-TS-2, the intensity of the bands due to both Brönsted and Lewis acid sites decrease systematically. It is, therefore, inferred that on increasing the Ti content keeping the number of Al atoms constant in the Al-TS-2 framework, the strengths of both types of acid sites decrease. This can be due to the inductive effect of the more polarizable Ti-O bond (compared to Al-O bond), which is present in the secondary sphere of interaction in the framework, on the bridging OH groups of Si and Al cations (Scheme 1).

C. UV-VIS spectroscopy

UV-VIS spectra of Al-TS-2 and Fe-TS-2 are compared with those of Al-MEL, Fe-MEL and TS-2 in Fig.3.15. Absence of a band at 326 nm characteristic of TiO_2 (anatase) and the presence of a band at 212 nm shows that most of the Ti is incorporated into MEL framework.

D. ESR and magnetic measurements

The ESR spectrum of Fe-TS-2 has two peaks at g = 4.3 and g = 2.0, the former is assigned to the presence of Fe^{3+} ions in a distorted tetrahedral position, possibly in the zeolite framework. Magnetic moment values of 5.8 and 5.7 BM at 298 and 97 K, respectively, and

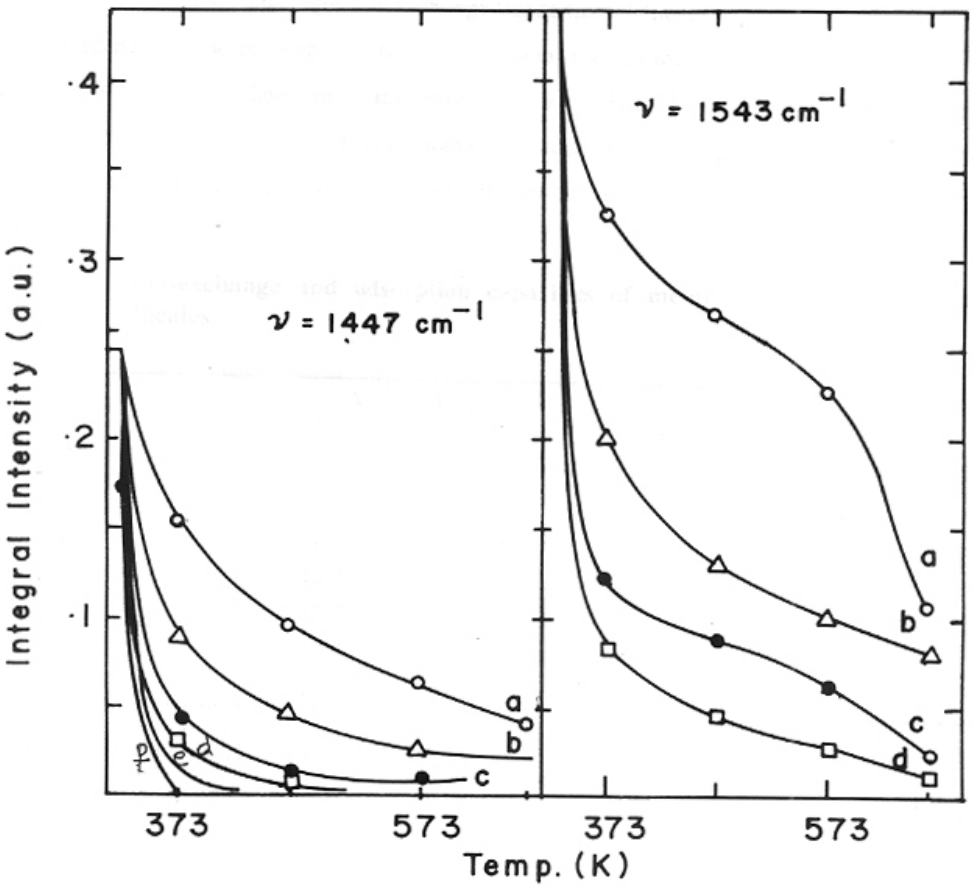

Fig.5.6. **Plot of intergral intensity (normalized) vs Temp. of desorption of pyridine.** Curves a-f correspond to samples a-f, respectively (Table 5.2).

white color of the Fe-TS-2 sample indicated the absence of condensed iron oxides[16]. These features are attributed to the presence of uniformly dispersed Fe (III) ions in a distorted tetrahedral environment in the molecular sieve framework.

E. Ion-exchange and adsorption capacities

Ion-exchange and adsorption capacities of metallo and metallo-titanium-silicates are reported in Table 5.3. The high ion exchange capacities of these materials can be taken as a direct evidence for the presence of the trivalent metal ions in the framework. Titaniumsilicate molecular sieves do not have any ion exchange capacity. The adsorption capacities (Table 5.3) of all the samples studied were comparable to those reported in the literature[17] for MEL zeotypes, indicating the absence of any significant amount of occluded material within the zeolite channels.

Table 5.3. Ion-exchange and adsorption capacities of metallo and metallo-titanium-silicates

Catalyst	Adsorption, wt %[a]		Ion-exchange capacity (K^+/MO_2^-)
	n-hexane	cyclohexane	
Al-MEL	12.4	6.9	0.90
Ga-MEL	12.5	6.6	0.90
Fe-MEL	12.3	6.2	0.84
Al-TS-2	12.7	8.2	0.91
Ga-TS-2	13.2	7.9	0.88
Fe-TS-2	12.8	7.5	0.87

a: $p/p_o = 0.5$; Temp. (K) = 298.

F. Scanning Electron Microscopy

SEM photographs of Ga-TS-2 and Fe-TS-2 samples are shown in Fig. 5.7. The photographs of the corresponding metallosilicates have already been presented in Chapter IV (Fig.4.3). The particle sizes of all the metallosilicates and metallo-titanium-silicate molecular sieves are similar. SEM photographs of Al-TS-2 samples having different Ti contents are shown in Fig.5.8. The replacement of Si by Ti in aluminosilicates did not affect the particle size or morphology. The crystals were about 1 μm in size, and cuboid in shape.

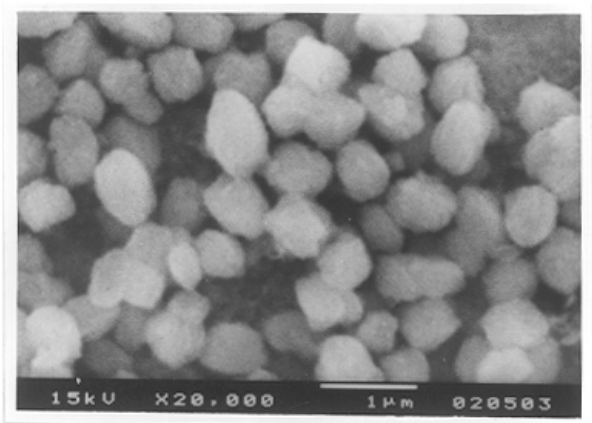

A

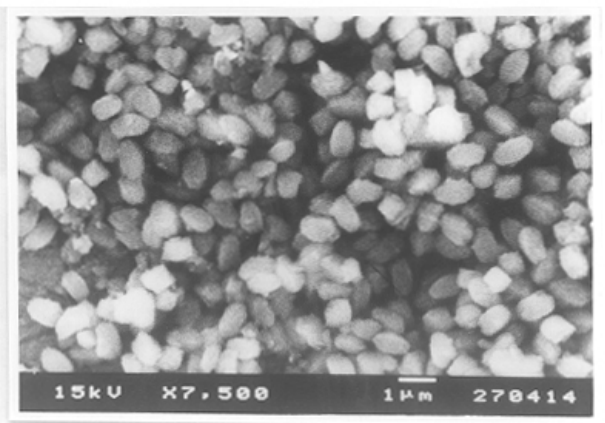

B

Fig.5.7. SEM photographs of Ga-TS-2 (A) and Fe-TS-2 (B).

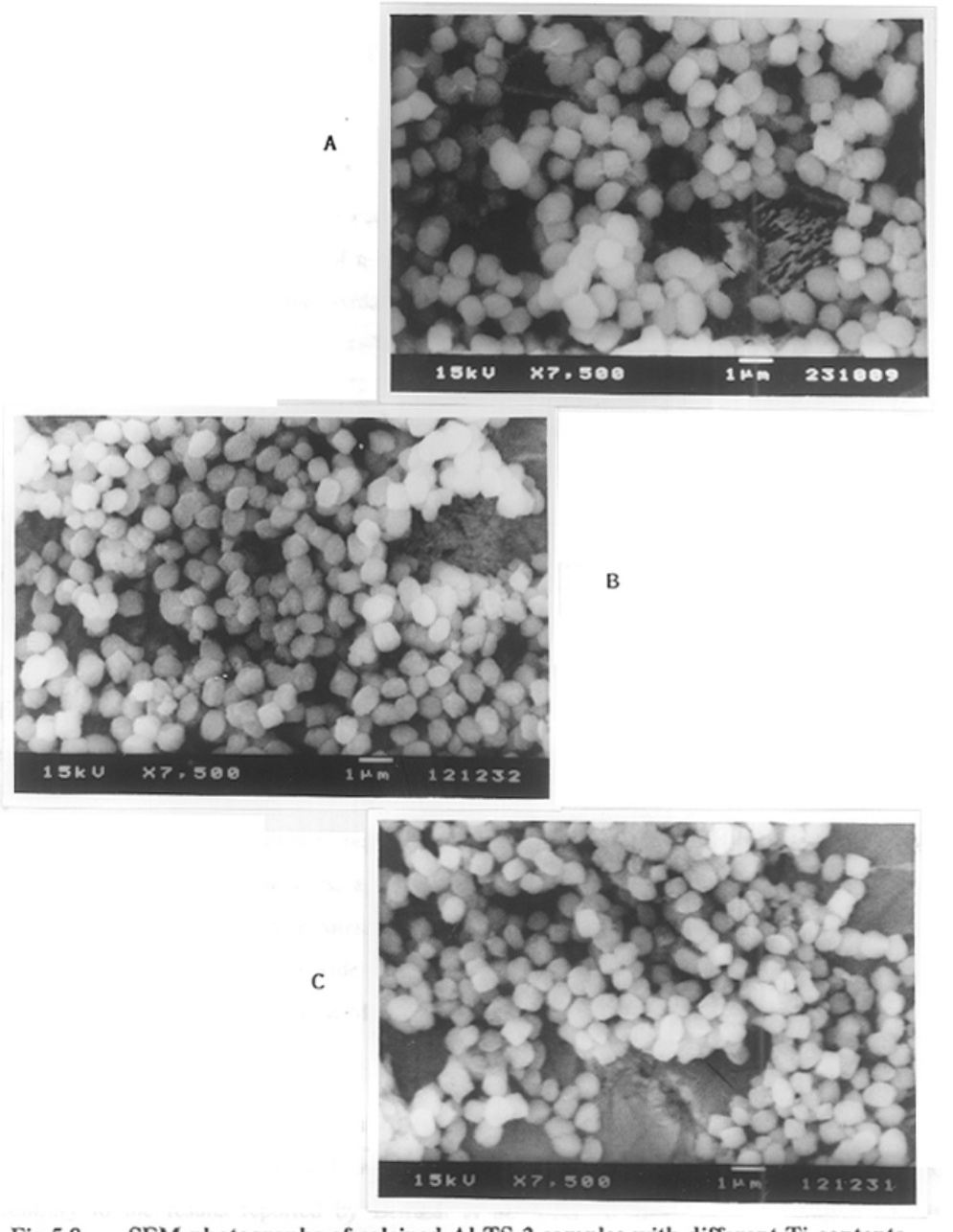

Fig.5.8. SEM photographs of calcined Al-TS-2 samples with different Ti contents. TBA-OH/SiO_2 = 0.2; SiO_2/Al_2O_3 = 90; H_2O/SiO_2 = 30; SiO_2/TiO_2 = 20, 65 and 180 for A, B and C, respectively.

5.2.3. CATALYTIC PROPERTIES

A. Oxidation reactions

i. Oxyfunctionalization of n-hexane

The catalytic activity and selectivity of silicalite-2, TS-2, Al-MEL, Al-TS-2 and Na-Al-TS-2 in the oxyfunctionalization of n-hexane are reported in Table 5.4. As expected, TS-2 is the most active catalyst in the oxidation of n-hexane. When Ti is present in the lattice, hydrogen peroxide is selectively utilized for the oxidation reaction. The catalytic activity decreases in the order: TS-2 > M-TS-2 > M-MEL ≈ silicalite-2. Brönsted acid sites in metallosilicate analogs decompose the hydrogen peroxide leading to lower H_2O_2 selectivity. This was confirmed by ion exchanging H-Al-TS-2 with Na^+. The non-acidic Na-Al-TS-2 has a higher H_2O_2 selectivity in n-C_6 oxidation than the acidic H-Al-TS-2 (Table 5.4).

ii. Hydroxylation of benzene

The activity and selectivity of various MEL zeolites in the hydroxylation of benzene are reported in Table 5.5. The hydrogen peroxide selectivity (benzene conversion) decreased in the following order: TS-2 > Fe-TS-2 > M-TS-2 > M-MEL (where M = Al or Ga). The significant activity of M-TS-2 zeolites in the hydroxylation of benzene indicates the presence of Ti species in the zeolite framework because neither TiO_2 nor physical mixtures of silicalite-2 and TiO_2 (both amorphous and crystalline) are active in this reaction. When the hydroxylation was carried out over M-MEL zeolites, a lot of heat was produced due to the decomposition of hydrogen peroxide by the acid sites. The lower activity of M-TS-2 samples is due to the decomposition of hydrogen peroxide by the acid sites present in it. This is further confirmed by the extremely low activity of M-MEL samples (not reported).

iii. Hydroxylation of phenol

This reaction has been extensively studied over titaniumsilicate molecular sieves TS-1 and TS-2. The results obtained over different MEL zeolites are reported in Table 5.6. Contrary to the results reported by Bellussi *et al.*[5] over Al-MFI, M-MEL samples exhibit considerable activity in the hydroxylation of phenol. Metallo-titanium-silicates exhibit H_2O_2 selectivities which are in between those of TS-2 and the corresponding metallosilicates. The conversion of phenol and the selectivity for hydrogen peroxide over different MEL zeolites decreases in the following order: TS-2 > H-Al-TS-2 > Na-Al-TS-2 > H-Ga-TS-2 > H-Al-MEL

Table 5.4. Oxidation of n-hexane over MEL molecular sieves.

Reaction conditions: Temp. (K) = 373; 0.58 moles n-C_6/g catalyst; n-C_6/H_2O_2 (moles) = 3; Solvent = Acetone; Reaction time = 5 h.

Catalyst	n-C_6 Conversion (wt. %)	H_2O_2[a] utilization (mole %)	2-/3- ratio[b]	Product selectivity[c]
TS-2[d]	11.3	33.0	1.2	85.5
H-Al-TS-2[d]	7.8	12.0	1.3	61.1
Na-Al-TS-2[e]	10.1	18.6	1.2	66.9
H/Al-MEL[e]	5.3	4.9	1.5	36.5
Silicalite-2	3.3	3.1	1.2	27.1

a: H_2O_2 utilized for oxyfunctional product formation.
b: 2-/3- ratio = (2-hexanol + 2-hexanone/3-hexanol + 3-hexanone).
c: Product selectivity = (Σ 2- and 3- compounds/n-hexane reacted) x 100.
d: TS-2: SiO_2/TiO_2 = 70; Al-TS-2: SiO_2/TiO_2 = 92, SiO_2/Al_2O_3 = 60; Al-MEL: SiO_2/Al_2O_3 = 74.
e: Al-TS-2 is refluxed twice in sodium sulfate and calcined at 773 K to obtain Na-Al-TS-2.

Table 5.5. Hydroxylation of benzene over different MEL zeolites

Catalyst	H_2O_2 Sel.[a]	Product distribution, wt.%[b]	
		Phenol	PBQ
TS-2	57	66	34
H-Fe-TS-2	42	76	24
H-Al-TS-2	34	80	20
H-Ga-TS-2	36	78	22

a: (moles of phenol and PBQ / moles of hydrogen peroxide fed) X 100.
b: PBQ: para benzoquinone.
Note: Silicalite-2 and TiO_2 were completely inactive.

> H-Fe-TS-2 > H-Fe-MEL. Unlike TS-2, M-MEL and M-TS-2 form tarry products immediately, which apparently deactivate the active sites responsible for the reaction. During the initial hours of the reaction, para benzoquinone was the major product. It disappeared with time to form tarry materials.

Table 5.6. Hydroxylation of phenol over different MEL zeolites

Reaction conditions: Catalyst = 0.2 g; Temp. (K) = 353 K; Phenol/H_2O_2 (moles) = 3; Solvent = H_2O (8 ml); Reaction duration (h) = 10.

Catalyst	H_2O_2 Sel., %[a]	Phenol Convn., %	Product distribution, wt.%[b]		
			PBQ	CAT	HQ
Silicalite-2	0.0	0.0	0.0	0.0	0.0
H-Al-MEL	11.3	29.7	1.6	57.4	40.9
H-Al-MEL[c]	15.5	40.5	0.1	59.6	34.3
Na-Al-MEL	16.6	46.9	8.7	63.5	27.1
H-Al-TS-2	15.2	30.0	0.7	48.7	50.6
H-Fe-MEL	4.6	13.4	6.9	51.2	42.0
H-Fe-TS-2	10.0	26.5	2.4	52.0	45.6
H-Ga-TS-2	11.5	30.2	1.4	55.4	43.3
TS-2	19.6	51.1	1.0	49.5	49.5

a : (H_2O_2 utilized for the product formation/H_2O_2 fed) x 100
b : PBQ = para benzoquinone; CAT = Catechol; HQ = Hydroquinone
c : Si/Al = 400.

In the presence of acid catalysts, hydrogen peroxide will be protonated to give hydrogen peroxonium ion[18], which supplies OH^+ ions for the hydroxylation of aromatic compounds.

$$H_2O_2 \xrightarrow{H^+} H_3O_2^+ \longrightarrow OH^+ + H_2O$$

OH^+ ion undergoes electrophilic substitution on the aromatic ring of phenol to give the dihydroxy phenol. The absence of the formation of resorcinol (meta hydroxy phenol) in the products strongly supports the electrophilic substitution of OH^+.

In the case of titaniumsilicates a different mechanism has been reported to take place[19]. Titaniumsilicates are known to form titanium peroxo complexes upon addition of hydrogen peroxide. The titaniumsilicate inserts the oxygen into the phenol ring to yield dihydroxy phenols. The detailed mechanism of hydroxylation of phenol over TS-2 has already been described in chapter III.

B. Acid-catalyzed reactions

i. m-xylene isomerization

Fig.5.9 compares the catalytic activity of Al-MEL and Al-TS-2 (Fig.5.9 A) and Fe-MEL and Fe-TS-2 (Fig.5.9 B) in the isomerization of m-xylene as a function of time-on-stream. The significant activity of Al-TS-2 and Fe-TS-2 in m-xylene isomerization strongly suggests the presence of Al^{3+} and Fe^{3+} ions in the MEL framework. Al-MEL deactivates faster than Al-TS-2. The former also has a higher para-selectivity (p-/o-ratio) than the latter (Fig.5.9). Both Fe-MEL and Fe-TS-2 possess similar deactivation characteristics. But Fe-TS-2 is less para-selective compared to Fe-MEL (Fig.5.9 C) . Since the crystal size and shape of all the MEL samples studied here are comparable (Table 5.9 and Fig.4.3), the lower para selectivity of Al-TS-2 and Fe-TS-2 vis-á-vis the corresponding strongly acidic M-MEL indicates the important role of the strength of acid sites in controlling product shape-selectivity. This has already been discussed earlier (Chapter IV) in the case of Al-, Ga- and Fe-MEL systems, where the p-/o-ratio decreases with decreasing acid strength. This is more clearly illustrated in Fig.5.10, where m-xylene conversion is plotted against p-/o-xylene ratio and selectivity for isomerization. At similar conversion levels the metallo-titanium-silicate analogs exhibit lower para-selectivity and higher selectivity for isomerization (lower TMB selectivity) vis-á-vis their metallosilicate analogs not containing Ti. In the alkylation of toluene with methanol, Corma *et al.*[20] have also reported that para-selectivity increases with the strength of the Brönsted acid sites. On weakly acidic catalysts the overall rate is probably controlled by the chemical reaction step. On strongly acidic catalysts, on the other hand, transport processes constitute the slow rate determining step and, hence, differences in the relative diffusivities of the various product molecules lead to the observed product shape-selectivity phenomenon.

Catalytic activity of Al-MEL, the Al-TS-2 series, TS-2 and silicalite-2 in m-xylene isomerization is included in Table 5.2. The conversion of m-xylene was the same over all the samples having similar Al^{3+} content. However, para-selectivity decreased upon replacement of Si by Ti in the aluminosilicate. In Fig.5.11 the p-/o- ratio in m-xylene isomerization is plotted against the total amount of pyridine retained at 473 K obtained by FTIR. There is a proportional decrease in para-selectivity on decrease in acid strength. Since the crystal size and shape of the samples studied here are nearly comparable, the origin of change in para-selectivity is most probably connected with the intrinsic rate of m-xylene isomerization and hence to the acidity. Chen *et al.*[21] have reported a lower n-hexane cracking rate for Al-TS-1 (SiO_2/Al_2O_3 = 20; SiO_2/TiO_2 = 200) compared to ZSM-5 (SiO_2/Al_2O_3 = 60).

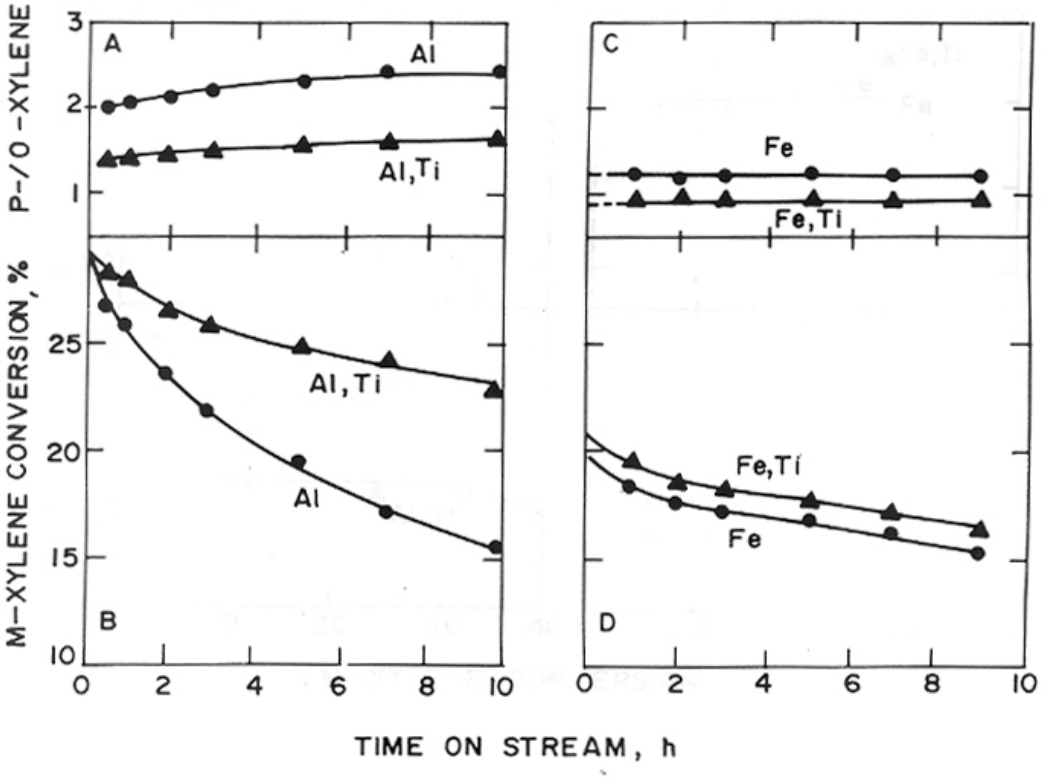

Fig.5.9. **Influence of time on stream on m-xylene conversion and p-/o-xylene ratio.** Temp. (K) = 553; LHSV (h^{-1}) = 4; H_2/m-xylene (mole) = 4.

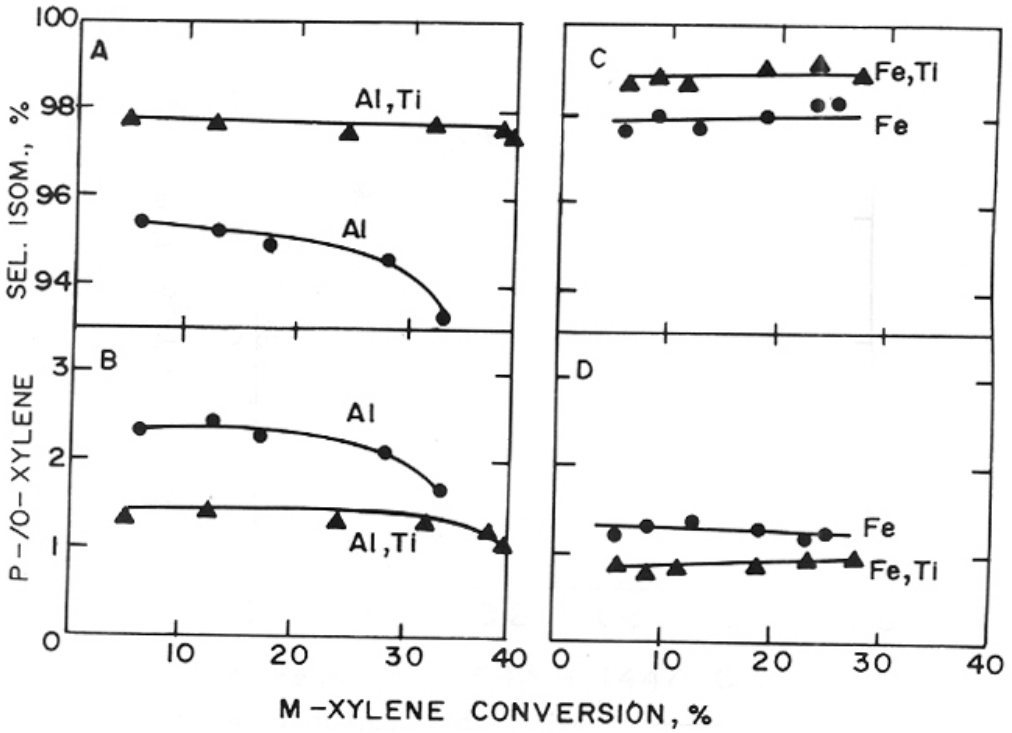

Fig.5.10. **Effect of m-xylene conversion on p-/o-xylene ratio and selectivity for isomerization.**
LHSV (h^{-1}) = 4; H_2/m-xylene (mole) = 4; Temperature was varied to get different conversions.

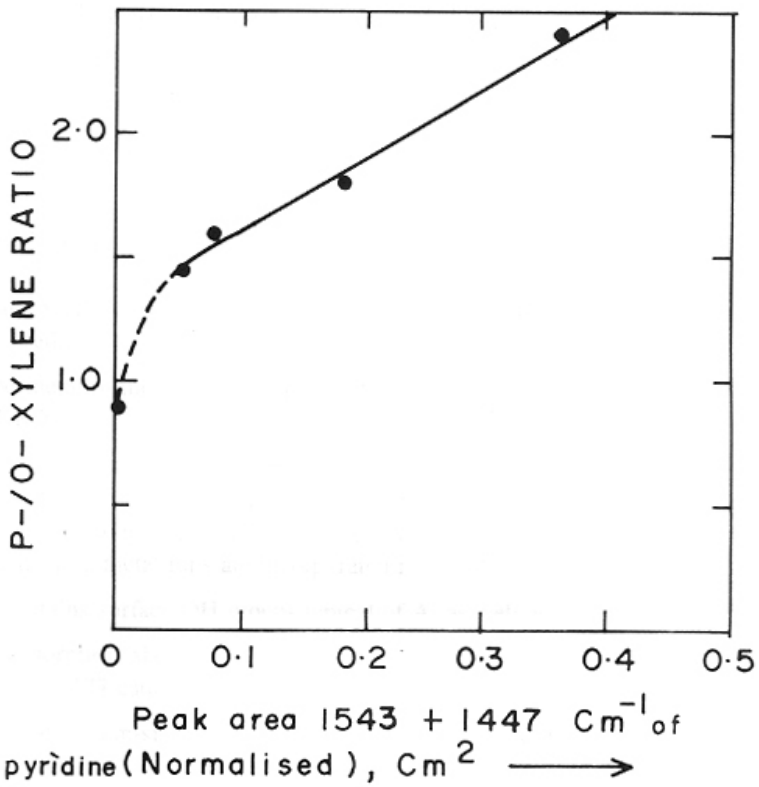

Fig.5.11. Influence of total acidity on p/o-xylene ratio in m-xylene isomerization reaction.

Temp. (K) = 533; LHSV (h^{-1}) = 4; H_2/m-xylene (mole) = 4.

ii. Ethylbenzene disproportionation

Fig.5.12 compares the catalytic activity and the rates of deactivation of H-Al-MEL, H-Al-TS-2, H-Fe-MEL and H-Fe-TS-2 in the disproportionation of ethylbenzene. The initial high activity of H-Al-MEL and H-Al-TS-2 vis-á-vis H-Fe-MEL and H-Fe-TS-2 can be attributed to the higher acid strength of the Al-analogs. However, metallo-titanium-silicates exhibited slower rates of deactivation compared to metallosilicate analogs suggesting that acid strength has an influence on the rate of deactivation. Probably, on weaker acid sites the secondary reactions (such as the further disproportionation/dealkylation of the products) causing coke formation/pore blocking in the zeolites is suppressed.

5.3. CONCLUSIONS

1) Incorporation Ti^{4+} as well as Al^{3+}, Ga^{3+} or Fe^{3+} into the MEL (Silicalite-2) framework has been achieved.
2) MEL type metallo-titanium-silicates do not contain any detectable amount of MFI impurities (by XRD).
3) Expansion in the unit cell parameters (XRD), the occurrence of the 960 cm^{-1} band in the framework IR spectra and a band at 212 nm in the UV-VIS spectra, ion-exchange capacities, ESR spectroscopy (g = 4.3) and magnetic moment values (μ = 5.6-5.8 BM) strongly suggest that these metal ions are incorporated in the MEL framework.
4) Al-TS-2 contains surface OH groups typical of Al as well as TS-2.
5) Pyridine adsorption shows that acidity of Al-MEL goes on decreasing with increasing incorporation of Ti cations.
6) The metallo-titanium-silicate analogs crystallize at a slower rate than the corresponding metallosilicates.
7) Metallo-titanium-silicates exhibit catalytic activity in both acid and oxidation reactions.
8) In m-xylene isomerization, H-M-TS-2 is less para-selective vis-á-vis H-M-MEL and p-/o-xylene ratio decreases parallelly with decreasing acidity.
9) In Brönsted acid catalyzed reactions metallo-titanium-silicates deactivate at a slower rate than the metallosilicate analogs.

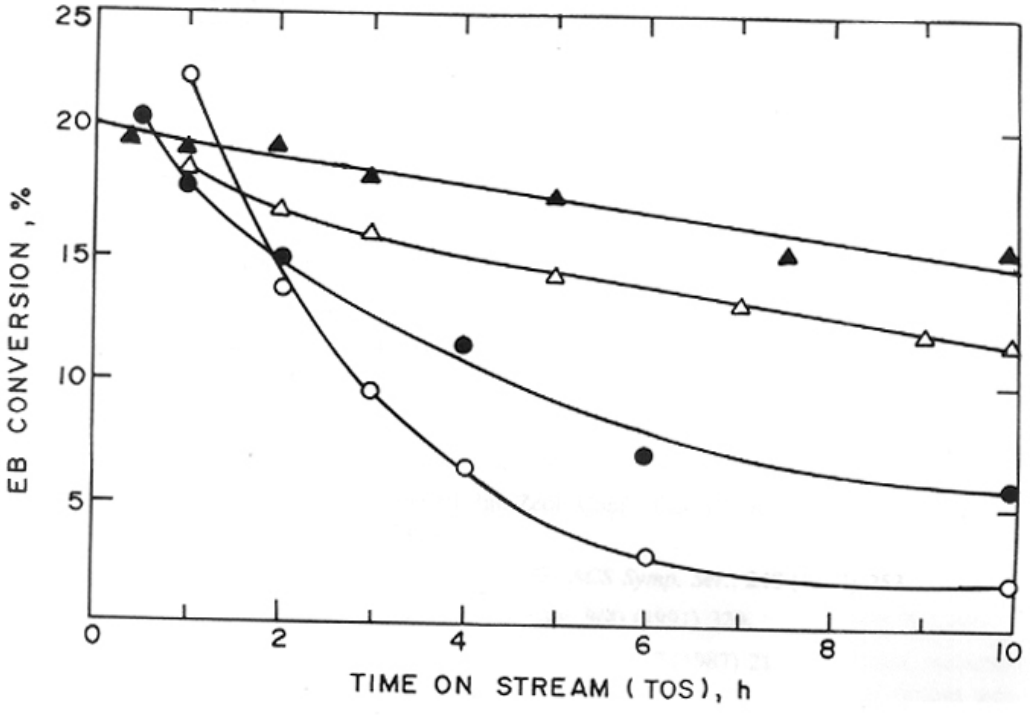

Fig.5.12. Influence of time on stream on EB conversion
(▲): Fe-TS-2; (△): Fe-MEL; (●): Al-TS-2; (○) Al-MEL.
Temp. (K) = 648; LHSV (h^{-1}) = 8 and 4 for Al and Fe analogs, respectively (10-20 mesh size).

5.4. REFERENCES

1. Bellusi, G., EP Applied A1 0 272 496 (1987).
2. Forni, L. and Pelozzi, M., *J. Mater. Chem.*, (1990) 1101; Forni, L., Pelozzi, M., Guisti, A., Fornasari, G. and Millini, R., *J. Catal.*, **122** (1990) 44.
3. Thangaraj, A., Kumar, R. and Ratnasamy, P., *Appl. Catal.*, **57**, L1, (1990); Thangaraj, A., Sivasanker, S. and Ratnasamy, P., *Zeolites*, **12** (1992) 135.
4. Reddy, J.S. and Kumar, R. in "Proc. 10th Natl. Symp. on Catal. And 4th INDO-USSR Symp. on Catal." Recent Developments in Catalysis, Theory and Practice, Eds. B.Viswanathan *et al.*, Narosa Pub., New Delhi, India, 1989, p.156.
5. Bellussi, G., Carati, A., Clerici, M.G. and Esposito, A., *Stud. Surf. Sci. Catal.*, **63** (1991) 421.
6. Reddy, J.S., Reddy, K.R., Kumar, R. and Csicsery, S.M., *J. Catal.*, (accepted).
7. Rollmann, L.D. and Valyocsik, E.W., Eur. Pat. EP. 21,675 (1981).
8. Rammanikov, V.N., Mastikhin, V.M., Hocevar, S. and Drzaj, B., *Zeolites*, **3** (1983) 311.
9. Ernst, S., Jacobs, P.A., Martens, J.A. and Weitkamp, J., *Zeolites*, **7**, (1987) 458.
10. Reddy, J.S. and Kumar, R., *Zeolites*, **12** (1992) 95.
11. Boccuti, M.R., Rao.,K.M., Zecchina, A., Leofanti, G. and Petrini, G., *Stud. Surf. Sci. Catal.*, **48** (1989) 133.
12. Thangaraj, A., Ph.D Thesis, submitted to University of Poona, 1991.
13. Morterra, C. and Cerrato, G., *Langmuir*, **6** (1990) 1810
14. Vedrine, J.C., in "Proc. of the 6th Int. Zeol. Conf." Eds. D. Olson and A. Basio, Butterworths, Guildford, UK, 1984, 497.
15. Vedrine, J.C, Aurox, A. and Coudurier, G., *ACS Symp. Ser.*, **248** (1984) 253.
16. Ratnasamy, P. and Kumar, R., *Catal. Today*, **9(4)** (1991) 329.
17. Harrison,I.D., Leach,H.F. and Whan,D.A., *Zeolites*, **7** (1987) 21.
18. Perot, G. and Guisnet, M., *J. Mol. Catal.*, **61** (1990) 173.
19. Reddy, J.S., Sivasanker, S. and Ratnasamy, P., *J. Mol. Catal.*, **71(3)** (1991) 373.
20. Corma, A., in "Guidlines for Mastering the Properties of Molecular Sieves" Eds. Barthomeuf, D. *et al.*, NATO ASI Series, Series B: Physics Vol.221, Plenum press, New York, 1990.
21. Chen, M.C., Chu, S.J., Chang, N.S., Chen, P.Y., Chuang, T.K. and Chen, L.Y., *Stud. Surf. Sci. Catal.*, **38** (1987) 253.

CONCLUSIONS

1. A new crystalline microporous titaniumsilicate molecular sieve, TS-2 has been synthesized.
2. The formation of TiO_2 precipitate or alkali metal titanates has to be avoided to ensure the incorporation of Ti in the lattice and to get an active titaniumsilicate catalyst.
3. The use of tetraethylorthosilicate (TEOS) and tetrabutylorthotitanate (TBOT) avoids the formation of TiO_2 precipitate during the preparation of the reaction mixture.
4. The presence of Ti in MEL framework has been established by different physicochemical techniques
5. Ti is found to more stable in the zeolite framework both under thermal and hydrothermal conditions when compared to Si and Al.
6. TS-2 is an active catalyst in the following oxidation reactions involving hydrogen peroxide as the oxidant.
   - Oxyfunctionalization of alkanes
   - Ammoximation of carbonyl compounds
   - Hydroxylation of aromatic compounds
   - Epoxidation of olefins
   - Oxidation of primary and secondary alcohols to aldehydes and ketones, respectively.
7. The Ti present in the zeolite framework is responsible for the activity of titanium silicates. Silicalite, TiO_2 and amorphous titaniumsilicates are inactive in these reactions.
8. Gallo-, ferri-, alumino-titanium-, gallo-titanium- and ferri-titanium-silicate molecular sieves with MEL structure have been synthesized and characterized using various techniques.
9. The rate of crystallization of different MEL molecular sieves follows the decreasing order: silicalite-2 > TS-2 ≈ Al-MEL > Ga-MEL ≈ Ga-TS-2 > Fe-MEL > Fe-TS-2.
10. The replacement of Si by Ti in metallosilicates decreases the strength of their acid centers.
11. Metallo-titanium-silicates possess dual-catalytic functions. They are active in both acid-catalyzed and oxidation reactions.
12. Metallo-titanium-silicates are more stable than the corresponding metallosilicates.

LIST OF PUBLICATIONS

PAPERS

1. J.S. Reddy and R. Kumar "*Synthesis, Characaterization and Catalytic Properties of Titanium Silicate, TS-2, with MEL Structure*" J. Catal., **130**, (1991) 440.
2. R.S. Reddy, J.S. Reddy, R. Kumar and P. Kumar "*Sulphoxidation of Thioethers using Titanium Silicate Molecular Sieves*" J. Chem. Soc., Chem. Commun., (1992) 84.
3. J.S. Reddy, K.R. Redy, R. Kumar and P. Ratnasamy "*Ferisilicate analogs of ZSM-11 (MEL)*" Zeolites, **11**, (1991) 553.
4. J.S. Reddy and R. Kumar "*Crystallization Kinetics of a new Titanium Silicate with MEL Structure (TS-2)*" Zeolites, **12** (1991) 95.
5. J.S. Reddy, S. Sivasanker and P. Ratnasamy "*Ammoximation of Cyclohexanone over a Titanium Silicate Molecular Sieve, TS-2*" J. Mol. Catal., **69** (**3**) (1991) 383.
6. J.S. Reddy, S. Sivasanker and P. Ratnasamy "*Selective Oxidation of n-hexane over a Titanium Silicate Molecular Sieve with MEL Structure*" J. Mol. Catal., **70** (**3**) (1991) 335.
7. J.S. Reddy, S. Sivasanker and P. Ratnasamy "*Hydroxylation of Phenol over TS-2, a Titanium Silicate Molecular Sieve*" J. Mol. Catal., **71** (**3**) (1992) 373.
8. J.S. Reddy, R. Kumar and P. Ratnasamy "*Synthesis, characterization and catalytic properties of Titanium silicalite (TS-2)*" Appl. Catal., **58**,(1990) L1-L4.
9. J.S. Reddy and S. Sivasanker "*Selective Oxidation of Cyclohexane over TS-2, a Titanium Silicate Molecular Sieve*" Catal. Lett., **11** (1990) 241.
10. Anuj Raj, J.S. Reddy and R. Kumar "*Catalytic Properties of [Al]-, [Ga]- and [Fe]-silicate Analogs of ZSM-11 in C_7 and C_8 Aromatic Hydrocarbon Reactions: Influence of Iomorphous Substitution*", 9th Int. Zeo. Conf., Full paper-poster presentation, Montreal, Canada.
11. Anuj Raj, K.R. Reddy, J.S. Reddy "*Catalytic Properties of Ferrisilicate Analogs of Some Medium Pore Zeolites in C_7 and C_8 Aromatic Hydrocarbon Reactions*" 10th Int. Cong. Catal., Poster presentation, Budapest, Hungary.
12. J.S. Reddy and S. Sivasanker "*Selective Oxidation of organic compounds over TS-2, a Titanium Silicate Molecular Sieve*", Ind. J. Technol., **11** (1992) 64.
13. J.S. Reddy and R. Kumar "*Metallo- and Metallo-Titanium-Silicate Molecular Sieves with MEL Topology*", B. Viswanathan and C.N. Pillai (Eds.), Recent Developments in Catalysis:Theory and Practice, Narosa, New Delhi, 1990, p.156.
14. J.S. Reddy, K.R. Reddy and R. Kumar "*Incorporation of Fe and Ga into MEL Framework*" B. Viswanathan and C.N. Pillai (Eds.), Recent Developments in Catalysis:Theory and Practice, Narosa, New Delhi, 1990, p.575.

15. Anuj Raj, J.S. Reddy and R. Kumar "*Selective formation of 1,2,4-trimethylbenzenes over different MEL metallosilicate Molecular Sieves*" J. Catal., (accepted).

16. J.S. Reddy, R. Kumar and S.M. Csicsery "*Synthesis, Characterization and Catalytic Properties of Metallo-Titanium-Silicates with MEL Topology*", J. Catal., (communicated).

17. J.S. Reddy, P. Ratnasamy and R.B. Mitra "*Cleavage of Carbon-Carbon Double Bond over Zeolites using Hydrogen Peroxide*", J. Chem. Soc., Chem. Commun., (communicated).

18. J.S. Reddy, R.S. Reddy, P. Kumar and R. Kumar "*Catalytic Sulfoxidation of Thioethers with Hydrogen Peroxide over Titanium Silicate Molecular Sieve*", Appl. Catal., (communicated)

19. J.S. Reddy, S. Sivasanker and P. Ratnasamy "*Vapour Phase Beckmann Rearrangement of Cyclohexanone Oxime over the Titanium Silicate, TS-2, and other MEL-analogs*", Catal. Lett., (communicated).

20. J.S. Reddy, S. Sivasanker and P. Ratnasamy "*Studies on Thermal and Hydrothermal Stabilities of Titanium silicates*", (in preparation).

21. J.S. Reddy, R. Kumar and P. Ratnasamy "*Factors influencing the occurrence of ZSM-5 (MFI) impurity/intergrowth during the synthesis of ZSM-11 (MEL) using TBA^+ as a templateN*", (in preparation).

22. J.S. Reddy, S.G. Hegde and P. Ratnasamy "*Influence of Replacement Si by Ti on Acidity and Activity in Aluminosilicates*", (in preparation)

23. J.S. Reddy, P. Ratnasamy and R.B. Mitra "*Cleavage of Carbon Carbon Double Bond During the Epoxidation of α-methylstyrene over Titanium Silicate Molecular Sieve, TS-2*", (in preparation).

24. J.S. Reddy, A. Raj, A.P. Singh and P. Ratnasamy "*Hydroxylation of Phenol over Various Metallo- and Metallo-Titanium-Silicate Analogs of MEL*", (in preparation).

PATENTS (FILED)

1. J.S. Reddy, A. Thangaraj, R. Kumar and P. Ratnasamy "Process for the Preparation of Crystalline Titanium Silicalite-2" - 954/DEL/1990.

2. J.S. Reddy, R. Kumar and P. Ratnasamy "Process for the Preparation of Crystalline Metallosilicate Catalyst Composite Material" - NF/42/89-PAT.

3. J.S. Reddy, R. Kumar and P. Ratnasamy "Process for the Preparation of Crystalline Metallo-Titanium-Silicate Catalyst Composite Material" - 1210/DEL/90.

4. J.S. Reddy, S.Sivasanker and P.Ratnasamy "An Improved Process for the Production of Cyclohexanone and Cyclohexanol" - 1097/DEL/90.

5. J.S. Reddy, S.Sivasanker and P.Ratnasamy "An Improved Process for the Manufacture of ε-caprolactam from Cyclohexane" - 1099/DEL/90.

6. J.S. Reddy, S.Sivasanker and P.Ratnasamy "An Improved Process for the Manufacture of ε-caprolactam - 1099/DEL/90.

7. J.S. Reddy, S.Sivasanker and P.Ratnasamy "A Process for the Production of Cyclohexanone Oxime - 1099/DEL/90.

8. J.S. Reddy, R.S. Reddy, P. Kumar and R. Kumar "An Improved Process for the Production of Sulfoxides and Sulfones" - NF/169/91-PAT.

9. M.K. Dongare, J.S. Reddy, Prabath Singh and P. Ratnasamy "Process for the Preparation of a Novel Porous Crystalline Material" - 1169/DEL/89.

10. R.S. Reddy, J.S. Reddy, P. Kumar and R. Kumar "An Improved Process for the Production of Sulfoxides and Sulfones" - NF/170/91-PAT.

11. P.P.Moghe, P.Ratnasamy, G.R.Venkatakrishanan, J.S.Reddy, A.V. Pol, M.G.Kotasthane, S.S.Biswas, A.S.Tambe and P.K.Bahirat "An Improved Process for the Preparation of Dihydroxy Benzenes and 1,4-benzoquinone by the Hydroxylation of Phenol using Hydrogen Peroxide and Titanium Containing Zeolites" - 170/DEL/90.

12. P.P.Moghe, P.Ratnasamy, G.R.Venkatakrishanan, J.S.Reddy, A.V. Pol, M.G.Kotasthane, S.S.Biswas, A.S.Tambe and P.K.Bahirat "An Improved Process for the Preperation of Phenol, Hydroxy Benzene and 1,4-benzoquinone by the Hydroxylation of Benzene using Titanium Containing Synthetic Zeolitic Catalyst" - 171/DEL/90.

13. Anuj Raj, J.S. Reddy, R. Kumar and P. Ratnasamy "A Process for the Production of 1,2,4 Trimethylbenzene" - (Applied).